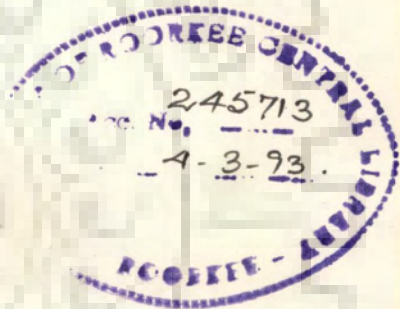# MODELLING OF SOLUTE TRANSPORT THROUGH AN UNSATURATED ZONE EXTENDING FROM GROUND SURFACE TO WATER TABLE

A THESIS

submitted in fulfilment of the
requirements for the award of the degree
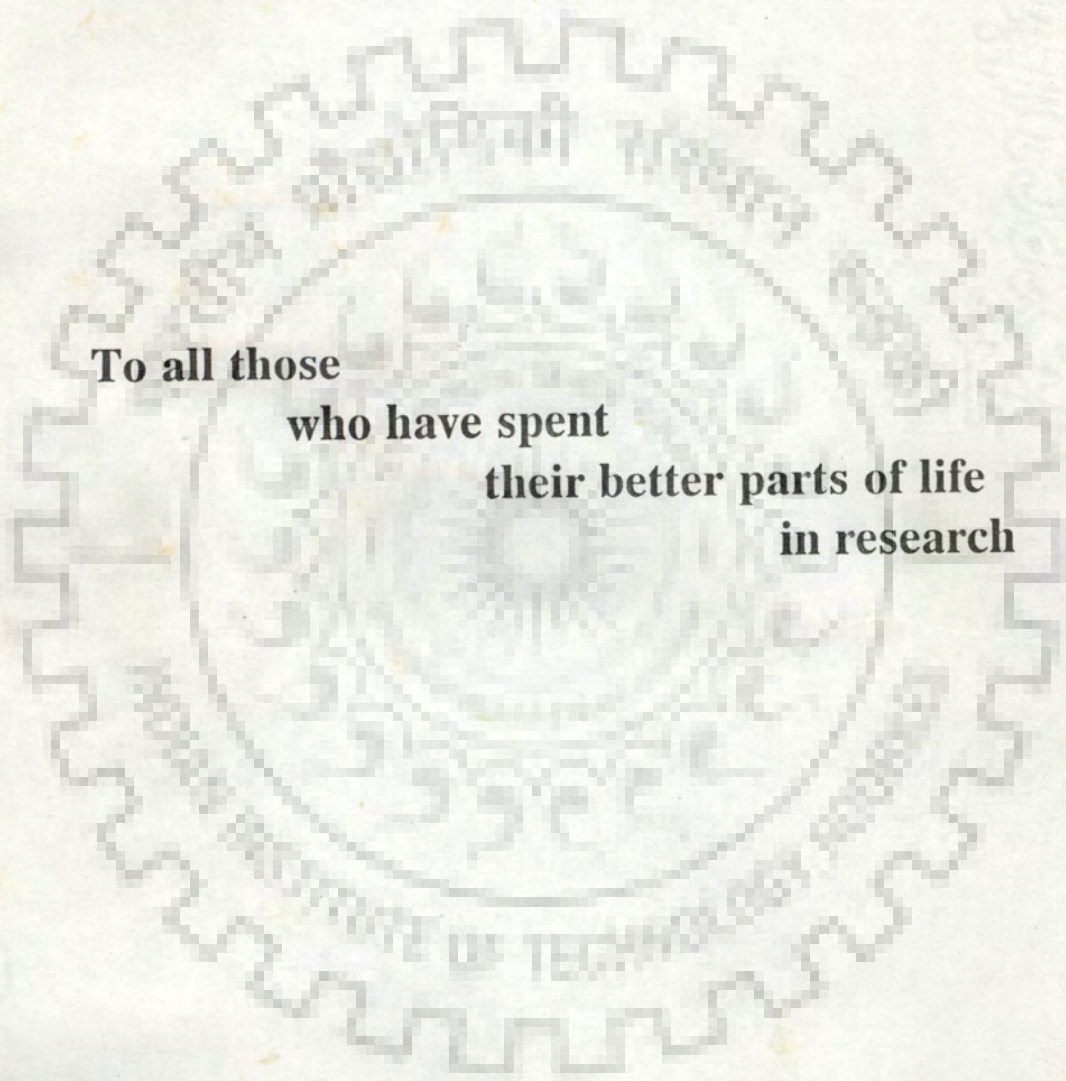of
DOCTOR OF PHILOSOPHY
in
HYDROLOGY

By

SULEKHA GUPTA

DEPARTMENT OF HYDROLOGY
UNIVERSITY OF ROORKEE
ROORKEE-247 667 (INDIA)

DECEMBER, 1991

To all those
who have spent
their better parts of life
in research

CANDIDATE'S DECLARATION

I hereby certify that the work which is being presented in the thesis entitled **MODELLING OF SOLUTE TRANSPORT THROUGH AN UNSATURATED ZONE EXTENDING FROM GROUND SURFACE TO WATER TABLE** in fullfilment of the requirements for the award of the degree of DOCTOR OF PHILOSOPHY, submitted in the Department of Hydrology, University of Roorkee, is an authentic record of my own work carried out during a period from November, 1987 to December 1991 under the supervision of Dr. Deepak Kashyap.

The matter embodied in this thesis has not been submitted by me for the award of any other degree.

Sulekha Gupta

(SULEKHA GUPTA)

Dated : 19 Dec. 1991

This is to certify that the above statement made by the candidate is correct to the best of my knowledge.

(DEEPAK KASHYAP)
Reader in Hydrology
Department of Hydrology
University of Roorkee
Roorkee (India)

The Ph.D viva-voce examination of Ms. Sulekha Gupta, research scholar has been held on. Sept 30, 1992

Signature of Guide(s) 30/9/92

Signature of External Examiner(s) 30/9/92

ABSTRACT

Waste disposal on land and application of fertilizers and pesticides to crop lands has become a common practice universally. Water infiltrating at the ground, dissolves such matter and carries it downward through the unsaturated zone. Many types of waste material (e.g., heavy metals, radioactive material) do not decompose easily. Such pollutants travelling through the unsaturated zone join the water table and may affect the water quality adversely. Further, fertilizers which are not utilized by crops are transported below the root zone by percolating water and pose a potential threat to the groundwater quality. In a reverse situation, evapotranspiration may lead to an accumulation of pollutants in the root zone. This may lead to a fall in crop yield and deterioration of top soil conditions. To avoid such problems and to design safe disposal systems, the time variant rate of pollutant transfer to the water table as well as depth and time variant concentrations need to be estimated.

In the present study an attempt has been made to develop a numerical model for simulating one dimensional (vertical) solute transport from ground to the water table. The mechanisms of solute transport accounted for are convection, hydrodynamic dispersion, lateral diffusion into/out of an immobile phase (in case of two phase solute transport) and linear adsorption - desorption in either or both the phases. The model is developed in the following four stages.

Stage I   Single phase non-reactive solute transport.

Stage II   Single phase reactive solute transport, accounting for first order linear kinetic adsorption-desorption.

Stage III Two phase non-reactive solute transport.

Stage IV Two phase reactive solute transport accounting for linear equilibrium adsorption-desorption.

The numerical methods employed for solving the solute transport equations are the method of characteristics (MOC) and the finite differences. The convective component is solved using MOC to overcome the problem of numerical dispersion encountered in solving convection dominated flow problems. Change in concentration due to hydrodynamic dispersion and adsorption-desorption is accounted for subsequently, using an implicit finite difference scheme. The soil moisture and flux distribution required for solving the solute transport equations is obtained by solving (Mohan Rao, 1986) the head form of Richards equation using a Crank-Nicolson finite difference scheme. The problem of non linearity arising due to dependence of scpecific moisture capacity and capillary conductivity on soil moisture (or capillary head) was taken care of by using Picard's Iteration method.

To account for solute transport due to convection by MOC the domain under consideration is discretized by a finite number of moving packets of a pre-assigned strip thickness. Each moving packet is defined by two co-ordinates (representing its upper and lower bounds) and the solute and water volumes contained in it. During simulation, the movement of these packets is traced. During each time step the new positions of moving packets are obtained by ensuring a compatibility between the cumulative water profiles obtained by the considerat of flow and transport.

Solute volumes (per unit plan area) of these moving packets were further redistributed amongst themselves to account for solute transport due to hydrodynamic dispersion. This is done by solving the

ii

governingdifferential equation using an implicit finite difference scheme. To compute further change in concentration due to adsorption-desorption of solute by the soil matrix or lateral diffusion of solute into/out of the immobile phase and subsequent adsorption-desorption a fixed grid system is superposed on the moving co-ordinate system. Concentration distribution of this grid is computed by identifying moving packets lying wholly or partially in the area of influence of any node. The governing differential equations are then solved using an implicit finite difference scheme. Further, change in solute volume (per unit plan area) at the nodes is attributed to the moving packets.

Thus, the model is capable of simulating spatial and temporal distribution of solute concentration and quantifying the volume of solute (per unit plan area) joining the water table.

The model was validated by comparing model simulated solute transport with the results of two analytical solutions of van Genuchten and Alves, 1982 (cited in Parker and van Genuchten, 1984) and Parker and van Genuchten, 1984. The analytical solution of van Genuchten and Alves', 1982 (cited in Parker and van Genuchten, 1984) pertains to flow conditions, accounting for linear equilibrium adsorption-desorption. Neglecting solute matrix interaction this solution was used to validate the stage I model. Results obtained by the two methods showed an excellent agreement. The analytical solution of Parker and van Genuchten (1984) pertains to single phase and two phase solute transport under steady state flow conditions. For single phase solute transport the sorption sites present in the soil matrix are assumed to comprise of two fractions i.e., equilibrium adsorption ('type-1' sites) and kinetic

equilibrium adsorption ('type-2' sites). For two phase solute transport the interaction between solute and soil matrix in both phases, is described by a linear equilibrium adsorption-desorption isotherm. By assigning appropriate values to the parameters, this solution was used to validate the stage II, III and IV model. An excellent agreement was obtained for most of the simulations.

The proposed model was also used to simulate reported experimental data of two field experiments (Warick et al, 1971; Bottcher and Strebel, 1989).

The model (Stage I) was used to simulate Chloride concentration profiles in depth under conditions identical to the experiments of Warrick et al. (transport of $CaCl_2$ and water in Panoche clay loam). The simulated and measured concentration profiles compared reasonably well, except for a lag between the simulated and measured depth of solute travel. The simulation was repeated considering the presence of an immobile phase (Stage III model) and neglecting solute transfer into/out of the immobile phase (equivalent to a case of anion exclusion, assuming the effect of osmotic potential on the fluid flow to be negligible). For θ_{im} = 0.06, the lag was almost eliminated.

A bromide leaching experiment was conducted by Böttcher and Strebel, 1989 (unpublished data) and breakthrough curves at 51 locations at depths of 120 cm were measured. Profiles of bromide amounts in depth at 26 boring sites were also made on two dates. The measured experimental data exhibited a considerable lateral variation in solute transport. Although, the proposed model does not account for horizontal transport, a reasonable agreement was observed between the model simulated and measured mean concentration distribution.

Model application to real life problems was demonstrated by simulating two problems of solute transport through the unsaturated zone. The model was used to simulate salt accumulation in the root zone of two crops (wheat and rice) assumed to grow over a period of one year and irrigated by considerably saline water (1.5 mmho/cm). Concentration profiles (ground to water table) at different discrete times, covering the entire period were also simulated. Evapotranspiration by the crops was accounted for (Doorenbos et al., 1979). Salt accumulation in the root zone was also estimated using the salt storage equation (Van der Molen, 1973). A considerable deviation was observed between the salt accumulation as computed by the salt storage equation and by the model. This deviation was possibly caused by the assumptions on which the salt storage equation is based.

The model was used to simulate solute travel of a conservative pollutant (assumed to be abundantly available on the ground) in two types of soils (loam and clay) under conditions of heavy monsoon rainfall. At the end of the simulation period (140 days) the solute joining the water table in case of clay was negligible - caused only by dispersion. However, in case of loam, the convective front reached the water table in about 80 days time, beyond which the solute joining the water table was appreciable.

ACKNOWLEDGEMENT

At the completion of this earnest attempt of my academic career it is natural that I express my gratefulness to the numerous individuals who unstintingly helped during the progress of this work. These few sentences will be encarved in my memory and the feelings will be everlasting.

The gratitude and indebtedness I feel towards my guide **Dr. Deepak Kashyap** is of infinite order. This work would have never taken the shape of a thesis without his able guidance and the encouragement provided throughout the course of this study. During these years I have been fortunate to have had the oppurtunity to assimilate from his thorough understanding and vast knowledge of the subject.

I am also specially thankful to Dr. W.H.M Duynisveld who gave me his invaluable time and also guided me in undertaking this research problem, during my visit to the Institue of Geo-sciences and Natural Resources, Hannover, Germany. The time I worked with him was short but there was a quantum leap in the knowledge gained.

Thanks are due to the experts of the Institute of Geosciences and Natural Resources, Hannover, Germany; **Dr Strebel**, who provided the required facilities available in his section and Dr. Bottcher who furnished the necessary data on a Bromide leaching experiment and also spared some of his invaluable time in useful discussion.

I am thankful to the Head and the other members of the teaching staff at the Department of Hydrology, University of Roorkee for the co-operation extended during the period of study.

I am also grateful to the staff of Roorkee University Regional computer centre for providing me with necessary computer facility.

The most difficult hurdles seem simple and easy when friends with their mere presence lead you across. **Ujjwala**, **Veena**, **Sagarika** and **Nirupama** will be remembered for their companionship and the soothing comfort in trying times .

Thanks are due to **Sandeep**, **Manoj** and **Patel** who with their friendly banter have always boosted my morale and reinforced my enthusiasm to work. **Glory**, **Anjana**, **Swagata**, **Ritu** and **Nandana** with their fun and laughter always managed to keep me in good spirits.

I am also thankful to my departmental colleagues who have always assisted me promptly whenever the need arose.

I fall short of words to express the support and encouragement which was provided by my parents, sisters and brother.

My hearty gratitude goes to my husband **Raj** for his patience and much needed moral support. His sense of humour has always helped me overcome difficult patches. I also feel a deep sense of gratitude towards his family.

I want to thank Mr. D.P.Sharma for meticulously typing the text and Mr. **Narendra** for preparing some of the drawings.

Sulekha Gupta
(SULEKHA GUPTA)

INDEX

LIST OF SYMBOLS

Symbol	Description	Dimension
	(Unless mentioned otherwise)	
a b	} empirical constants characterizing the soil.	$[*]$
c	solute concentration	$[ML^{-3}]$
d_{in}	depth of infiltrated solute	$[L]$
d_t	depth of root zone	$[L]$
f	fraction of adsorption sites located in the mobile phase	$[*]$
f_e	fraction of the percolating solute having a concentration of the soil solution	$[*]$
h	capillary pressure head	$[L]$
h_b	bubbling pressure	$[L]$
im	suffix representing the immobile phase	$[*]$
k_d	empirical distribution coefficient	$[L^3 M^{-1}]$
m	suffix representing the mobile phase	$[*]$
n	total number of nodes in the finite difference grid	$[*]$
np	total number of moving packets	$[*]$
$ns_{j,k}$	volume of solute (per unit plan area) at node j at k^{th} discrete time	$[ML^{-2}]$
$nv_{j,k}$	volume of water (per unit plan area) at node j at k^{th} discrete time	$[L]$
q	volumetric flux	$[LT^{-1}]$
s	adsorbed concentration	$[MM^{-1}]$

$sl_{p,k}$ volume of solute (per unit plan area) contained

in the pth packet at k^{th} discrete time $[ML^{-2}]$

t time $[T]$

Δt_k time step from k^{th} to $(k+1)^{th}$ discrete time levels $[T]$

v seepage velocity $[LT^{-1}]$

$vl_{p,k}$ volume of water (per unit plan area) contained

in the pth moving packet at k^{th} discrete time $[L]$

$x_{p,k}$ lower bound of the pth moving packet at k^{th}

discrete time $[L]$

$\Delta x_{p,k}$ length of pth moving packet at k^{th} discrete time $[L]$

$xs_{p,k}$ volume of solute (per unit plan area) contributed

to the jth node by p^{th} moving packet at k^{th}

discrete time $[L]$

$xv_{p,k}$ volume of water (per unit plan area) contributed

to the jth node by p^{th} moving packet at k^{th}

discrete time $[L]$

$xw_{p,k}$ cumulative volume of water (per unit plan area)

corresponding to $x_{p,k}$ $[L]$

$y_{p,k}$ upper bound of pth moving packet at k^{th} discrete

time $[L]$

$yw_{p,k}$ cumulative volume of water (per unit plan area)

corresponding to $y_{p,k}$ $[L]$

z co-ordinate along the vertical direction (+ve

upwards) $[L]$

Δz_j spatial distance between the jth and $(j+1)^{th}$ node $[L]$

of the finite difference grid

C_u specific moisture capacity $[L^{-1}]$

D	hydrodynamic dispersion coefficient	$[L^2T^{-1}]$
D_o	molecular diffusion coefficient in a free water system	$[L^2T^{-1}]$
E	sink term	$[T^{-1}]$
F	fraction of type-1 sorption sites	$[*]$
I_c	infiltration capacity	$[LT^{-1}]$
K	capillary conductivity	$[LT^{-1}]$
K_s	saturated capillary conductivity	$[LT^{-1}]$
P	factor to define the threshold moisture content value	$[*]$
Q	input intensity	$[LT^{-1}]$
R	retardation factor	$[L]$
R^*	net downward percolation	$[L]$
W_{fc}	amount of moisture in the root zone assuming the moisture content to be at field capacity	$[L]$
X	total depth of solute domain	$[L]$
Z	total salt content of the root	$[L^3]$
Z'_1	initial salt content of the root zone	$[L^3]$
Z'_2	salt content in the root zone at the end of the period	$[L^3]$
$\Delta Z'$	change in salt content in the root zone	$[L^3]$
α	first order rate coefficient governing transfer of solute into/out of the immobile phase	$[T^{-1}]$
β	first order rate coefficient governing exchange between solute and soil matrix (kinetic adsorption-desorption)	$[T^{-1}]$
γ_s	rate constant for zero order production in the soil	

	matrix	$[T^{-1}]$
γ_w	rate constant for zero order production in the solute	$[ML^{-3}T^{-1}]$
θ	soil moisture content	$[L^3L^{-3}]$
θ_{fc}	soil moisture content at field capacity	$[L^3L^{-3}]$
θ_t	threshold moisture content	$[L^3L^{-3}]$
θ_{wp}	soil moisture content at wilt point	$[L^3L^{-3}]$
λ	dispersivity	$[L]$
μ_s	rate constant for first order decay in the soil matrix	$[T^{-1}]$
μ_w	rate constant for first order decay in solute	$[T^{-1}]$
ξ	co-ordinate along the vertical direction (+ve downwards)	$[L]$
ξ_o	small positive value to define permissible error in Picard's ineration method	$[*]$
ρ	soil bulk density	$[ML^{-3}]$
ϕ	porosity	$[L^3L^{-3}]$

* - dimensionless

List of Figures

I am also grateful to the staff of Roorkee University Regional computer centre for providing me with necessary computer facility.

The most difficult hurdles seem simple and easy when friends with their mere presence lead you across. **Ujjwala, Veena, Sagarika** and **Nirupama** will be remembered for their companionship and the soothing comfort in trying times .

Thanks are due to **Sandeep, Manoj** and **Patel** who with their friendly banter have always boosted my morale and reinforced my enthusiasm to work. Glory, Anjana, Swagata, Ritu and Nandana with their fun and laughter always managed to keep me in good spirits.

I am also thankful to my departmental colleagues who have always assisted me promptly whenever the need arose.

I fall short of words to express the support and encouragement which was provided by my parents, sisters and brother.

My hearty gratitude goes to my husband Raj for his patience and much needed moral support. His sense of humour has always helped me overcome difficult patches. I also feel a deep sense of gratitude towards his family.

I want to thank Mr. D.P.Sharma for meticulously typing the text and Mr. Narendra for preparing some of the drawings.

Sulekha Gupta

(SULEKHA GUPTA)

List of Tables

CHAPTER 1

INTRODUCTION

1.1   GENERAL

The unsaturated zone acts as a conduit for the passage of water from the ground to the water table. For a very long time it had been believed that this zone serves as a filter and the quality of water finally joining the water table is relatively good. After many instances of water pollution in drinking water sources, scientists began to realize the vital role played by the unsaturated zone in controlling the quality of groundwater. In the past few decades research workers have turned their attention towards the various processes taking place in this zone, a complete description of which involves many physical, chemical and biological processes. Thus, making it highly impossible for any single discipline to tackle the encountered problems.

Any material present on the ground, which can be dissolved and carried by water infiltrating into the ground is a potential threat to groundwater quality. In addition to natural waste, the rapid growth of industry has largely contributed to the numerous types of contaminants, rendering waste management an almost Herculean task. Disposal of domestic and industrial waste, directly on land or with the help of disposal systems, which may be improperly designed and poorly maintained, contributes significant amounts of leachate carried by the rainfall percolating through them, to the soil. This leachate in due

time travels through the unsaturated zone and joins the water table, affecting the water quality.

The second most critical role, in deterioration of water quality as well as soil conditions is played by agriculture, the main thrust of which has always been optimal crop production, disregarding all other adverse effects caused on a long term basis. Excess application of pesticides and fertilizers not required by the plants leads to their leaching below the root zone. They further travel through the unsaturated zone and gradually join the water table. These are mainly composed of complex organic chemicals and have adverse health effects, if present in toxic levels. Also long term use of saline irrigation water combined with poor management and adverse climatic conditions i.e., low rainfall and high evapotranspiration, leads to accumulation of salts in the root zone. This results in a loss of crop yield and deterioration of soil conditions.

In order to prevent or minimize such a water quality hazard, a thorough understanding of the flow process combined with the mechanism of solute transport in the unsaturated zone is essential. Solute transport in a porous medium involves transport by convection, mechanical dispersion and molecular diffusion. The source-sink term includes solid-solute interaction, various chemical reactions and decay phenomena.

1.2   PRESENT STUDY

In the present study an attempt has been made to develop a numerical model simulating one dimensional vertical two phase reactive solute transport through the unsaturated zone, extending from ground to

water table. The head form of Richards equation governing one dimensional vertical flow was solved (Mohan Rao, 1986) using a Crank - Nicolson finite difference scheme and Picard's iteration method.

To avoid problems of numerical dispersion and oscillations, encountered in solving convection dominated solute transport problems, the convective component was solved by the method of characteristics. The diffusive - dispersive component was subsequently solved by an implicit finite difference scheme. The model can also account for two phase flow (a feature of aggregated and unsatuarated flow conditions) comprising of mobile and immobile liquid zones, linear equilibrium adsorption and first order linear kinetic adsorption.

The model was validated using two analytical solutions. The analytical solution of van Genuchten and Alves', 1982 (Parker and van Genuchten, 1984), pertains to single phase reactive (linear equilibrium adsorption-desorption) solute transport under steady state flow conditions. Neglecting solute matrix interaction this solution was used to compare results of the model accounting for single phase non-reactive solute transport. Agreement between the results obtained by the two solutions was excellent.

The analytical solution of Parker and van Genuchten (1984) pertains to single phase and two phase solute transport under steady state flow conditions. For single phase solute transport the sorption sites present in the soil matrix are assumed to comprise of two fractions. Adsorption on one fraction ('type-1' sites) is assumed to be instantaneous i.e., equilibrium adsorption, while adsorption on the other fraction ('type-2' sites) is time dependent i.e., kinetic equilibrium

adsorption. For two phase solute transport the interaction between solute and soil matrix in both the phases is described by a linear equilibrium adsorption-desorption isotherm. Assigning appropriate values to the parameters, this solution was used to compare results with the model accounting for,

(i) single phase reactive (kinetic adsorption-desorption),

(ii) two phase non-reactive,

and (ii) two phase reactive (linear equilibrium adsortption - desorption) solute transport.

Again, an excellent agreement was observed for most of the simulations.

The proposed model was also used to simulate reported experimental data of two field experiments (Warrick et al., 1971; Böttcher and Strebel, 1989). Warrick et al. (1971) conducted a field experiment to study transport of calcium chloride through Panoche clay loam. The model accounting for single phase non-reactive solute transport was used to simulate concentration profiles under conditions indentical to that of the experiment. The simulated and measured concentration profiles compared reasonably well. However, a lag between the simulated and measured depth of the solute travel was observed. This indicates towards an increasd solute velocity, which may have been caused by the phenomenon of anion exclusion. Therefore the simulation was repeated considering the presence of an immobile phase and neglecting solute transfer into/out of the immobile phase (equivalent to a case of anion exclusion, assuming the effect of osmotic potential on the fluid flow to be negligible). For an immobile moisture content value of 0.06, the lag was almost eliminated.

A Bromide leaching experiment was conducted by Böttcher and Strebel, 1989 (unpublished data, details of experiment received by personal communication). Monitoring of solute transport at different locations showed a considerable variation in the time of arrival of solute at a specified depth, possibly caused by horizontal transport. The proposed model does not account for horizontal transport. Still, the simulated concentration distribution in space and time compared reasonably well with the measured mean distribution of concentration.

Application of the model to real life problems has been demonstrated by simulating two problems of solute transport through the unsaturated zone.

The model was used to estimate salt accumulation in the root zone for two crops (wheat and rice) assumed to grow over a period of one year. Concentration profiles (ground to water table) at differnt discrete times, covering the entire period were also simulated. The water used for irrigating the crops was assumed to be considerably saline (1.5 mmho/cm). Evapotranspiration by the crops was accounted for (Doorenbos et al., 1979). Salt accumulation in the root zone was also estimated using the salt storage equation (Van der Molen, 1973). A considerable deviation was observed between the salt accumulation as computed by the salt storage equation and by the model. This deviation was possibly caused by the assumptions on which the salt storage equation is based.

Water percolating through waste material present at the ground dissolves pollutants and carries them through the unsaturated zone. Non-conservative pollutants may get adsorbed or degraded, however

conservative pollutants will sooner or later join the water table. Again, the travel time of conservative pollutants to join the water table would be lesser compared to pollutants which react with the soil matrix and in the process get retarded. Thus, if the time of degeneration of a pollutant is less than the travel time of a conservative pollutant under identical conditions, its disposal on the ground could be assumed to be safe.

The model was used to simulate solute travel of a conservative pollutant (assumed to be abundantly available on the ground) in two types of soils (loam and clay) under conditions of heavy monsoon rainfall. At the end of the simulation period (140 days) the solute joining the water table in case of clay was negligible- caused only by dispersion. However, in case of loam, the convective front reached the water table in about 80 days time. Thus beyond 80 days, the solute joining the water table was appreciable.

CHAPTER 2

LITERATURE REVIEW

'Solute transport in a porous medium', has gained much attention during the past few decades. Considering its importance in different areas, like agriculture, waste management, water quality etc., research workers have made immense efforts towards understanding the complexities underlying this phenomenon. Following is a brief review of significant research studies carried out involving some of the various aspects of solute transport occuring in the unsaturated zone of the earth.

2.1   MISCIBLE DISPLACEMENT IN POROUS MEDIA

Slichter, 1905 (cited in Bear, 1979) was one of the first ones to observe that tracer movement in a porous medium doesn't follow piston flow, as would be the case if there was complete displacement and no mixing occured at the boundary of the tracer and tracer free water. He injected salt into an aquifer and observed that a general spreading took place from the point of injection. Scheideggar, 1954 (cited in Scheideggar, 1961) suggested the term dispersion for this spreading phenomenon, in order to distinguish it from the process of diffusion which is superficially similar. The dispersion process is a result of the complexities of the pore system, where as diffusion is caused by the intrinsic motion of molecules. Either of the two processes may dominate depending on the flow conditions in a system. Nielsen and Biggar (1961)

and Biggar and Nielsen (1963) conducted laboratory experiments for different types of soils and glass bead media, under saturated and unsaturated soil conditions at different average pore water velocities for chloride and tritium tracers. They obtained concentration break through curves which were skewed and sigmoid in nature as compared to a sharp concentration front, which would have resulted in case of piston flow. The deviation from flow appeared to increase as the average pore water velocity decreased.

The shape and time of arrival of the break through curve depends on different physical and chemical processes taking place between the solute and solid medium (Nielsen and Biggar, 1962). One of the important physical feature observed during these experiments was the magnitude of the volume of water not readily displaced at saturation, increased as desaturation of the soil took place. This indicated towards the presence of a region of water which was either stagnant or moved at a very low velocity compared to the average pore water velocity. This region of water termed as an immobile water zone, acts as a static sink and material can be transferred to and from it only by a process of lateral diffusion. Krupp and Elrick (1968) conducted a series of miscible displacement experiments in an unsaturated glass bead medium maintaining a constant average water content during each experiment. Decrease in water content again resulted in early breakthrough and tailing of the concentration curve, caused by slow transfer of concentration from immobile to mobile water. Gupta et al. (1973) measured concentration vs time data at selected points along a column for different solution contents and seepage velocities. At solution contents close to saturation the breakthrough curves were symmetrical

and regularly spaced. As the solution content decreased, the curves became asymmetrical with a pronounced tailing of concentration. They also attributed this phenomenon to the presence of an immobile water zone, which increased as the solution content in the column decreased. De Smedt and Wierenga (1984) have pointed out that some of the observed phenomena of early breakthrough and tailing could be explained on the basis of anion exclusion and adsorption. However, the case of a glass bead medium (experiments conducted by them also) eliminates the possibility of such an explanation. Henceforth, miscible displacement in the absence of an immobile liquid zone will be referred to as single phase solute transport and in the presence of an immobile liquid zone reference will be made to as two phase solute transport.

2.2 DEVELOPMENT OF DIFFUSION - DISPERSION MODELS

The oldest approach to dispersion problems is based on the analogy between a porous medium and bundles of capillaries. Taylor, (1953) (cited in Nielsen and Biggar, 1962) used solute flow in a single circular cylindrical capillary tube as a basis to macroscopic flow. He assumed that longitudinal molecular diffusion was negligibly small compared to radial diffusion. Again, radial diffusion counteracts velocity dispersion by trying to establish a uniform concentration distribution over a cross-section. Thus, for a symmetrical concentration profile about the axis of the capillary he gave the following equation,

$$\frac{\partial^2 c}{\partial r^2} + \frac{1}{r}\frac{\partial c}{\partial r} = \frac{1}{D}\frac{\partial c}{\partial t} + \frac{U_o}{D}(1-\frac{r^2}{a})\frac{\partial c}{\partial x}$$

Where, a is the radius of the capillary, c is the concentration, r is the distance along the capillary axis, U_o is the maximum velocity on the

axis of the cylinder (velocity distribution in a cross-section is parabolic), t is time and D is the molecular diffusion coefficient which is constant and independent of the concentration.

Aris, 1956 (cited in Fried and Combarnous, 1971) generalized Taylor's approch to irregularly shaped capillaries in which local velocity distributions may not be parabolic, and the molecular diffusion coefficient D varies with concentration. He inferred that the mean concentrtion distribution about a point moving at a mean flow velocity is dispersed according to a Gaussian distribution, and based on the variance of this distribution he gave the following relation for an effective diffusion coefficient,

$$K = D + \alpha^* [(a^2 U_m^2)/D]$$

Where, K is the effective diffusion coefficient, D is the molecular diffusion coefficient, a is a characteristic dimension of the cross section, U_m is the mean flow velocity and α^* is a dimensionless number depending upon the capillary cross section.

The theories of Taylor and Aris were not successful as flow in a porous medium is very different from the flow in a capillary. Most of the dispersion in a porous medium results from its complexity of structure, and is not caused by the existence of a velocity profile in each pore as in a tube. The models of Klinkenberg, 1957 (cited in Fried and Combarnous, 1971) which represent the porous medium as a bundle of straight non-connected capillaries and that of Marle and Defrenne, 1960 (cited in Fried and Combarnous, 1971), assuming regularly spaced connections between capillaries also failed as the complexity of a porous medium cannot be described by a fixed capillary pattern.

In an attempt to describe the porous medium more closely De Josselin de Jong (1958) and Saffman (1959), (1960) introduced random networks of capillaries. The model of De Josselin de Jong was very restrictive. He neglected molecular diffusion and assumed that the velocities in a capillary cross-section were constant. However, he was the first one to express the fact that transverse dispersion is smaller than longitudinal dispersion. The model of Saffman was more general and consisted of a network of randomly oriented and distributed pores connected to each other, in each of which the flow was uniform. The pore sizes were comparable to a real porous medium. The path followed by fluid particles in such a medium was regarded as a random walk in which the length, direction and duration of each time step were random variables. Saffman calculated the probability distribution function of the displacement of a particle after a given time and deduced values of dispersion. He considered cases where molecular diffusion was neglected and where both molecular diffusion and dispersion were important.

A further improvement in random capillary models was given by Bear and Bachmat, 1967 (cited in Fried and Combarnous, 1971), Bear et al., 1968 (cited in Fried and Combarnous, 1971) and Bachmat (1969). They represented porous medium as a continuum at the macroscopic scale by averaging microscopic quantities in a representative element of volume REV at a point. The REV was defined with respect to porosity. Their model yielded results closer than Saffman's model and was a step towards freeing models from a rigid geometrical frame.

Geometrical models were followed by a statistical approach which was general, as no assumptions on the geometrical structure of the

medium are required. The most important model was derived by Scheideggar (1963), who used a random walk process. He derived the equation for a homogeneous, isotropic medium and laminar flow conditions. Based on experimental studies he realized that the dispersion coefficient was not a scalar quantity and depended on the direction of the concentration gradient. He gave the following equation,

$$\frac{\partial c}{\partial t} + \bar{v} \cdot \text{grad } c = \text{div} \left(\bar{D} \cdot \text{grad } c \right)$$

Where, $\bar{v}$ is the mean velocity and $\bar{D}$ is the tensor of dispersion. Discrepencies were observed between experimental and theoretical results computed by the above equation. In order to account for these deviations Scheideggar introduced autocorrelation between subsequent time steps and ended up with a telegraph equation. However, he could not improve the match. An interesting improvement was made by Coats and Smith, 1964 (cited in Fried and Combarnous, 1971) who introduced the concept of dead end pores. Fluid in these pores was assumed to be static and subjected only to molecular diffusion. They gave the following macroscopic equation,

$$\frac{\partial c}{\partial t} + v \frac{\partial c}{\partial x} = D \frac{\partial^2 c}{\partial x^2} - (1-f) \frac{\partial c_1}{\partial t}$$

Where, f is the fraction of pore volume occupied by the moving fluid and c_1 is the concentration in the dead end pores. The equation describing diffusion into and out of the dead end pores was given by,

$$\gamma(c-c_1) = (1-f) \frac{\partial c_1}{\partial t}$$

where, γ is a transfer coefficient between dead end pores and

other pores.

The equation of Coats and Smith was a significant improvement, however they were not quite successful in explaining the observed discrepencies between experimental and theoretical results.

Whitaker (1967) and Fried, 1968 (cited in Fried and Combarnous, 1971) objected to the mode of derivation of the equation given by Scheideggar, and stated that it did not account for the fact that the quantities involved were not functions, but distributions in the sense of Schwartz. They proposed a method based on the theory of scale change and gave the following macroscopic equation,

$$\text{div } [D \times \text{grad } c] - \text{div } (cv) = \frac{\partial c}{\partial t}$$

The above equation is one of the most accurate representations of the classical convective dispersive equation (CDE). Source/sink terms and scale change effects have been included in various studies to represent problem specific phenomenon.

2.2.1   Parameters of Dispersion

The coefficient of molecular diffusion (D_p) and mechanical dispersion (D_h) have been subject to many theoretical and experimental investigations. They have been observed to depend on the flow pattern and some basic medium characteristics.

The effective molecular diffusion coefficient of ions in a soil medium is less than that in a free water system (D_0). Based on theoretical consiserations of a porous medium, Porter et al. (1960) gave

the following relationship between D_p and D_0,

$$D_p = D_o \alpha \gamma \, (L/L_e)^2 \theta$$

where, θ is the volumetric water content of the soil, and $(L/L_e)^2$, α and γ are factors accounting for reduction in ion velocity due to toruosity, reduced fluidity of the water and electrostatic interactions.

They also measured chloride diffusivities in medium and fine textured soils and observed a linear relationship between $(L/L_e)^2$ and θ i.e. $(L/L_e)^2 \alpha\gamma = a\theta + b$, where a and b are constants characterizing the given soil.

Kemper and Van Schaik (1966) studied rates of salt difusion in clay plugs and observed that the diffusion coefficients increased as an exponential function of the water content, but for practical purposes, were independent of the salt concentration. They gave the following relationship between D_p and D_o,

$$D_p = D_o a \, e^{b\theta}$$

Olsen and Kemper (1968) reported that data collected on soils fit the above equation reasonably well with b=10 and a ranging from 0.005 to 0.001, for sandy loam to clay soils.

The coefficient of mecahanical dispersion has been observed to depend on the average flow velocity and characteristics of the medium. One dimensional analysis show D_h to be proportional to, either the first (Bear and Todd, 1960 cited in Bear, 1972) or second (Taylor, 1953 cited in Bear, 1972) power of the average flow velocity(v), with a proportionality constant λ, being a characteristic length of the medium.

Thus,

$$D_h = \lambda \, |v|$$

or $\quad D_h = \lambda \, |v^2|$

2.3 SINGLE PHASE SOLUTE TRANSPORT

2.3.1 Analytical Solutions

A number of analytical solutions (exact and approximate) of the one-dimensional CDE have been given by several research workers.

Lapidus and Amundson (1952) were one of the first ones to present an analytical solution, which took into account longitudinal diffusion and/or dispersion. The solution was valid for a system having a constant average flow velocity and a constant diffusion coefficient. They also accounted for linear adsorption and first order kinetics.

The solution presented by Brenner (1962) is applicable to beds of finite length, initially containing a uniform distribution of solute. He has computed numerical values of the solution and presented them in a dimensionless form for, (i) the instantaneous concentration of solute leaving the bed, and (ii) the average solute concentration in the bed at any instant.

Lindstorm et al., 1967 (cited in Cleary and Adrian, 1973) considered a flux type upper boundary condition and a semi-infinite soil column. Gehrson and Nir (1969) studied the effect of initial and boundary conditions on the distribution of a tracer in space and time for various infinite, semi-infinite and finite soil systems. They also accounted for a linear equilibrium adsorption isotherm and a

radioactive tracer (considered stable in case of a long half life compared to the experiment duration). Analytical solutions exhibited that results of steady state experiments were influenced only upto 0.5% by changes in the boundary conditions. However unsteady state results were influenced upto 5% in the region $c/c_0 = 0.5$ (where, c is the solute concentration and c_0 is the concentration of the input tracer).

Warrick et al. (1971) gave an approximate analytical solution of the CDE in order to simulate data from a field experiment. They used a constant apparent diffusion coefficient and assumed that the time taken to attain steady state is much less compared to the total time of infiltration. On analyzing the results they found that dispersion caused by the average flow velocity was significant and that the apparent diffusion coefficient increased with time or distance of solute travel.

Solution for the case of a finite soil medium accounting for linear adsorption and a first type of boundary condition was reported by Cleary and Adrian (1973). Marino (1974) presented an analytical solution for a semi-infinite, homogeneous isotropic porous medium subject to source concentrations varying exponentially with time. He also accounted for decay of a radio-active contaminant and linear equilibrium adsorption.

The solution given by Selim and Mansell (1976) is applicable to a finite soil column, subject to the third type of boundary condition i.e., accounting for convection and dispersion across the surface. The solution incorporates reversible and irreversible linear adsorption in the form of a source/sink term which may be constant or concentration dependent. Neglecting the source/sink term, comparisons were made with

earlier analytical solutions of Lindstorm et al., 1967 (cited in Cleary and Adrian, 1973) and Cleary and Adrian (1973). The model of Cleary and Adrian provided higher concentration values throughout the soil column. However, the results matched well with the model of Lindstorm et al., 1967, except at the exit end of the soil column. This was understood to be caused by the semi-infinite boundary condition. Computed break through curves were found to lie between the previous two models. For higher peclet numbers the deviation between the three models decreased.

A combination of a linear freundlich isotherm and first order reversible kinetic adsorption was included in an analytical solution by Cameron and Klute (1977). Comparison with experimental data gave a good agreement. Parameters for adsorption-desorption were obtained by fitting the simulated results to experimental data. Individually neither of the two isotherms gave a good match with the experimental data.

Parlange and Starr (1978) presented a closed form approximate analytical solution for a finite soil column accounting for linear adsorption, first and zero order reactions. The solution is valid for peclet numbers greater than 4 for break through curves and concentration profiles within the soil columns. Earlier, solutions, which consider an infinite soil column and first type boundary condition although simpler are valid for peclet numbers greater than 16 for concentration profiles within the soil column.

De Smedt and Wierenga (1978a) presented an approximate analytical solution for solute movement in soils with an initial non-uniform water content distribution leached at a steady rate. Linear variation of dispersion coefficient with velocity was considered.

Computed results matched with a CSMP[*] simulation model (van Genuchten and Wierenga, 1974) and were also in agreement with results obtained by an exact analytical solution (Lindstorm, et al., 1967 cited in Cleary and Adrian, 1973) for a case of uniform water content distribution. They concluded that the approximate analytical solution could be applied to field problems with variational flow velocity, water content and dispersion coefficient. In case of breakthrough curves, no significant effect was observed by variation in flow velocity and dispersion coefficient, implying that the use of average values was good enough.

Another approximate solution by the same authors (1978b) describes solute movement in soils during infiltration and redistribution. The solution requires solute penetration depths. For the case of infiltration (under ponded conditions) this was obtained by dividing the cumulative infiltration depths by the moisture content value at field capacity . Hydrodynamic dispersion was varied linearly with pore water velocity. Concentration profiles were simulated neglecting molecular diffusion and accounting for both molecular diffusion and mechanical dispersion. Results were compared with a CSMP simulation model (IBM, 1972 cited in De Smedt and Wierenga, 1978b)). A good agreement was not obtained in case of redistribution, unless molecular diffusion was accounted for.

---

[*] CSMP : Continuous System Modelling Program, IBM, 1967 (cited in Bolt, 1982). In the CSMP approach the spatial derivatives are approximated with suitable finite differences, while the integration in time is performed using a predictor-corrector Runge-Kutta type algorithm.

Gupta and Singh (1980) developed an analytical solution for a semi-infinite soil medium in order to leach existing saline soils. The initial salt concentration profile was approximated by an exponentially decreasing concentration profile, uniform average salt concentration or by fitting straight line segments to it. Reasonable accuracy in predicting salt concentration profiles was obtained in case of closely fitting straight line segments to the initial profile. A zero surface boundary condition i.e. concentration at the ground surface instantaneously becomes zero, when ponding of solute free water occurs, was compared to a time varying (concentration decreases exponentially with time) boundary condition at the ground surface. The difference between the two was not significant. Thus a zero surface boundary condition is a good enough approximation in case of ponding of solute free water. They also observed that the time taken for leaching decreased in case of high average pore water velocity leading to higher dispersion values and flatter concentration profiles.

The analytical solution given by van Genuchten (1981) for a semi-infinite soil profile under various boundary conditions, accounts for linear equilibrium adsorption, zero order production and first order decay. The solution holds good for the limiting case of neglecting zero order production. However, in order to neglect first order decay the solution had to be modified. The modified solution has also been presented.

Approximating the initial salt concentration profile with an exponentially varying concentration profile for leaching saline soils has also been done by Misra and Mahapatra (1989). In their solution the

slopes of the initial concentration profiles are varied with the help of a parameter. The solution of Gupta and Singh (1980) is a limiting case of their solution, when the concentration at the lower boundary becomes zero. Linear variation of the hydrodynamic dispersion coefficient has also been taken care of.

2.3.2   Numerical Solutions

Till date many numerical techniques have been applied for solving the solute transport equation. The literature reviewed here pertains only to the numerical methods of finite differences, finite elements and Method of Characteristics.

2.3.2.1   Finite Difference Methods

Bresler and Hanks (1969) solved the solute transport equation using an explicit finite difference technique in order to simulate salt movement in unsaturated soils. They only considered convective transport and neglected any effects on salt distribution, caused by the diffusion process. Solutions were obtained for infiltration, redistribution and evaporation for flooded and rainfall conditions. The results were reasonable and an improvement between measured and computed salt concentration profiles was observed on adding a source term to the computations.

Lai and Jurinak (1971) gave an explicit solution involving cation exchange in soil columns. They used three different soils and found that the cation exchange isotherms were non-linear, by plotting the normalized concentration in solution and in the adsorbed phase. The developed numerical method was capable of solving the equation for both

linear and non-linear cation exchange isotherms. Agreement between numerical solution and experimental values was fairly good. They further (Lai and Jurinak, 1972) applied the method to predict cation adsorption in systems involving five different types of exchange isotherms. For convex isotherms they found that the concentration profiles were sharp and the adsorbed phase advanced ahead of the solution phase. For concave isotherms the concentration profiles were diffused and the adsorbed phase lagged behind the solution phase. For the case of a linear exchange isotherm, the numerical solution was compared with the analytical solution of Lindstrom et al.,1967 (cited in Cleary and Adrian, 1973). A small deviation was observed between the two, which was attributed to numerical dispersion.

Kirda et al. (1973) also presented an explicit finite difference solution of the CDE for a non-reactive solute. Assuming the apparent diffusion coefficient to be a constant, they studied displacement of Chloride during infiltration using soil columns. A deeper and more complete displacement of Chloride was observed in case of maintaining a constant moisture content having a value below saturation at the ground surface. For flow velocities below 0.1 cm/min the apparent diffusion coefficient depended mainly on molecular diffusion.

The finite difference solution for a non-interacting solute given by Bresler (1973a) is one of the most significant solutions given so far and has been used and modified by many subsequent research workers. He has used an implicit scheme of solution and accounted for numerical dispersion following Chaudhary, 1971 (cited in Bresler, 1973a)

by considering the second derivatives in Taylor's series. A variable diffusion-dispersion coefficient was introduced by combining the relations given by Kemper and Van Schaik (1966), for molecular diffusion and by Ogata, 1970 (cited in Bresler, 1973a) for mechanical dispersion. Results obtained for a steady state case were compared with the analytical solution of Brenner (1962). An exact match was achieved only after accounting for numerical dispersion. For transient infiltration the results were compared with field data reported by Warrick et al. (1971). Cases of redistribution and evaporation were also studied and they found that mechanical dispersion dominated during infiltration as compared to molecular diffusion, which was more important during the process of redistribution and evaporation.

Bresler (1973b) extended his model to account for the phenomenon of anion exclusion . He again simulated the data of Warrick et al. and observed an improvment of fit between the observed and theoretical results. However, contribution of osmotically induced flow to total flow was negligibly small in most parts of the system.

Wood and Davidson (1975) presented an implicit-explicit finite difference solution, accounting for non-linear equilibrium adsorption-desorption. Numerical dispersion in the solution was accounted for following Chaudhari, 1971 (cited in Bresler, 1973a). Comparison with experimental data gave a good agreement barring a slight lag between the two.

An implict finite difference solution using a second order accurate difference form as suggested by Chaudhari, 1971 (cited in Bresler, 1973a) was also given by Gureghian et al. (1979). They

accounted for soil layering and included a sequential chemical reaction of ammonium getting converted to Nitrite and then Nitrate.

The model of Bresler (1973a) was modified by Russo (1988a) to account for physical and chemical reactions between soil solution and soil matrix in terms of hydraulic conducivity and retentivity functions, anion exclusion and cation exchange. Solute transport was studied for three different homogeneous soils under different sets of initial and boundary conditions. Comparisons were made with results obtained for transport of an inert solute under the same set of conditions. To account for inhomogeneity of the soil profile the model was further modified (Russo, 1988b) and solute transport through layered sequences of soil were studied.

Russo et al. (1989a) has again used the solution of Bresler (1973a) for non-reactive solute transport. Assuming scale heterogeneity of the medium in a vertical direction he accounted for hysteresis in the soil hydraulic properties and studied their effect on field scale transport.

2.3.2.2   Finite Element Methods

Cavalieri and Russo Spena (1984) solved the solution transport equation including an irreversible adsorption isotherm with the help of galerkin finite element method. First order approximations were used and convergence of the numerical scheme may or may not be guaranteed depending on the particular choice of the space and time step. Infiltration of solute into a loam soil profile was studied, neglecting and accounting for adsorption. Incorporation of the irreversible

adsorption isotherm resulted in a retardation of the solute movement and decrease of solute concentration.

2.3.2.3 Method of Characteristics (MOC)

This numerical technique was introduced by Garder et al., 1964 (cited in Smajstrla et al., 1975) to overcome problems encountered in solving convection-dominated solute transport. He used it to solve a miscible displacement problem for unsteady unsaturated solute infiltration into a homogeneous, isotropic porous medium. The method has subsequently been used for solving solute transport problems in porous media.

Smajstrla et al. (1975) solved the CDE for transient unsaturated flow conditions. They used MOC to solve for convective transport and subsequently solved for dispersive transport using an explicit finite difference scheme. A set of moving points was distributed throughout the entire grid system (1 point per grid) at the beginning of simulation and each moving point was assigned an initial depth and solute concentration. During subsequent time steps new moving points were generated at the top and existing ones were moved using linearly interpolated values of pore water velocity at the grid boundaries. To avoid overcrowding of moving points at the front, moving points were removed when they became closer than 0.2 times of the grid thickness. Results were compared with earlier reported experimental results and analytical solutions under steady state saturated flow conditions. A close agreement was obtained between the various results. During steady state flow a weighted averaging scheme was used to obtain grid concentrations. However, it was not feasible to use this scheme for

unsteady state flow. For unsteady unsaturated flow conditions field experimental data of Warrick et al. (1971) was used. Employing a constant dispersion coefficient given by Warrick et al. or the dispersion coefficient relation proposed by Bresler (1973a). The simulated results agreed reasonably well with the numerically simulated results of Bresler and those obtained by Warrick et al. using an approximate analytical solution. However, a lag between the experimental and simulated data was observed.

Charbeneau (1981) solved the transport equation accounting for adsorption and cation exchange. He assumed dispersion to be negligibly small and solved only for the convective component using MOC. Both adsorption and ion-exchange served to retard the contaminant movement. In case of ion-exchange the ion preferred on the exchange site was retarded to the greatest extent.

Khaleel et al. (1985) again used MOC to solve for the convective component of the solute transport equation. The dispersive component was subsequently solved using an explicit centered in space finite difference approximation. They also simulated the field data of Warrick et al. (1971) for unsaturated transient conditions and found a lag between the observed and simulated concentration profiles.

2.3.3 Numerical Dispersion and Oscillations

It is well known, that while solving the CDE numerically if the term proportional to the second order is neglected in approximating the first order derivative, it results in a numerical dispersion i.e., smearing of the concentration front. Also in case of steep concentration

fronts oscillations of the solution are observed at the upstream side i.e., overshoot and downstream side i.e., undershoot of the concentration front. Oscillations manifest themselves as concentration values higher than the maximum value and negative concentration values. These two errors are interrelated and numerical schemes selected to reduce the magnitude of one problem generally increases the other. Several numerical schemes have been introduced and modified since these problems were detected in numerical solutions of convection dominated solute transport. Following is a brief review of some of these schemes including comparisons amongst different numerical techniques (again restricted to finite differrences, finite elements and MOC). In all of these techniques the one-dimensional CDE under steady state flow and constant moisture conditions has been solved and compared with exact analytical solutions, although most of them are valid under transient unsaturated flow conditions.

For very small values of D, solution of the CDE equation develops discontinuities in the dependent variable referred to as shock waves or shock fronts. Von Neuman and Richtermeyer, 1950 (cited in Stone and Brian, 1963) proposed the use of large dispersion coefficients, the effect of which was to smear out these discontinuities, by replacing them with thin layers, in which the dependent variable varied rapidly and continuously.

Stone and Brian (1963) were one of the first ones to suggest the use of a weighted finite difference scheme to overcome this problem. They were able to almost get rid of the oscillations. Comparison with an analytical solution was not very good. However, there was a considerable

improvement over earlier solutions.

The finite difference method adopted by Bresler (1973a) to eliminate numerical dispersion has already been mentioned (refer section 2.3.2.1). A considerably good match was obtained on comparison with Brenner's (1962) analytical solution for high Brenner numbers (low dispersion coefficients).

Gray and Pinder (1976) have used the Fourier series analysis to demonstrate the accuracy of finite difference and finite element (Galerkin's approach using different types of basis functions) schemes. They found that the solution obtained by finite differences was consistently inferior to the ones obtained using finite element schemes for a given number of degrees of freedom. In case of the different finite element schemes, hermite polynomials exhibited decreased amounts of oscillation and numerical smearing as compared to quadratic elements. On including a correction factor to account for numerical dispersion in the solution, the finite difference scheme remained relatively unaffected. However a substantial improvement in the finite element method was observed. Again, upstream weighting of the convective term generated unacceptable solutions as selection of an appropriate weighting factor to minimize overshoot resulted in increased smearing of the front.

van Genuchten (1976) has also compared solutions obtained by finite difference and finite element methods and reported conclusions similar to Gray and Pinder. He also stated that first and second order continuous hermitian polynomial solutions, exhibit lesser numerical dispersion and oscillations compared to the various zero order

continuous elements. Quadratic and cubic elements fare better than linear elements and depending upon the time step size, quadratic elements may be preferred to cubic elements. The relative indifference of the finite difference scheme to a correction factor for numerical dispersion has also been shown.

Varoglu and Finn (1978) presented a finite element method (based on Galerkin's approach) incorporating the method of characteristics (FEMIC) to take care of convection dominated solute transport. This was achieved by using spatial and temporal elements and incorporating the method of characteristics by orienting the sides of the elements joining the nodes at subsequent time levels, in a particular direction. For very low values of dispersion the method yields results which are very close to the exact solution. For the case of pure convection, the method predicts the exact solution.

van Genuchten and Gray (1978) presented high order accurate finite difference and finite element schemes to solve the CDE. The various schemes were made high order accurate in time through the introduction of appropriate dispersion corrections in the numerical formulations. The most accurate finite difference and finite element schemes were obtained when fourth order space-time corrections were applied to each of the two schemes, in which case the two methods became identical. The quadratic finite element schemes which provided the best results were based on third and fourth order correct difference equations in time. Superior results were obtained with the dispersion corrected Hermitian schemes.

Neuman (1981) solved the convective component by MOC on a fixed grid in space. Dispersion was handled by finite element on a separate grid which may or may not coincide with the former at selected points in space and time. Information from one grid to another was projected by local interpolation. Results were free from oscillations, but numerical dispersion existed. However, it could be brought under control by reducing the spatial increment of the convective grid or by increasing the time step. Best results were obtained for courant numbers exceeding one.

van Genuchten (1982) compared several numerical schemes for solving the CDE under transient flow conditions. For steep moisture/concentration fronts he concluded that finite difference and mass lumped linear finite element schemes generated the most stable solutions while the hermitian finite element scheme gave a better spatial location of the front. However, some oscillations developed near the toe of the front. Temporal approximation was done using a Crank - Nicolson scheme with correction applied to the dispersion coefficient.

Neuman and Sorek (1982) compared three different Eularian -Lagrangian schemes for solving the one-dimensional CDE. The first two methods decouple the CDE into convection and dispersion problems. The problem of convection was solved by the method of reverse streaklines (developed by the authors in question) and continuous particle tracking (based on the MOC presented by Garder et al., 1964), while the dispersion problem was subsequently handled by implict finite elements on a fixed grid using linear and quadratic basis functions. A comparison with analytical solutions exhibited that the first two methods worked

well for convection dominated problems but irregularities appeared in certain dispersion dominated problems. The third method sufferred from numerical dispersion and overshoot in case of convection dominated problems, but works well when dispersion is dominant.

Khaleel et al. (1986) solved the one dimensional CDE under steady state uniform flow conditions using MOC to solve for the convective component. An explicit centred in space finite difference scheme was used to solve for the dispersive component. Comparison with an analytical solution using a small dispersion coefficient is quite good. However no comparison with purely convective solute flow or very small dispersion coefficients was shown. Documented list of the fortran program has also been presented.

2.4 TWO PHASE SOLUTE TRANSPORT

Deans, 1963 (cited in van Genuchten and Wierenga, 1976) modified the CDE to include transfer by diffusion from mobile to immobile water. However, he neglected the effect of longitudinal dispersion. Similar concepts were proposed by Gottschlich (1963) and Skopp and Warrick (1974). Coats and Smith, 1964 (cited in van Genuchten and Wierenga, 1976) modified the model of Deans and accounted for longitudinal dispersion. Subsequent authors adopted the model of Coats and Smith.

2.4.1 Analytical Solution

The solution of van Genuchten and Wierenga (1976) includes a linear equilibrium adsorption-desorption isotherm, for a semi-infinite soil column and a pulse input of solute. The model is capable of

simulating concentration profiles in both the mobile and immobile liquid regions. They computed effluent concentration curves to study the effect of various parameters on the solution. The model was further used by them (cited in van Genuchten and Wierenga, 1977) to simulate tritium effluent concentration curves, which were compared with the observed concentration distribution. Necessary parameters were computed by curve fitting of simulated and experimental data. They gave the following conclusions.

(i) The amount of immobile water generally decreases with increasing flow velocity.

(ii) The coefficient of mass transfer increases with decreasing flow velocity, which may be a consequence of an increased amount of immobile water and hence an increase in the diffusion path length.

(iii) A decrease in the size of aggregates decreases the amount of dead water in the column.

(iv) A reduction in bulk density appeared to increase the amount of immobile water.

(v) The dispersion coefficient appeared to some what increase with an increasing aggregate size and decreasing bulk density.

van Genuchten et al. (1977) again made comparisons between observed 2,4,5-T herbicide effluent concentration curves for 30 cm long unsaturated soil column and simulated concentration curves using the previous solution. Theoretical curves were also calculated using a CSMP model (van Genuchten and Wierenga, 1974 cited in van Genuchten et al., 1977), accounting for non-linear hysteretic adsorption-desorption. The simulated curves gave a reasonably good description of the observed data. They also stated that in case of two phase solute transport the

effect of hysteresis did not appear to be very significant as compared to single phase solute transport.

De Smedt and Wierenga (1979a) presented an analytical solution valid for both a finite and semi-infinite soil column and concentration or flux type boundary condition leached at constant rate. They conducted column experiments under saturated and unsaturated soil conditions. On comparing simulated and observed data they found that a good match could not be obtained for unsaturated soils, unless the presence of an immobile liquid phase was accounted for.

Analytical solutions for a flux type and concentration type upper boundary condition for finite and semi-infinite soil columns were again given by De Smedt and Wierenga (1979b). They compared observed and simulated effluent concentration curves and concluded that effluent concentration curves for finite soil columns leached at a steady rate of infiltration may be computed with a relatively simple solution, derived for semi-infinite soil columns and a concentration type upper boundary condition, provided the peclet number is greater than 9. Also concentration distribution inside the column could be computed if the peclet number is greater than 40.

In a subsequent study De Smedt and Wierenga (1984) conducted column experiments using a porous medium consisting of glass beads so as to eliminate the ambiguity of asymmetric concentration curves being caused by anion exclusion or adsorption, in case of unsaturated flow. They conducted a wide range of experiments, both for saturated and unsaturated flow conditions at different steady flux rates and initial uniform water contents. Theoretical curves were computed for the one

phase and two phase CDE and compared with observed experimental curves. For unsaturated displacement experiments they found that a reasonable match using the one phase CDE, could only be obtained in case of using very large dispersion coefficients (almost 20 times greater than those used for saturated conditions). However, a good match was obtained between the two, if the two phase CDE solution was considered. Also the dispersion coefficient was comparable with saturated conditions. For very long soil columns, symmetric concentration curves were obtained, but again they could not be reproduced by the one phase CDE solution, unless a large dispersion coefficient was used. Other conclusions regarding the fraction mobile water (ratio of mobile to total water content) and value of mass transfer coefficient were similar to those reported earlier.

2.4.2 Numerical Solutions

2.4.2.1 Finite Difference Methods

Gaudet et al. (1977) gave an explicit finite difference solution of the two phase solute transport equation. They conducted experiments at different steady flux rates and initial water content values. Curve fitting techniques were used to determine the parameter values. A sensitivity analysis indicated that the fraction mobile water was the most sensitive parameter and primarily affected the time of appearance of the solute. A good match between the calculated and experimental data was observed for all the different experiments.

Russo et al. (1989b) modified the solution of Bresler (1973a) to include the presence of an immobile water zone. They simulated

concentration profiles for irrigation, redistribution and evaporation, using different values of the mass transfer coefficient and compared them with concentration curves simulated using the one phase CDE. In the two region case, the concentration profiles were characterized by higher dispersion and low concentration peaks compared to the single region case. The effect of the rate of mass transfer was manifested as low concentration peaks, and significant tailing in case of low values of the mass transfer coefficient. As the rate of transfer increased, the difference in concentration of the two regions decreased and eventually led to a new equilibrium. For the limiting case, where its value tends to infinity, concentration in the two regions became equal and the solution reduced to that of the one phase CDE.

2.5 Field Tracer Experiments

Solute transport under field conditions was studied by several research workers, as experiments conducted under laboratory conditions are far from representing complexities encountered in the field.

Miller et al. (1965) conducted a field experiment to study chloride (applied in the form of KCl) displacement through Panoche clay loam. They found that more efficient leaching of the soil profile was achieved in case of intermittent ponding as compared to continuous ponding i.e., application of a certain amount of water by intermittent ponding provided a lower average concentration distribution. However, the time taken by intermittent ponding was much higher than continuous ponding to achieve the same distribution. They gave two main conclusions, (i) the amount of chloride displaced from a depth was not uniquely related to the volume of displacing water and (ii) the chloride

concentration attained at any depth could be either less than or greater than the concentration above or below that depth.

A field experiment was conducted by Biggar and Nielsen (1976). They leached solute pulses of chloride and nitrate in twenty plots over an area of 150 ha. Steady state conditions were established, before applying the solute pulses. They observed extremes in solute leaching at equal or different depths within relatively small areas, exhibiting the significance of spatial variability in field soils even at small distances.

Similar conclusions were drawn by Van de Pol (1977), who studied solute (labelled with chloride and tritium) and water movement under steady state flow conditions in a field soil, consisting of a 70 cm clay layer over medium sand.

Butters et al. (1989) conducted a two year field study of mobile solute transport over an area of 0.64 ha to a depth of 25 cm. Prior to tracer application the field was leached to free it from residual salts and achieve a uniform water content profile to a depth in excess of 3 m. A pulse of NaBr (aq) was applied and subsequently leached downward, monitored by vacuum solution samplers replicated at different depths. Although mass recovery was nearly 100% at all depths, the coefficient of variation of mass recovery between samplers at a given depth was nearly 50%. Lateral variations in vertical solute velocities at shallow depths was considerable, causing rapid solute breakthrough at some sites, in contrast to late arrival at the others. The average pore water velocity at shallow depths was found to be greater than the average solute velocity. This difference decreased with depth and was

attributed to the transient irrigation regime near the surface.

Van Ommen et al. (1989a) applied a small pulse of KBr to a strip of land (260m x 12m). The landuse pattern was grass and corn and both the areas were treated separately. Concentration profiles were measured in depth at different times and locations. Large local variations were observed at seemingly homogeneous and small areas. A mean concentration profile was compared with CDE predicted results and a reasonably good match was observed upto a depth of 70 cm. Parameter estimation for the model was done by curve fitting. Effluent concentrations were measured in drains and simulated solute travel depths were underestimated, unless the soil profile was divided into two layers. The first layer consisted of the top 25 cms characterized by a low average velocity while the solute travelled at higher velocities in the second layer. They attributed the accelerated breakthrough curves to the phenomenon of preferential flow. An iodide tracer experiment was carried out at the same site to examine preferential flow paths (Van Ommen et al., 1989b). The solute front shape was more irregular in case of the grassland compared to the corn field. However, moisture content profiles exhibited no significant difference within and outside a preferred flow zone. Solute penetration depths were underestimated using the parameters estimated for the bromide tracer experiment (Van Ommen et al., 1989a) assuming a homogeneous soil profile. On the other hand they were over estimated using the parameters estimated assuming a two layered soil profile. A good agreement was observed only in case of obtaining parameters by fitting the model results to the iodide tracer experiment. The accelerated breakthrough curve that was observed during the bromide experiment could not be reproduced. The authors deduced that

the antecedent moisture content and rainfall intensity may have an important effect on the formation of preferred flow zones.

2.6   UNSATURATED FLOW

To solve the equation governing solute transport in an unsaturated porous medium, it is necessary to obtain a solution of the eqution governing unsaturated flow. Again, the work done in this direction is immense. A brief review of the reported work is as follows.

Green and Ampt, 1911 (cited in Childs, 1967 and Philip, 1969) were among the first ones to propose a model for water movement in soils. They assumed that for surface flooding the advancing moisture profile exhibited a sharp front, above which the soil was saturated and below which it remained at the initial moisture content value. They expressed the rate of infiltration in terms of depth penetration and a uniform conductivity. As time increases the rate of infiltration approaches a constant value.

Richards, 1931 (cited in Swarzentruber, 1969) extended Darcy's law for saturated flow to unsaturated flow and combining it with the continuity equation gave the partial differential equation governing flow through unsaturated soils.

Klute (1952) also derived the equation for flow of water for unsaturated porous materials by combining the continuity equation with Darcy's law. Neglecting the effect of gravity he solved the moisture flow equation numerically for semi-infinite horizontal systems and applied it to several examples.

Philip, 1957a (cited in Philip, 1969) gave a quasi-analytical solution of the moisture flow equation for absorption (horizontal flow) and infiltration (vertical flow) into an effectively semi-infinite homogeneous soil. It was assumed that the soil had a constant initial moisture content and was submerged under a thin layer of water which instantaneously increases the wetness at the surface to near saturation and remains constant thereafter. For infiltration his solution is in the form of a power series, which reduces to the first term of the series in case of absorption. The coefficients of the power series are expressed in the form of ordinary integro-differential equations including the diffusivity and conductivity functions and are solved using appropriate finite differences and forward integration.

The series solution however fails for large values of time exhibited by the infiltration rate, which after reaching a minimum starts increasing. Restating the infiltration equation as diffusion equations in terms of moisture gradient, flux and flux gradient, philip (1957b) has established certain theorems about the moisture profile. With the help of these theorems he has solved the moisture flow equation under conditions stated above (Philip, 1957a), for large times (approaching infinity). It is shown that the moisture profile approaches a constant shape and travels down the column at a constant velocity, confirming to theory.

Youngs (1957) solved the moisture flow equation for, (i) vertical infiltration into an initially dry semi-infinite column of porous material, with the surface moisture content maintained at saturation, and (ii) vertical infiltration at a constant rate into a

column draining to the water table, numerically using integration and finite differences. Comparison between theoretical and experimental moisture profiles exhibited good agreement.

Philip (1958) extended his series solution to account for ponded water at the ground surface by defining a depth at which the hydrostatic pressure becomes zero. Solutions are presented for one dimensional absorption and infiltration. Theoretical profiles indicate an increased rate of infiltration by increasing the depth of ponding at small times.

Hanks and Bowers (1962) gave an implicit finite difference solution of the head form of Richards equation for vertical infiltration into layered soils. The hydraulic conductivity was computed using an average moisture diffusivity, while specific moisture capacities were computed from a table of θ vs h. To evaluate the numerical model, results for a case of horizontal infiltration into a homogeneous soil at uniform initial soil moisture content were compared with those obtained by the methods of Scott et al., 1962 (cited in Hanks and Bowers, 1962) and Philip, 1955 (cited in Hanks and Bowers, 1962). In both the cases the agreement was considerably good. Vertical infiltration into a layered soil indicated that infiltration is governed by the least permeable layer, once the wetting front reaches that layer.

Rubin and Steinhardt (1963) solved the moisture form of Richards equation for a nonponding infiltration condition using an implicit finite difference scheme. The equation was linearized employing linear extrapolation. They numerically simulated moisture profiles in depth for constant rainfall intensities (R) and confirmed the following

analytical considerations.

(i) If the rainfall intensity $R \leq K(\theta_{sat})$ (i.e. capillary conductivity at saturation), infiltration will continue indefinitely without giving rise to ponding. However, if $R > K(\theta_{sat})$, ponding will occur after infiltration is allowed to proceed for a finite time.

(ii) During rain infiltration the soil moisture contents at finite depths proceed to increase, till a definite limit defined by the relation $R = K(\theta_L)$ is reached.

The numerical solution only holds good as long as $R \leq K(\theta_{sat})$.

Experiments of infiltration into soils using constant rainfall intensities were conducted by Rubin et al. (1964). They simulated moisture profiles with the help of the earlier developed numerical model (Rubin and Steinhardt, 1963) using the average moisture content of the transmission zone to compute capillary conductivity values. Comparison with experimental results exhibited a good agreement for low rainfall intensities but a departure was observed as the intensity increased.

Remson and Drake (1965) solved the moisture flow equation using an explicit finite difference scheme and applied it to the following cases,

(i) Moisture content specified at the top and bottom of the soil.

(ii) Zero moisture flux across the soil surface.

Staple (1966) solved the moisture flow equation using an explicit finite difference scheme to simulate infiltration and redistribution. For redistribution in the upper part of the soil profile he accounted for hysteresis, both in the capillary pressure and capillary conductivities by interpolating the appropriate scanning

curve. However, it was assumed that after partial drying of the soil, wetting did not take place. Neglecting hysteresis only in the hydraulic conductivity gave results closer to the ones obtained by accounting for hysteresis, as compared to the results obtained by neglecting hysteresis entirely.

Rubin (1967) solved the moisture flow equation using an implicit finite difference scheme and accounted for hysteresis in the retention curve during redistribution. He used empirical equations, based on experimental data for the wetting, drying and scanning curves. He assumed that during the process if significant drying was exhibited by a soil element, then wetting of it does not take place. For a case of redistribution he observed that hysteresis retarded the process of drainage as compared to using only wetting or drying curves for simulation. The method is also applicable to cases, where evaporation and redistribution take place simultneously.

The numerical method developed by Hanks and Bowers (1962) to solve the head form of Richards equation was modified by Hanks et al. (1969). They incorporated a code to account for hysteresis in the capillary pressure and moisture content relation. They conducted experiments for infiltration followed by redistribution, followed by evaporation. Comparison of the depth of wetting front and average moisture content with numerically simulated results, exhibited a good agreement. However, the measured cumulative infiltration and evaporation values were higher than the computed values.

Bresler et al. (1969) conducted column experiments to study the effect of hysteresis on infiltration, redistribution and evaporation

for three different wetting rates. An earlier developed numerical simulator (Hanks et al, 1969) was also used to simulate moisture profiles in depth and time. Based on experimental and numerical results they stated.

(i) During infiltration no drying occurred and constant moisture content values were approached in the transmission zone depending on the wetting rate.

(ii) During redistribution the h vs θ relation followed separate drying scanning curves. As observed earlier (Rubin, 1967 ; Hanks et al, 1969) the hysteresis effect tends to keep the water content higher and zone of wetting shallower. This effect increased with an increase in the wetting rate.

(iii) Due to the high water contents and a shallow wetting zone, evaporation subsequent to redistribution was higher as compared to the case where hysteresis was neglected. Thus, evaporation was directly related to the wetting rate. The same observation held good when the redistribution stage was also accompanied by evaporation.

The head form of Richards equation was solved using a Crank-Nicolson finite difference scheme and Jacobi Iteration method, by Giesel et al. (1973). Hysteresis in the h vs θ relation was accounted for. They simulated results in accordance with the experiments conducted by Vachaud and Thony (1971) for the following two cases.

(i) Constant head infiltration followed by redistribution with no evaporation.

(ii) Constant flux infiltration followed by redistribution, accompained by evaporation.

A good agreement between the simulated and experimental results was observed.

Bruch and Zyvoloski (1974) presented a finite element solution of the moisture flow equation using a Galerkin approach. Finite elements in space and time and linear shape functions were used for two different element configurations; triangles and rectangles. A quadratic form was used for the diffusion co-efficients and capillary conductivities based on curve-fitting of experimental data of these funtions. Results were compared with the finite difference solution of Remson et al. (1965) and series solution of Nielsen et al., 1961 (cited in Swartendruber, 1969). A good agreement between the different results was observed.

Dane and Mathis (1981) solved the head form of Richards equation using an implicit finite difference scheme. Boundary conditions were experessed so that they could easily be changed from pressure head to flux boundary. The method allows for variable space and time steps as smaller time and space steps are required in regions where changes in the pressure head gradients are large. The time step was changed on the basis of mass balance. In the space direction a fixed number of grid points were used, which were continuously redistributed to give the best possible piecewise interpolation of the pressure head at the end of the time step. For required values of pressure head and flux at grid points not present at the previous time level, linear interpolation was carried out. Earlier reported experimental data was simulated using the numerical model and a good agreement was observed.

Parlange et al (1982) added a new parameter to the two parameter Green and Ampt equation. Addition of this parameter resulted

in a more accurate description of infiltration. Also it is not very sensitive to soil structure.

Mohan Rao, 1986 solved the head form of Richards equation using a Crank-Nicolson finite difference scheme and Picard's iteration method. His model can account for a time variant water table as a lower boundary condition. The upper boundary condition (Neuman or Dirichlet) is automatically identified and assigned, Evapotranspiration has been computed. A good agreement was observed between simulated and experimental data.

2.6.1   Soil Characteristics

Along with the solution of Richards equation research workers realized the necessity of a K vs θ (or h) and h vs θ relation, which could be used for different soils in absence of elaborate experimental data. Following is a brief description of some of the research studies carried out in this direction.

Childs and Collis George, 1950 (cited in Bear, 1979) gave a relationship for capillary conductivity relating it to the soil moisture content and the specific surface area of the soil phase.

Irmay, 1954 (cited in Bear, 1979) derived a relationship assuming that the resistance to flow offered by the solid matrix is proportional to the solid liquid interfacial area. For a cubic arrangement of spheres he gave the following relation.

$$K = K_o \left[\frac{S - S_r}{1 - S_r} \right]^3$$

where, K is capillary conductivity at saturation S, K_o is saturated hydraulic conductivity and S_r is the residual saturation.

Corey, 1957 (cited in Brooks and Corey, 1964) called the quantity $(S-S_r)/(1-S_r)$, as effective porosity S_e and found that for a large number of soils, relative permeability K_r (= K/K_o) is equal to the fourth power of S_e.

Brooks and Corey (1964) gave a relation between S_e and capillary pressure and defined a characteristic constant of the medium known as bubbling pressure, below which the soil is more or less saturated. They further gave relations of K_r in terms of capillary pressure.

Another empirical equation to compute capillary conductivity from the moisture content value using the satu-rated moisture content and capillary conductivity, has been presented by Campbell (1974). His equation is based on the approach of Childs, 1969 (cited in Campbell, 1974), and requires an empirical equation between capillary pressure and moisture retention.

Mualem (1976) presented a simple analytic model based on the approach of Burdine, 1953 (cited in Brooks and Corey, 1964). The expression is in an integral form related to moisture content, capillary pressure and saturated capillary conductivity.

van Genuchten (1980) derived a closed form analytic expression for predicting relative capillary conductivity, using the model of Mualem (1976). This was done by using an equation for the soil water retention curve in the expression of Mualem (1976). The resulting

expression for relative capillary conductivity contained three unknown parameters, which were determined by fitting the proposed soil water retention model to experimental data. For comparing simulated and experimental results, five different types of soils were used. The agreement was found to be good in four cases.

Mohan Rao et al. (1989) gave a functional relation for h vs θ in terms of well defined soil properties i.e., porosity, residual moisture content and bubbling pressure. Piecewise functional approximations were presented for h above and below the bubbling pressure. An exponential decay relation ensures that at higher values of capillary pressure, the moisture content tends to the residual moisture content.

CHAPTER 3

MODEL DEVELOPMENT

3.1   MECHANISMS OF SOLUTE TRANSPORT

3.1.1.   Convection and Diffusion-Dispersion

Assuming no interaction between solute and soil matrix,
transport of solute in a soil system depends on the average flow
velocity i.e., viscous movement of the soil solution and is known as
convective transport. Further spreading of the tracer solution takes
place due to molecular diffusion and mechanical dispersion. The combined
effect of the two is known as hydrodynamic dispersion.

The rate of solute transport in soils is also affected by the
presence of an immobile fluid phase. In this phase the fluid does not
move/moves negligibly by the process of convection. In homogeneous soils
this condition is created by continued desaturation of the soil,
eliminating the larger pores for transport. However, in aggregated
soils, fluid located in micro-pores and dead end pores is also
stagnant. Thus, the entire flow region is effectively partitioned into
an immobile phase and a mobile phase. Transport of solute in the mobile
phase is governed by convection and hydrodynamic dispersion. The
transfer of solute into and out of the immobile phase can only take
place by the process of lateral diffusion. In the following discussion,
solute transport in the absence of an immobile phase has been referred

to as single phase solute transport. Again, the transport in the presence of an immobile phase has been referred to as two phase solute transport.

3.1.2   Adsorption-Desorption

In case of a reactive solute, one of the additional mechanisms affecting the transport is the process of adsorption-desorption. Adsorption is a physico-chemical process by which molecules or ions of the solute are immobilized/fixed by the soil matrix (e.g. cations present in the solute held by anions present in the soil matrix). Further the adsorbed concentration i.e., the amount of salt per unit mass of soil adsorbed by the soil matrix, is described as a function of the solute concentration at a fixed temperature and is known as an adsorption isotherm. Equilibrium between the solute and adsorbed concentration may be attained very rapidly i.e., almost instantaneously or at a finite rate. The two modes of reaching equilibrium are known as equilibrium adsorption and kinetic adsorption respectively.

For the two phase solute transport, the soil matrix can be conceptualized as being made up of two separate regions. The region in contact with the solute in the mobile phase, termed as mobile soil matrix; and the region in contact with the solute in the immobile phase, termed as immobile soil matrix. When a solute invades such a soil, only part of the adsorption sites i.e., the ones located in the mobile soil matrix may be readily accessible. However, some of the solute after being diffused into the immobile phase may also get adsorbed at the adosrption sites located in the immobile soil matrix.

3.2   PROBLEM DEFINITION

The present study is aimed at developing a numerical model to simulate vertical two phase transport of a reactive solute through the unsaturated zone extending from ground surface to the water table.

The mechanisms of solute transport accounted for in the present model are convection, hydrodynamic dispersion, lateral diffusion of solute into/out of the immobile phase and linear adsorption desorption in either or both the phases. The model is capable of simulating simpler cases of solute transport by assigning appropriate values to the concerned parameters. The simplest case being single phase non-reactive solute transport brought about only by the mechanism of convection. For such a case the immobile moisture content and hydrodynamic dispersion are assigned zero values and inter-action between the solute and soil matrix is neglected.

The model was developed in the following four stages.

Stage I   Single phase non-reactive solute transport.

Stage II Single phase reactive solute transport accounting for first order linear kinetic adsorption-desorption.

Stage III Two phase non-reactive solute transport.

Stage IV Two phase reactive solute transport accounting for linear equilibrium adsorption-desorption.

The model output (as per requirement) comprises of,

(i) Concentration distribution in space at pre-specified discrete times.

(ii) Concentration distribution (referred to as a breakthrough curve) in time at pre-specified depths.

(iii)   Volumes of solute (per unit plan area) transferred to the water table till different pre-assigned discrete times.

3.3   GOVERNING DIFFERENTIAL EQUATIONS

3.3.1   Single Phase Solute Transport

(i) Non - reactive solute

The equation governing one-dimensional solute transport in an unsaturated porous medium can be written as,

$$\frac{\partial(c\theta)}{\partial t} = \frac{\partial}{\partial z}\left(\theta D \frac{\partial c}{\partial z}\right) - \frac{\partial}{\partial z}(qc) \qquad (3.1)$$

where, z is a co-ordinate along the vertical direction t is time θ $(=\theta(z,t)$ is the volumetric moisture content, $c(=c(z,t)$ is the solute concentration, $D(= D(\theta,z,t))$ is the hydrodynamic dispersion coefficient and $q = (q(z,t))$ is the volumetric flux.

The hydrodynamic dispersion coefficient D represents the combined effect of both molecular diffusion and mechanical dispersion, and can be defined as follows (Bresler, 1973a),

$$D = D_o ae^{b\theta} + \lambda \mid v \mid \qquad (3.2)$$

where, a and b are empirical constants characterizing the soil, λ is dispersivity, v $(=q/\theta)$ is seepage velocity and D_o is the molecular diffusion coefficient in a free water system.

(ii) Reactive solute

Accounting for first order linear kinetic adsorption-desorption,

equation (3.1) can be rewritten as,

$$\frac{\partial(c\theta)}{\partial t} + \rho \frac{\partial s}{\partial t} = \frac{\partial}{\partial z}\left(\theta D \frac{\partial c}{\partial z}\right) - \frac{\partial}{\partial z}(qc) \qquad (3.3)$$

where, s is the adsorbed concentration of the soil matrix, and ρ is the bulk density of the soil.

The linear kinetic adsorption - desorption rate equation can be written as,

$$\frac{\partial s}{\partial t} = \beta(k_d c - s) \qquad (3.4)$$

where, β is a kinetic rate coefficient governing exchange between solute and soil matrix and k_d is an empirical distribution constant.

3.3.2 Two Phase Solute Transport

(i) Non-reactive solute

Considering the presence of an immobile phase alongwith the mobile solute phase, the equation governing one - dimensional solute transport can be written as,

$$\frac{\partial(c_m\theta_m)}{\partial t} + \frac{\partial(c_{im}\theta_{im})}{\partial t} = \frac{\partial}{\partial z}\left(\theta_m D_m \frac{\partial c_m}{\partial z}\right) - \frac{\partial}{\partial z}(qc_m) \qquad (3.5)$$

where, subscript m represents the mobile phase and im the immobile phase. The total moisture content in the soil comprises of the moisture contents in the two phases ($\theta = \theta_m + \theta_{im}$).

The hydrodynamic dispersion coefficient defined for the mobile

phase, can be written as,

$$D_m = D_o ae^{b\theta}_m + \lambda \mid v_m \mid \qquad (3.6)$$

where, $v_m(=q/\theta_m)$ is the seepage velocity in the mobile phase.

The lateral diffusion of concentration into and out of the immobile phase, can be defined by the following rate equation,

$$\theta_{im} \frac{\partial c_{im}}{\partial t} = \alpha (c_m - c_{im}) \qquad (3.7)$$

where, α is a first order rate constant governing the rate of solute exchange between the two phases.

(ii)   Reactive solute

Accounting for a linear equilibrium adsorption-desortion isotherm, with adsorption occuring in either or both phases, equation (3.5) can be rewritten as,

$$\frac{\partial c_m (\theta_m + \rho f k_d)}{\partial t} + (\theta_{im} + \rho(1-f)k_d) \frac{\partial c_{im}}{\partial t} =$$

$$\frac{\partial}{\partial z} (\theta_m D_m \frac{\partial c_m}{\partial z}) - \frac{\partial}{\partial z} (qc_m) \qquad (3.8)$$

where, f is the fraction of adsorption sites located in the mobile phase.

Again, the rate equation for lateral diffusion into and out of the immobile phase and subsequent adsorption-desorption can be written

as,

$$(\theta_{im} + \rho(1-f)k_d) \; \frac{\partial c_{im}}{\partial t} = \alpha(c_m - c_{im})$$
(3.9)

3.3.3 Fluid Flow

To quantify the distribution of moisture (θ) and volumetric flux (q) required for solving the solute transport equations (3.1-3.9) the partial differential equation governing flow in an unsaturated porous medium has to be solved. The head form of Richards equation governing one dimensional vertical flow in an unsaturated porous medium can be written as,

$$C_u \; \frac{\partial h}{\partial t} = \frac{\partial}{\partial z} \; (K \; \frac{\partial(-h + z)}{\partial z}) - E$$
(3.10)

where, h (=h(θ)) is the capillary pressure head, K (=K(θ)) is the unsaturated hydraulic conductivity (known as capillary conductivity), C_u (=dθ/dh) is the specific moisture capacity and E is sink term representing volume of water extracted/unit volme of soil/unit time. h(θ) and K(θ) are the soil characteristics.

3.4 THE SOLUTION

3.4.1 Solution Strategy

The solute transport equations (eqns. 3.1-3.9) comprise of among others, a convective and a diffusive – dispersive component. Solving for these two components simultaneously using a finite difference approximation scheme results in an artificial dispersion known as numerical dispersion. Numerical dispersion is a truncation

error and results by neglecting the term proportional to the second order derivative in the Taylor's series, while approximating for the first order derivative. To overcome this problem, the convective component is solved using the Method of Characteristics (MOC). The change in concentration due to hydrodynamic dispersion and adsorption-desorption is accounted for subsequently using an implicit finite difference scheme. However, for such a solution space and time distributions of q and θ form a pre -requisite. To obtain these distributions, Richards equation has been solved.

3.4.2   Co-ordinate System

Two co-ordinate systems in depth have been used. The z co-ordinate system begins with a zero value at the lower boundary, (+ve upwards and has been used for solving Richards equation. The ξ co-ordinate system begins with a zero value at the upper boundary (+ve downwards) and has been used for solving the solute transport equations.

3.4.3   Solution of Richards Equation

Richards equation i.e., equation (3.10) has been solved for a capillary pressure distribution in space and time which also leads to the spatial and temporal moisture distribution using the h vs θ relation (soil characteristic). The method of solution has been adopted from Mohan Rao (1986). Following is a brief description of it.

Richards equation is a non-linear second order partial differential equation. The non-linearity arises due to the dependence of C_u and K on θ (and h). In order to solve this equation the flow domain under consideration (for example ground to water table) is discretized by a finite number of nodes. Similarly the time domain is discretized by

a finite number of discrete times. Thus, $h(z,t)$ at the jth node and k^{th} discrete time is represented as, $h_{j,k}$ (refer Fig.3.1). Using a central finite difference scheme, the difference approximation of equation (3.10) for an interior node j and time step Δt_k, from k^{th} to $k+1^{th}$ discrete time can be written as,

$$C_{u_{j,k+1/2}} \frac{h_{j,k+1} - h_{j,k}}{\Delta t_k} = \frac{1}{2} \left[\left\{ K_{j-1/2,k} \frac{h_{j,k} - h_{j-1,k} + \Delta z_{j-1}}{\Delta z_{j-1}} \right. \right.$$

$$\left. + K_{j-1/2,k+1} \frac{h_{j,k+1} - h_{j-1,k+1} + \Delta z_{j-1}}{\Delta z_{j-1}} \right\} -$$

$$\left\{ K_{j+1/2,k} \frac{h_{j+1,k} - h_{j,k} + \Delta z_j}{\Delta z_j} + K_{j+1/2,k+1} \frac{h_{j+1,k+1} - h_{j,k} + \Delta z_j}{\Delta z_j} \right\} \right]$$

$$\frac{2}{\Delta z_{j-1} + \Delta z_j} - E_{j,k+1/2} \qquad (3.11)$$

$$j = 2,3,4\ldots\ldots\ldots n-1$$

where, n is the total number of nodes.

This provides (n-2) non-linear simultaneous equations. Two additional equations are obtained by assigning upper and lower boundary conditions.

(i) Upper Boundary Condition

The upper boundary condition i.e., the boundary condition at the ground may be of Neuman type (entire input infiltrates) or Dirichlet type (ponding occurs or just saturation is maintained), depending upon the relative magnitude of input intensity (Q), infiltration capacity
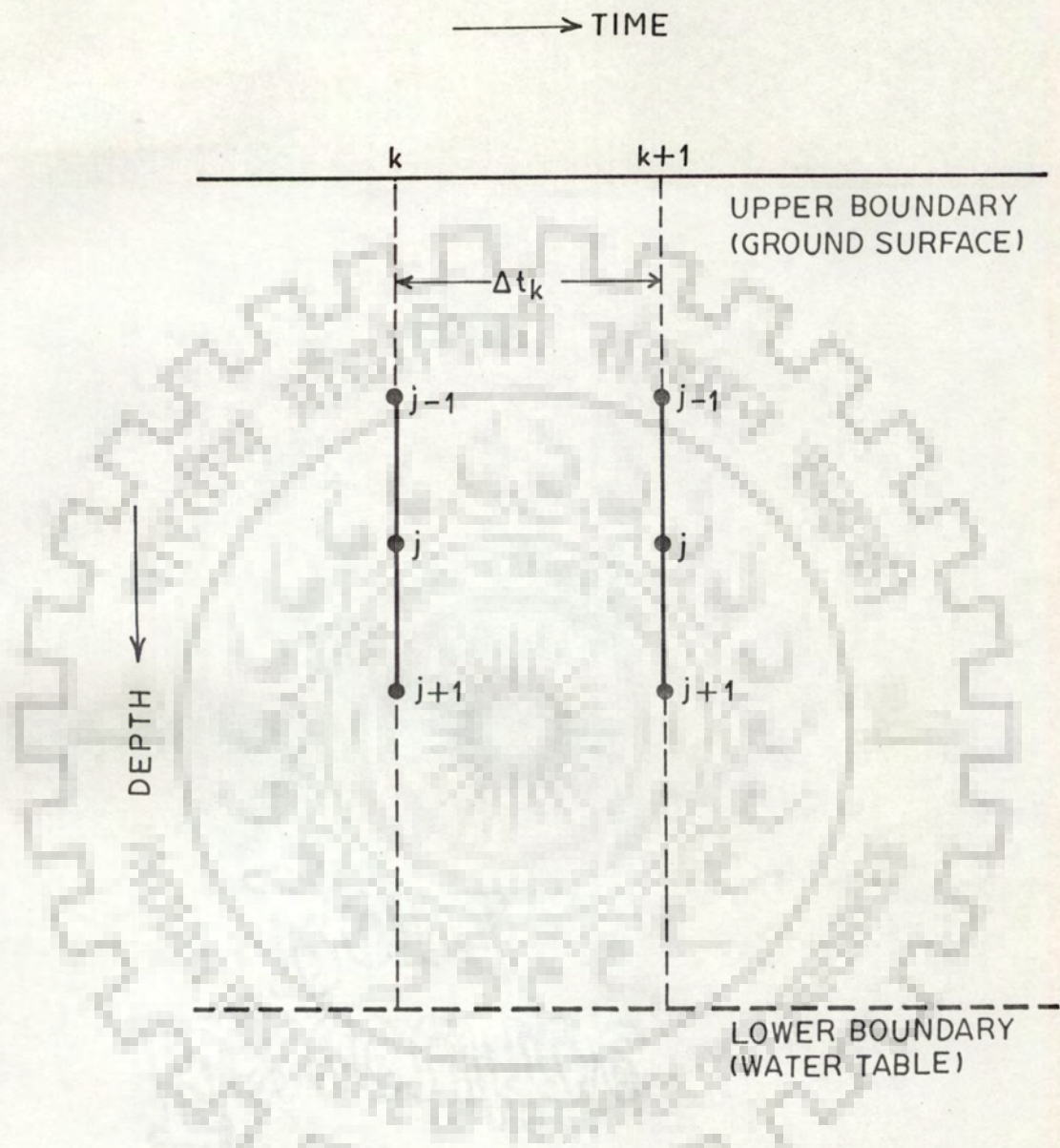
Fig. 3.1. Finite difference grid for solving Richards equation.

(I_c) and saturated capillary conductivity (K_s). Thus, assuming Q to be constant for a sufficiently long period, either of the following three situations may arise,

(a) $Q < K_s$ The entire input will be infiltrated. The top soil remains unsaturated (i.e., h > 0).

(b) $K_s < Q < I_c$ Saturation will occur after infiltration is allowed to proceed for a finite time. The top soil becomes saturated (i.e., h = 0).

(c) $Q > I_c$ Saturation will occur and will be followed by ponding after infiltration is allowed to proceed for a finite time (i.e., h < 0)

In case of a time variant input intensity the above three situations may change from one to another. In the present solution, a change over of the boundary condition is assigned based on the capillary head value. The adopted algorithm is given in annexure 1.

(ii) Lower Boundary Condition

The lower boundary condition is taken as a constant head boundary condition (h = 0, for a water table) and may be time variant i.e., a fluctuating water table. This will cause a change in the depth of the flow domain i.e., an increase (falling water table) or a decrease (rising water table). To account for this change, the number of nodes discretizing the domain are modified accordingly.

This leads to a determinate system of equations. The system of non-linear simultaneous equations is solved using Picard's iteration method (Remson et al., 1971). According to this method the system of equations is linearized and solved successively by evaluating K and C_u

in accordance with the known values of h arrived at in the previous iteration. Thus for the mth iteration equation (3.11) is rewritten with the following substitutions,

$$h_{j-1,k+1} = h_{j-1,k+1}^{(m)} \; ; \; h_{j,k+1} = h_{j,k+1}^{(m)}; \; h_{j+1,k+1} = h_{j,k+1}^{(m)}$$

$$C_{u_{j,k+1/2}}^{(m)} = C_u \left(\frac{h_{j,k+1}^{(m-1)} + h_{j,k}}{2} \right)$$

$$K_{j-1/2,k+1}^{(m)} = 0.5 \left[K \left(\theta_{j-1,k+1}^{(m-1)} \right) + K \left(\theta_{j,k+1}^{(m-1)} \right) \right]$$

$$K_{j+1/2,k+1}^{(m)} = 0.5 \left[K \left(\theta_{j,k+1}^{(m-1)} \right) + K \left(\theta_{j+1,k+1}^{(m-1)} \right) \right]$$

$$K_{j-1/2,k+1}^{(0)} = K_{j-1/2,k} \quad \text{and} \quad C_{u_{j,k+1/2}}^{(0)} = C_{u_{j,k}}$$

The resulting system of equations is tridiagonal and is solved for ($h_{j,k+1}^{(m)}$, j = 1,2,......n) using Thomas algorithm (Remson et al., 1971). As the iteration index approaches infinity $h_{j,k+1}^{(m)}$ converges to the unknown true solution $h_{j,k+1}$ of the non - linear simultaneous equations.

$$| h_{j,k+1}^{(m)} - \hat{h}_{j,k+1} | = 0 \tag{3.12}$$

To avoid too large a number of iterations, the iterations are stopped when the following check is satisfied,

$$| h_{j,k+1}^{(m)} - h_{j,k+1}^{(m-1)} | \le \xi_o \, h_{j,k+1}^{(m-1)} \tag{3.13}$$

where, ξ_o is a small +ve value.

Thus, the distribution of h in space and time is obtained. The corresponding distribution of θ in space and time is obtained by the θ vs h relation.

Again, using the known h distribution, the distribution of q is computed as follows,

$$q_{j+1/2,k+1/2} = \left[q_{j+1/2,k} + q_{j+1/2,k+1} \right]/2 \qquad (3.14)$$

where,

$$q_{j+1/2,k} = K_{j+1/2,k} \frac{h_{j+1,k} - h_{j,k} + \Delta z_j}{\Delta z_j}$$

$$q_{j+1/2,k+1} = K_{j+1/2,k+1} \frac{h_{j+1,k+1} - h_{j,k+1} + \Delta z_j}{\Delta z_j}$$

3.4.4   Single Phase Non-reactive Solute Transport

This requires the coupled solution of equation (3.1) and equation (3.10). The solution of equation (3.10) i.e., Richards equation has already been described (Section 3.4.3).

An equivalent set of ordinary differential equations for solving equation (3.1) can be written as,

$$\frac{dz}{dt} = \frac{q}{\theta} \qquad (3.15)$$

$$\frac{d(c\theta)}{dt} = \frac{\partial}{\partial z} \left(\theta D \frac{\partial c}{\partial z} \right) \qquad (3.16)$$

Thus, equation (3.1) can be solved by solving equations (3.15) and (3.16), which comprise of the convective and diffusive - dispersive transport respectively.

3.4.4.1 Convective Transport

The initial solute domain is discretized into a finite number (np) of moving packets, each moving packet having a pre-assigned strip thickness (ts). The first packet lies at the lower boundary, while the np^{th} packet lies at the upper boundary (Fig. 3.2). Each moving packet is defined by two co-ordinates (x) and (y) representing its lower and upper bounds. Further, the solute (sl) and water (vl) volumes (per unit plan area) contained in each moving packet are quantified based upon the known initial soil moisture and solute concentration distributions. The variables x,y,vl,sl are defined as double subscripted variables, the first subscript represents the serial number of the moving packet, while the second subscript represents the discrete time (the initial discrete time is designated as $zero^{th}$ time). Thus, for p^{th} moving packet, $x_{p,0}, y_{p,0}, vl_{p,0}$ and $sl_{p,0}$ at the beginning of simulation are defined as follows,

$$x_{p,0} = (np - p + 1). \, ts \tag{3.17}$$

$$y_{p,0} = (np - p). \, ts \tag{3.18}$$

$$vl_{p,0} = (x_{p,0} - y_{p,0}). \, \theta_{p,0} \tag{3.19}$$

where, $\theta_{p,0}$ is an average moisture content of the pth moving packet. It is estimated by taking an arithmatical mean of the moisture contents at the lower and upper bounds of the pth moving packet. These moisture contents in turn are estimated by linearly interpolating the initial soil moisture distribution known at the fixed nodal points.
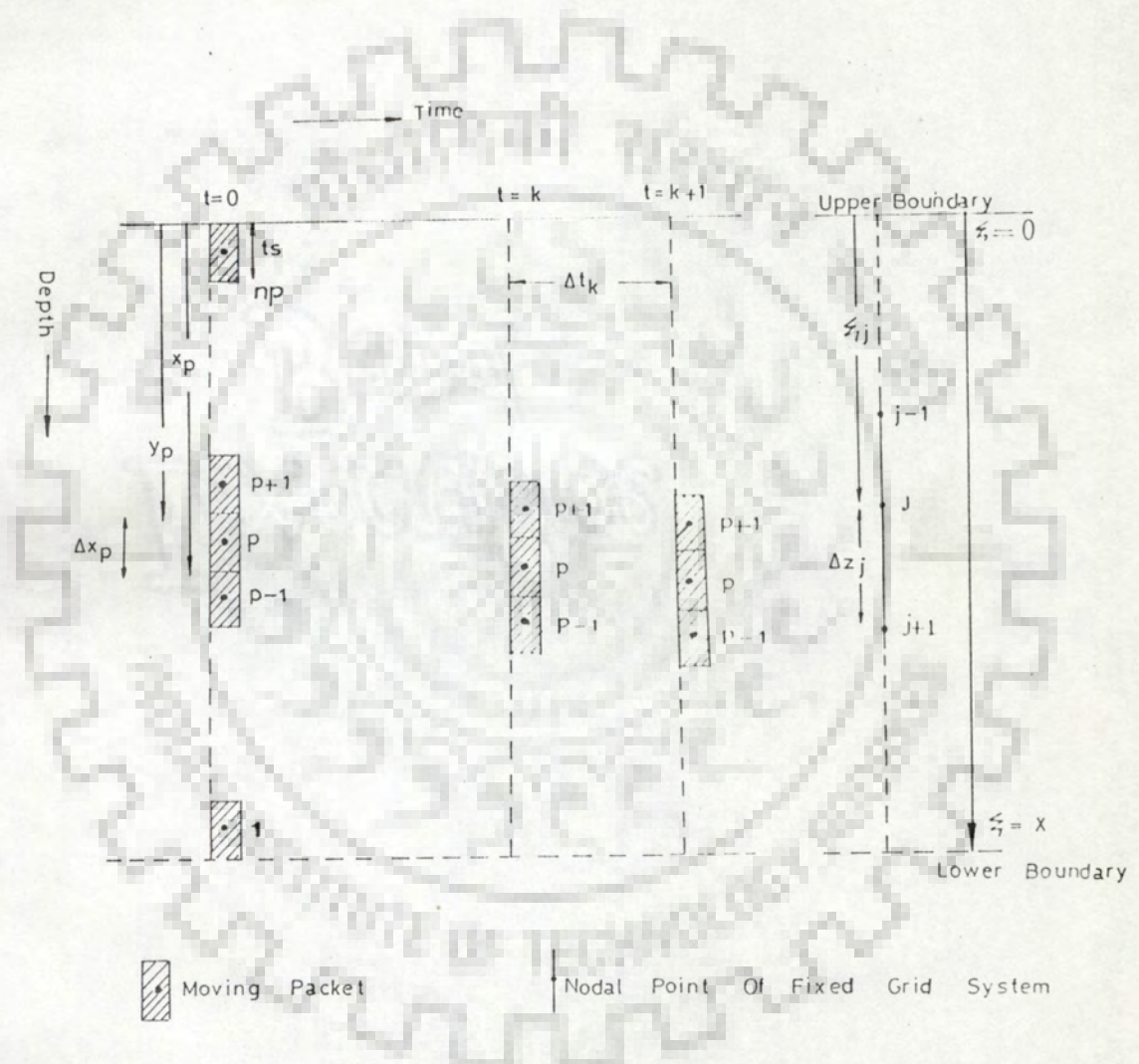
Fig. 3.2. Moving and fixed co-ordinate systems for simulation of solute transport.

$$sl_{p,0} = vl_{p,0} \cdot c_{i_{p,0}}$$

(3.20)

where, $c_{i_{p,0}}$ is an average concentration of the pth moving packet. It is estimated by taking an arithmatical mean of the concentrations at the lower and upper bounds of the pth moving packet. These concentrations in turn are estimated by linearly interpolating the initial concentration distribution known at the fixed nodal points.

It is to be noted that the water volumes (per unit plan area) assigned to the moving packets remain the same throughout the simulation (except when evapotranspiration is accounted for). However, any change in moisture distribution is manifested as a change in the length of the moving packets (length of the pth moving packet = $x_{p,0} - y_{p,0}$).

3.4.4.1.1 Convection of Moving Packets

For known positions of the moving packets at the beginning of a time step Δt_k (i.e., at k^{th} discrete time), the new positions at the end of the time step [i.e., at $(k+1)^{th}$ discrete time] are computed in the following steps.

(i) Computation of cumulative water volume (per unit plan area) profile from the flow consideration : Using the moisture content distribution ($\theta_{j,k+1}$, j=1,2.....n) known at the end of the time step (obtained by the solution of Richards equation; refer section 3.4.3) cumulative water volumes (per unit plan area) at the fixed nodal points (used for solving Richards equation) are computed. For the jth node at $(k+1)^{th}$ discrete time, the cumulative water volume ($cw_{j,k+1}$) (per unit plan area) is computed as,

$$cw_{j,k+1} = \sum_{i=2}^{j} \frac{\theta_{i,k+1} + \theta_{i-1,k+1}}{2} \cdot \Delta z_{i-1} \qquad (3.21)$$

$$j = 2, 3, \ldots \ldots n$$

$$cw_{1,k+1} = 0.0$$

The nodal depth ξ_j, at node j is computed as,

$$\xi_j = \sum_{i=2}^{j} \Delta z_{i-1} \qquad (3.22)$$

$$j = 2, 3, \ldots \ldots n$$

$$\xi_1 = 0.0$$

where, Δz_i is the spatial distance between i^{th} and $(i+1)^{th}$ fixed node, of the finite difference grid used for solving Richards equation. Thus, a cumulative water volume profile $cw_{j,k+1}$ vs ξ_j ($j=1,2,\ldots n$) is obtained.

(ii) Computation of cumulative water volume (per unit plan area) profile from the transport consideration : The cumulative water volumes ($xw_{p,k+1}$ and $yw_{p,k+1}$) (per unit plan area) at the lower and upper bounds ($x_{p,k+1}$ and $y_{p,k+1}$) of each moving packet at the end of the time step Δt_k i.e., $(k+1)^{th}$ discrete time are computed using the known cumulative water volumes ($xw_{p,k}$ and $yw_{p,k}$) (per unit plan area) at k^{th} discrete time and the infiltration during the time step Δt_k, known from the solution of Richards equation. Thus, $xw_{p,k+1}$ and $yw_{p,k+1}$ are computed as follows,

$$xw_{p,k+1} = xw_{p,k} + I_{1,k+1/2} \cdot \Delta t_k \qquad (3.23)$$

$$yw_{p,k+1} = yw_{p,k} + I_{1,k+1/2} \cdot \Delta t_k \qquad (3.24)$$

where, $I_{1,k+1/2}$ is the rate of infiltration at the upper boundary during Δt_k [for a Dirichlet boundary condition $I_{1,k+1/2} = q_{1,k+1/2}$; refer eqn(3.14), while for a Neuman boundary condition $I_{1,k+1/2}$ is the assigned net input intensity].

At the beginning of each time step $xw_{p,k}$ and $yw_{p,k}$ are known from the solution of the preceding time step. However, at the beginning of simulation $xw_{p,0}$ and $yw_{p,0}$ are computed using the initial soil moisture distribution and spatial location of moving packets [refer eqn (3.17),(3.18) and (3.19)].

$$xw_{p,0} = \sum_{i=p}^{np} vl_{i,0} \qquad (3.25)$$

$$yw_{p,0} = \sum_{i=p-1}^{np} vl_{i,0} \qquad (3.26)$$

(iii) New positions of the moving packets : Finally the new positions of the moving packets (i.e., co-ordinates $x_{p,k+1}$ and $y_{p,k+1}$) at $(k+1)^{th}$ discrete time are computed by ensuring a compatibility between the cumulative water volume (per unit plan area) profiles computed from the considerations of flow [step(i)] and of transport [step(ii)]. Thus, for the pth moving packet $x_{p,k+1}$ and $y_{p,k+1}$ are obtained as follows.

(a) Locate two nodal points j and $j+1$ at which the computed cumulative water volumes (cw) (per unit plan area) lie just below and just above the $xw_{p,k+1}$ i.e.,

$$cw_{j,k+1} \leq xw_{p,k+1} \leq cw_{j+1,k+1}$$

Similarly for $yw_{p,k+1}$,

$$cw_{j,k+1} \leq yw_{p,k+1} \leq cw_{j+1,k+1}$$

(b) The ξ co-ordinate at which the cumulative water volume (per unit plan area) just equals $xw_{p,k+1}$ is estimated by assuming a linear variation of cw in between the nodal points j and j+1 (Fig. 3.3).

$$\xi = \xi_j + (xw_{p,k+1} - cw_{j,k+1})(\xi_{j+1} - \xi_j)/(cw_{j+1,k+1} - cw_{j,k+1})$$
$$(3.27)$$

Similarly the ξ co-ordinate corresponding to $yw_{p,k+1}$ is obtained.

$$\xi = \xi_j + (yw_{p,k+1} - cw_{j,k+1})(\xi_{j+1} - \xi_j)/(cw_{j+1,k+1} - cw_{j,k+1})$$
$$(3.28)$$

The two ξ co-ordinates obtained in step(b) represent the new positions of the pth moving packet i.e., the co-ordinates $x_{p,k+1}$ and $y_{p,k+1}$ respectively at the end of the time step Δt_k.

Thus, the new positions of all the moving packets at $(k+1)^{th}$ discrete time are obtained.

To account for the downward movement out of the domain, of the moving packet closest to the water table, the cumulative water volume (per unit plan area) profile computed in step (i) (same section) is extended to a certain depth below the water table using the moisture content value of the last node i.e., porosity.

3.4.4.1.2 Generation of New Moving Packets

In case of continued solute infiltration at the upper boundary, there will be a continuous downward movement of the packets.
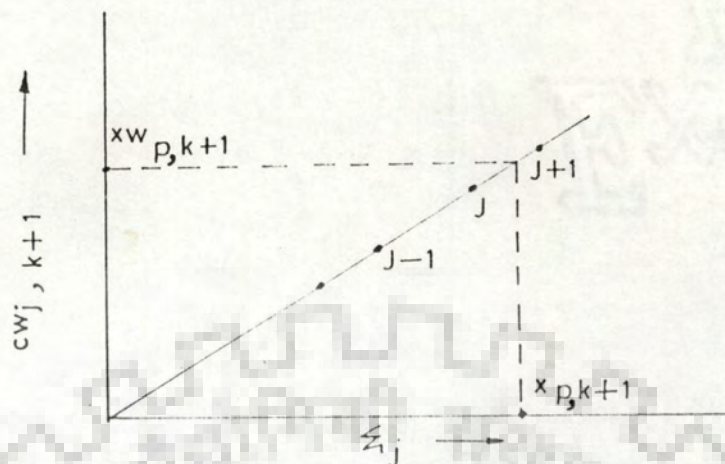
Fig. 3.3. Interpolation of the new position of the moving packet.
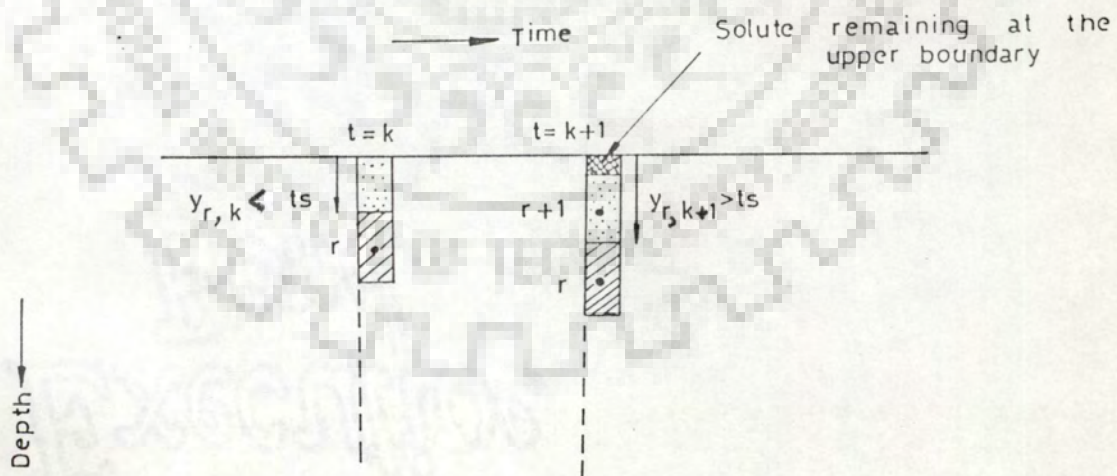
Fig. 3.4. Generation of a new moving packet.

To quantify the infiltrating solute, new moving packets are generated as follows.

When the upper co-ordinate (y) of the moving packet closest to the ground equals or just exceeds the strip thickness ts a new moving packet is introduced into the flow domain (Fig. 3.4). The moving packet is described as follows,

Serial number = r + 1

where, r is the number of moving packets present in the flow domain till the kth discrete time,

$$x_{r+1,k+1} = y_{r,k+1} \tag{3.29}$$

$$y_{r+1,k+1} = (y_{r,k+1} - ts) \tag{3.30}$$

$$vl_{r+1,k+1} = cv. \; ts \; /y_{r,k+1} \tag{3.31}$$

$$sl_{r+1,k+1} = cs. \; ts \; /y_{r,k+1} \tag{3.32}$$

where, cv and cs are the volumes (per unit plan area) of water and solute respectively, infiltrated during the time interval between the subsequent entry of two moving packets. And are computed as follows.

$$cv = \sum_{k1} I_{1,k+1/2} \cdot \Delta t_k \tag{3.33}$$

$$cs = \sum_{k1} I_{1,k+1/2} \cdot \Delta t_k \cdot c_o \tag{3.34}$$

where, k1 is the number of time steps occuring between the subsequent entry of two moving packets, c_o is concentration of the solute infiltrating during the time step Δt_k.

$$xw_{r+1,k+1} = x_{r+1,k+1} \cdot cv /y_{r,k+1} \tag{3.35}$$

$$yw_{r+1,k+1} = y_{r+1,k+1} \cdot cv / y_{r,k+1} \tag{3.36}$$

Again from Fig. 3.4, it can be seen that after the new moving packet is generated, a certain volume of solute, in excess of the new moving packet may remain at the upper boundary. During the subsequent time steps it is constantly incremented till it attains the status of a moving packet i.e., when its thickness equals or just exceeds ts. However, to account for its presence during each time step it is treated as a moving packet and is defined as,

$$x^*_{k+1} = y_{r+1,k+1} \tag{3.37}$$

$$y^*_{k+1} = 0 \tag{3.38}$$

$$vl^*_{k+1} = cv - vl_{r+1,k+1} \tag{3.39}$$

$$sl^*_{k+1} = cs - sl_{r+1,k+1} \tag{3.40}$$

$$xw^*_{k+1} = cv - vl_{r+1,k+1} \tag{3.41}$$

$$yw^*_{k+1} = 0 \tag{3.42}$$

It does not add to the total number of moving packets.

3.4.4.1.3 Solute Leaving the Domain at the Lower Boundary

When the co-ordinates of a moving packet exceed the total dpeth (Z) of the solute domain under consideration some solute has left the domain at the lower boundary. The moving packets leaving the domain at the lower boundary are identified as follows.

(i) if $x_{p,k+1} > Z$ and $y_{p,k+1} < Z$, implies that the pth moving packet has partially left the domain.

(ii) if $x_{p,k+1} > Z$ and $y_{p,k+1} \geq Z$, implies that the moving packet has

completely left the flow domain.

On encountering either of the two conditions stated above, for the pth moving packet the following procedure is carried out.

Condition(i) : If a moving packet partially leaves the flow domain, the volumes (per unit plan area) of solute leaving the domain and remaining in the domain are quantified based on the ratio of the length $(x_{p,k+1}-Z)$ of the moving packet which has left the flow domain and the total length $(x_{p,k+1}-y_{p,k+1})$ of the moving packet. Thus,

(a) To account for partial exit of the pth moving packet during the time step Δt_k, the variables $sl_{p,k+1}, vl_{p,k+1}, xw_{p,k+1}, yw_{p,k+1}, x_{p,k+1}$ and $y_{p,k+1}$ are modified as follows.

$$sl_{p,k+1_{new}} = sl_{p,k+1_{old}} - sl_{p,k+1_{old}}(x_{p,k+1_{old}} - Z)/$$

$$(x_{p,k+1_{old}} - y_{p,k+1_{old}}) \tag{3.43}$$

$$vl_{p,k+1_{new}} = vl_{p,k+1_{old}} - vl_{p,k+1_{old}}(x_{p,k+1_{old}} - Z)/$$

$$(x_{p,k+1_{old}} - y_{p,k+1_{old}}) \tag{3.44}$$

$$xw_{p,k+1_{new}} = xw_{p,k+1_{old}} - vl_{p,k+1_{old}}(x_{p,k+1_{old}} - Z)/$$

$$(x_{p,k+1_{old}} - y_{p,k+1_{old}}) \tag{3.45}$$

$$x_{p,k+1_{new}} = Z \tag{3.46}$$

There is no change in $y_{p,k+1}$ and $yw_{p,k+1}$.

(b) The volume (per unit plan area) of solute (vsl) leaving the domain due to partial exit of the pth moving packet during the time step Δt_k is quantified as,

$$vsl_{p,k+1} = sl_{p,k+1_{old}} (x_{p,k+1_{old}} - Z)/(x_{p,k+1_{old}} - y_{p,k+1_{old}}) \quad (3.47)$$

Condition (ii) : If a moving packet leaves the flow domain completely, it is excluded from the total number of moving packets. The remaining ones are renumbered. Volume of solute (vsl) (per unit plan area) leaving the domain due to exit of the pth moving packet during the time step Δt_k is,

$$vsl_{p,k+1} = sl_{p,k+1}$$

Similarly, the positions of all the moving packets are checked. Thus, total solute volume leaving the domain during the time step Δt_k

$$= \sum_{p \in p1} vsl_{p,k+1}$$

where, p1 is a subset of np and is the number of moving packets leaving the domain completely or partially during the time step Δt_k.

Thus, the cumulative volume (per unit plan area) of solute transported to the water table till different discrete times is estimated by constantly adding up the solute leaving the system during each preceding time step.

3.4.4.1.4 Concentration of Moving Packets

Concentration of the pth moving packet (due to convection only) at $(k+1)^{th}$ discrete time is computed as follows,

$$\hat{c}_{p,k+1} = sl_{p,k+1} / vl_{p,k+1}$$

$$p = 1, 2, \ldots \ldots n.$$

During computation of convective solute transport the volumes of solute of all the moving packets ($sl_{p,k+1}$, p=1,2,....np) remain time invariant from k^{th} (known from the solution of the preceding time step) to $(k+1)^{th}$ discrete time. There may be a change in the solute volume of the temporary moving packet lying at the top (which is incremented due to solute infiltration during the time step Δt_k). Also, at the lower boundary, in case of partial exit of a moving packet its solute volume gets modified during the time step Δt_k. However, when accounting for hydrodynamic dispersion and adsorption-desorption by the soil matrix (described subsequently), there is a change in the solute volumes of moving packets caused by redistribution of the solute amongst themselves and adsorption by the soil matrix.

3.4.4.2   Diffusive-Dispersive Transport

Subsequent to accounting for the process of convective transport, diffusive-dispersive transport is accounted for by solving equation (3.16). The solution is carried out using an implicit finite difference scheme for all the moving packets in the flow domain. The finite difference approximation for the pth packet from k^{th} to $(k+1)^{th}$ discrete time is written as,

$$\frac{c_{p,k+1} \theta_{p,k+1} - \hat{c}_{p,k+1} \theta_{p,k}}{\Delta t_k} = \left[(\theta_{p-1,k+1} + \theta_{p,k+1})/2 \right.$$

$$D_{p-1/2,k+1/2} \; \frac{c_{p-1,k+1} - c_{p,k+1}}{(\Delta x_{p-1,k+1} + \Delta x_{p,k+1})/2} \; - (\theta_{p,k+1} - \theta_{p+1,k+1})/2$$

$$D_{p+1/2,k+1/2} \; \frac{c_{p,k+1} - c_{p+1,k+1}}{(\Delta x_{p,k+1} + \Delta x_{p+1,k+1})/2} \Bigg] \; \frac{1}{\Delta x_{p,k+1}} \tag{3.50}$$

where, $\hat{c}_{p,k+1}$ is the concentration at $(k+1)^{th}$ discrete time due to convection only.

The other required variables $\Delta x_{p,k+1}$ (length), $\theta_{p,k+1}$ (moisture content) and $D_{p,k+1/2}$ (hydrodynamic dispersion coefficient) for the pth moving packet at $(k+1)^{th}$ discrete time are computed as,

$$\Delta x_{p,k+1} = x_{p,k+1} - y_{p,k+1} \tag{3.51}$$

$$\theta_{p,k+1} = vl_{p,k+1} \; /\Delta x_{p,k+1} \tag{3.52}$$

$$D_{p+1/2,k+1} = D_o ae^{b(\theta_{p,k+1} + \theta_{p+1,k+1})/2} + \lambda |v_{p+1/2,k+1}| \tag{3.53}$$

The seepage velocity $v_{p+1/2,k+1}$ is computed using the positions of the co-ordinates at the kth and $(k+1)^{th}$ discrete times. Thus,

$$v_{p+1/2,k+1} = (y_{p,k+1} - y_{p,k})/\Delta t_k \tag{3.54}$$

Similarly,

$$D_{p-1/2,k+1} = D_o ae^{b(\theta_{p-1,k+1} + \theta_{p,k+1})/2} + \lambda |v_{p-1/2,k+1}| \tag{3.55}$$

where,

$$v_{p-1/2, k+1} = (x_{p, k+1} - x_{p, k})/\Delta t_k \qquad (3.56)$$

Similarly, writing difference approximations for all the interior moving packets results in (np-2) (where, np is the total number of moving packets at $(k+1)^{th}$ discrete time including the temporary moving packet, which lies at the top) equations.

The np^{th} packet lies at the upper boundary. Thus, the difference approximation for the np^{th} packet from k^{th} to $(k+1)^{th}$ discrete time is written as,

$$\frac{c_{np, k+1}\, \theta_{np, k+1} - \hat{c}_{np, k+1}\, \theta_{np, k}}{\Delta t_k} = \left[(\theta_{np, k+1} + \theta_{np-1, k+1})/2 \right.$$

$$\left. D_{np-1/2}\, \frac{c_{np, k+1} - c_{np-1, k+1}}{(\Delta x_{np, k+1} + \Delta x_{np-1, k+1})/2} \right] \frac{2}{\Delta x_{np, k+1}} \qquad (3.57)$$

Again, the 1st packet lies at the lower boundry and the difference approximation for it is written as,

$$\frac{c_{1, k+1}\, \theta_{1, k+1} - \hat{c}_{1, k+1}\, \theta_{1, k}}{\Delta t_k} = \left[(\theta_{2, k+1} + \theta_{1, k+1})/2 \right.$$

$$\left. D_{1+1/2}\, \frac{c_{1, k+1} - c_{2, k+1}}{(\Delta x_{1, k+1} + \Delta x_{2, k+1})/2} \right] \frac{2}{\Delta x_{1, k+1}} \qquad (3.58)$$

This leads to a determinate system of equations and is solved for $c_{p, k+1}$ (p = 1,2.......np) using Thomas algorithm (Remson et al., 1971). Thus, the solute concentration distribution accounting for

convection and hydrodynamic dispersion is obtained.

3.4.4.2.1 Change in Solute Volumes (per unit plan area)of Moving Packets

To account for solute exchanged between the moving packets due to diffusive dispersive transport, the solute volumes (per unit plan area)of the moving packets are recomputed. Thus, for the pth moving packet at $(k+1)^{th}$ discrete time $sl_{p,k+1}$ is computed as,

$$sl_{p,k+1} = c_{p,k+1} \cdot vl_{p,k+1} \qquad (3.59)$$

$p=1,2,\ldots\ldots\ldots np.$

3.4.5 Single Phase Reactive (first order linear kinetic adsorption-desorption) Solute Transport.

The model described previously has been extended by incorporating an additional equation, describing the rate of solute-matrix interaction. For a first order linear kinetic adsorption-desorption isotherm, the problem is defined by equations (3.3),(3.4) and (3.10) alongwith the appropriate boundary conditions. Combining equtions (3.3) and (3.4) as follows,

$$\frac{\partial(c\theta)}{\partial t} = \frac{\partial}{\partial z}(\theta D \frac{\partial c}{\partial z}) - \frac{\partial}{\partial z}(qc) - \beta(k_d c - s)\rho \qquad (3.60)$$

The set of ordinary differential equations to be solved for solving the above partial differential equation can be written as,

$$\frac{dz}{dt} = \frac{q}{\theta} \qquad (3.61)$$

$$\frac{d(c\theta)}{dt} = \frac{\partial}{\partial z}(\theta D\frac{\partial c}{\partial z}) - \beta (k_d c - s)\rho \qquad (3.62)$$

Neglecting the second term on the R.H.S of eqution (3.62) the solution reduces to that of, single phase non-reactive solute transport. Thus, the solution described previously is followed to obtain the solute concentration distribution ($\hat{c}_{p,k+1}$, p=1,2,....np) ignoring solute matrix interaction (refer section 3.4.4). To account for linear adsorption - desorption, the following additional steps are taken.

3.4.5.1 Computation of Nodal Concentration

To compute nodal concentration values, a fixed grid system is superposed on the solution domain. This grid system coincides with the one used for solving the flow equation. However, it extends to a certain depth below the water table [refer section 3.4.4.1.1; step (ii)]. Each node is assumed to have an area of influence. For j^{th} node this area of influence extends from ($\xi_j - \Delta z_{j-1}/2$) to ($\xi_j + \Delta z_j/2$) (Fig. 3.5a). All moving packets lying wholly or partially within the area of influence of a certain node at any instant contribute towards the concentration of the node.

The following possibilities may arise,

(a) If the pth moving packet satisfies the conditions,

$$\xi_{j-1/2} \leq x_{p,k+1} \leq \xi_{j+1/2}$$
and

$$\xi_{j-1/2} \leq y_{p,k+1} \leq \xi_{j+1/2} ,$$

it lies wholly within the area of influence of node j (Fig. 3.5a). The solute volume ($xs_{p,k+1}$) (per unit plan area) contributed to

node j by it, is

$$xs_{p,k+1} = sl_{p,k+1} \qquad (3.63)$$

(b) If the pth moving packet satisfies the conditions,

$$\xi_{j-1/2} < x_{p,k+1} \leq \xi_{j+1/2}$$

and

$$y_{p,k+1} < \xi_{j-1/2} ,$$

it lies partially (towards the upper side of node j) within the area of influence of node j (Fig. 3.5b). The solute volume $(xs_{p,k+1})$ (per unit plan area) contributed to node j by it, is

$$xs_{p,k+1} = (x_{p,k+1} - \xi_{j-1/2})sl_{p,k+1}/(x_{p,k+1} - y_{p,k+1}) \qquad (3.64)$$

(b) If the pth moving packet satisfies the conditions,

$$\xi_{j-1/2} \leq y_{p,k+1} < \xi_{j+1/2}$$

and

$$\xi_{j+1/2} < x_{p,k+1} ,$$

it lies partially (towards the lower side of node j) within the area of influence of node j (refer Fig. 3.5c). The solute volume $(xs_{p,k+1})$ (per unit plan area) contributed to node j, by it is,

$$xs_{p,k+1} = (\xi_{j+1/2} - y_{p,k+1})sl_{p,k+1}/(x_{p,k+1} - y_{p,k+1}) \qquad (3.65)$$

Thus, the total solute volume $(ns_{j,k+1})$ (per unit plan area) of node j is computed by summing up the separate contributions of the moving packets lying wholly or partially within the area of influence of
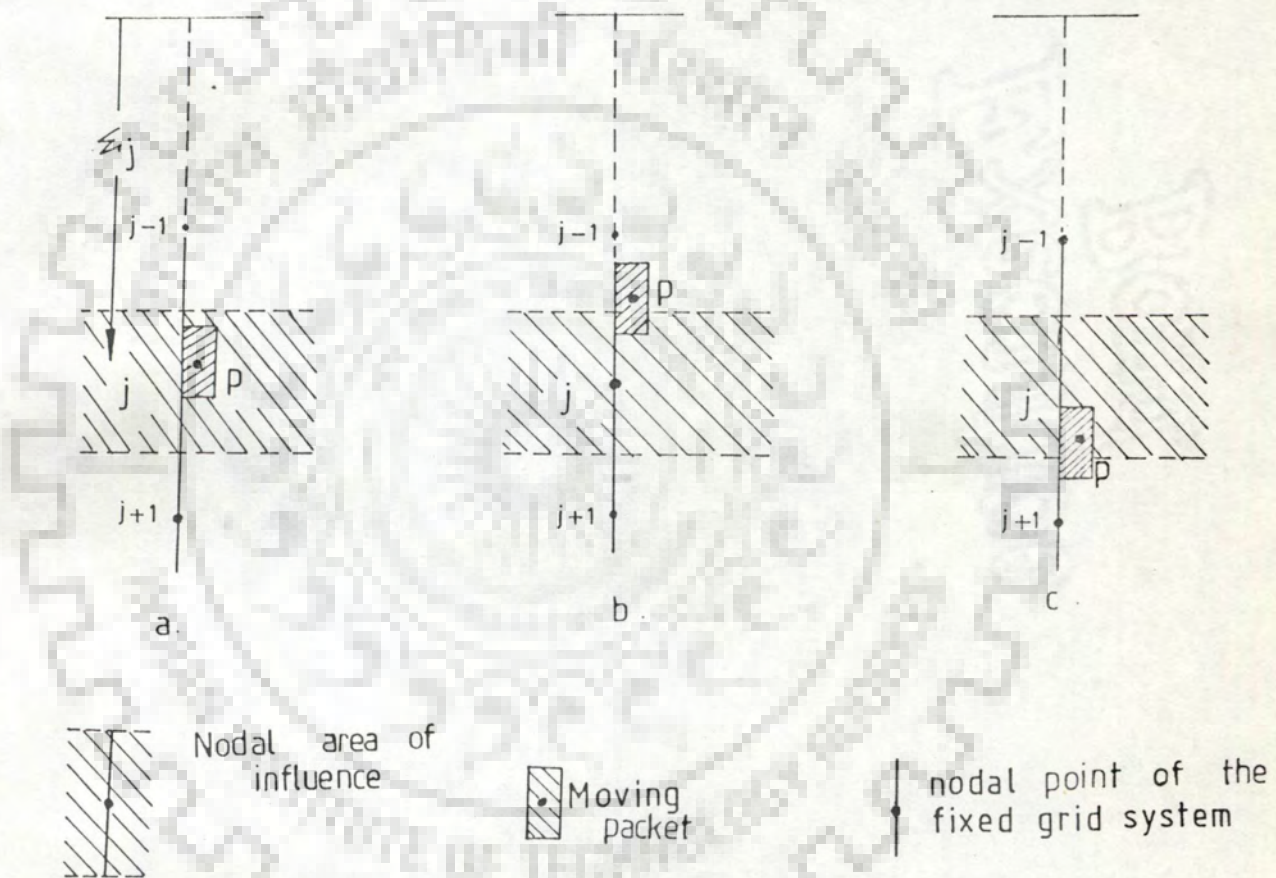
Fig. 3.5. Nodal area of influence and moving packets lying (a) wholly, (b) partially towards the upper side, (c) partially towards the lower side, in it.

node j.

$$ns_{j,k+1} = \sum_{p \in J} xs_{p,k+1} \qquad (3.66)$$

where, J is a subset of moving packets comprising of all the moving packets lying wholly or partially within the area of influence of node j.

The water volume $(nv_{j,k+1})$ (per unit plan area) of jth node is computed using a similar procedure. The separate contributions of water volumes $(xv_{p,k+1})$ (per unit plan area) by different moving packets are computed as,

(a) if

$$\xi_{j-1/2} \leq x_{p,k+1} \leq \xi_{j+1/2}$$
$$\text{and} \quad \xi_{j-1/2} \leq y_{p,k+1} \leq \xi_{j+1/2} \ ,$$

$$xv_{p,k+1} = vl_{p,k+1} \qquad (3.67)$$

(b) if

$$\xi_{j-1/2} < x_{p,k+1} \leq \xi_{j+1/2}$$
$$\text{and} \quad y_{p,k+1} < \xi_{j-1/2} \ ,$$

$$xv_{p,k+1} = (x_{p,k+1} - \xi_{j-1/2})vl_{p,k+1}/(x_{p,k+1} - y_{p,k+1}) \qquad (3.68)$$

(c) if

$$\xi_{j-1/2} \leq y_{p,k+1} < \xi_{j+1/2}$$
$$\text{and} \quad \xi_{j+1/2} < x_{p,k+1} \ ,$$

$$xv_{p,k+1} = (\xi_{j+1/2} - y_{p,k+1})vl_{p,k+1}/(x_{p,k+1} - y_{p,k+1}) \qquad (3.69)$$

Again,

$$nv_{j,k+1} = \sum_{p \in J} xv_{p,k+1} \qquad (3.70)$$

The solute concentration ($cc_{j,k+1}$) at the jth node at $(k+1)^{th}$ discrete time is computed as,

$$cc_{j,k+1} = ns_{j,k+1}/nv_{j,k+1} \qquad (3.71)$$

Similarly, solute concentrations ($cc_{j,k+1}$, $j=1,2,\ldots n$) of all the nodes are computed.

3.4.5.2 Adsorption - desorption of Solute by the Soil Matrix

To further account for first order linear kinetic adsorption - desorption, equation (3.4) is solved. For any interior node j, the finite difference approximation of equation (3.4) can be written as,

$$\frac{s_{j,k+1} - s_{j,k}}{\Delta t_k} = \beta (k_d \, cc_{j,k+1} - s_{j,k+1}) \qquad (3.72)$$

Similarly, writing for all the nodes and solving renders the adsorbed concentration distribution ($s_{j,k+1}$, $j=1,2\ldots n$) of the soil matrix.

Adsorption-desorption of solute by the soil matrix results in a change of solute concentration ($cc_{j,k+1}$, $j = 1,2,\ldots\ldots n$). The volume (per unit plan area) of solute adsorbed ($\Delta sd_{j,k+1}$ is +ve) - desorbed ($\Delta sd_{j,k+1}$ is -ve) at the jth node is computed as,

$$\Delta sd_{j,k+1} = (s_{j,k+1} - s_{j,k})(\rho_j(\Delta z_{j-1} + \Delta z_j)/2) \qquad (3.73)$$

Thus, the solute concentration of the jth node is recomputed

as,

$$c_{j,k+1} = cc_{j,k+1} - \Delta sd_{j,k+1}/nv_{j,k+1} \qquad (3.74)$$

where, $nv_{j,k+1}$ is the nodal water volume (per unit plan area) at node j (refer section 3.4.5.1).

Similarly, writing for all the nodes and solving, the solute concentration distribution ($c_{j,k+1}$, j=1,2...n) accounting for first order linear kinetic adsorption – desorption is obtained.

3.4.5.3 Attributing Change in Nodal Solute Volume (per unit plan area) to the Moving Packets

Change in nodal solute volumes ($\Delta sd_{j,k+1}$, j=1,2...n) (per unit plan area) at all the nodes is attributed to the solute volumes (per unit plan area) of the moving packets as follows.

For any node j,

If $\Delta sd_{j,k+1} < 0$, the solute volume $sl_{p,k+1_{new}}$ of the pth moving packet is computed as,

$$sl_{p,k+1_{new}} = sl_{p,k+1_{old}} + \frac{\Delta x_{p,k+1}}{(\Delta z_{j-1} + \Delta z_j)/2} \Delta sd_{j,k+1} \qquad (3.75)$$

If, $\Delta sd_{j,k+1} > 0$, the solute volume $sl_{p,k+1_{new}}$ (per unit plan area) of the pth moving packet is computed as,

$$sl_{p,k+1_{new}} = sl_{p,k+1_{old}} + \frac{sl_{p,k+1_{old}}}{ns_{j,k+1}} \Delta sd_{j,k+1} \qquad (3.76)$$

Where, $ns_{j,k+1}$ is the solute volume (per unit plan area) at node j (refer section 3.4.5.1).

Similarly, the solute volumes of (per unit plan area) all the moving packets are modified.

3.4.6   Two Phase Non-reactive Solute Transport

The model described previously has been modified to account for two phase non-reactive solute transport. To represent two phase solute transport, the soil moisture (θ) present in the domain is conceptually divided into an immobile and a mobile phase. The soil moisture content in the immobile phase (θ_{im}) is assumed to remain constant. The moisture content in the mobile phase (θ_m) will remain constant for steady state flow conditions (constant θ). However, for unsteady state flow conditions, it will vary as a result of varying θ. Transport of solute in the mobile phase is governed by the process of convection and hydrodynamic dispersion. However, transfer of solute into/out of the immobile phase takes place only through the process of lateral diffusion.

The problem of two phase non-reactive solute transport is defined by equations (3.5)-(3.7) and (3.10), alongwith appropriate boundary conditions. Combining equations (3.5) and (3.7) as follows,

$$\frac{\partial(c_m\theta_m)}{\partial t} = \frac{\partial}{\partial z}(\theta_m D_m \frac{\partial c_m}{\partial z}) - \frac{\partial}{\partial z}(qc_m) - \alpha(c_m - c_{im}) \qquad (3.77)$$

The set of ordinary differential equations to be solved, for solving the above partial differential equation can be written as,

$$\frac{dz}{dt} = \frac{q}{\theta_m} \tag{3.78}$$

$$\frac{d(c_m \theta_m)}{dt} = \frac{\partial}{\partial z} (\theta_m D_m \frac{\partial c_m}{\partial z}) - \alpha (c_m - c_{im}) \tag{3.79}$$

Equations (3.78) and (3.79) are first solved neglecting the second term on the R.H.S of equations (3.79) (i.e., neglecting transfer of solute into/out of the immobile phase).

3.4.6.1 Convective Transport

The solution follows directly from section 3.4.4.1 with θ being replaced by θ_m. The equations modified as a consequence of such replacements are as follows.

$$vl_{p,k} = (x_{p,k} - y_{p,k}) \theta_{m_{p,k}} \tag{3.80}$$

[refer eqn. (3.19)]

where, $\theta_{m_{p,k}} = \theta_{p,k} - \theta_{im}$

$$cw_{j,k+1} = \sum_{i=2}^{J} \frac{(\theta_i - \theta_{im}) + (\theta_{i-1} - \theta_{im})}{2} . \Delta z_{i-1} \tag{3.81}$$

[refer eqn. (3.21)]

$$\hat{c}_{m_{p,k+1}} = sl_{p,k+1} / vl_{p,k+1} \tag{3.82}$$

[refer eqn. (3.49)]

3.4.6.2 Diffusive-Dispersive Transport

The solution follows directly from section 3.4.4.2 with θ being replaced by θ_m. The equations modified as a consequence of such

replacements are as follows.

$$\frac{c_{m_{p,k+1}} \theta_{m_{p,k+1}} - \hat{c}_{m_{p,k+1}} \theta_{m_{p,k+1}}}{\Delta t_k} = \left[(\theta_{m_{p-1,k+1}} + \theta_{m_{p,k+1}})/2 \right.$$

$$D_{m_{p-1/2,k+1}} \frac{c_{m_{p-1,k+1}} - c_{m_{p,k+1}}}{(\Delta x_{p-1,k+1} + \Delta x_{p,k+1})/2} - (\theta_{m_{p,k+1}} + \theta_{m_{p+1,k+1}})/2$$

$$D_{m_{p+1/2,k+1}} \frac{c_{m_{p,k+1}} - c_{m_{p+1,k+1}}}{(\Delta x_{p,k+1} + \Delta x_{p+1,k+1})/2} \left. \right] \frac{1}{\Delta x_{p,k+1}} \tag{3.83}$$

[refer eqn. (3.50)]

$$\theta_{m_{p,k+1}} = vl_{m_{p,k+1}}/\Delta x_{p,k+1} \tag{3.84}$$

[(refer eqn. (3.52)]

$$D_{m_{p+1/2,k+1}} = D_o a e^{b(\theta_{m_{p,k+1}} + \theta_{m_{p+1,k+1}})/2} + \lambda \left| v_{m_{p+1/2,k+1}} \right|$$

$$\tag{3.85}$$

[refer eqn. (3.53)]

$$v_{m_{p+1/2,k+1}} = (y_{p,k+1} - y_{p,k})/\Delta t_k \tag{3.86}$$

[refer eqn. (3.54)]

$$D_{m_{p-1/2,k+1}} = D_o a e^{b(\theta_{m_{p-1,k+1}} + \theta_{m_{p,k+1}})/2} +$$

$$\lambda \left| v_{m_{p-1/2,k+1}} \right| \tag{3.87}$$

[refer eqn. (3.55)]

$$v_{m_{p-1/2,k+1}} = (x_{p,k+1} - x_{p,k})/\Delta t_k \tag{3.88}$$

[refer eqn. (3.56)]

$$\frac{c_{m_{np,k+1}} \theta_{m_{np,k+1}} - \hat{c}_{m_{np,k+1}} \theta_{m_{np,k}}}{\Delta t_k} = \left[(\theta_{m_{np,k+1}} + \theta_{m_{np-1,k+1}})/2 \right.$$

$$\left. D_{m_{np-1/2}} \frac{c_{m_{np,k+1}} - c_{m_{np-1,k+1}}}{(\Delta x_{np,k+1} + \Delta x_{np-1,k+1})/2} \right] \frac{2}{\Delta x_{np,k+1}}$$

$$\tag{3.89}$$

[refer eqn. (3.57)]

$$\frac{c_{m_{1,k+1}} \theta_{m_{1,k+1}} - \hat{c}_{m_{1,k+1}} \theta_{m_{1,k}}}{\Delta t_k} = \left[(\theta_{m_{1,k+1}} + \theta_{m_{2,k+1}})/2 \right.$$

$$\left. D_{m_{1+1/2}} \frac{c_{m_{1,k+1}} - c_{m_{2,k+1}}}{(\Delta x_{2,k+1} + \Delta x_{1,k+1})/2} \right] \frac{2}{\Delta x_{1,k+1}} \tag{3.90}$$

[refer eqn. (3.58)]

$$sl_{p,k+1} = c_{m_{p,k+1}} vl_{p,k+1} \tag{3.91}$$

[refer eqn. (3.59)]

3.4.6.3 Computation of Nodal Concentration

Nodal solute concentrations are computed following section 3.4.5.1.

$$cc_{m_{j,k+1}} = ns_{j,k+1}/nv_{j,k+1} \tag{3.92}$$

[refer eqn. (3.68)]

3.4.6.4 Transfer of Solute into/out of the Immobile Phase due to Lateral Diffusion

To further account for transfer of solute into/out of the immobile phase, equation (3.7) is solved. For any interior node j the difference approximation of equation (3.7) can be written as,

$$\theta_{im} \frac{c_{im_{j,k+1}} - c_{im_{j,k}}}{\Delta t_k} = \alpha \left(cc_{m_{j,k+1}} - c_{im_{j,k}} \right) \tag{3.93}$$

Similarly, writing for all the nodes and solving renders the concentration distribution ($c_{im_{j,k+1}}$, $j=1,2........n$) of the immobile phase.

Transfer of solute into/out of the immobile phase results in a change of mobile solute concentration ($cc_{m_{j,k+1}}$, $j=1,2.....n$). The volume of solute (per unit plan area) transferred into ($\Delta cd_{j,k+1}$ is +ve)/out of ($\Delta cd_{j,k+1}$ is -ve) the immobile solute phase, at node j is computed as,

$$\Delta cd_{j,k+1} = \left(c_{im_{j,k+1}} - c_{im_{j,k}} \right) . \theta_{im} (\Delta z_{j-1} + \Delta z_j)/2 \tag{3.94}$$

Thus, the mobile solute concentration at the node j is computed as,

$$c_{m_{j,k+1}} = cc_{m_{j,k+1}} - \Delta cd_{j,k+1}/nv_{j,k+1} \tag{3.95}$$

Where, $nv_{j,k+1}$ is the volume of water (per unit plan area) at node j (refer section 3.4.5.1).

Similarly, writing for all the nodes and solving, the mobile

solute concentration distribution ($c_{m_{j,k+1}}$,j=1,2.....n) accounting for transfer of solute into/out of the immobile phase is obtained.

3.4.6.5 Attributing Change in Nodal Solute Volumes (per unit plan area) to Moving Packets

Change in solute volume (per unit plan area) in the mobile phase ($\Delta cd_{j,k+1}$,j=1,2.....n) at all the nodes is further attributed to the solute volumes (per unit plan area) of the moving packets. Thus, the solute volumes (per unit plan area) of all the moving packets are modified, following the procedure described in section 3.4.5.3.

3.4.7 Two Phase Reactive (linear equilibrium adsorption-desorption) Solute Transport.

The model was further modified to account for linear equilibrium adsorption-desorption during two phase solute transport. The problem is defined by equations (3.8), (3.9) and (3.10) alongwith appropriate boundary conditions. Combining equations (3.8) and (3.9) as follows,

$$\frac{\partial c_m (\theta_m + \rho f k_d)}{\partial t} = \frac{\partial}{\partial z}(\theta_m D_m \frac{\partial c_m}{\partial z}) - \frac{\partial}{\partial z}(qc_m)$$
$$- \alpha (c_m - c_{im}) \qquad (3.96)$$

The set of ordinary differential equations to be solved, for solving the above partial differential equation can be written as,

$$\frac{dz}{dt} = \frac{q}{(\theta_m + \rho f k_d)} \qquad (3.97)$$

$$\frac{dc_m(\theta_m + \rho fk_d)}{dt} = \frac{\partial}{\partial z}\left(\theta_m D_m \frac{\partial c_m}{\partial z}\right) - \alpha(c_m - c_{im}) \qquad (3.98)$$

Equations (3.97) and (3.98) are first solved neglecting the second term on the R.H.S of equation (3.98) (i.e., neglecting transfer of solute into/out of the immobile phase and subsequent adsorption-desorption), which are accounted for subsequently.

3.4.7.1   Convective transport

The solution follows directly from section 3.4.4.1 and section 3.4.6.1 with θ_m being replaced by $(\theta_m + \rho fk_d)$. The equations modified as a consequence of such replacements are as follows.

$$vl_{p,k} = (x_{p,k} - y_{p,k})(\theta_{m_{p,k}} + \rho fk_d) \qquad (3.99)$$

[refer eqn. (3.80)]

$$cw_{j,k+1} = \sum_{i=2}^{j} \frac{[(\theta_i - \theta_{im}) + \rho fk_d] + [(\theta_{i-1} - \theta_{im}) + \rho fk_d]}{2} \Delta z_{i-1}$$

$$(3.100)$$

[refer eqn. (3.81)]

$$\hat{c}_{m_{p,k+1}} = sl_{p,k+1}/vl_{p,k+1} \qquad (3.101)$$

[refer eqn 3.49)]

3.4.7.2   Diffusive-Dispersive Transport

The solution follows directly from section 3.4.4.2 and 3.4.6.2 with θ_m being replaced by $(\theta_m + \rho fk_d)$, as and when required. The equations modified as a consequence of such replacements are as follows.

$$\frac{c_{m_{p,k+1}}(\theta_{m_{p,k+1}} + \rho f k_d) - \hat{c}_{m_{p,k+1}}(\theta_{m_{p,k}} + \rho f k_d)}{\Delta t_k} =$$

$$\left[\frac{(\theta_{m_{p-1,k+1}} + \theta_{m_{p,k+1}})}{2} D_{m_{p+1/2,k+1}} \frac{c_{m_{p-1,k+1}} - c_{m_{p,k+1}}}{(\Delta x_{p-1,k+1} + \Delta x_{p,k+1})/2} \right.$$

$$\left. - \frac{(\theta_{m_{p,k+1}} + \theta_{m_{p+1,k+1}})}{2} D_{m_{p+1/2,k+1}} \frac{c_{m_{p,k+1}} - c_{m_{p+1,k+1}}}{(\Delta x_{p,k+1} + \Delta x_{p+1,k+1})/2} \right]$$

(3.102)

[refer eqn. (3.83)]

$$\theta_{m_{p,k+1}} = vl_{p,k+1}/\Delta x_{p,k+1} - \rho f k_d$$ (3.103)

[refer eqn. (3.84)]

$$\frac{c_{m_{np,k+1}}(\theta_{m_{np,k+1}} + \rho f k_d) - \hat{c}_{m_{np,k+1}}(\theta_{m_{np,k}} + \rho f k_d)}{\Delta t_k} =$$

$$\left[\frac{(\theta_{m_{np,k+1}} + \theta_{m_{np-1,k+1}})}{2} D_{m_{np-1/2,k+1}} \right.$$

$$\left. \frac{c_{m_{np,k+1}} - c_{m_{np-1,k+1}}}{(\Delta x_{np,k+1} + \Delta x_{np,k+1})/2} \right] \frac{2}{\Delta x_{np,k+1}}$$ (3.104)

[refer eqn. (3.89)]

$$\frac{c_{m_{1,k+1}}(\theta_{m_{1,k+1}} + \rho f k_d) - \hat{c}_{m_{1,k+1}}(\theta_{m_{1,k}} + \rho f k_d)}{\Delta t_k} =$$

$$\left[\frac{\theta_{m_{1,k+1}} + \theta_{m_{2,k+1}}}{2} D_{m_{1+1/2,k+1}} \frac{c_{m_{1,k+1}} - c_{m_{2,k+1}}}{(\Delta x_{1,k+1} + \Delta x_{2,k+1})/2}\right] \frac{2}{\Delta x_{1,k+1}}$$

(3.105)

[refer eqn.(3.89)]

3.4.7.3 Computation of Nodal Concentration

Nodal solute concentrations are computed following section 3.4.5.1.

$$cc_{m_{j,k+1}} = ns_{j,k+1}/nv_{j,k+1}$$

(3.106)

[refer eqn.(3.89)]

3.4.7.4 Transfer of Solute into/out of the immobile Phase due to Lateral diffusion (accounting for linear equilibrium adsorption-desorption)

To further account for transfer of solute into/out of the immobile phase (accounting for linear equilibrium adsorption-desorption), equation (3.9) is solved. For any interior node j the difference approximation of equation (3.9) is written as,

$$(\theta_{im} + \rho(1-f)k_d) \frac{c_{im_{j,k+1}} - c_{im_{j,k}}}{\Delta t_k} = \alpha(cc_{m_{j,k+1}} - c_{im_{j,k+1}})$$

(3.107)

[refer eqn.(3.93)]

Similarly, writing for all the nodes and solving renders the concentration distribution $(c_{im_{j,k+1}}, j=1,2......n)$ of the immobile phase (accounting for linear equilibrium adsorption-desorption).

Transfer of solute into/out of the immobile phase results in a change of mobile solute concentration $(cc_{m_{j,k+1}}, j=1,2.....n)$. The volume of solute (per unit plan area) transferred into $(\Delta cd_{j,k+1}$ is +ve)/out of $(\Delta cd_{j,k+1}$ is -ve) the immobile solute phase (accounting for linear equilibrium adsorption-desorption), at node j is computed as,

$$\Delta cd_{j,k+1} = (c_{im_{j,k+1}} - c_{im_{j,k}})(\theta_{im} + \rho(1-f)k_d)(\Delta z_{j-1} + \Delta z_j)/2$$

(3.108)

[refer eqn.(3.94)]

Thus, the mobile solute concentration at node j is computed as,

$$c_{m_{j,k+1}} = cc_{m_{j,k+1}} - \Delta cd_{j,k+1}/nv_{j,k+1}$$

(3.109)

[refer eqn.(3.95)]

Similarly, writing for all the nodes and solving, the mobile solute concentration distribution $(c_{m_{j,k+1}}, j=1,2.......n)$ accounting for transfer of solute into/out of the immobile phase and linear equilibrium adsorption-desorption is obtained.

3.4.7.5 Attributing Change in Nodal Solute Volumes (per unit plan area) to Moving Packets

Change in solute volume (per unit plan area) in the mobile phase $(\Delta cd_{j,k+1}, j=1,2.....n)$ at all the nodes is further attributed to the solute volumes (per unit plan area) of the moving packets. Thus, the

solute volumes (per unit plan area) of all the moving packets are modified, following the procedure described in section 3.4.5.3.

3.5   Mass Balance

Mass balance calculations were performed to check the accuracy of the solution. The principle of conservation requires that the difference between the solute inflowing into and outflowing from a spatial domain in a given time must equal the change of solute in the domain at the same time. Thus, considering a spatial domain extending from the ground surface to water table,

| Total solute volume (per unit plan area) infiltrated into the unsaturated zone at the ground surface. (SV_{inf}) | − | Total solute volume (per unit plan area) joining the _water_ table. (SV_{efl}) | = | Change in solute volume (per unit plan area) in the domain. (ΔSV) |

The relative mass balance error (ERR) was computed as follows,

$$ERR(\%) = \frac{SV_{inf} - SV_{ef} - \Delta SV}{SV_{inf}}$$

The relative mass balance error is computed at the end of each time step as follows,

(a)   The total solute volume (per unit plan area) infiltrated into the system till any discrete time t_k is computed by integrating the product of infiltration rate (q) and the concentration (c_o) of the infiltrating solute ($\int_o^{t_k} q\, c_o\, dt$).

(b)   The change in solute volume (per unit plan area) in the domain at any discrete time t_k, for the four different stages of the model are computed as follows.

Stage I

Change in solute volume (per unit plan area)

$$= \sum_{p=1}^{np} sl_{p,k} + sl_k^* - \sum_{p=1}^{np} sl_{p,0}$$

Stage II

Change in solute volume (per unit plan area)

$$= \sum_{p=1}^{np} sl_{p,k} + sl_{p,k}^* - \sum_{p=1}^{np} sl_{p,0} + \sum_{j=1}^{n} s_{j,k} \rho (\Delta z_{j-1} + \Delta z_j)/2$$

$$- \sum_{j=1}^{n} s_{j,0} \rho (\Delta z_{j-1} + \Delta z_j)/2$$

Stage III

Change in solute volume (per unit plan area)

$$= \sum_{p=1}^{np} sl_{p,k} + sl_{p,k}^* - \sum_{p=1}^{np} sl_{p,0} + \sum_{j=1}^{n} c_{im_{j,k}} \theta_{im} (\Delta z_{j-1} + \Delta z_j)/2$$

$$- \sum_{j=1}^{n} c_{im_{j,0}} \theta_{im} (\Delta z_{j-1} + \Delta z_j)/2$$

Stage IV

Change in solute volume (per unit plan area)

$$= \sum_{p=1}^{np} sl_{p,k} + sl_{p,k}^* - \sum_{p=1}^{np} sl_{p,0} + \sum_{j=1}^{n} c_{im_{j,k}} [\rho(1-f)k_d \theta_{im}]$$

$$(\Delta z_{j-1} + \Delta z_j)/2 - \sum_{j=1}^{n} c_{im_{j,0}} [\rho(1-f)k_d \theta_{im}](\Delta z_{j-1} + \Delta z_{j+1})/2$$

(c)   The solute volumes (per unit plan area) joining, the water table till different discrete times are computed throughout the simulation period (refer section 3.4.4.1.3).

3.6   MODEL PARAMETERS

For simulation of spatial and temporal variation of concentration using the numerical model described so far, the following parameters are required.

D   -   hydrodynamic dispersion

D is expressed by equation (3.2) and in turn requires parameters D_o, a, b, and λ.

D_o -   molecular diffusion coefficient in a free water system.

a
b $\Big\}$ -   empirical constants characterizing the soil.

λ -   dispersivity

β -   first order rate coefficient governing exchange between solute and soil matrix (kinetic adsoprtion-desorption)

k_d -   empirical distribution coefficient

α -   first order rate coefficient governing exchange of solute between mobile and immobile phase.

f   -   fraction of adosprtion sites, located in the mobile phase.

θ_{im} -   immobile moisture content.

3.7.   COMPUTER CODE

The computer code for performing the calculations of the distributed model, has been written in FORTRAN IV. The program consists of four functions, twelve subroutines and a main program. Role of the

main program and each subroutine is described briefly in the following paragraphs.

3.7.1   MAIN PROGRAM

The following tasks are performed.

1.   Reading of input data. The details of the read statements are as follows.

(i)   NDP: number of nodes in the flow domain, NMAX: number of nodes in the solute domain, NT: Number of time steps, NOB: number of daily observations, ITR: maximum number of iterations used in Picard's iteration method; Conditional switches [IOPT = 0: Neuman boundary condition, IOPT=2: Dirichlet boundary condition, NWTV = 1: time variant water table (Default time invariant water table), NETS=1: evapotranspiration not occounted for (default evapotranspiration accounted for, NMKT=1: linear kinetic adsorption-desorption not accounted for (default linear kinetic adsopriton-desorption accounted for)].

(ii)   DTM: time step, TOTIRR: time duration of a single irrigation application, EPS: small positive value for defining permissible error in Picard's iteration method.

(iii)   POR(ϕ): porosity (L^3L^{-3}), SAT(K_s): saturated capillary conductivity (LT^{-1}), SSM(h_b): bubbling pressure (L), FFC (θ_{fc}): field capacity (L^3L^{-3}), WP (θ_{wp}): wilt point of the crop (L^3L^{-3}), THR (θ_r): residual moisture content (L^3L^{-3}), PAT: minutes in a day (T).

(iv)   CO(c_o): input solute concentration (ML^{-3}), TSTR(ts): strip thickness, parameters [THC (θ_{im}): immobile moisture content (L^3L^{-3}); DO(D_o): molecular diffusion coefficient in a free water system, (AO(a),A10(b)): empirical constants characterizing the soil, AML(λ):

dispersivity (L), p(f): fraction of adsorption sites located in the mobile soil matrix, RO(ρ): bulk density of soil (ML^{-3}), CONS (k_d): empirical distribution coefficient (L^3M^{-1})].

(v)   DELZ (Δz): spatial increment for solving flow equation (L).

(vi) HPR1(h): cpillary pressure at the beginning of simulation/a time step (L^3L^{-3}).

(vii)   DZS (Δz): spatial increment for solving solute transport equation (L).

(viii)   CI(c_i): initial concentration distribution in the soil profile (ML^{-3}).

2.   Computation of nodal depth co-ordinates and nodal area of influence.

3.   Computation of total number of moving packets, upper and lower coordinates of each moving packet, water volumes and solute volumes (per unit plan area) contained in the moving packets, cumulative water volumes (per unit plan area) corresponding to coordinates.

4.   Computation of nodal solute and water volumes (per unit plan area).

5.   Reading daily input data. Details of the read statements are as follows.

(i)   NYR : year of simulation, NMNTH: month of simulation, NDT: date of simulation, RAIN: rainfall intensity (daily), PET: potential evapotranspiration (daily), PF: P factor, API: depth of applied irrigation.

(ii)   RZD: root zone depth, NOROOT: node number at which root zone ends.

6.   Computation of number of nodes in the flow domain, in case of

time variant water table.

7.   Computation of capillary head and moisture distribution, accounting for evapotranspiration, if required.

8.   Computation of cumulative water volume (per unit plan area) profile, based on moisture distribution.

9.   Modifying water volumes (per unit plan area) of moving packets lying in the root zone caused by evapotranspiration and subsequent modification of cumulative water volumes (per unit plan area) corresponding to coordinates, if required.

10.   Computation of solute concentration by solving for the various components of transport.

11.   Printing the computed results.

3.7.2   SUBROUTINES

DPEC :   Computes nodal depths and upper and lower limits of the nodal areas of influence. Data supplied are total number of nodes and nodal spacing for the solute domain.

INICON: Computes total number of moving packets, their upper and lower coordinates, moisture contents, solute and water volumes (per unit plan area)contained in them and the cumulative water volumes (per unit plan area)correponding to the coordinates. Data supplied are strip-thikness, total depth of domain, initial concentration and moisture distributions.

VOLSOL: Computes nodal concentration, solute and water volumes (per unit plan area). Data supplied are the output of INICON, total number of nodes and nodal area of influence.

WATBLE   Computes total number of nodes in the domain, additional nodal spacing and capillary head values, in case of a fluctuating

water table. Data supplied are depths to water table (before and after fluctuation), number of nodes and nodal spacing (before fluctuation).

SOLVE   Computes the latest capillary head and moisture distribution. Data supplied are capillary head and moisture distribution at the beginning of the time step, upper and lower boundary conditions at the beginning of the time step, maximum permissible number of iterations for Picard's iteration method, permissible convergence error and time step.

SINK   Computes nodal values of evapotranspiration (restricted to the root zone depth). Data supplied are depth of root zone, node number at which the root zone ends, moisture content values at the beginning and end of the time step/iteration, daily value of potential evapotranspiration, wilt point of the crop, field capacity of the soil, residual moisture content, nodal area of influence and time step.

TRANS   Computes the latest solute concentration distribution. Data supplied are input flux, input concentration, total number of nodes in the solute domain, total number of moving packets, their upper and lower coordinates, the solute and water volumes (per unit plan area) contained in the moving packets, the cumulative water volumes (per unit plan area) corresponding to the coordinates, total depth of solute domain, the amount of solute which has already left the domain, nodal area of influence, nodal spacing, strip thickness, molecular diffusion coefficient, empirical constants characterizing the soil, dispersivity, bulk density of soil, empirical distribution coefficient, first order rate

98

coefficient governing exchange of solute between solute and soil matrix, immobile moisture content, rate coefficient governing transfer of solute into/out of the immobile phase fraction of the adsorption sites located in the mobile phase.

MCURVE   Computes the cumulative water content profile based on the nodal moisture distribution, obtained by solving Richards equation. Data supplied are latest moisture distribution, nodal spacing, immobile moisture content value, bulk density of soil, fraction of adsorption sites located in the mobile phase and empirical distribution coefficient.

MODCOR   Increments cumulative water volumes (per unit plan area) corresponding to the coordinates and computes their latest positions. Data supplied are input flux, cumulative water volumes (per unit plan area) corresponding to the coordinates at the beginning of the time step and the output of subroutine MCURVE.

MODSOL   Modifies solute volumes (per unit plan area) of the moving packets. Data supplied are solute volumes (per unit plan area) of the moving packets at the beginning of the time step and change in nodal solute volume (per unit plan area).

DONNA   Carries out linear iterpolation.

BST   Solves the tridiagonal coefficient matrix.

3.7.3   FUNCTIONS

THETA   Computes moisture content values corresponding to the supplied capillary head value. Other data supplied are porosity, residual moisture content, bubbling pressure (in accordance with the h vs θ relation).

COND   Computes capillary conductivity values corresponding to the supplied moisture content values. Other data supplied are porosity, residual moisture content, saturated capillary conductivity (in accordance with the K vs θ relation).

DIFU   Computes specific moisture capacity corresponding to the capillary head values at the beginning and end of the time step. Other data supplied are porosity, residual moisture content, bubbling pressure (in accordance with the h vs θ relation).

TREP   Computes change in moisture storage. Data supplied are moisture distribution at the beginning and end of a time step, number of nodes and nodal spacing.

For listing of the computer code refer to annexure 2.

CHAPTER 4

MODEL VALIDATION

The model described in chapter 3 was validated by comparing the simulated results with available analytical solutions and reported experimental data.

4.1 COMPARISON WITH ANALYTICAL SOLUTIONS

The model simulated transport was compared with the results of two analytical solutions (van Genuchten and Alves, 1982 cited in Parker and van Genuchten, 1984 and Parker and van Genuchten, 1984). Both the analytical solutions have been programmed by Parker and van Genuchten, 1984 and are contained in a package called CXTFIT. Thus, CXTFIT was used to obtain the spatial and temporal distributions pertaining to the analytical solutions. The model was operated under conditions consistent with the assumptions of the analytical solutions.

4.1.1 van Genuchten and Alves' Solution (van Genuchten and Alves, 1982 cited in Parker and van Genuchten, 1984)

The solution pertains to single phase reactive solute transport under steady state flow conditions. The interaction between solute and soil matrix is described by a linear equilibrium adsorption-desorption isotherm. The source/sink term accounted for are first order decay and zero order production. The details of the solution are as follows.

4.1.1.1 Differential Equation

The differential equation governing one dimensional solute transport under conditions described above is written as,

$$R \frac{\partial c}{\partial t} = D \frac{\partial^2 c}{\partial z^2} - v \frac{\partial c}{\partial z} - \mu c + \gamma \qquad (4.1)$$

where, v is the steady state velocity

The dimensionless factor R is defined as,

$$R = 1 + \frac{k_d}{\theta}$$

and

$$\mu = \mu_\omega + \mu_s \frac{k_d}{\theta}$$

$$\gamma = \gamma_\omega + \gamma_s \frac{\rho}{\theta}$$

where, μ_ω and μ_s are rate constants for first order decay in the solute and soil matrix respectively, γ_ω and γ_s are rate constants for zero order production in the solute and soil matrix respectively.

Neglecting the source/sink terms μ and γ and assuming R to be 1, equation (4.1) reduces to the form of equation (3.1).

4.1.1.2 Initial and Boundary Conditions

The initial condition is assumed to be of the form,

$$c(z, o) = c_i \qquad (4.2)$$

where, c_i is a constant

For a pulse type input the upper boundary condition is written as,

$$c - \frac{D}{v} \left. \frac{\partial c}{\partial z} \right|_{z=0} = \begin{cases} c_o & 0 < t \le t_o \\ 0 & t > t_o \end{cases} \qquad (4.3)$$

where, c_o is the input concentration and is a constant.

For a semi-infinite system the lower boundary condition is written as,

$$\frac{\partial c}{\partial z} (\infty, t) = \text{finite} \qquad (4.4)$$

4.1.1.3 Assumptions

The solution of equation (4.1) subject to the initial and boundary conditions described in equations 4.2 - 4.4 is based upon the following assumptions.

(i)   Flow velocity is time independent.

(ii)   Soil medium is homogeneous.

(iii)   The system is semi-infinite.

(iv)   Backmixing at the exit boundary is negligible.

4.1.1.4 Analytical solution

For $\mu = 0$ and subject to boundary and initial conditions (4.2), (4.3) and (4.4), the solution of equation (4.1) is reported as follows.

$$c(z,t) = \begin{cases} c_i + (c_o - c_i)A(z,t) + B(z,t) & 0 < t < t_o \\ \\ c_i + (c_o - c_i)A(z,t) + B(z,t) - c_o A(z, t-t_o) & t > t_o \end{cases} \qquad (4.5)$$

Where,

$$A(z,t) = \frac{1}{2}\,erfc\left[\frac{Rz - vt}{2(DRt)^{1/2}}\right] + \left(\frac{v^2 t}{\pi DR}\right)^{1/2}\exp\left[-\frac{(RZ-vt)^2}{4DRt}\right]$$

$$-\frac{1}{2}\left(1+\frac{vz}{D} + \frac{v^2 t}{DR}\right)\exp\left(\frac{vz}{D}\right)erfc\left[\frac{Rz + vt}{2(DRt)^{1/2}}\right]$$

$$B(z,t) = \frac{\gamma}{R}\left\{ t + \left(\frac{Rz}{2v} - \frac{t}{2} + \frac{DR}{2v^2}\right)erfc\left[\frac{Rz - vt}{2(DRt)^{1/2}}\right]\right.$$

$$- \left(\frac{t}{4\pi DR}\right)^{1/2}\left(Rz + vt + \frac{2DR}{v}\right)\exp\left[-\frac{(Rz - vt)^2}{4DRt}\right]$$

$$+ \left[\frac{t}{2} - \frac{DR}{2v^2} + \frac{(Rz + vt)^2}{4DR}\right]\exp\left(\frac{vz}{D}\right)erfc\left[\frac{Rz + vt}{2(DRt)^{1/2}}\right]\left.\right\}$$

4.1.1.5   Model Operation

The model accounting for single phase non-reactive solute transport (refer section 3.4.4) was operated under the following conditions.

4.1.1.5.1 Time and space Domains

The depth of the solution domain was taken as 180 cms. At the beginning of simulation the domain was subdivided into 180 moving packets using a strip thickness (ts) of 1 cm.

The total time duration of each simulation was 1980 mins. A time step of 1 min was used. However, to check the effect of a large time step, the simulations were repeated using a time step of 15 mins.

4.1.1.5.2 Parameter values

The following parameter values were used for simulation.

$$a = 0.002$$

$$b = 10.0$$

$$D_o = 0.000667 \ cm^2/min.$$

For λ, a range of values, 0.0, 0.1, 0.5 and 1.0 cms, was taken.

4.1.1.5.3 Initial and Boundary Conditions

$$c_i(z,0) = 0.0 \qquad\qquad 0 \le z \le Z \qquad\qquad (4.6)$$

where, Z (180 cm) is the total depth of the domain.

The upper boundary condition is a pulse type input, and is written as,

$$qc - \theta D \left.\frac{\partial c}{\partial z}\right|_{z=0} = \begin{cases} qc_o & d_{in} \le x \\ 0 & d_{in} > x \end{cases} \qquad\qquad (4.7)$$

where, c_o is the concentration of the infiltrated solute , d_{in} is the depth of infiltration and x is the depth of the solute to be infiltrated.

If t_o is the time taken for x cms of solute to infiltrate and θ and q are time independent, eqn(4.7) can be written as,

$$c - \frac{D}{v}\left.\frac{\partial c}{\partial z}\right|_{z=0} = \begin{cases} c_o & t \le t_o \\ 0 & t > t_o \end{cases} \qquad\qquad (4.8)$$

where, $v = q/\theta$

Thus, the boundary conditions described by eqns (4.7) and (4.3) are the same.

The following values were assigned.

$$c_o = 209 \text{ meq/l}$$

$$x = 7.62 \text{ cms}$$

The solute was followed by fresh water infiltration till the end of simulation. The soil moisture content θ is maintained constant at 0.38. The corresponding value of q is 0.026 cm/min.

The lower boundary condition is assigned as,

$$\frac{\partial c(Z,t)}{\partial z} = 0 \qquad\qquad (4.9)$$

4.1.1.5.4 Results

(i)   The model computed variation of c with respect to z at times 120,540,1020 and 1980 mins are presented in Figs. 4.1-4.4 (Δt=1 min) and Figs. 4.5-4.8 (Δt=15 mins).

(ii)   Breakthrough curves at depths 20,40,60,80 and 100 cms are presented in Figs. 4.1-4.4 (Δt=1 min) and Figs 4.5-4.8 (Δt=15 mins).

4.1.1.6   Computation of Analytical Solution

CXTFIT was used to obtain c vs z and c vs t curves for identical parameters.

4.1.1.6.1 Parameter Values

For the solution [described by equation (4.5)] to be valid for single phase non-reactive solute transport, the dimensionless parameter R was assigned a value of 1 and γ was assigned a value of 0.

The parameters v and D were computed for the pre-assigned values of θ,q (refer section 4.1.1.5.3), a,b,D_o and λ (refer section 4.1.1.5.2).

$$v = q/\theta = 0.0684 \text{ cm/min.}$$
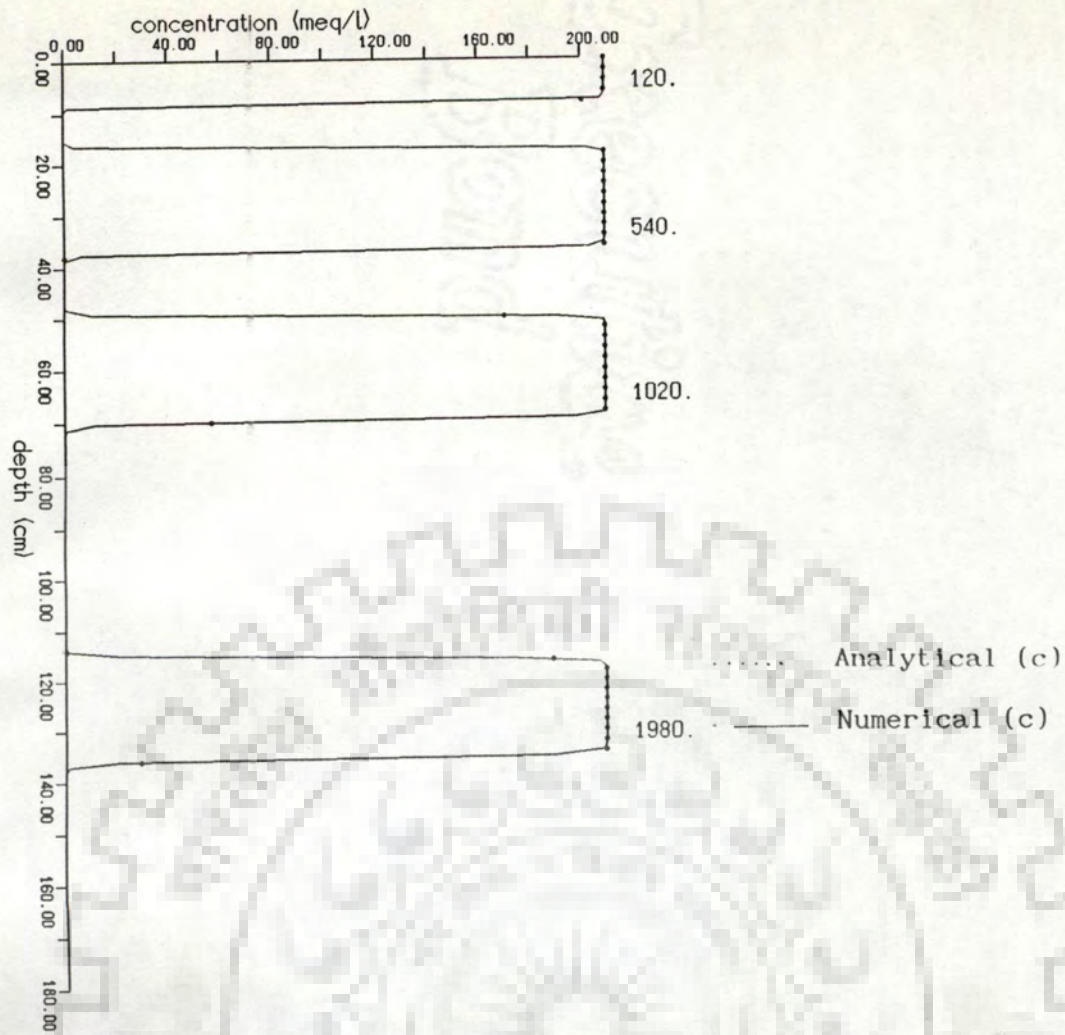
Concentration profile
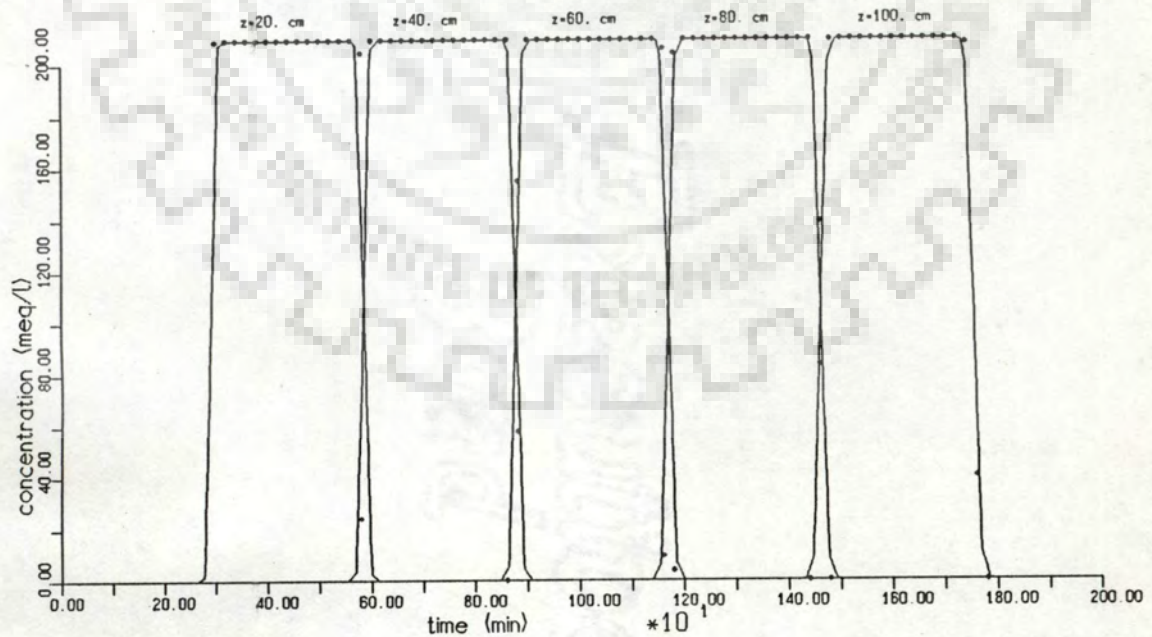
Concentration breakthrough curve

Fig. 4.1. Comparison with analytical solution for single phase non -reactive solute transport (λ=0.0 cm, Δt=1.0 min).

concentration (meq/l)

Concentration profile

Concentration breakthrough curve
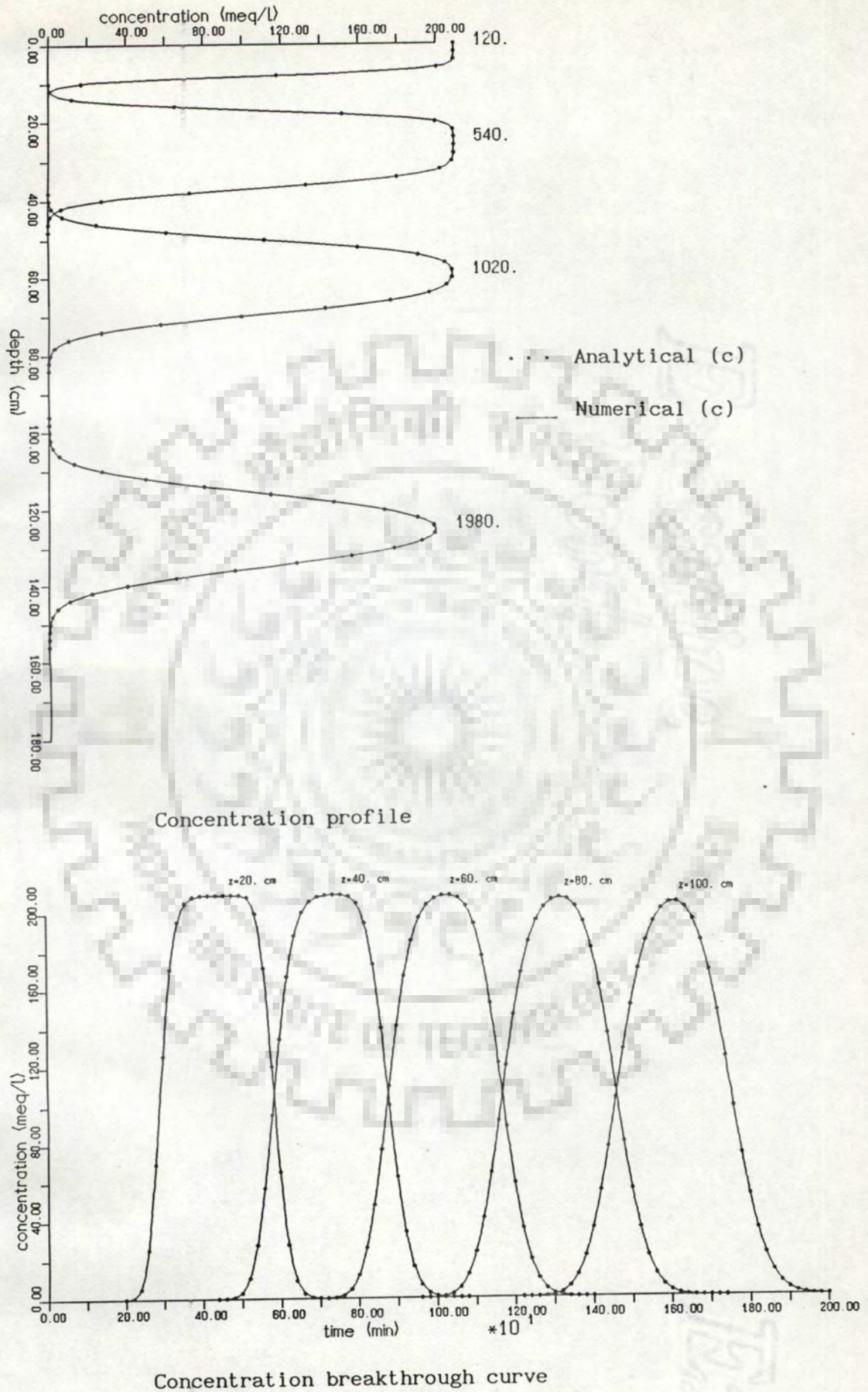
Fig. 4.2. Comparison with analytical solution for single phase non -reactive solute transport ($\lambda=0.1$ cm, $\Delta t=1.0$ min).
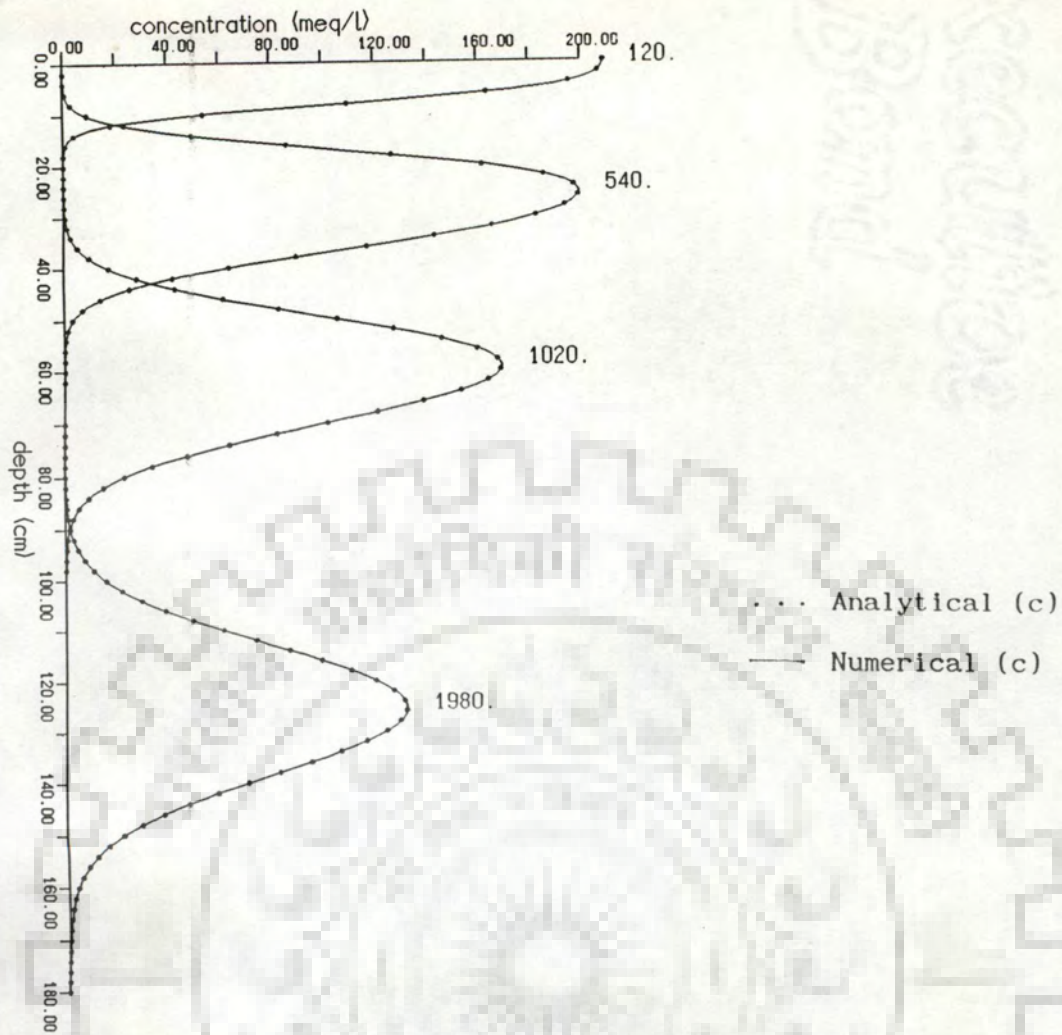
Concentration profile
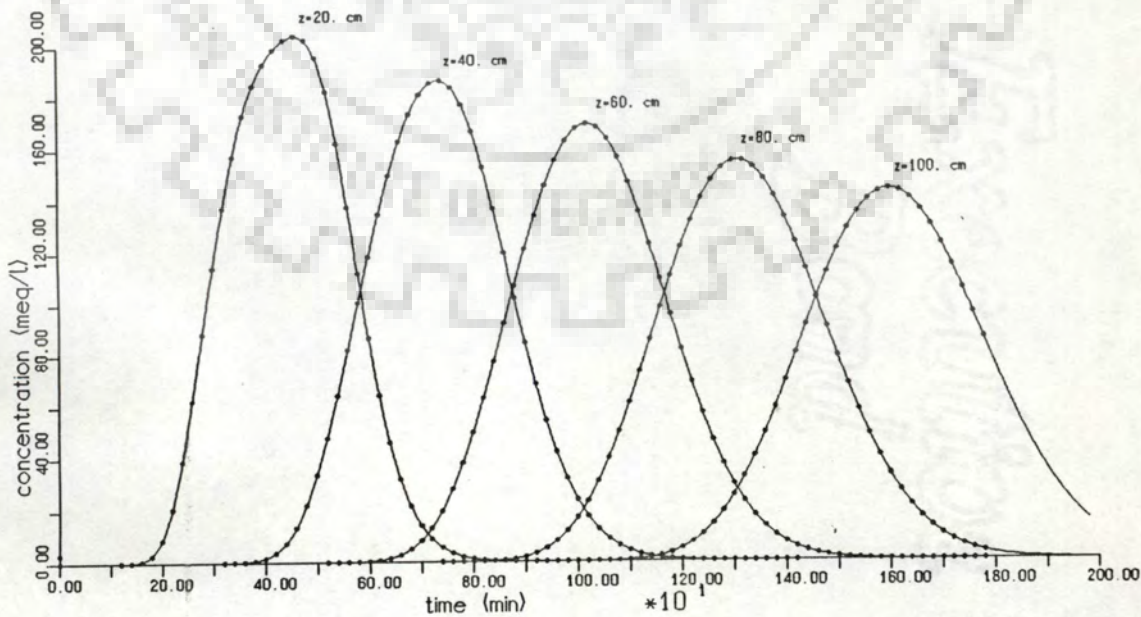
Concentration breakthrough curve

Fig. 4.3. Comparison with analytical solution for single phase non -reactive solute transport ($\lambda=0.5$ cm, $\Delta t=1.0$ min).

concentration (meq/l)

Concentration profile

· · · Analytical (c)

———— Numerical (c)

Concentration breakthrough curve

Fig. 4.4. Comparison with analytical solution for single phase non -reactive solute transport (λ=1.0 cm, Δt=1.0 min).

Concentration profile

Concentration breakthrough curve

Fig. 4.5. Comparison with analytical solution for single phase non reactive solute transport ($\lambda=0.0$ cm, $\Delta t=15.0$ min).

Concentration profile

Concentration breakthrough curve

Fig. 4.6. Comparison with analytical solution for single phase non -reactive solute transport (λ=0.1 cm, Δt=15.0 min).

concentration (meq/l)

Concentration profile

··· Analytical (c)

— Numerical (c)

Concentration breakthrough curve

Fig. 4.7. Comparison with analytical solution for single phase non -reactive solute transport ($\lambda=0.5$ cm, $\Delta t=15.0$ min).

concentration (meq/l)

depth (cm)

120.

540.

1020.

1980.

. . . Analytical (c)

—— Numerical (c)

Concentration profile

concentration (meq/l)

z=20. cm

z=40. cm

z=60. cm

z=80. cm

z=100. cm

time (min)   *10^1

Concentration breakthrough curve

Fig. 4.8. Comparison with analytical solution for single phase non -reactive solute transport ($\lambda=1.0$ cm, $\Delta t=15.0$ min).

The D values [refer equation(3.2)] computed for different λ values are as follows,

λ(cm)	$D(cm^2/min)$
0.0	0.00006
0.1	0.00689
0.5	0.03425
1.0	0.06846

4.1.1.6.2 Initial and Boundary Conditions

The initial and boundary conditions are assigned in accordance with eqns (4.2)-(4.4).

For the upper boundary condition, t_o was computed as follows,

$t_o = x/q = 7.62/0.026 = 293.077$ mins (refer section 4.1.1.5.3)

The value of c_o and θ were taken as 209 meq/l and 0.38 respectively (refer section 4.1.1.5.3).

4.1.1.6.3 Results

The concentration distributions obtained in space and time, from the analytical solution were superposed on the model computed results and are presented in Figs. 4.1-4.8.

4.1.1.7 Comparison

The two solutions (section 4.1.1.5 and 4.1.1.6) pertain to identical conditions except for the space domain (the analytical solution holds good for a semi-infinite system, where as the model has been operated for a system having a finite length of 180 cms). However, as the change in concentration at the lower boundary is negligible the

during the time period of simulation is negligible, the domain used for numerical simulation can also be considered as effectively semi-infinite.

4.1.1.8   Discussion

For different values of λ, an excellent agreement between the two solutions, represented by concentration profiles in depth and breakthrough curves (Figs. 4.1-4.4) was observed.

Even, for a considerably large time step ($\Delta t=15$ mins), the agreement between the two solutions remained excellent (Figs. 4.5-4.8).

4.1.2   Parker and van Genuchten's Solution (Parker and van Genuchten 1984, and van Genuchten, 1981 cited in Parker and van Genuchten, 1984)

The solution pertains to single phase and two phase reactive solute transport under steady state flow conditions. For single phase solute transport the sorption sites present in the soil matrix are assumed to comprise of two fractions. Adsorption on one fraction (type-1 sites) is assumed to be instantaneous i.e., equilibrium adsorption, while adsorption on the other fraction (type-2 sites) is time dependent i.e. kinetic equilibrium adsorption. For two phase solute transport the interaction between solute and soil matrix in both the phases is described by a linear equilibrium adsorption-desorption isotherm.

4.1.2.1   Differential Equations

The differential equation governing one-dimensional single phase solute transport under conditions described above is written as,

$$(1+ \frac{F\rho k_d}{\theta}) \frac{\partial c}{\partial t} + \frac{\rho}{\theta} \frac{\partial s}{\partial t} = D \frac{\partial c^2}{\partial z} - v \frac{\partial c}{\partial z} \qquad (4.10)$$

The linear kinetic adsorption-desorption equation is written as,

$$\frac{\partial s}{\partial t} = \beta [(1-F)k_d c - s] \qquad (4.11)$$

where, F is the fraction of type-1 sorption sites. For F=0, equations (4.10) and (4.11) reduce to equations (3.3) and (3.4).

Introducing the following dimensionless variables,

$$T = vt/L \qquad (4.12)$$

$$X = z/L \qquad (4.13)$$

$$P = vL/D \qquad (4.14)$$

$$R = 1 + \rho k_d / \theta \qquad (4.15)$$

$$\delta = \frac{\theta + F\rho k_d}{\theta + \rho k_d} \qquad (4.16)$$

$$\omega = \beta(1- \delta)RL/v \qquad (4.17)$$

$$c_1 = \frac{c - c_i}{c_o - c_i} \qquad (4.18)$$

$$c_2 = \frac{s - (1-F)k_d c_i}{(1-F)k_d(c_o -c_i)} \qquad (4.19)$$

where, L is an arbitrary positive distance from the origin.

Equations (4.10) and (4.11) are rewritten as,

$$k_d \frac{\partial c_1}{\partial t} +(1 - \delta)R \frac{\partial c_2}{\partial t} = \frac{1}{P} \frac{\partial c_1}{\partial x^2} - \frac{\partial c_1}{\partial x} \qquad (4.20)$$

$$(1-\delta)R \frac{\partial c_2}{\partial t} = \omega (c_1 - c_2) \qquad (4.21)$$

The differential equation governing one dimensional two phase solute transport under steady state flow conditions accounting for linear equilibrium adsorption - desorption is written as,

$$(\theta_m + \rho f k_d)\frac{\partial c_m}{\partial z} + \left[\theta_{im} + \rho(1-f)k_d\right]\frac{\partial c_{im}}{\partial t} = \theta_m D_m\frac{\partial^2 c}{\partial z^2} - q\frac{\partial c}{\partial z} \qquad (4.22)$$

$$\left[\theta_{im} + \rho(1-f)k_d\right]\frac{\partial c_{im}}{\partial t} = \alpha(c_m - c_{im}) \qquad (4.23)$$

The above equations are the same as eqns (3.5) and (3.7). The dimensionless forms of equations (4.22) and (4.23) remain the same as equations (4.20) and (4.21), if equations (4.22) and (4.23) are expressed in terms of T, x and R, and the following reduced variables.

$$p = v_m L/D_m \qquad (4.24)$$

$$\delta = \frac{\theta_m + f\rho k_d}{\theta + \rho k_d} \qquad (4.25)$$

$$\omega = \alpha L/q \qquad (4.26)$$

$$c_1 = \frac{c_m - c_i}{c_o - c_i} \qquad (4.27)$$

$$c_2 = \frac{c_{im} - c_i}{c_o - c_i} \qquad (4.28)$$

where $v_m = q/\theta_m$.

Eqn (4.14) is the same as (4.24) if D for the two phase model is defined as,

$$D = D_m \theta_m / \theta \qquad (4.29)$$

4.1.2.2   Initial and Boundary Conditions

The intial and boundary conditions are assigned in accordance with eqns (4.2) - (4.4). For eqn (4.11) an additional initial condition is required, which is in the form of,

$$s(x,0) = (1-F) \, k_d c_i \tag{4.30}$$

4.1.2.3   Analytical Solution

Solution of equations (4.20) and (4.21) in terms of the reduced variables, is reported as,

$$c(x,t) = \begin{cases} c_i + (c_o - c_i)A(x,T) & 0 < T < T_o \\ c_i + (c_o - c_i)A(x,T) - c_o A(x,T-T_o) & T > T_o \end{cases} \tag{4.31}$$

where,

$$A(x,t) = \int_0^T g(x,\tau) J(a,b) d\tau$$

$$g(x,\tau) = (\frac{P}{\pi \delta R \tau})^{1/2} \exp\left[-\frac{P(\delta Rx-\tau)^2}{4\delta R\tau} - \frac{P}{2\delta R} \exp(Px)\right]$$

$$\text{erfc}\left[(\frac{P}{4\delta RT})^{1/2}(\delta Rx+\tau)\right]$$

$$J(a,b) = 1 - e^{-b}\int_0^a e^{-\sigma} I_o\left[2(b\sigma)^{1/2}\right]d\sigma$$

$$a = \frac{\omega\tau}{\delta R}$$

and

$$b = \frac{\omega(t-\tau)}{(1-\delta)R}$$

The function J(a,b) is referred to as Goldstein's J-function and I is zero order Bessel's function. The above analytical solution for c represents the concentration of the entire solute phase if applied to the two site model, while for the two phase model the solution represents the concentration of the mobile phase.

The model simulated transport was compared with the above analtyical solution. The comparison was done for the following three cases.

Case I

Single phase reactive (first order linear kinetic adsorption-desorption) solute transport.

Case II.

Two phase non-reactive solute transport.

Case III.

Two phase reactive (linear equilibrium adsorption-desorption) solute transport.

4.1.3 Case I

Single phase reactive (first order linear kinetic adsorption-desorption) solute transport.

4.1.3.1 Model Operation

The model accounting for single phase reactive solute transport (refer section 3.4.5) was operated under the following conditions.

4.1.3.1.1 Time and space Domains

The depth of the solution domain was taken as 180 cms. At the beginning of simulation the domain was subdivided into 180 moving packets using a strip thickness (ts) of 1 cm.

The total time duration of each simulation was 1980 mins. A time step of 1 min was used. However, to check the effect of a large time step, the simulations were repeated using a time step of 15 mins.

4.1.3.1.2 Parameter Values

The following parameter values were used for simulation.

$a = 0.002$

$b = 10.0$ (refer section 4.1.1.5.2)

$D_o = 0.000667$

$\rho = 1.6$ gm/cm^3

$k_d = 0.5$ cm^3/gm

The sets of values of λ and β used are as follows,

λ(cm)	β(min^{-1})
0.5	0.01
0.1	0.01
0.5	0.001
0.5	0.1

4.1.3.1.3 Initial and Boundary Conditions

In addition to the intial and boundary conditions, assigned in accordance with eqns (4.6)-(4.8), the initial condition for the adsorbed concentration of the soil matrix (refer eqn (3.4)) is assigned as,

$$s(z,0) = 0.0 \qquad 0 \leq z \leq Z \qquad\qquad (4.32)$$

For the upper boundary condition (refer equation (4.7)), the depth of solute to be infiltrated (x) was taken as 10 cms. This was followed by infiltration of fresh water till the end of simulation. The values of infiltrated solute concentration (c_o), moisture content (θ) and volumetric flux (q) were taken as 209 meq/l, 0.38 and 0.026 cm/min respectively (refer section 4.1.1.5.3).

4.1.3.1.4 Results

Model computed breakthrough curves at depths of 20, 40, 60, 80 and 100 cm are presented in Figs. 4.9-4.12.

4.1.3.2   Computation of Analytical Solution

CXTFIT was used to obtain c vs z and c vs t curves for identical parameters.

4.1.3.2.1 Parameter Values

For the solution [described by equation (4.31)] to be valid for single phase reactive (first order kinetic adsorption-desorption) solute transport a zero value was assigned to F.

The parameters R, δ, D and ω were computed for the pre-assigned values of θ, v (refer section 4.1.3.1.3 and 4.1.1.6.1), ρ, k_d, a, b, D_o, λ, β (refer section 4.1.3.1.2), F and L (where, L is the depth at which the breakthrough curve is computed) in accordance with the equations (4.15), (4.16), (3.2) and (4.17). The computed parameter values are as follows,

$$R = 3.1053 \qquad\qquad \text{[refer equation (4.15)]}$$

$$\delta = 0.32203 \qquad\qquad \text{[refer equation (4.16)]}$$
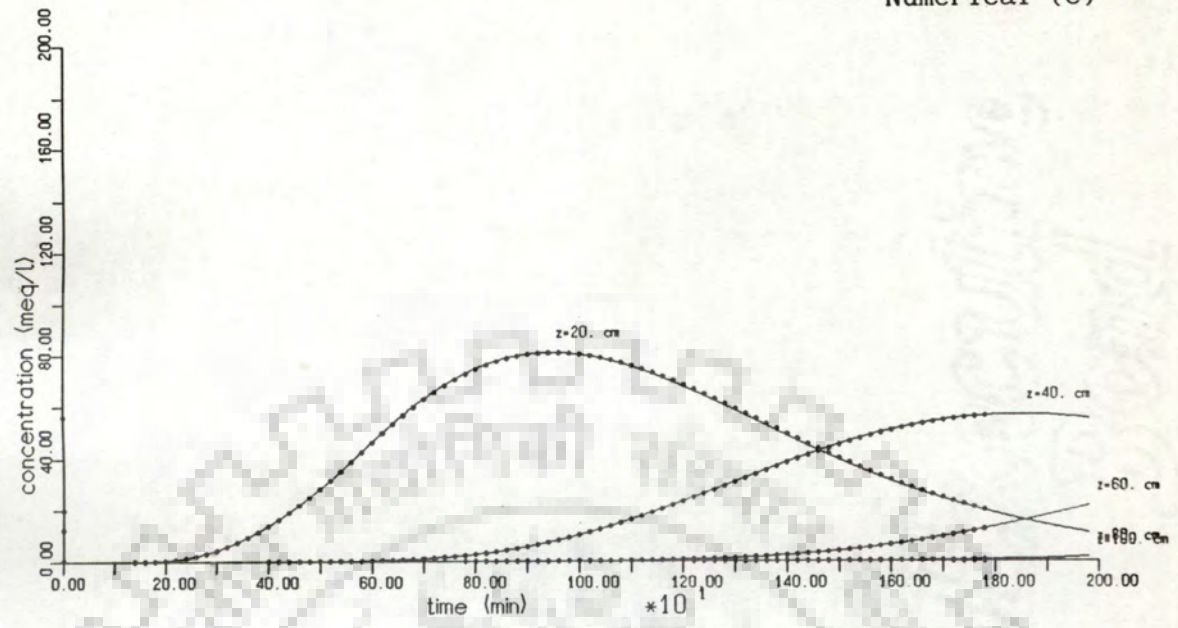
Fig. 4.9. Comparison with analytical solution for single phase reactivesolute transport ($\lambda=0.5$ cm, $\beta=0.01$ min^{-1}).
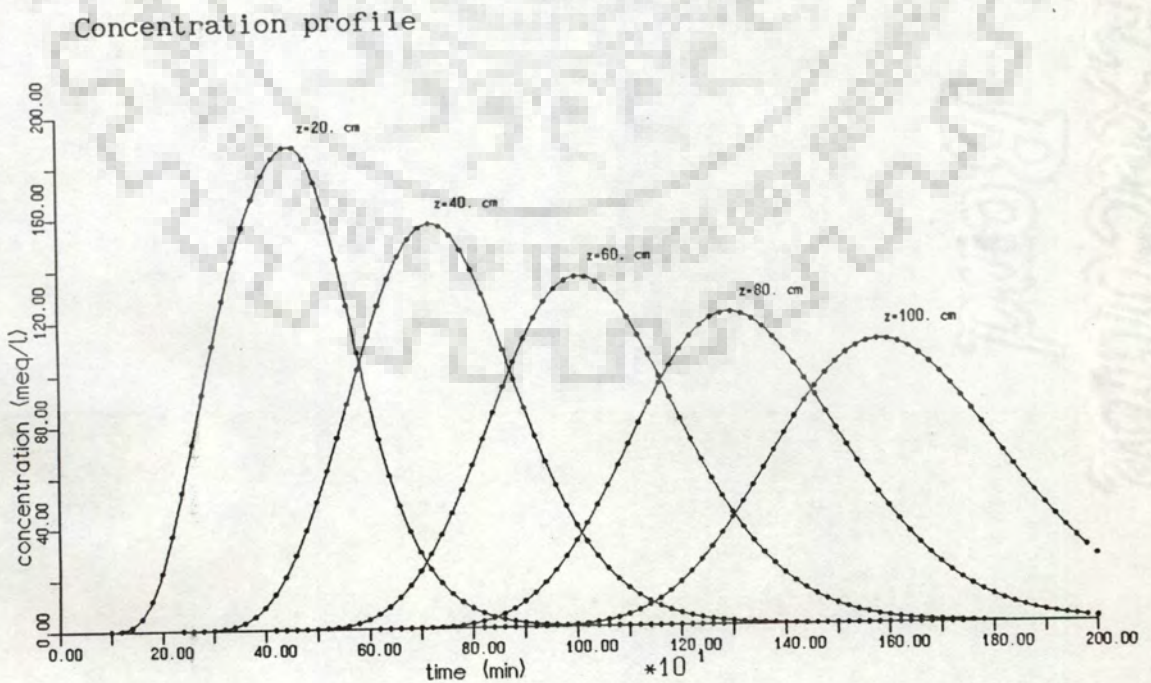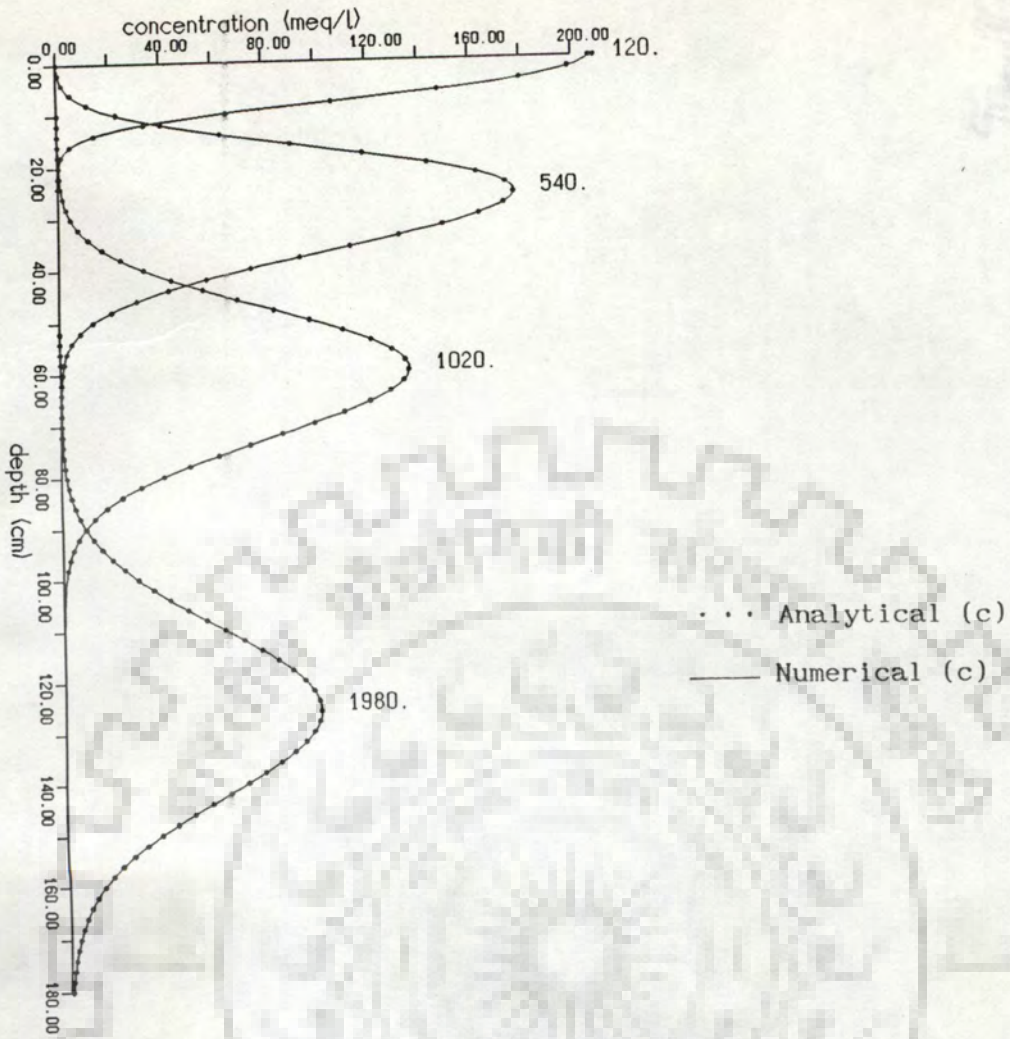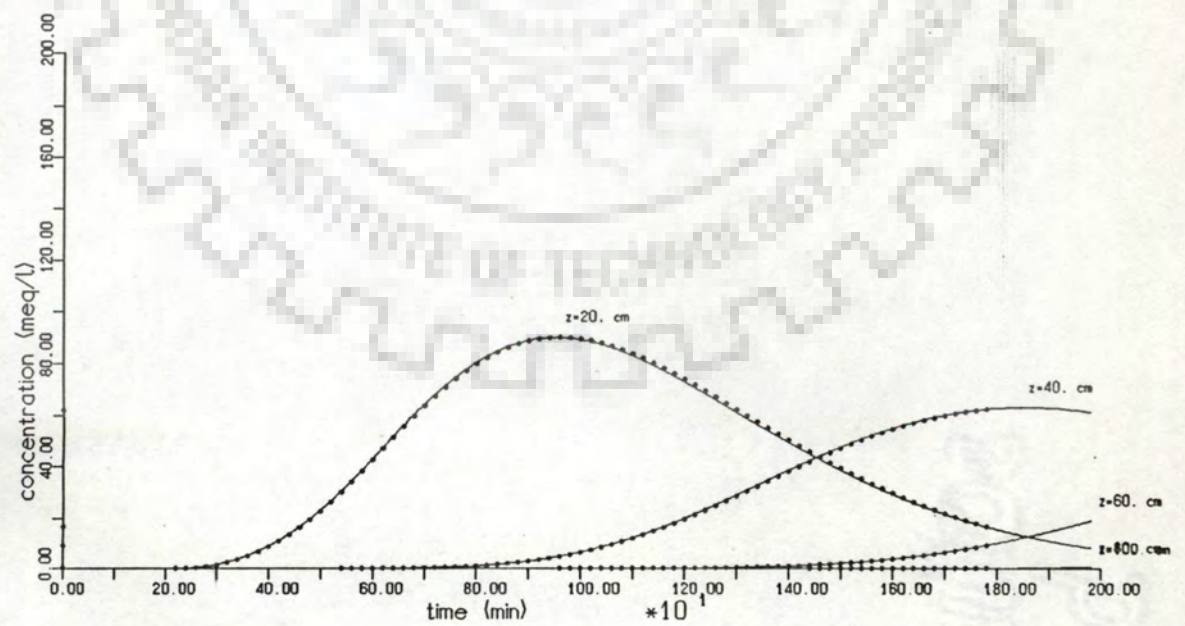

Concentration breakthrough curve

Fig. 4.10. Comparison with analytical solution for single phase reactive solute transport ($\lambda=0.1$ cm, $\beta=0.01$ min^{-1}).
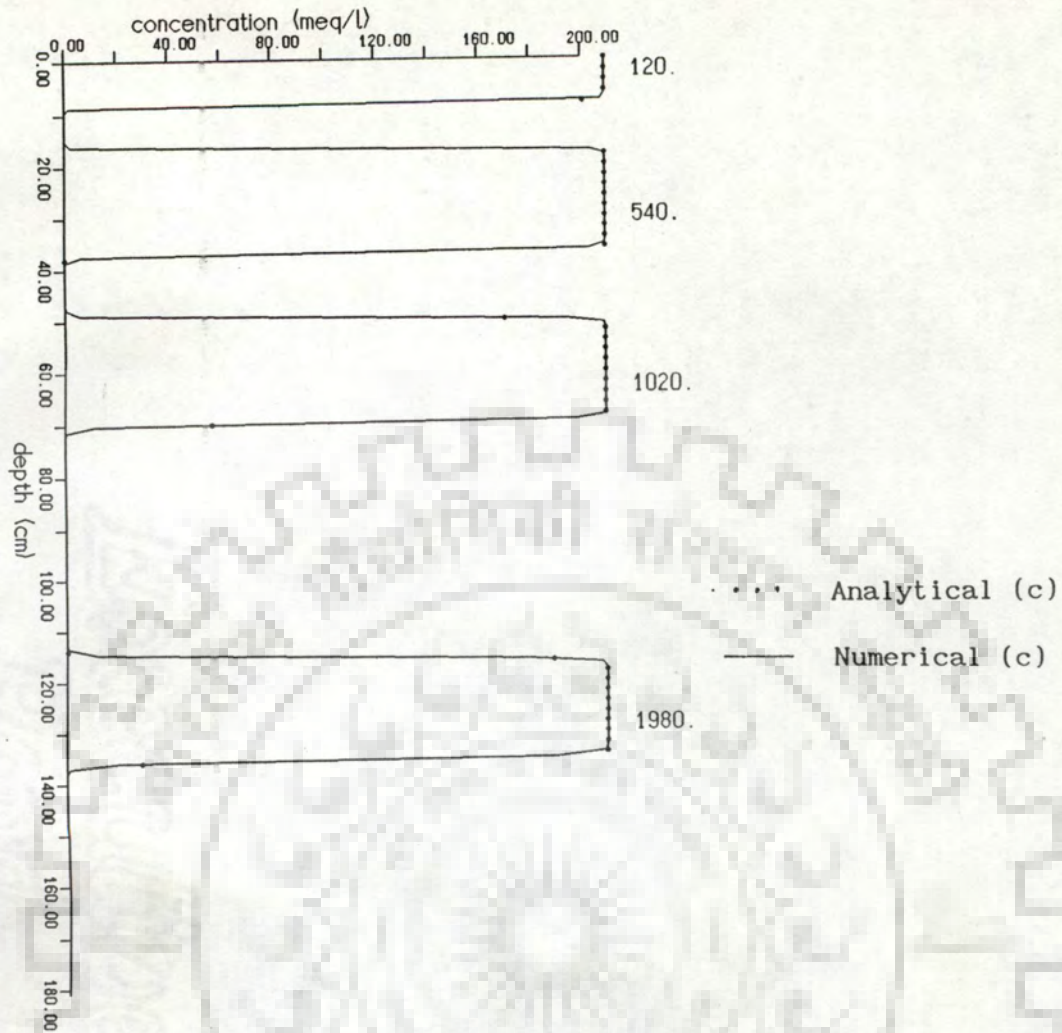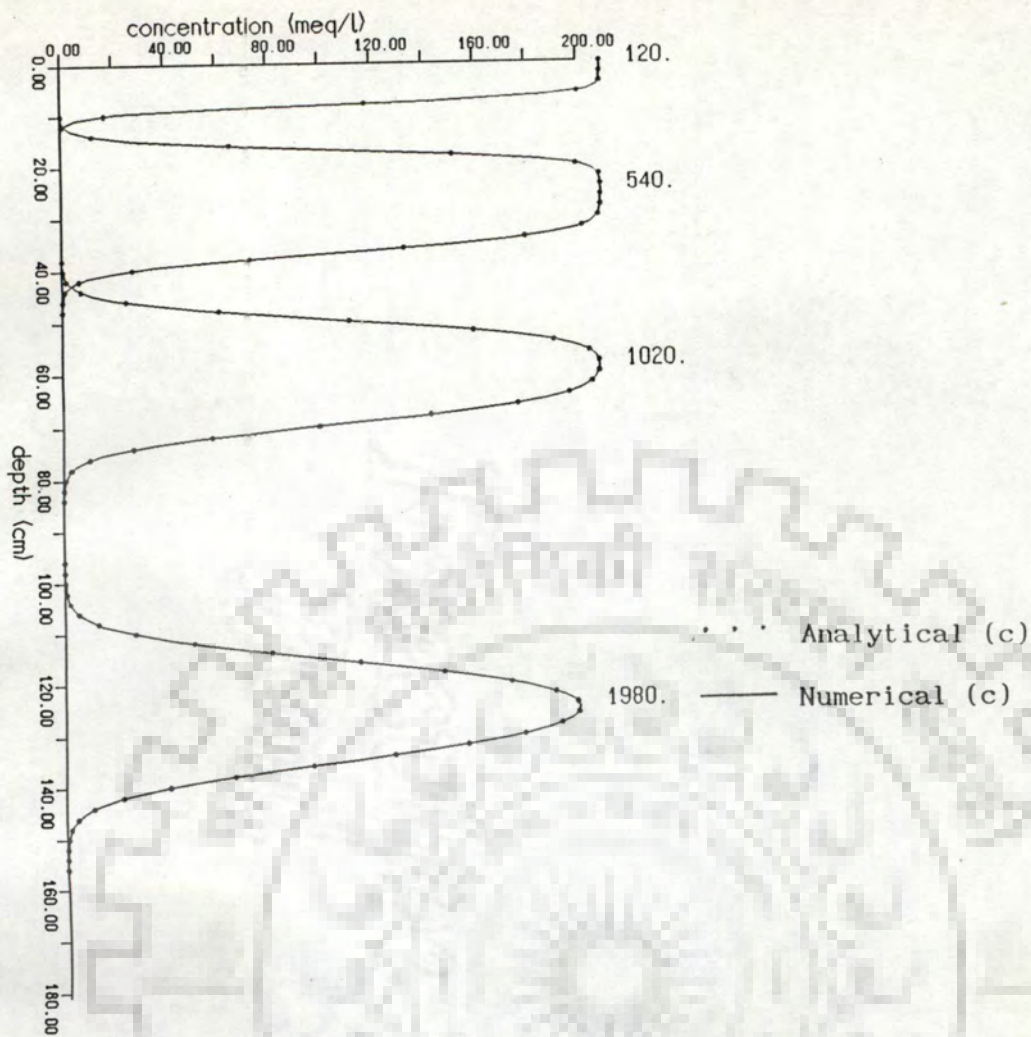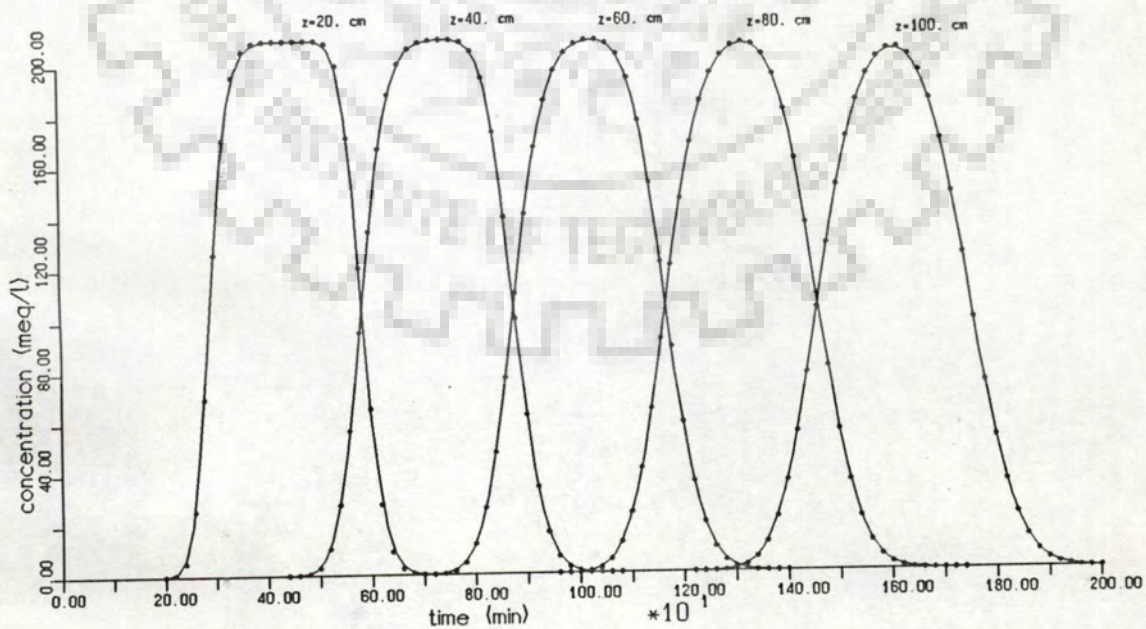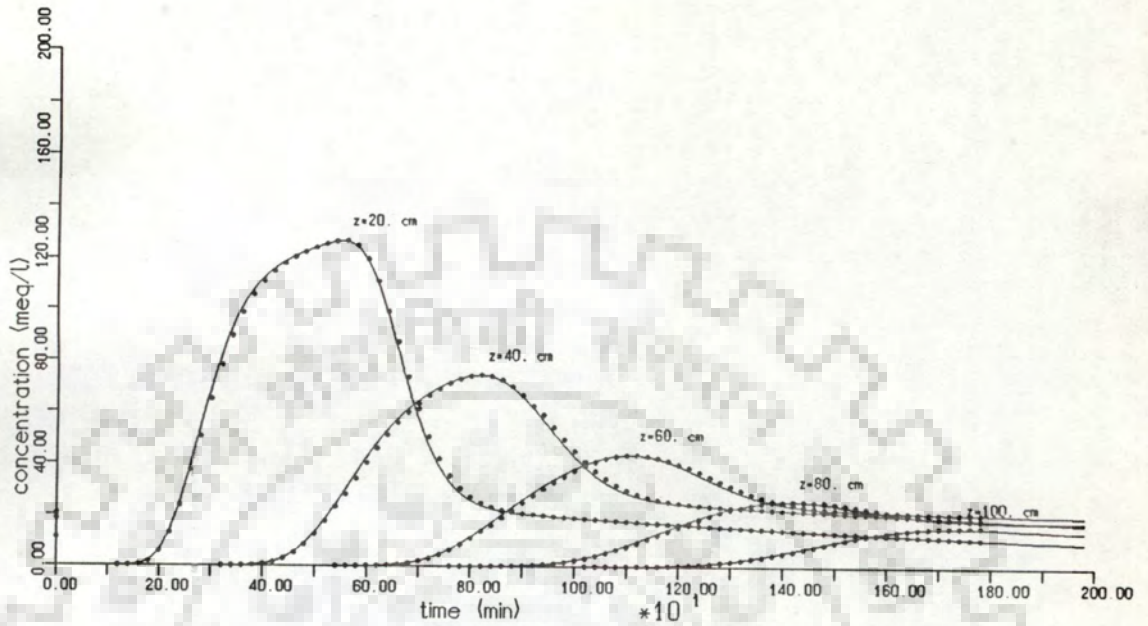
Concentration breakthrough curve

Fig. 4.11. Comparison with analytical solution for single phase reactive
solute transport ($\lambda=0.5$ cm, $\beta=0.001$ min^{-1}).
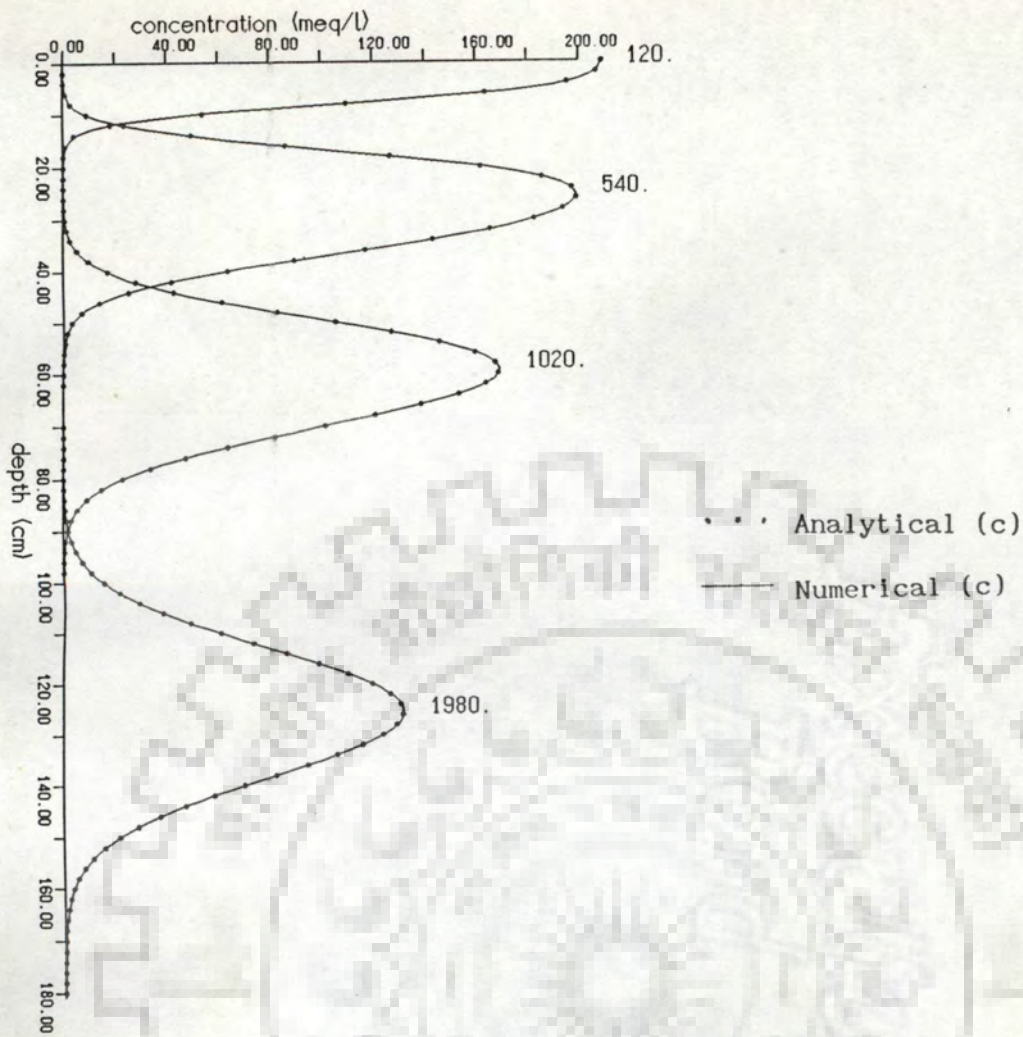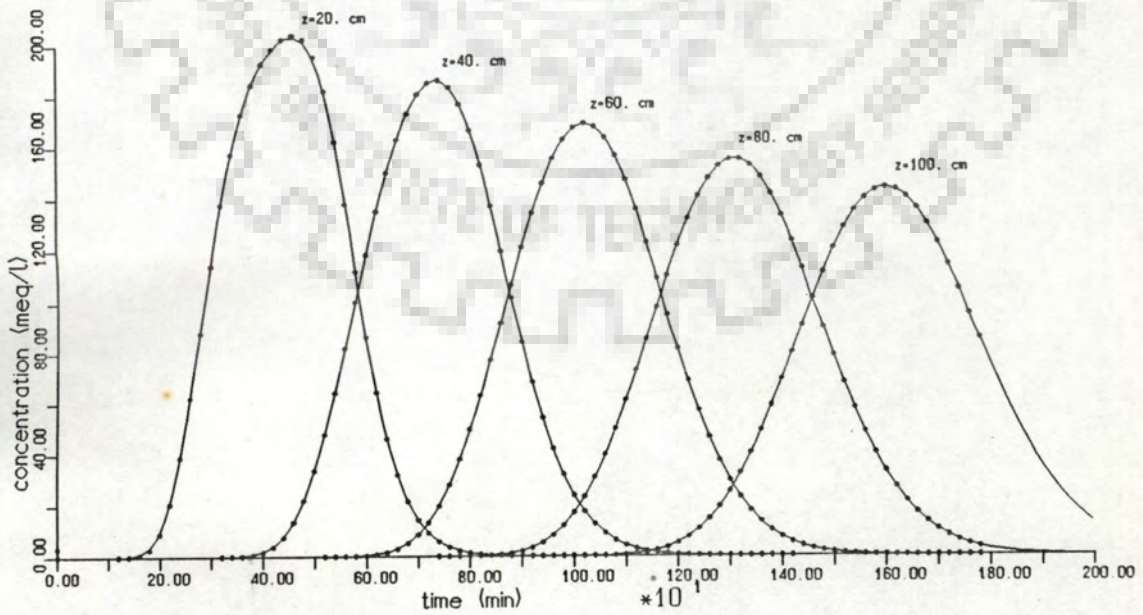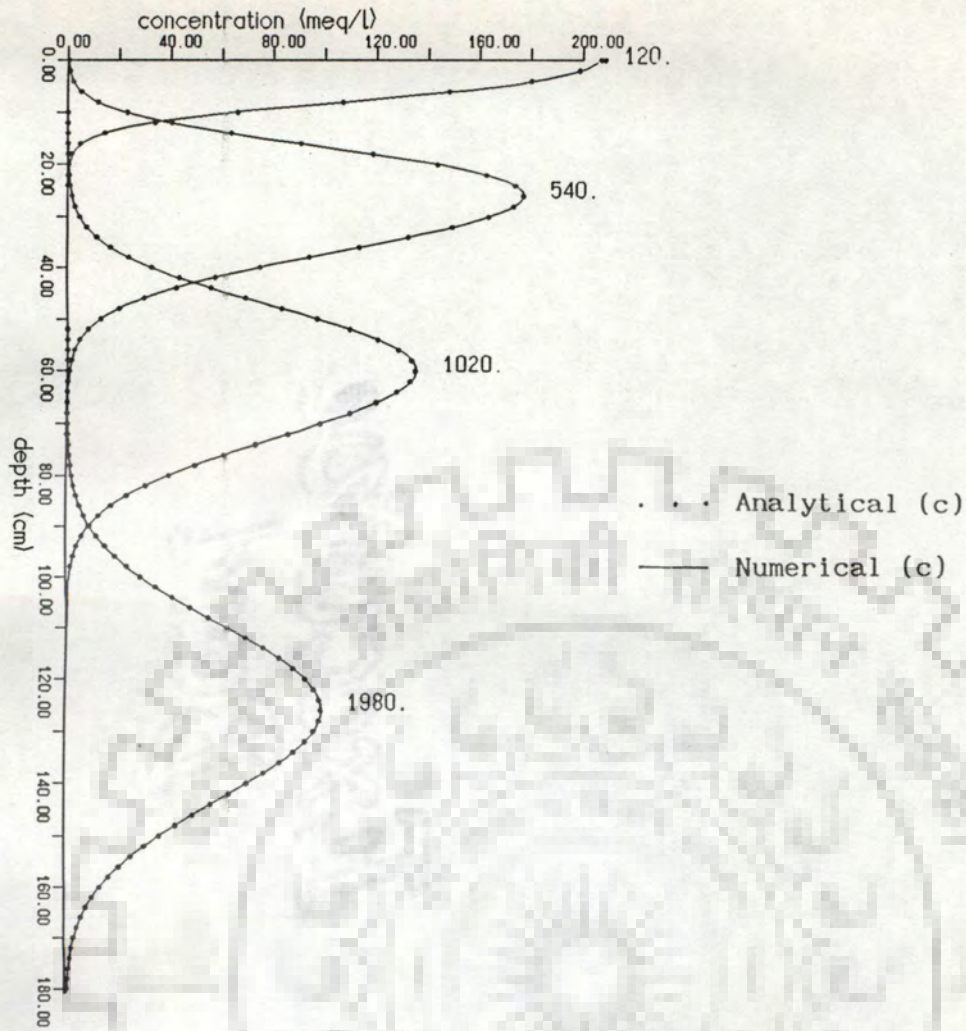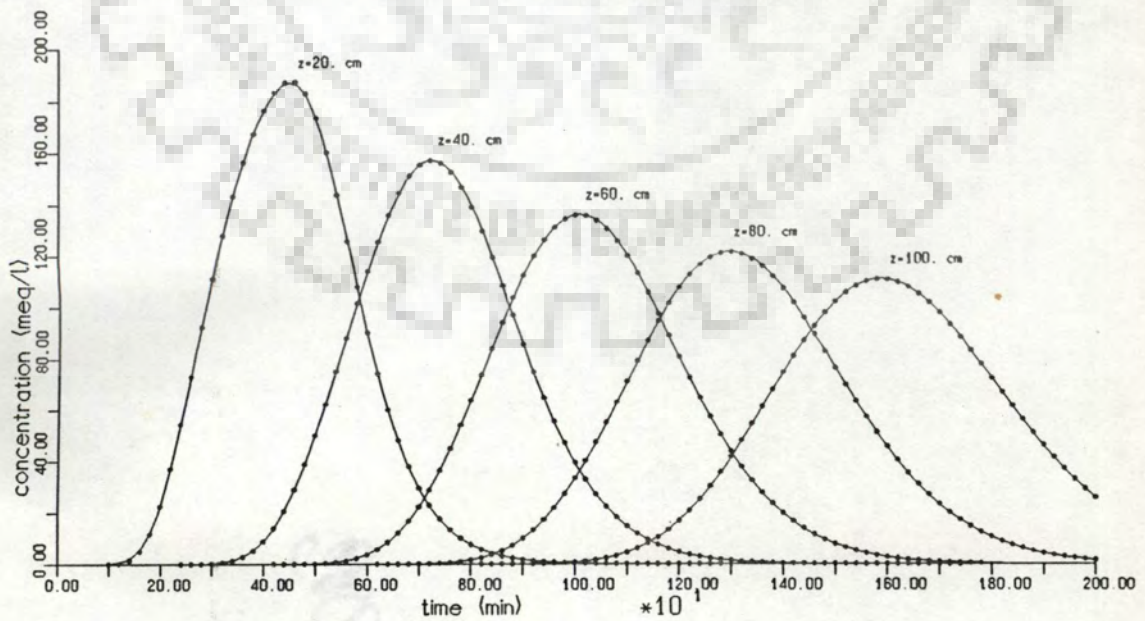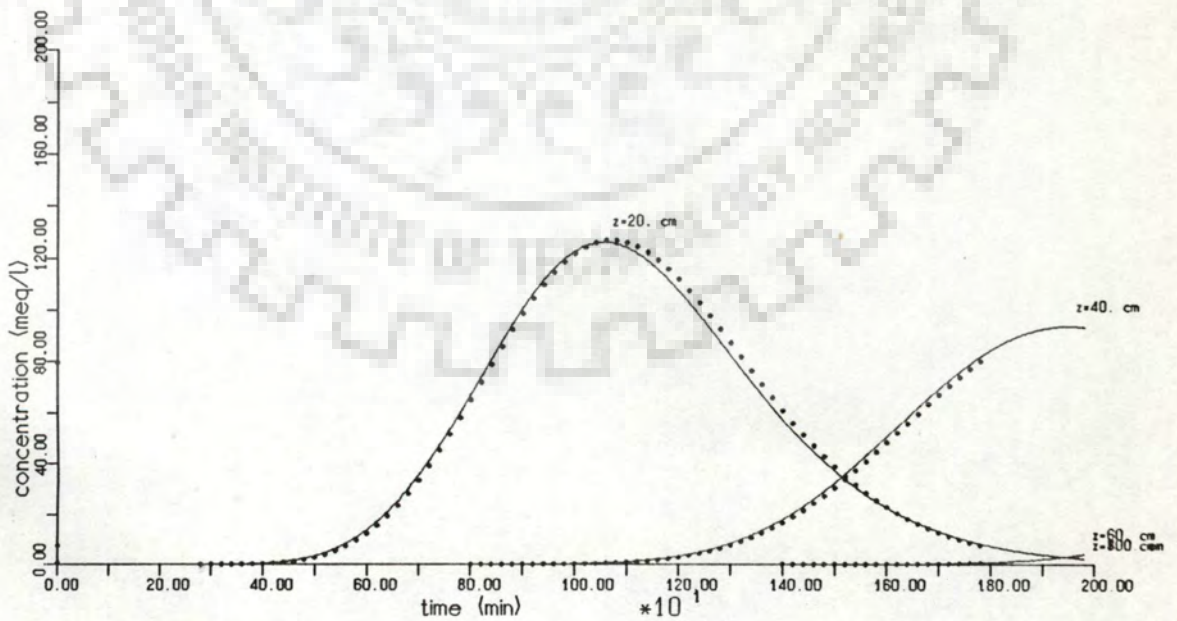

Concentration breakthrough curve

Fig. 4.12. Comparison with analytical solution for single phase reactive
solute transport ($\lambda=0.5$ cm, $\beta=0.1$ min^{-1}).

The D values [refer equation(3.2)] computed for different λ values are as follows,

λ(cm)	$D(cm^2/min)$
0.5	0.03425
0.1	0.00689

The ω values [refer equation (4.17)] computed for different values of L and β are as follows,

L(cm)	$\omega(\beta=0.01min^{-1})$	$\omega(\beta=0.001min^{-1})$	$\omega(\beta=0.1min^{-1})$
20	6.1558	0.61558	61.558
40	12.3117	1.23117	123.117
60	18.4675	1.84675	184.675
80	24.6234	2.46234	246.234
100	30.7792	3.07792	307.792

4.1.3.2.2 Initial and Boundary Conditions

The initial and boundary conditions are assigned in accordance with eqns (4.2)-(4.4) and equation (4.29);($c_i=0.0$). As the depth of solute (x) infiltrated was 10 cms, the value of t_o was 384.615 min (refer section 4.1.1.6.2).

The value of c_o and θ were taken as 209.0 meq/l and 0.38 respectively (refer section 4.1.1.5.3). Values of T_o [$=vt_o/L$, refer equation (4.12)], corresponding to the different values of L were computed as,

L(cm)	T_o
20	1.3154
40	0.6577

60	0.4385
80	0.3288
100	0.2631

4.1.3.2.3 Results

The concentration distribution in depth and time obtained from the analtyical solution were superposed on the model computed results and are presented in Figs. 4.9-4.12.

4.1.3.3 Comparison

The two solutions (section 4.1.3.1 and 4.1.3.2) pertain to identical conditions, except for the space domain (the analytical solution holds good for a semi-infinite system, where as the model has been operated for a system having a finite length of 180 cms). However, as the change in concentration at the lower boundary during the time period of simulation is negligible, the domain used for numerical simulation can also be considered as effecvtively semi-infinite.

4.1.4   Case II

Two phase non-reactive solute transport

4.1.4.1   Model Operation

The model accounting for two phase non reactive solute transport (refer section 3.4.6) was operated under the following conditions.

4.1.4.1.1 Time and space Domains

The depth of the solution domain was taken as 180 cms. At the beginning of simulation the domain was subdivided into 180 moving packets using a strip thickness (ts) of 1 cm.

The total time duration of each simulation was 1980 mins. A time step of 1 min was used. However, to check the effect of time step variation, for a sigle set of parameters simulations were carried out using 3 time steps of 5,10 and 15 mins.

4.1.4.1.2 Parameter Values

The following parameter values were used for simulation.

a = 0.002

b = 10   (refer section 4.1.1.5.3)

D_o = 0.000667 cm^2/min

λ = 0.5 cm.

The sets of values of θ_{im} and α used, are as follows,

θ_{im}	$\alpha(min^{-1})$
0.1	0.001
0.171	0.001
0.3	0.001
0.1	10.0
0.3	0.1

4.1.4.1.3 Initial and Boundary Conditions

The initial and boundary conditions are assigned in accordance with eqns (4.6)-(4.8). However, for the present simulation they

represent concentration and moisture content in the mobile phase. An additional initial condition for concentration in the immobile phase [refer equation (3.7)] is assigned in accordance with the following equation,

$$c_{im}(z,0) = 0.0 \qquad 0 \leq z \leq Z \qquad (4.33)$$

For the upper boundary condition [refer equation (4.7)] the depth of solute to be infiltrated (x) was taken as 10 cms, except when the simulation was carried out using an α value of 10 min^{-1}. For that simulation the value of x was taken as 7.62 cms. The values of the concentration of the infiltrated solute (c_o), moisture content (θ) and volumetric flux (q) were taken as 209 meq/l, 0.38 and 0.026 cm/min respectively (refer section 4.1.1.5.3).

4.1.4.1.4 Results

(i)   Model computed variation of concentrations in the mobile and immobile phase, with respect to depth, at times 120,540,1020 and 1980 mins are represented in Figs. 4.15-4.17.

(ii)   Model computed breakthrough curves (represent concentration only in the mobile phase) at depths 20,40,60,80 and 100 cms are represented in Figs. 4.13-4.20.

4.1.4.2   Computation of Analytical Solution

CXTFIT was used to obtain c vs z and c vs t curves for identical parameters.

• • • Analytical (c_m)

—— Numerical (c_m)

Concentration breakthrough curve

Fig. 4.13. Comparison with analytical solution for two phase non-reactive solute transport (θ_{im}=0.1 cm, α=0.001 min^{-1}).

Concentration breakthrough curve

Fig. 4.14. Comparison with analytical solution for two phase non-reactive solute transport (θ_{im}=0.171 cm, α=0.001 min^{-1}).

concentration (meq/l)

0.00   40.00   80.00   120.00   160.00   200.00   120.

depth (cm)

540.

1020.

1980.

$\cdots$ Analytical (c_m)

--- Numerical (c_m)

$\cdots$ Numerical (c_{im})

Concentration profile

concentration (meq/l)

z=20. cm

z=40. cm

z=60. cm

z=80. cm

z=100. cm

0.00   20.00   40.00   60.00   80.00   100.00   120.00   140.00   160.00   180.00   200.00

time (min) $*10^1$

Concentration breakthrough curve

Fig. 4.15. Comparison with analytical solution for two phase non-reactive solute transport (θ_{im}=0.3 cm, α=0.001 min^{-1}).

concentration (meq/l)

depth (cm)

120.

540.

1020.

· · · Analytical (c_m)

— Numerical (c_m)

1980.

Concentration profile

z=20. cm

z=40. cm

z=60. cm

z=80. cm

z=100. cm

concentration (meq/l)

time (min) $*10^1$
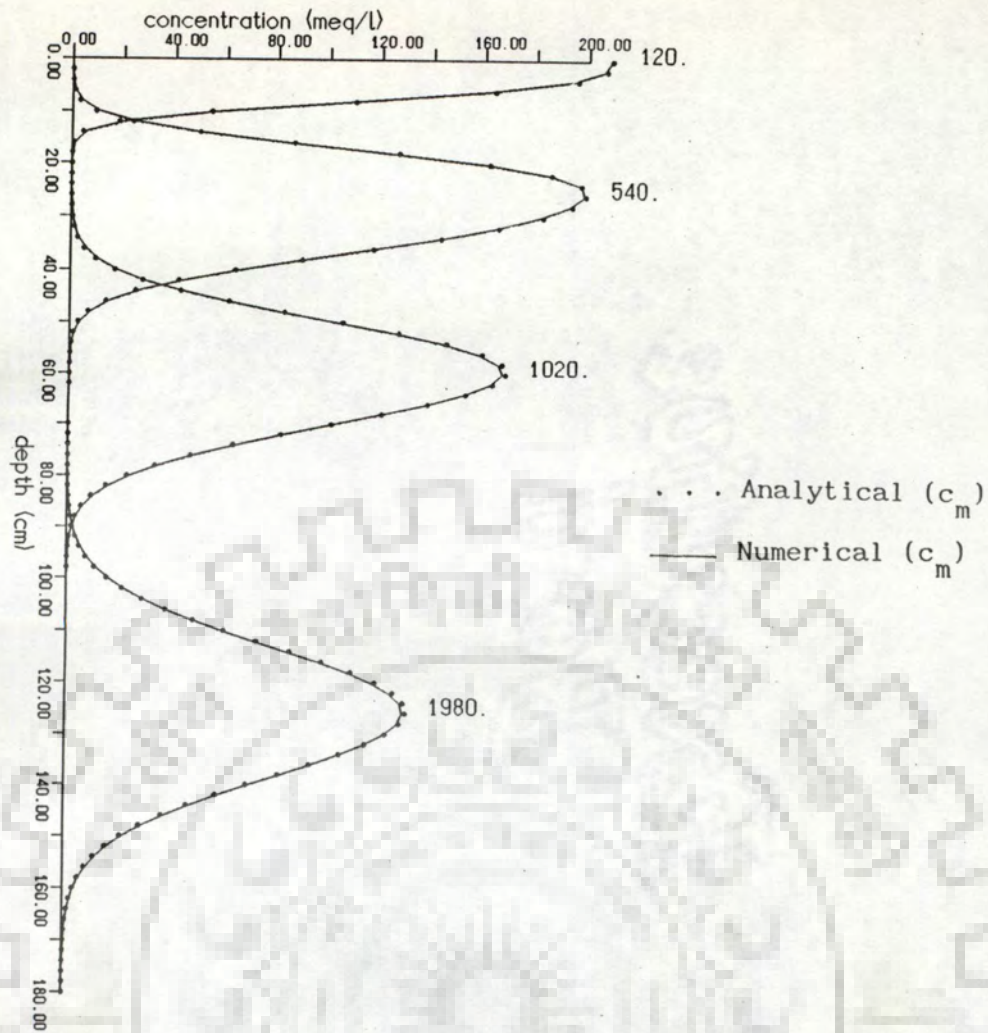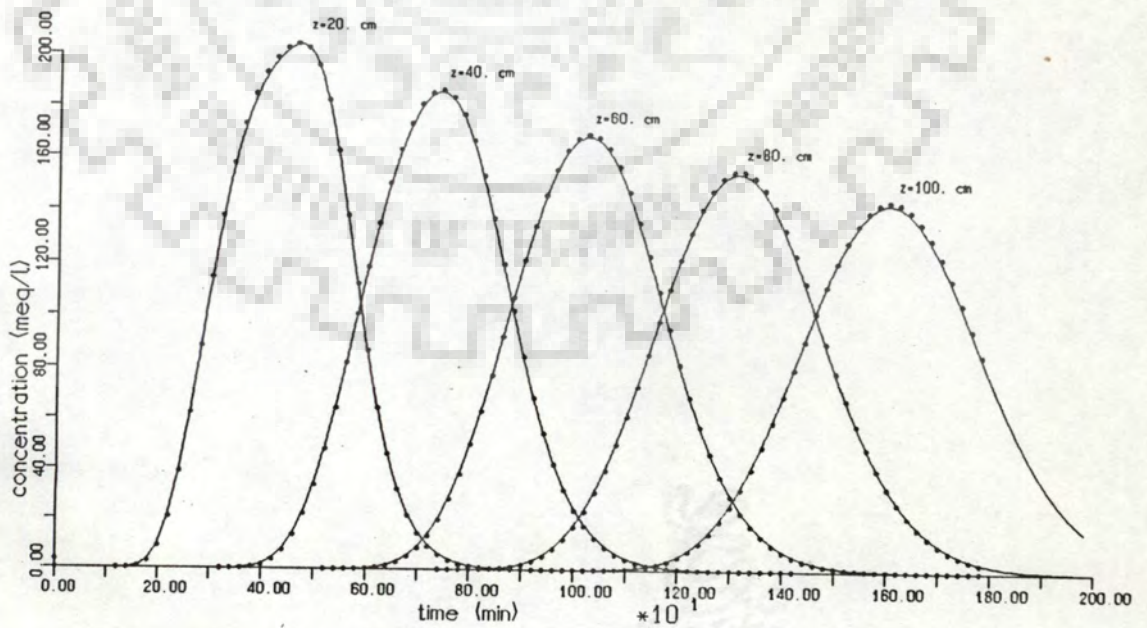
Concentration breakthrough curve

Fig. 4.16. Comparison with analytical solution for two phase non-reactive solute transport (θ_{im}=0.1 cm, α=10 min^{-1}).
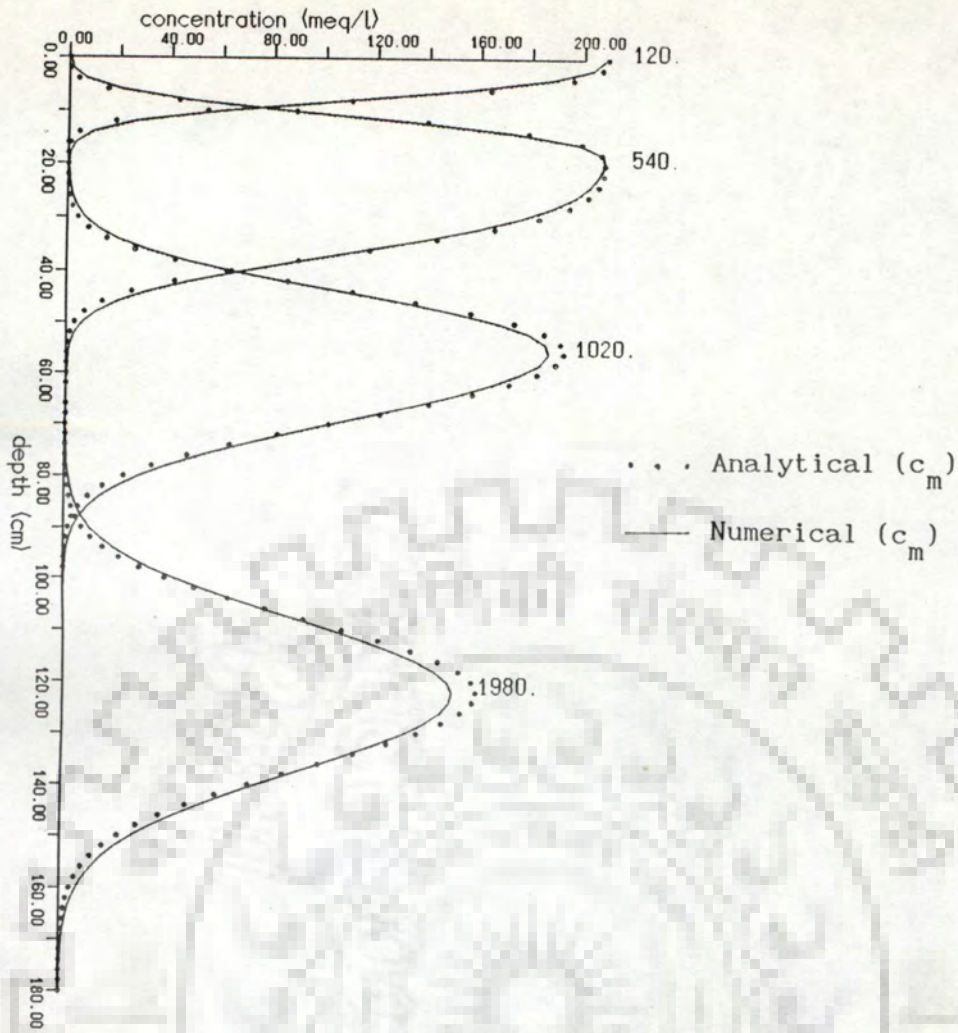
Concentration profile
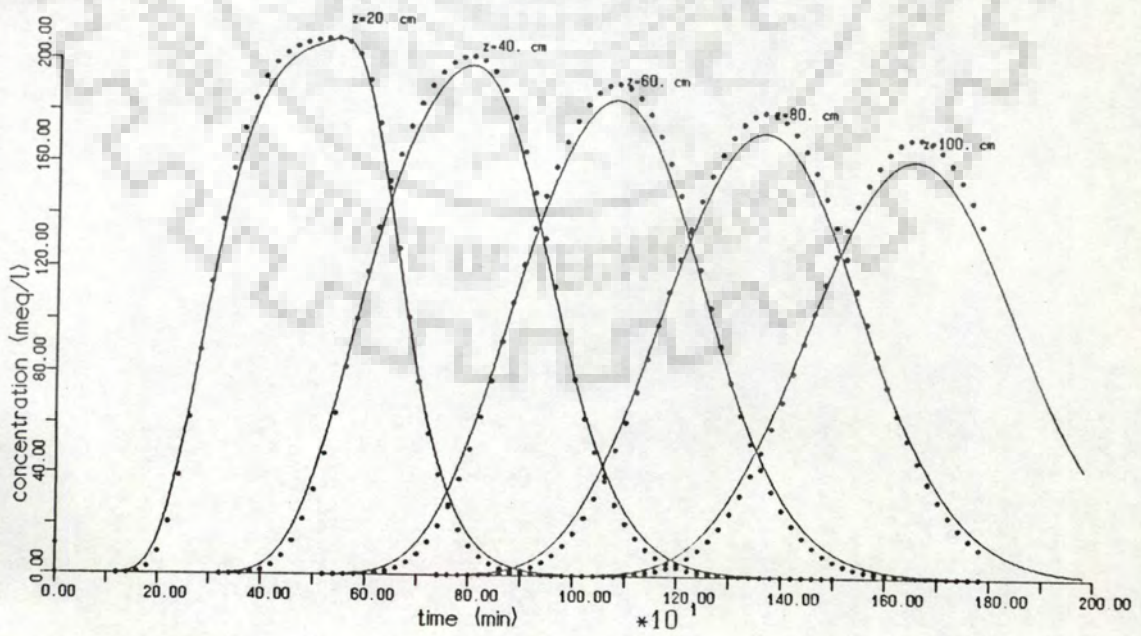
Concentration breakthrough curve

Fig. 4.17. Comparison with analytical solution for two phase non-reactive solute transport (θ_{im}=0.3 cm, α=0.1 min^{-1}).

Concentration breakthrough curve

Fig. 4.18. Comparison with analytical solution for two phase non-reactive solute transport (θ_{im}=0.171 cm, α=0.001 min^{-1}, Δt=5 min).

Concentration breakthrough curve
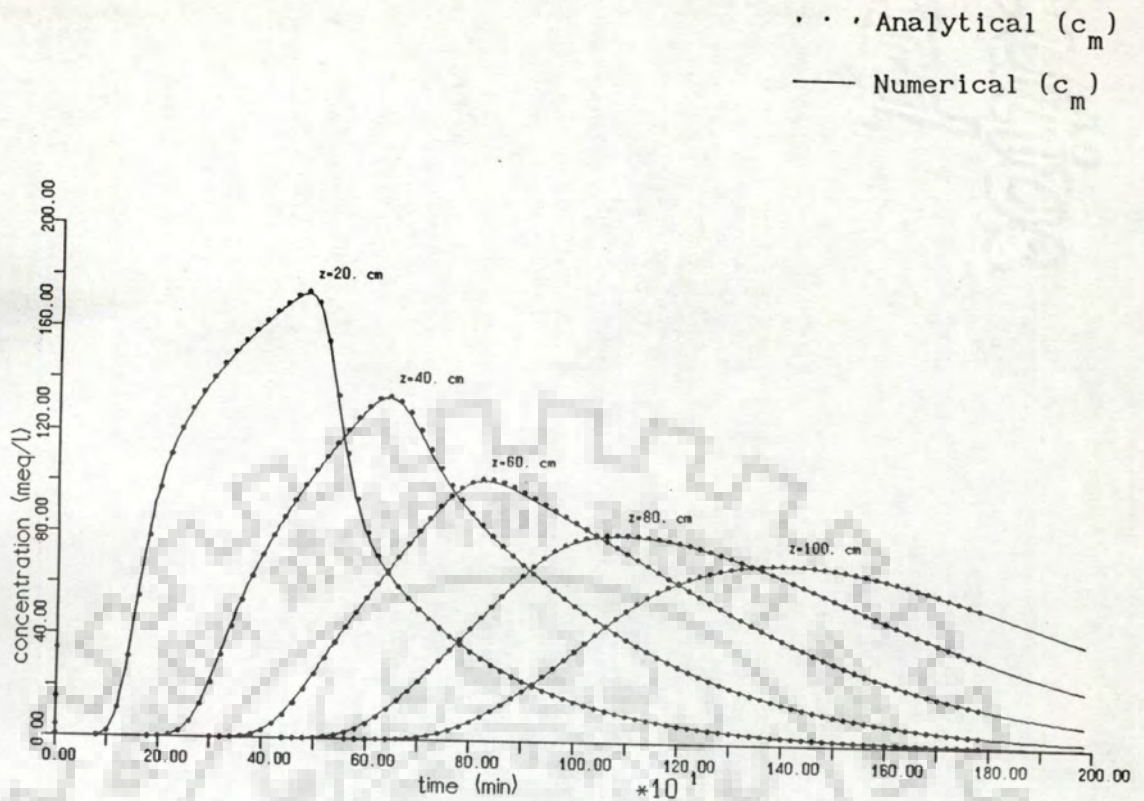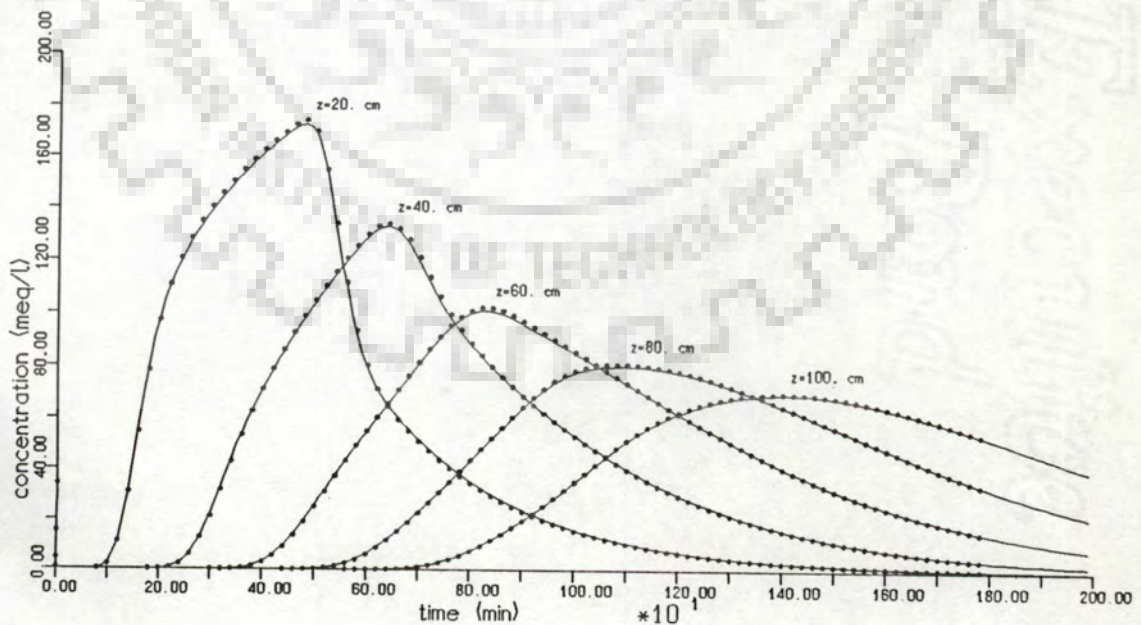
Fig. 4.19. Comparison with analytical solution for two phase non-reactive solute transport (θ_{im}=0.171 cm, α=0.001 min^{-1}, Δt=10 min).
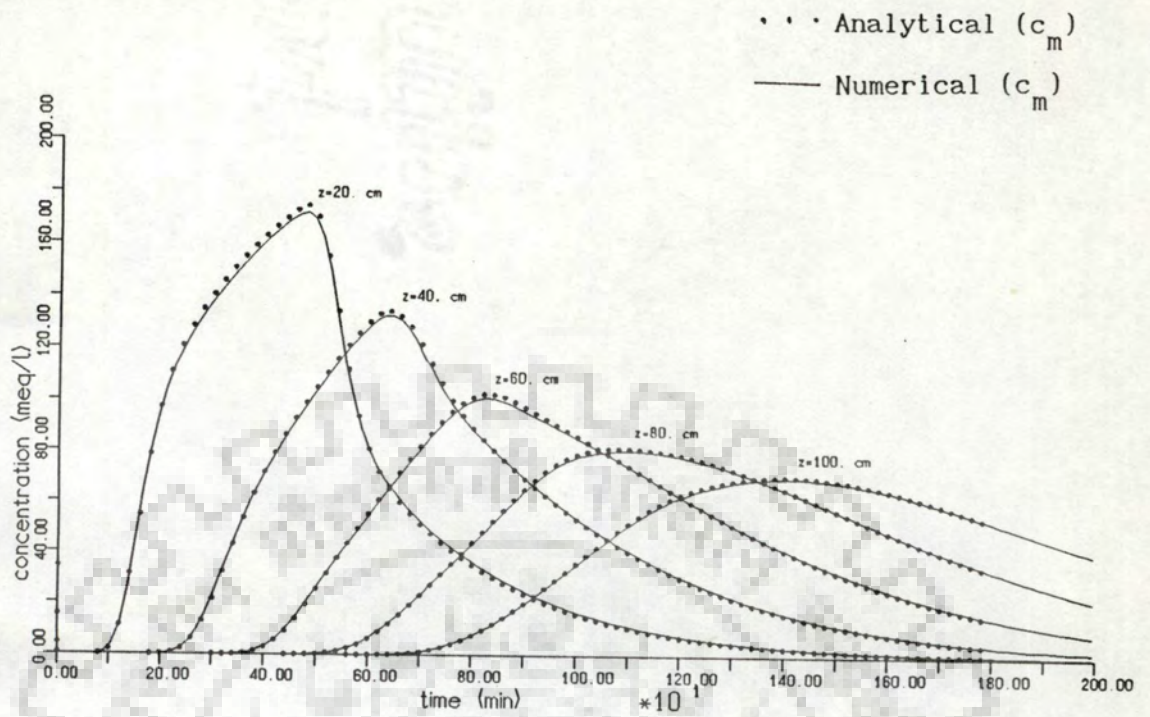
Concentration breakthrough curve

Fig. 4.20. Comparison with analytical solution for two phase non-reactive solute transport (θ_{im}=0.171 cm, α=0.001 min^{-1}, Δt=15 min).

4.1.4.2.1 Parameter Values

For the solution [described by equation (4.31)], to be valid for two phase non-reactive solute transport, a zero value is assigned to k_d.

The parameters R, δ, D and ω were computed for the pre-assigned values of θ, v (refer section 4.1.4.1.3 and 4.1.1.6.1) a, b, D_o, λ, α, θ_{im} (refer section 4.1.4.1.2), k_d and L (where, L is the depth at which the breakthrough curve is computed) in accordance with equations (4.15), (4.25), (4.29) and (4.26). The computed parameter values are as follows,

R =1   [refer equation (4.15)]

The different values of δ [refer equation (4.25)] and D [refer equation (4.29); equation (3.6) for computing D_m] computed corresponding to the values of θ_m ($=\theta-\theta_{im}$) are as follows,

θ_m (cm^3/cm^3)	δ	D
0.28	0.7368	0.03423
0.08	0.2105	0.03421
0.209	0.55	0.03422

The ω values [refer equation (4.26)] computed for different L and α values are as follows,

L(cm)	$\omega(\alpha=0.001\ \text{min}^{-1})$	$\omega(\alpha=0.1\text{min}^{-1})$	$\omega(\alpha=10\text{min}^{-1})$
20	0.7692	76.923	7692.31
40	1.5385	153.85	15384.6
60	2.3077	230.77	23076.9
80	3.0769	307.69	30769.2
100	3.8461	384.61	38461.5

4.1.4.2.2 Initial and Boundary Conditions

The initial and boundary conditions are assigned in accordance with eqns (4.2)-(4.4). However, they represent the concentrations of the mobile phase only. The initial condition for equation (4.23) is assigned in accordance with eqn (4.33) (refer section 4.1.4.1.3). The value of t_o for 10 cms and 7.62 cms of solute infiltration were computed as 384.615 mins and 293.077 mins (refer section 4.1.3.2.2 and section 4.1.1.6.2).

For t_o = 384.615 and 293.077 mins, the T_o [$=vt_o/L$, refer equation (4.12)] values, corresponding to the different values of L were computed as,

L(cm)	T_o(t_o=384.615)	T_o(t_o=293.077)
20	1.3154	1.0023
40	0.6577	0.5012
60	0.4385	0.3341
80	0.3288	0.2506
100	0.2631	0.2005

4.1.4.2.3 Results

The concentration (of the mobile phase) distribution in depth and time obtained from the analytical solution were superposed on the model computed results and are presented in Figs. 4.13-4.20.

4.1.4.3 Comparison

The two solutions (section 4.1.4.1 and 4.1.4.2) pertain to identical conditions, except for the space domain (The analytical solution holds good for a semi-infinite system, where as the model has

been operated for a system having a finite length of 180 cms). However, the change in concentration at the lower boundary during the time period of simulation is negligible, except at 1980 mins. Thus, the domain used for numerical simulation can also be considered as effectively semi-infinite.

4.1.5   Case III

Two phase reactive solute transport.

4.1.5.1   Model Operation

The model accounting for two phase reactive solute transport (refer section 3.4.7) was operated under the following conditions.

4.1.5.1.1 Time and space Domains

The depth of the solution domain was taken as 180 cms. At the beginning of simulation the domain was subdivided into 180 moving packets using a strip thickness (ts) of 1 cm.

The total time duration of each simulation was 1980 mins. A time step of 1 min was used.

4.1.5.1.2 Parameter Values

The following parameter values were used for simulation.

a = 0.002

b = 10.0   (refer section 4.1.1.5.2)

D_0= 0.000667 cm^2/min

ρ = 1.6 gm/cm^3

λ = 0.5 cm

The sets of values of θ_{im}, α, k_d, and f used, are as follows,

θ_{im}	$\alpha(min^{-1})$	$k_d(cm^3/gm)$	f
0.0	0.0	0.5	1.0
0.0	0.0	1.0	1.0
0.171	0.001	0.5	0.0
0.1	0.0005	0.5	0.5
0.171	0.001	0.5	0.5
0.1	0.0005	1.0	0.5
0.1	0.0005	0.1	0.5

4.1.5.1.3 Initial and Boundary Condition

The initial and boundary conditions are assigned in accordance with eqns (4.6)-(4.8). Again, for the present simulation they represent concentration and moisture content in the mobile phase (refer section 4.1.4.1.3). The initial condition assigned for the concentration in the immobile phase [eqn(3.9)] is assigned in accordance with the following equation.

$$[\theta_{im} + \rho(1-f)k_d] \, c_{im}(z,0) = 0.0 \quad 0 \le z \ge z \qquad (4.34)$$

For the upper boundary condition [refer equation (4.7)], the depth of solute to be infiltrated (x) was taken as 10 cms. The values of, the concentration of the infiltrated solute (c_o), moisture content (θ) and volumetric flux (q) were taken as 209 meq/l, 0.38 and 0.026 cm/min respectively (refer section 4.1.1.5.3).

4.1.5.1.4 Results

(i)   Model computed variation of concentration in the mobile and immobile phase with respect to depth, at times 120,540,1020 and 1980 mins are represented in Figs. 4.21, 4.22 and 4.25.

(ii)   Model computed breakthrough curves (represent concentration

only in the mobile phase) at depths 20,40,60,80 and 100 cms are represented in Figs. 4.21-4.27.

4.1.5.2 Compuation of Analytical Solution

CXTFIT was used to obtain c vs z and c vs t curves for identical parameters.

4.1.5.2.1 Parameter Values

The parameters R, D, δ and ω were computed for the pre-assigned values of θ, v (refer section 4.1.5.1.3 and 4.1.1.6.1), $k_d, a, b, D_o, \lambda, f, \alpha, \theta_{im}$ (refer section 4.1.5.1.2) and L (where L is the depth at which the breakthrough curve is computed) in accordance with equation (4.15), (4.29), (4.25) and (4.26). The computed parameter values are as follows,

The values of R [refer equation (4.15)], computed for the different values of k_d are as follows,

k_d	R
0.1	1.4210
0.5	3.1053
1.0	5.2105

The values of D [refer equation (4.29); equation (3.6) for computing D_m], computed for the different values of $\theta_m (= \theta - \theta_{im})$ are as follows,

θ_m	$D(cm^2/min)$
0.28	0.03423
0.209	0.03422
0.38	0.03425

concentration (meq/l)

Concentration profile

· · · Analytical (c_m)

—— Numerical (c_m)
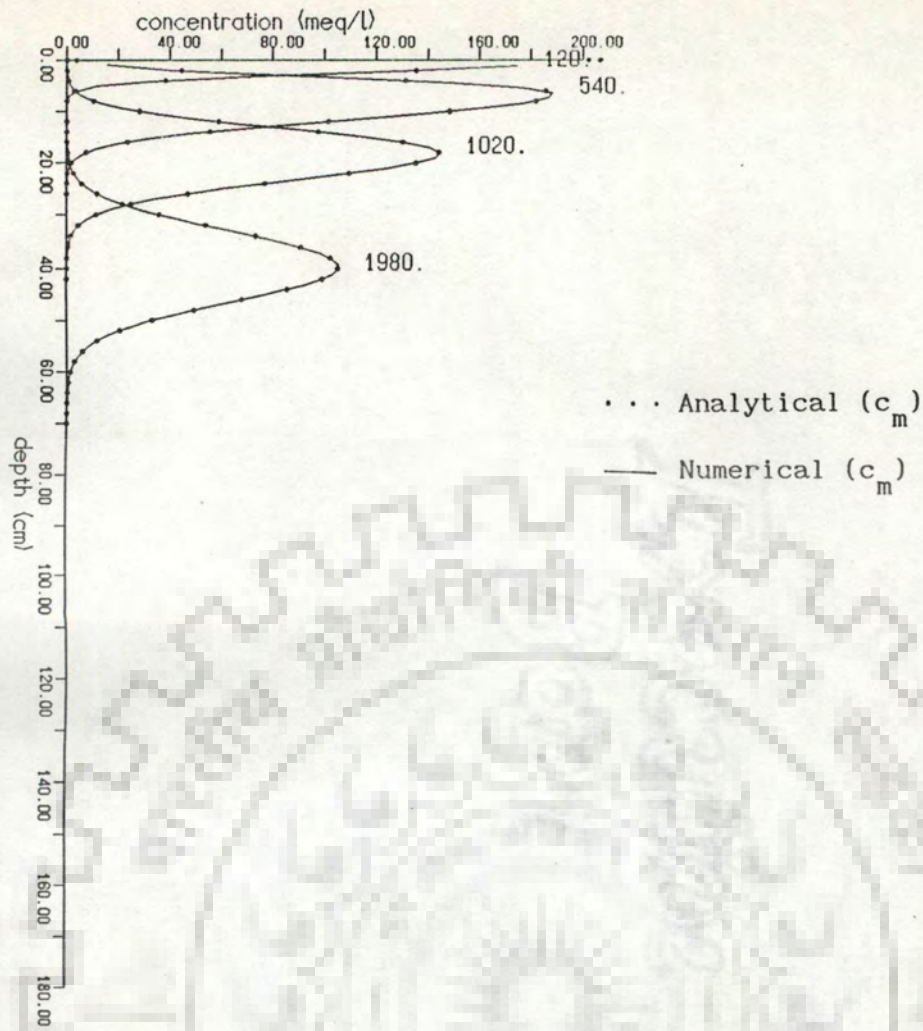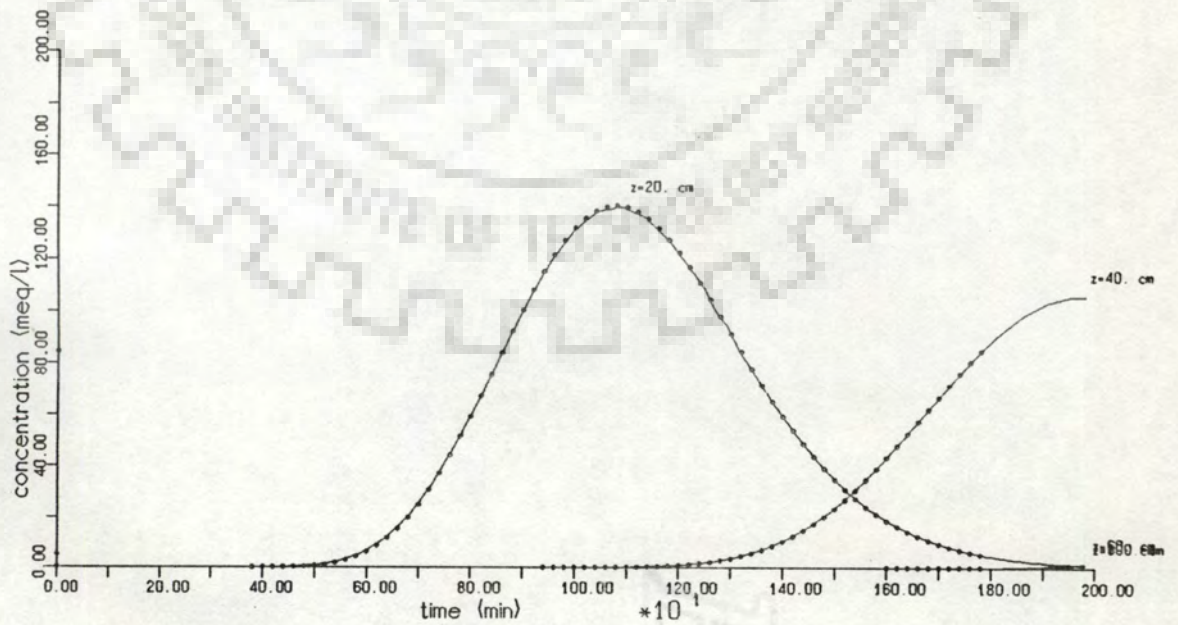
Concentration breakthrough curve

Fig. 4.21. Comparison with analytical solution for two phase reactive solute transport (θ_{im}=0.0 cm, α=0.0 min^{-1}, k_d=0.5 cm^3/gm, f=1.0).

concentration (meq/l)

depth (cm)

· · · Analytical (c_m)

—— Numerical (c_m)

Concentration profile

concentration (meq/l)

time (min)
$*10^1$

z=20. cm

z=600. cm
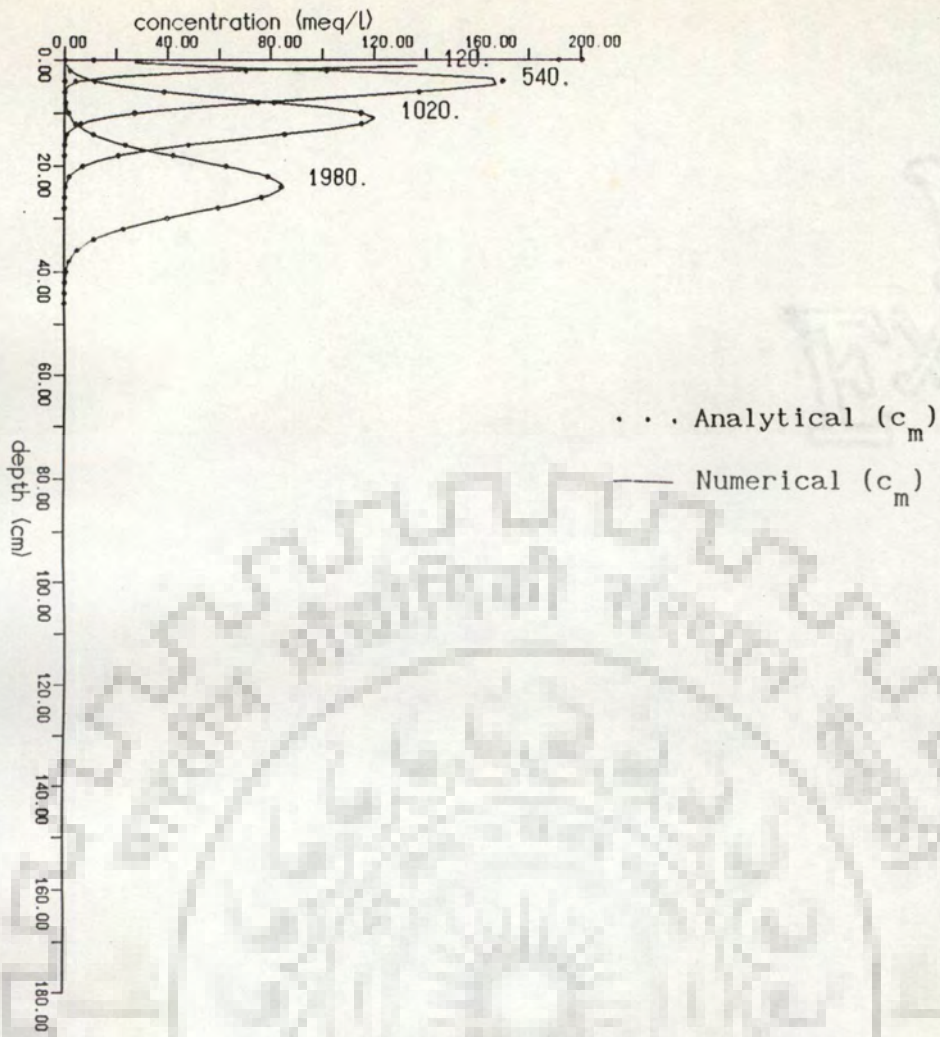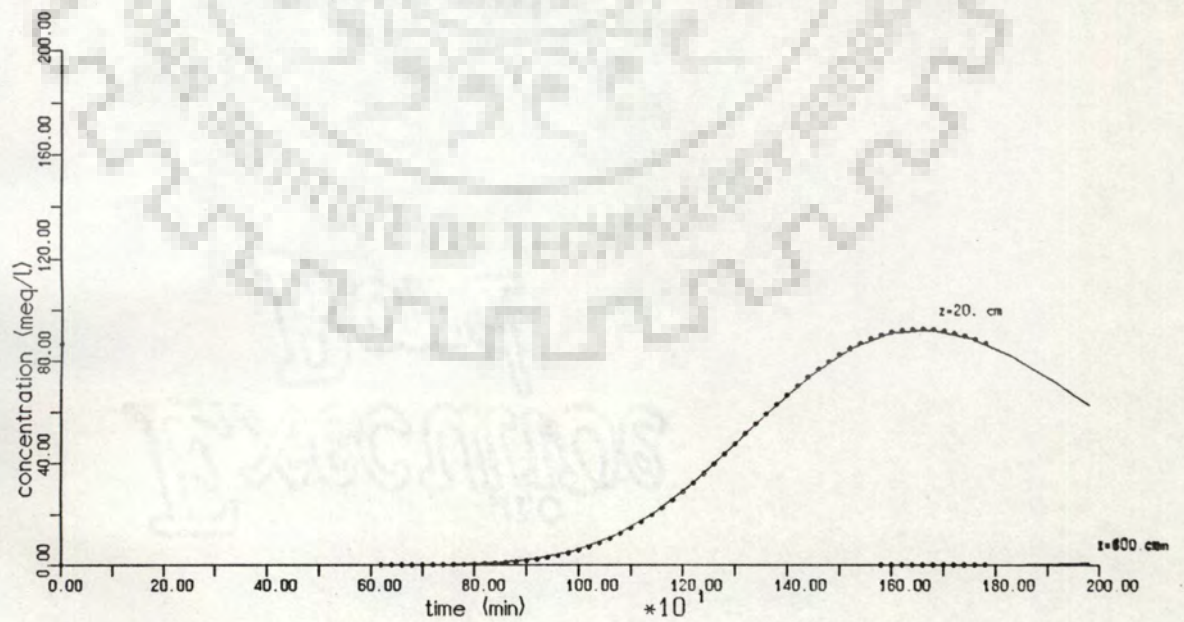
Concentration breakthrough curve

Fig. 4.22. Comparison with analytical solution for two phase reactive solute transport (θ_{im}=0.0 cm, α=0.0 min^{-1}, k_d=1.0 cm^3/gm, f=1.0).
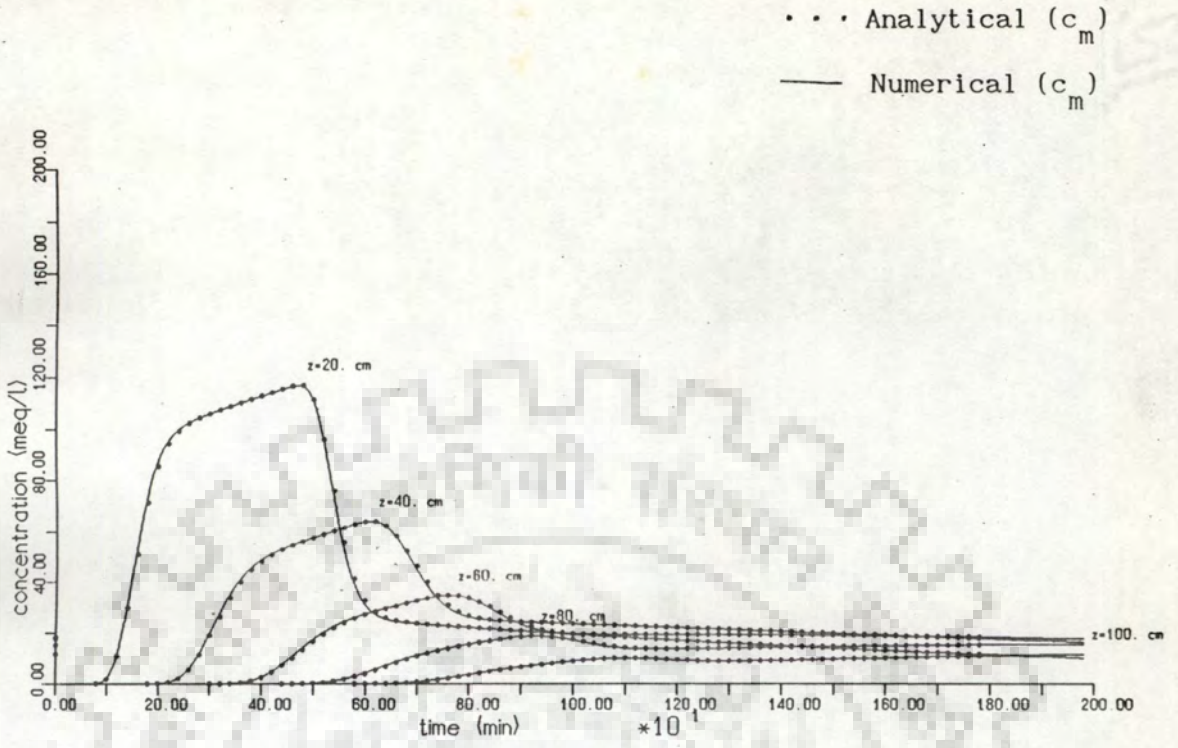
Concentration breakthrough curve

Fig. 4.23. Comparison with analytical solution for two phase reactive solute transport (θ_{im}=0.171 cm, α=0.001 min^{-1}, k_d=0.5 cm^3/gm, f=0.0).
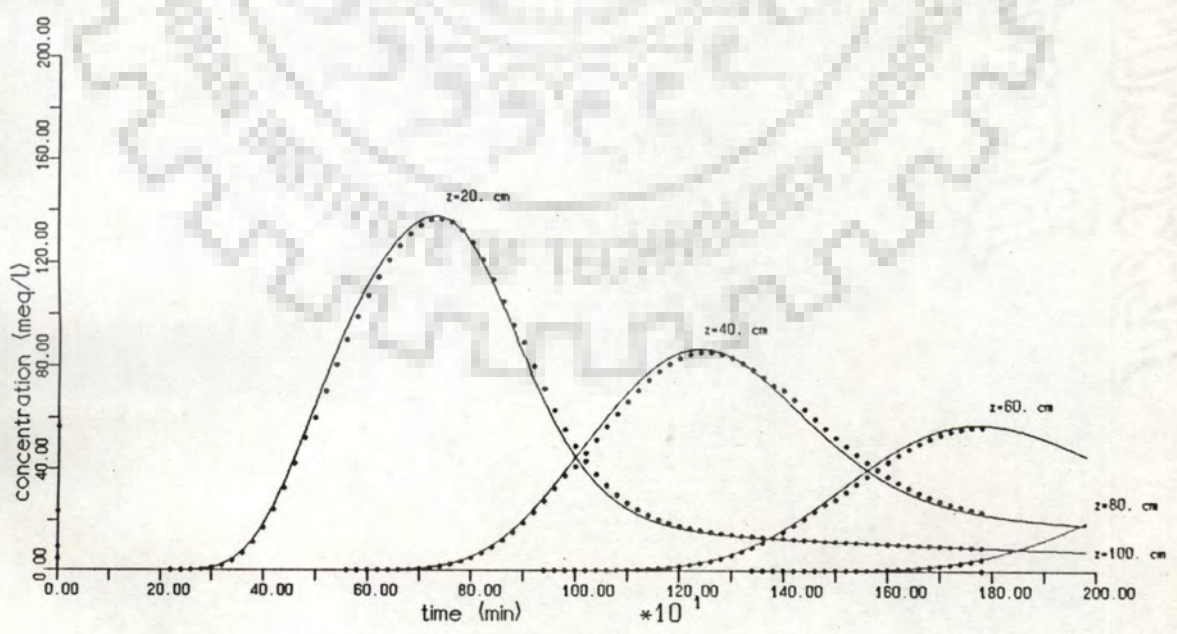
Concentration breakthrough curve

Fig. 4.24. Comparison with analytical solution for two phase reactive solute transport (θ_{im}=0.1 cm, α=0.0005 min^{-1}, k_d=0.5 cm^3/gm, f=0.5).
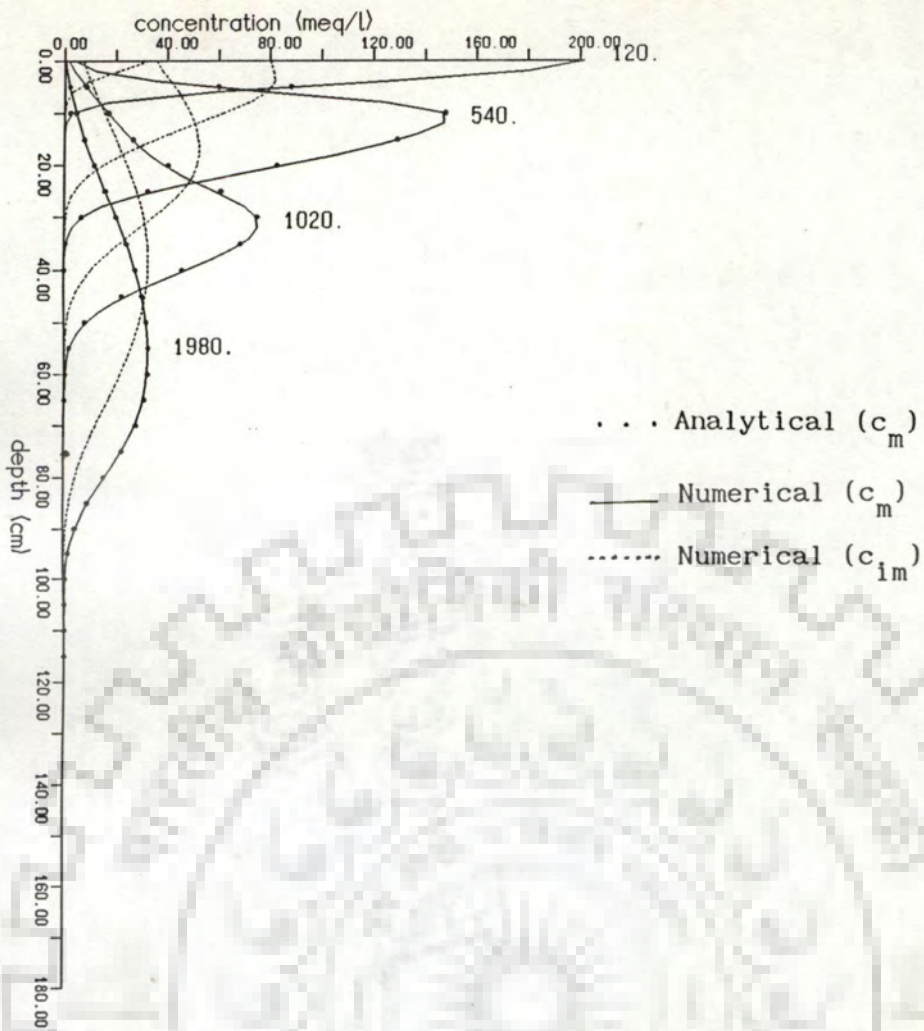
Concentration profile
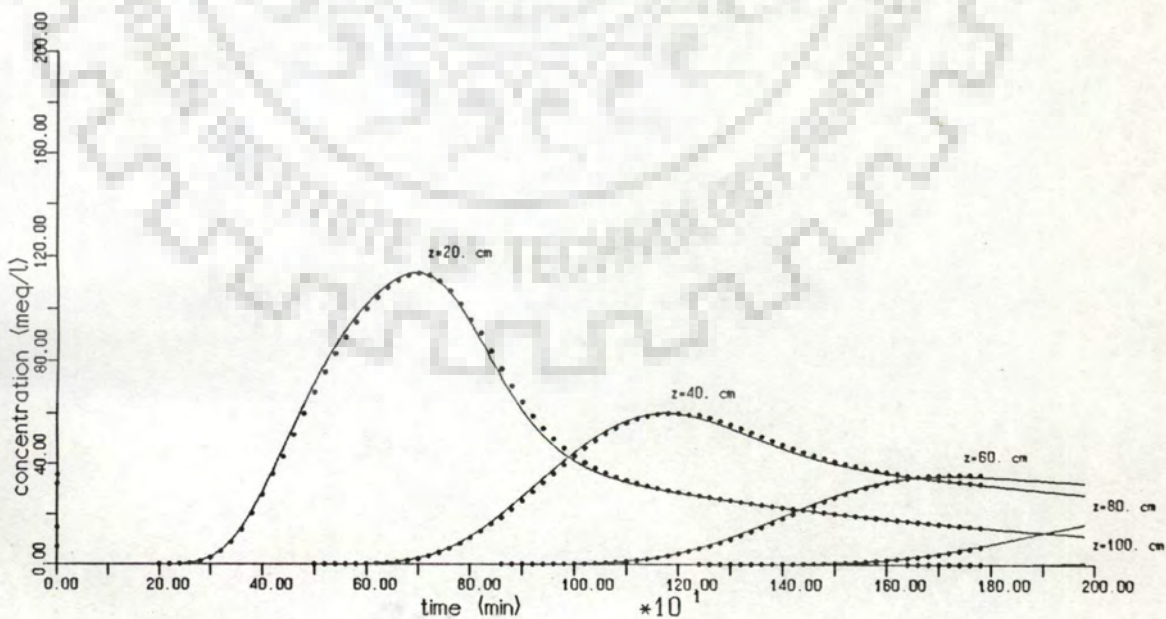
Concentration breakthrough curve

Fig. 4.25. Comparison with analytical solution for two phase reactive solute transport (θ_{im}=0.171 cm, α=0.001 min^{-1}, k_d=0.5 cm^3/gm, f=0.5).

Concentration breakthrough curve
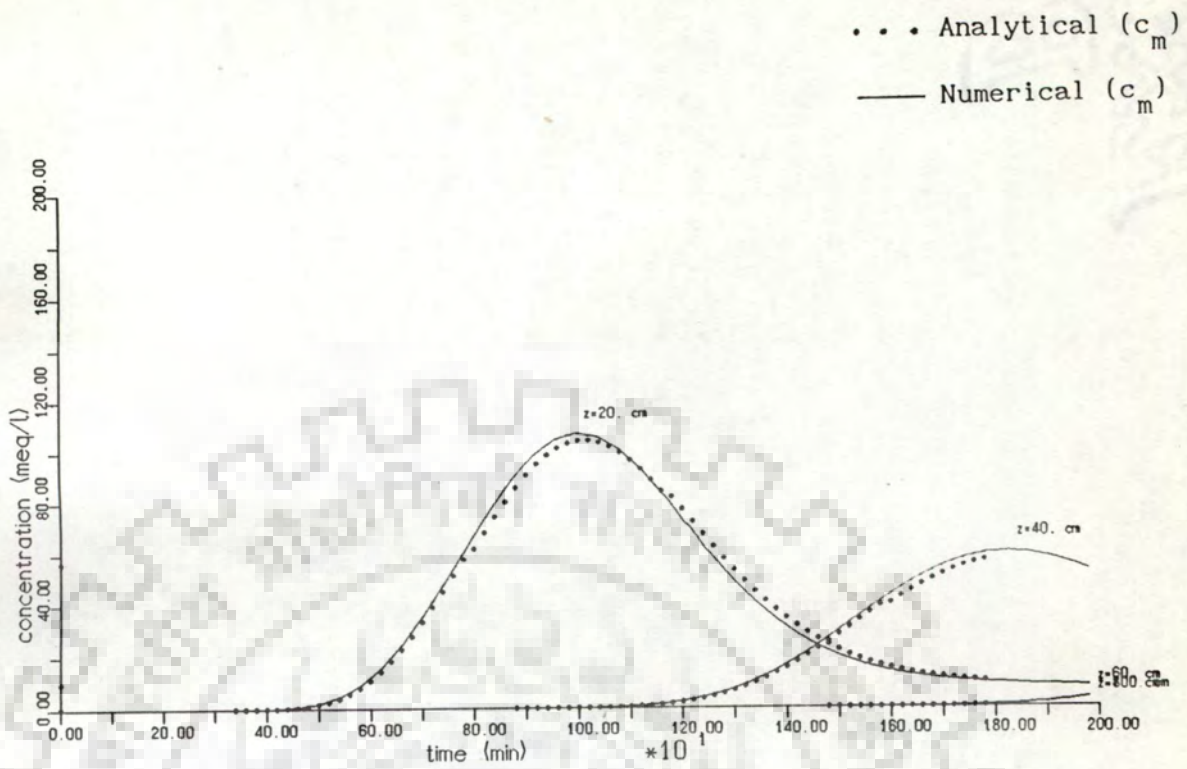
Fig. 4.26. Comparison with analytical solution for two phase reactive solute transport (θ_{im}=0.1 cm, α=0.0005 min^{-1}, k_d=1.0 cm^3/gm, f=0.5).

Concentration breakthrough curve
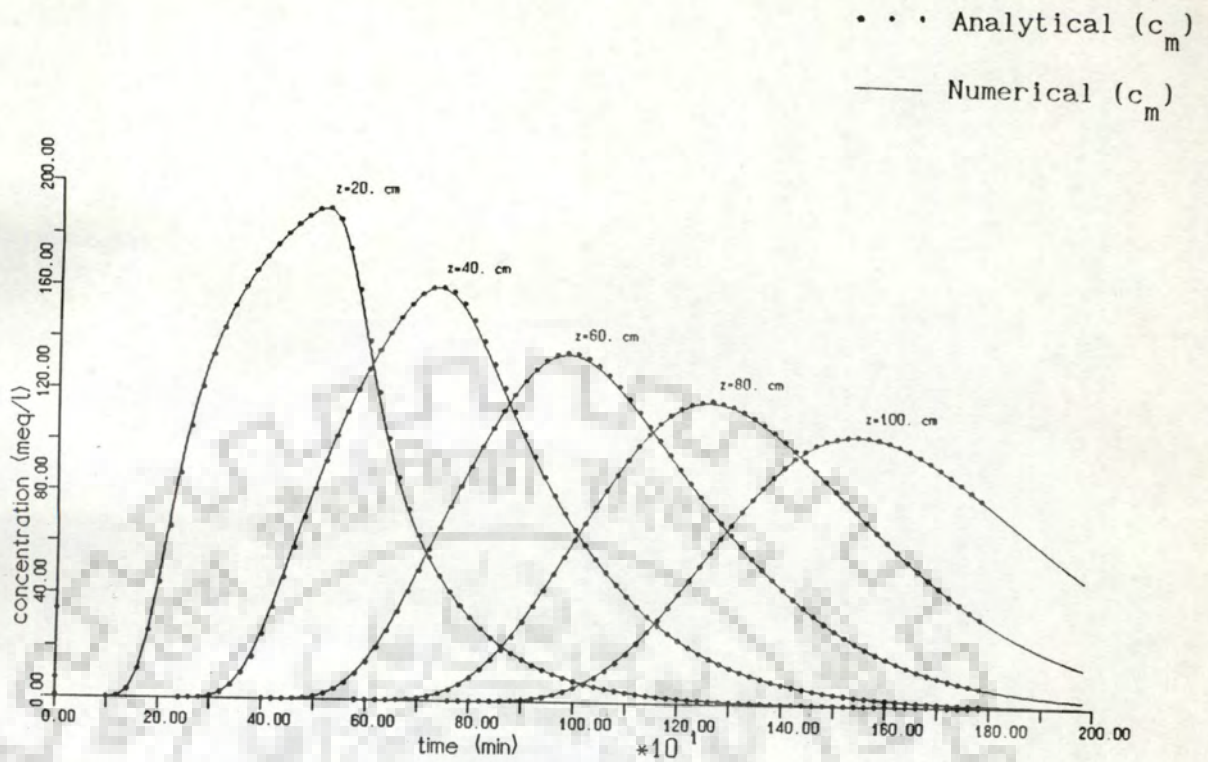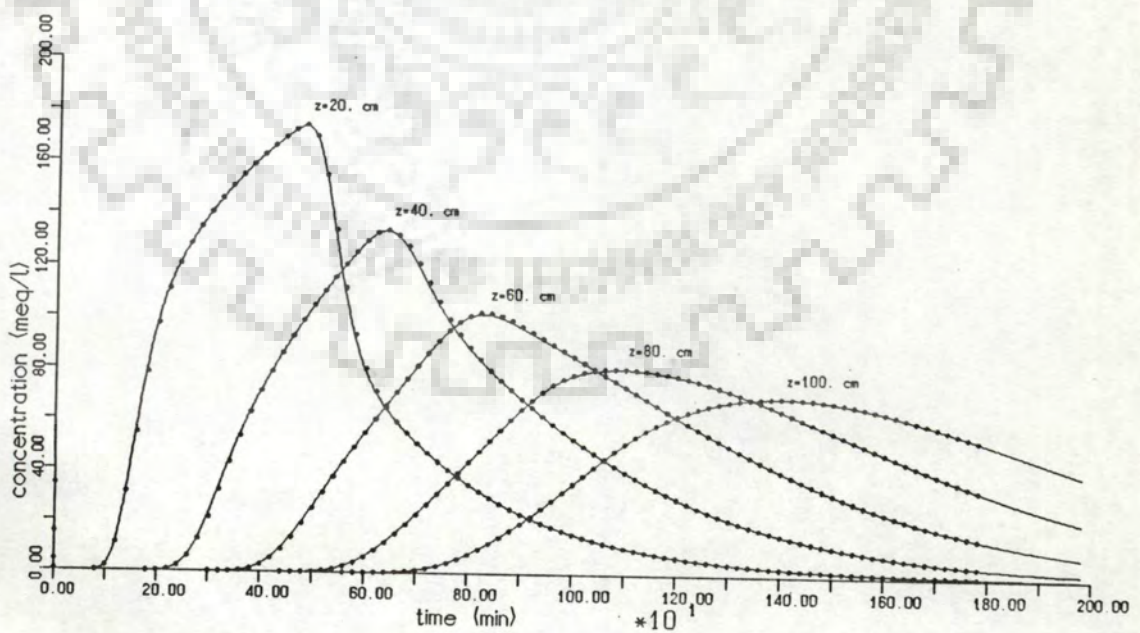
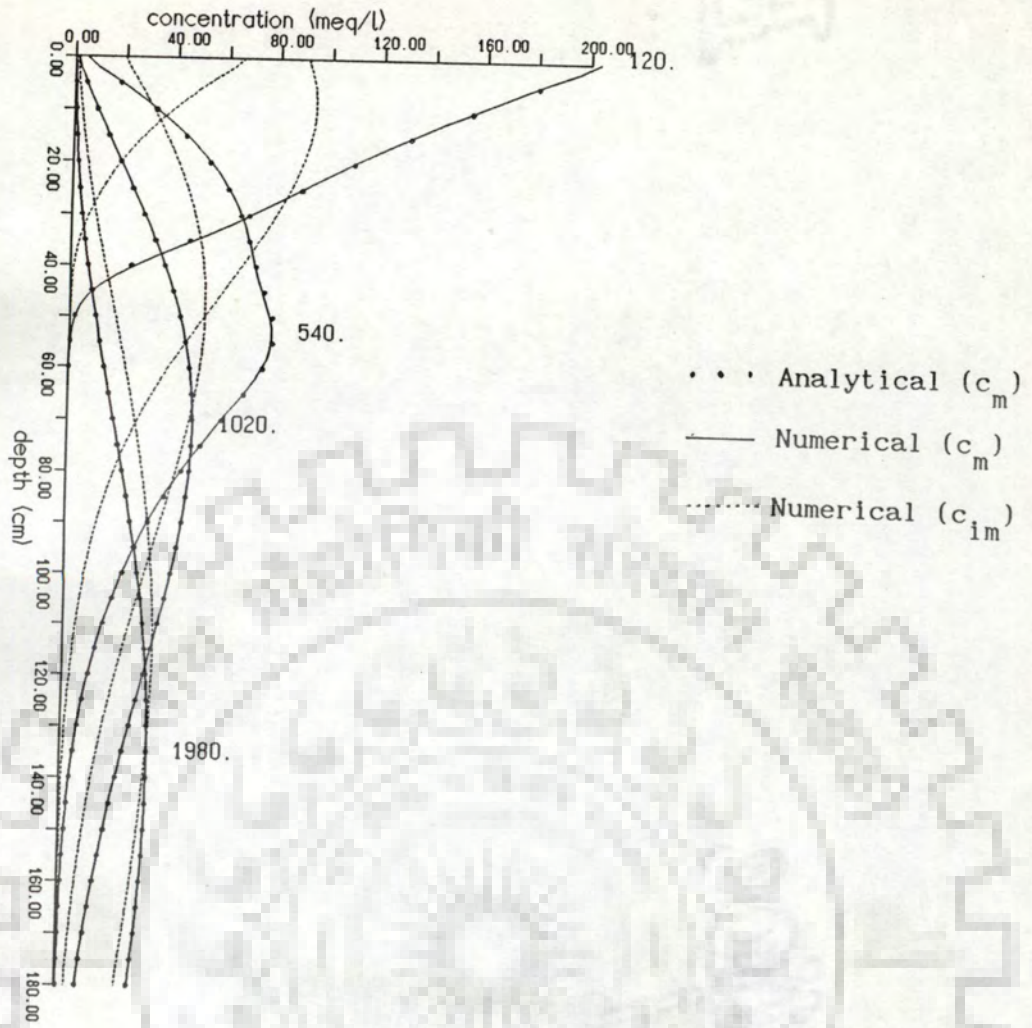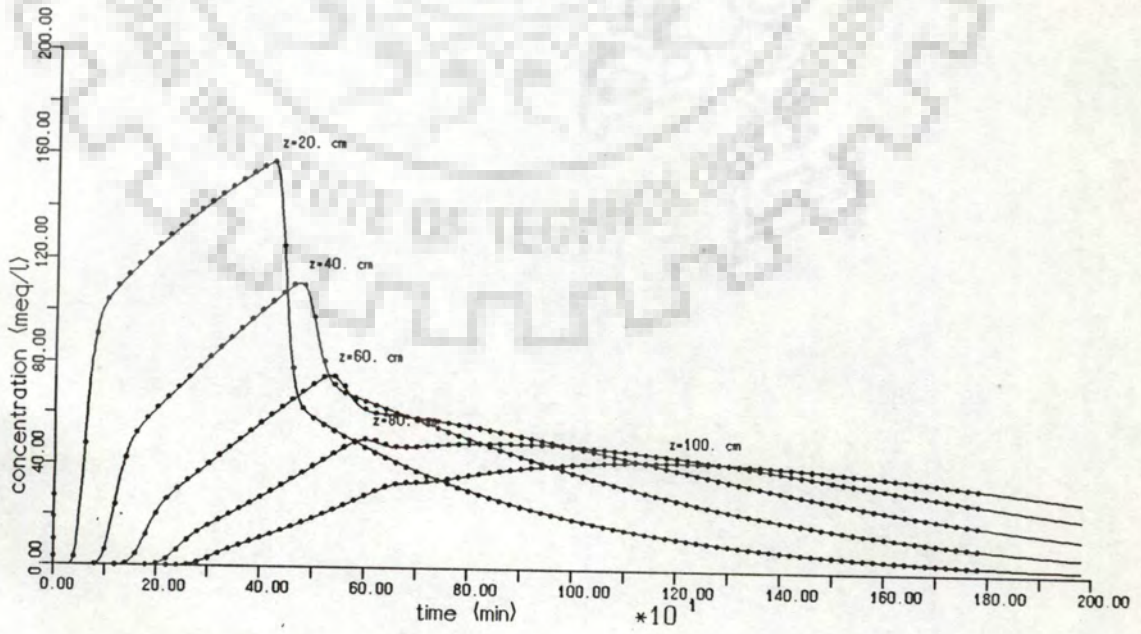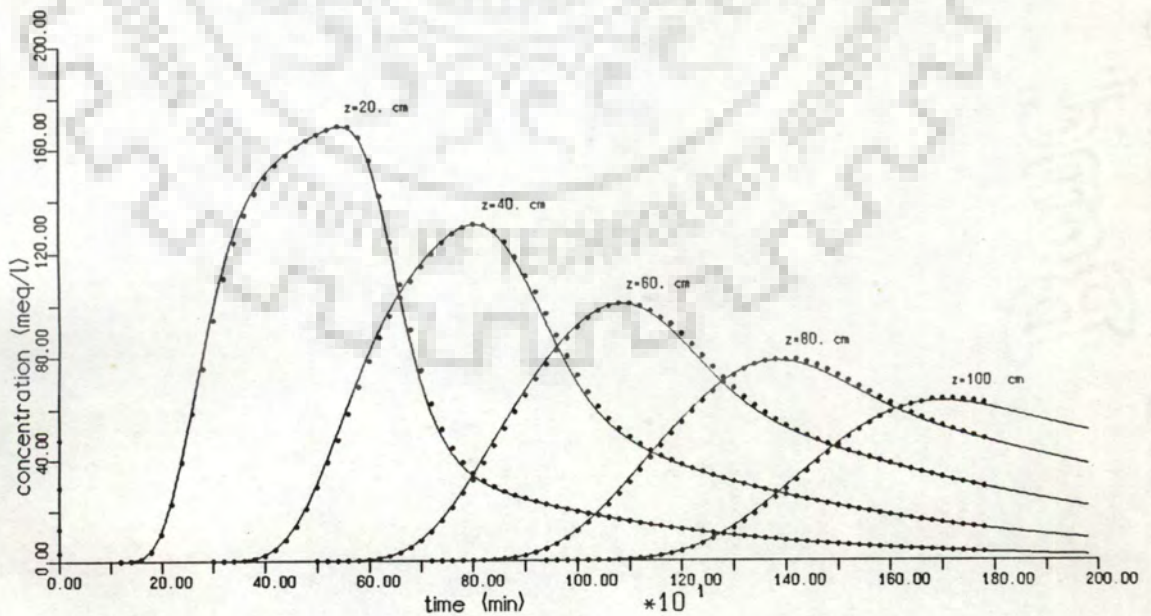Fig. 4.27. Comparison with analytical solution for two phase reactive solute transport (θ_{im}=0.1 cm, α=0.0005 min^{-1}, k_d=0.1 cm^3/gm, f=0.5).

The values of δ [refer equation (4.25)], computed for the different values of θ_m, k_d and f are as follows,

θ_m	$k_d(cm^3/gm)$	f	δ
0.38	0.5	1.0	0.678
0.38	1.0	1.0	0.8081
0.209	0.5	0.0	0.1771
0.28	0.5	0.5	0.5763
0.209	0.5	0.5	0.5161
0.28	1.0	0.5	0.5454
0.28	0.1	0.5	0.8372

The values of ω [refer equation (4.26)], computed for the different values of L and α are as follows,

$L(cm)$	$\omega(\alpha=0.0min^{-1})$	$\omega(\alpha=0.001min^{-1})$	$\omega(\alpha=0.0005min^{-1})$
20	0.0	0.7692	0.3846
40	0.0	1.5385	0.7692
60	0.0	2.3077	1.1538
80	0.0	3.0769	1.5385
100	0.0	3.8461	1.9231

4.1.5.2.2 Initial and Boundary Conditions

The initial and boundary conditions are assigned in accordance with eqns (4.2)-(4.4). However, they represent the concentration and moisture content of the mobile phase only. The initial condition for the immobile phase is assigned in accordance with eqn (4.34).

The value of t_o for 10 cms of solute infiltration was computed

as 384.615 mins (refer section 4.1.3.2.2). For t_0 = 384.615 mins, the T_0[=vt_0/L, refer equation (4.12)] values, corresponding to the different values of L were computed as,

L(cm)	T_0
20	1.3154
40	0.6577
60	0.4385
80	0.3288
100	0.2631

4.1.5.2.3 Results

The concentration (of the mobile phase) distribution in depth and time, obtained from the analytical solution were superposed on the model computed results and are presented in Figs. 4.21-4.27.

4.1.5.3 Comparison

The two solutions (section 4.1.5.1 and 4.1.5.2) pertain to identical conditions, except for the space domain (the analytical solution holds good for a semi-infinite system, where as the model has been operated for a system having a finite length of 180 cms). However, as the change in concentration at the lower boundary during the time period of simulation is negligible, the domain used for numerical simulation can also be considered as effectively semi-infinite.

4.1.6 DISCUSSION

Case I.

A very good agreement can be observed between the results

obtained by the two solutions (Figs. 4.9-4.11). However, for a high value of β (=0.1 min^{-1}) some numerical dispersion is observed (Fig. 4.12). Again, from Figs 4.9 and 4.10 it can be seen that the sensitivity of the peak concentration to the dispersivity value (λ=0.5, λ=0.1) is much less compared to that of the non-reactive case (Figs. 4.3 and 4.2).

Case II

For different values of θ_{im} (Figs. 4.13 to 4.15) an excellent agreement between the two solutions can be observed. From Fig. 4.16 it can be seen that, for a very high value of α(=10 min^{-1}) the solutions converge to that of single phase solute transport i.e., the concentration in the mobile and immobile phase become equal. For a high value of θ_{im} (=0.3) and α(=0.1 min^{-1}), again some numerical dispersion is observed (Fig. 4.17). The effect of the time step variation can be observed in Figs. 4.18 to 4.20. Deviations in the two solutions is negligible till the time step is such that a moving packet travels more than half the nodal spacing during a single time step.

Case III

An excellent agreement between the two solutions can be observed till all the adsorption sites are either located in the mobile (Fig. 4.21 and Fig. 4.22) or in the immobile soil phase (Fig. 4.23). For partial location of adsorption sites in both the soil phases, the agreement between the two solutions is not very good (Figs. 4.24-4.27). However, it is considerably close.

4.2   COMPARISON WITH EXPERIMENTAL DATA

4.2.1   Warrick's Experiment (Warrick et al., 1971)

A field experiment, to study transport of calcium chloride and water in an unsaturated soil medium, has been reported by Warrick et al. (1971). The experiment was conducted in the summer of 1970 on the University of California West side field station near Fresno. The soil is classified as Panoche clay loam. A 6.1- by 6.1- meter plot (Fig. 4.28) was wetted with 7.62 cm of 0.2N $CaCl_2$, followed immediately by 22.9 cm of solute free water. The total infiltration occurred in 17.5 hrs. Tensiometers were installed in duplicate at depths of 30,60,90,120,150 and 180 cm below the surface in a 1-meter square, located in the centre of the plot (Fig. 4.28) and were used to monitor values of the soil-water pressure head. Ceramic cups were also installed in duplicate at each 30 cm increment as shown in Fig. 4.28 to obtain solute samples during the infiltration process.

Numerical simulation of the concentration and moisture profiles in depth, under conditions identical to the field experiment was carried out using the model for single phase non-reactive solute transport. The simulated results were compared with the reported observed profiles.

4.2.1.1   Data

4.2.1.1.1 Soil Characteristics

The following relations were used.

(i) h vs θ relation
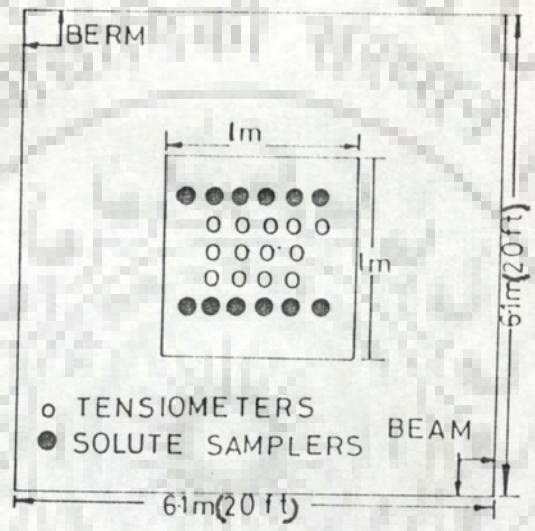
Fig. 4.28. Schematic diagram of field site (Warrick's experiment).

$$\theta(h) = \begin{cases} 0.6829-0.09524 \ \ln(|h|) & h \ge 29.5 \\ 0.4531-0.02732 \ \ln(|h|) & 29.5 > h \ge 14.495 \end{cases} \tag{4.34}$$

(ii) K vs θ relation

$$K(\theta) = 3.24 \times 10^{-8} \ \exp \ (35.8\theta) \tag{4.35}$$

where, K is in cm/min.

4.2.1.1.2 Initial and Boundary Conditions (Soil-Moisture)

(i) Initial condition

$$\theta(z,0) = f(z) \qquad\qquad 0 \le z \le Z \tag{4.36}$$

where, Z is the total depth of the flow domain.

(i) Upper boundary condition

$$h(0,t) \qquad = h_s \tag{4.37}$$

(ii) Lower boundary condition

$$h(Z,t) \qquad = h_i \tag{4.38}$$

where, h_s is the capillary head at the saturated soil moisture content value and h_i is the initial capillary head at depth Z.

4.2.1.1.3 Initial and Boundary Condition (Solute Concentration)

(i) Initial condition

$$c(z,0) \qquad = 0.0 \qquad\qquad 0 \le z \le Z \tag{4.39}$$

(i) Upper boundary condition

$$qc(0,t) - \theta D \ \frac{\partial c(0,t)}{\partial t} = \begin{cases} qc_o & d_{in} \le 7.62 \\ 0 & d_{in} > 7.62 \end{cases} \tag{4.40}$$

where, d_{in} is the cumulative depth of infiltration in cms.

(ii) Lower boundary condition

$$\frac{\partial c(Z, t)}{\partial z} = 0 \qquad\qquad (4.41)$$

where, z is in cm, θ is in cm^3/cm^3, c is in meq/l and t is in mins. The value of c_o i.e,. concentration of the solute being infiltrated is 209 meq/l. To compute the hydrodynamic dispersion co-efficient [eqn (3.2)], the following values of a, b and D_o (Bresler, 1973) were taken,

$$a = 0.002$$

$$b = 10.0$$

$$D_o = 0.000667 \ cm^2/min$$

where, D_o is the molecular diffusion coefficient of chloride in a free water system. For the dispersivity λ a range of values was taken to get the best possible match between the observed and computed profiles.

4.2.2   RESULTS AND DISCUSSION

The measured and computed soil moisture profiles at 2, 9, 11 and 17 hrs of infiltration are shown in Fig. 4.29. An examination of the profiles reveals that there is a close agreement between the observed and computed distribution of moisture in space and time. According to the reported data, the infiltration of the solute (7.62 cm) and water (22.9cm) required a time period of 1050 minutes (17.5 hrs). The model simulated period of infiltration is 1044 minutes (17.4 hrs).

The reported and computed solute concentration profiles at 2, 9, 11 and 17 hrs are plotted in Fig. 4.30. It is revealed that at 9 hrs $\lambda=0.7$ yields the peak concentration value. However, at subsequent times higher λ values ($\lambda =0.9$, at 11 hrs, $\lambda=1.0$ at 17 hrs) are necessary for matching the peak concentration values. This corroborates the time
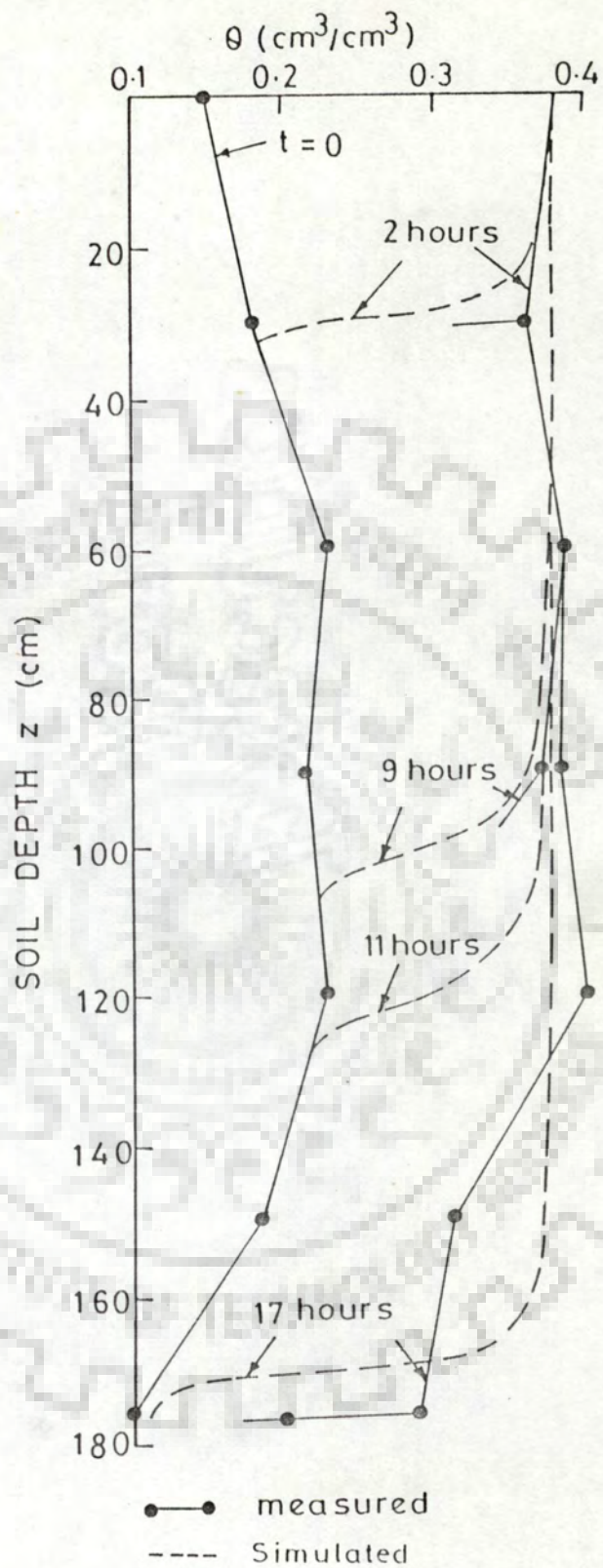
Fig. 4.29. Measured and simulated soil moisture profiles.
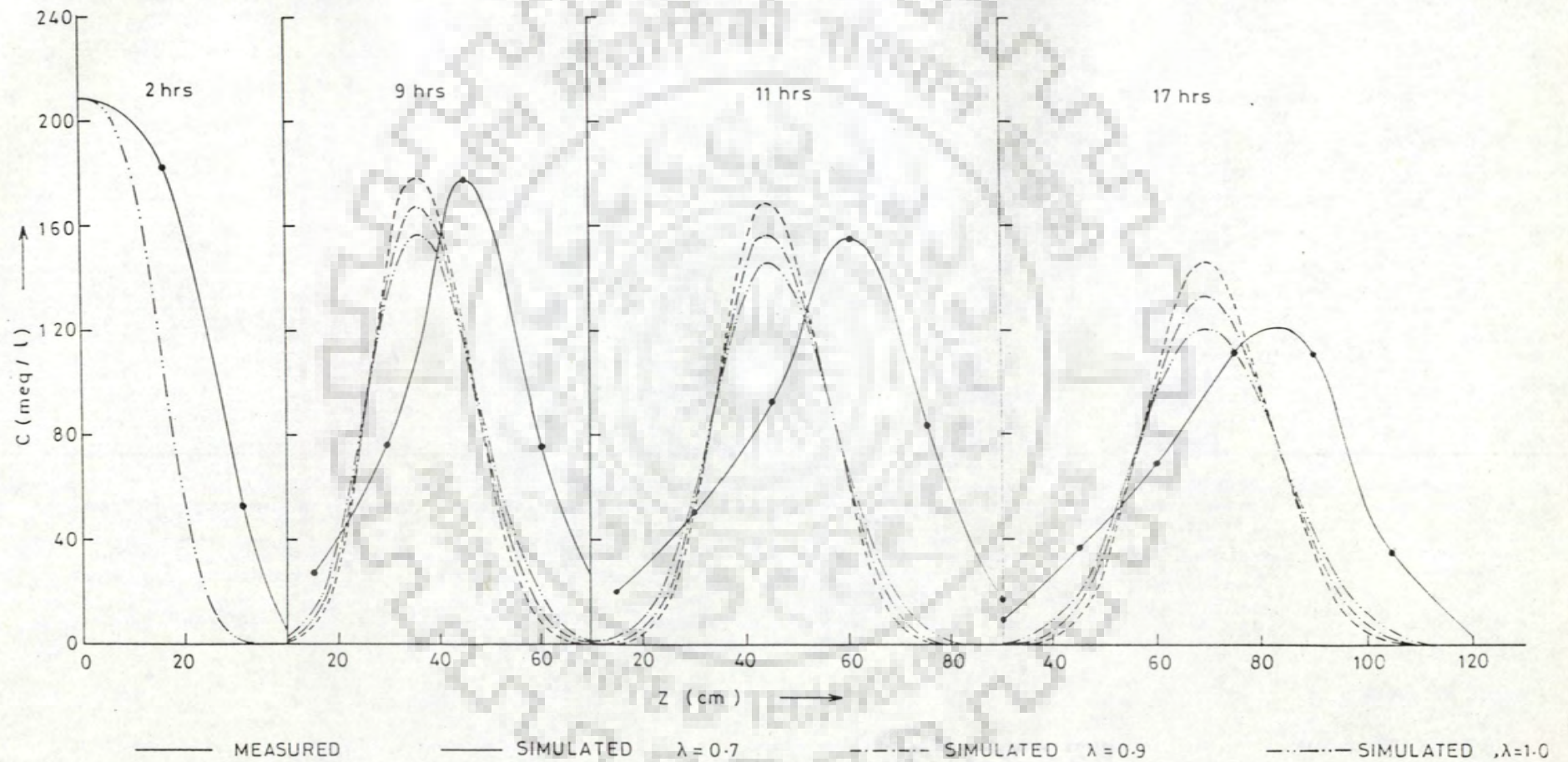
Fig. 4.30. Measured and simulated chloride concentration profiles.

(depth) variability of λ reported by Corey et al., 1970 (cited in Warrick et al., 1971).

An apparent lag between the simulated and measured solute concentration profiles is observed at all time levels. Thus, the measured depth of solute travel is higher, in comparison to the simulated depth of solute travel. This indicates towards an increased solute velocity, which may have been caused by the phenomenon of anion-exclusion. To verify this hypothesis, the simulation was repeated using the two phase non-reactive solute transport model, neglecting transfer of solute into out of the immobile solute phase. The solution carried out in this manner is similar to a single phase solute transport accounting for anion-exclusion, where θ_{im} acts as θ_{ex} i.e., the equivalent volume of anion free solution per unit volume of bulk soil. Concentration profiles were again simulated, varying the values of θ_{im} and λ. The best reproduction of the measured concentration profiles was obtained with θ_{im} = 0.06 and λ = 1.5 cm. The results are plotted in Fig. 4.31. It can be seen that the lag between the observed and measured profiles has considerably reduced.

4.2.3   Bromide leaching experiment (Böttcher and Strebel, 1990)

A bromide leaching experiment was conducted in the Fuhrberger field (Hannover, Germany) during the period 22.9.1989 to 26.3.1990. Fig. 4.32 is a schematic sketch of the area (3x12m). A bromide solution was applied on 22.9.1989 and concentrations were monitored reguarly at a depth of 120 cms, with the help of 51 suction cups. Profiles of bromide amounts in depth were also measured on two dates (15.11.1989 and 6.2.1990) (Unpublished data, the experimental data were obtained through
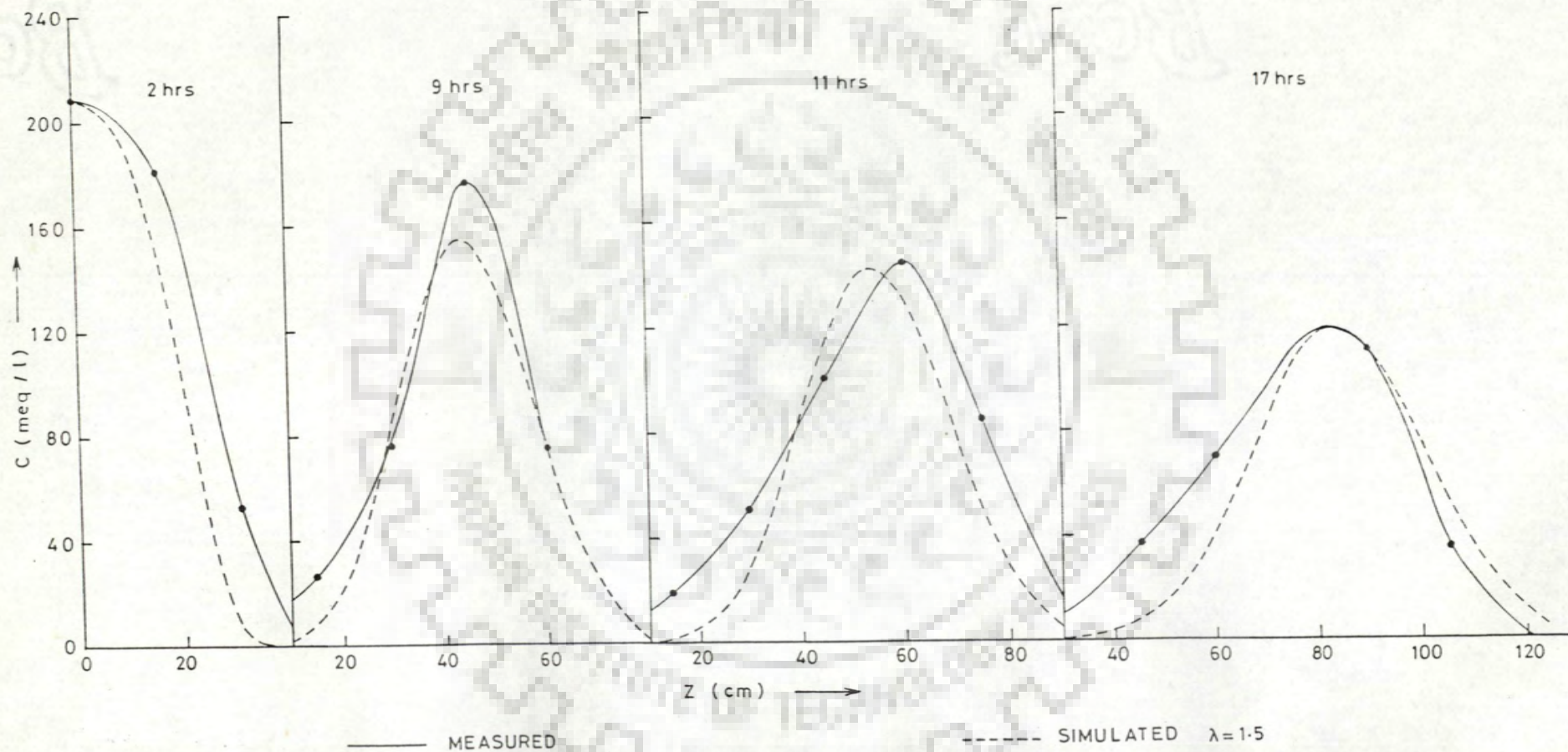
Fig. 4.31. Measured and simulated chloride concentration profiles (considering the presence of an immobile phase and neglecting transfer of solute into/out of the immobile phase).
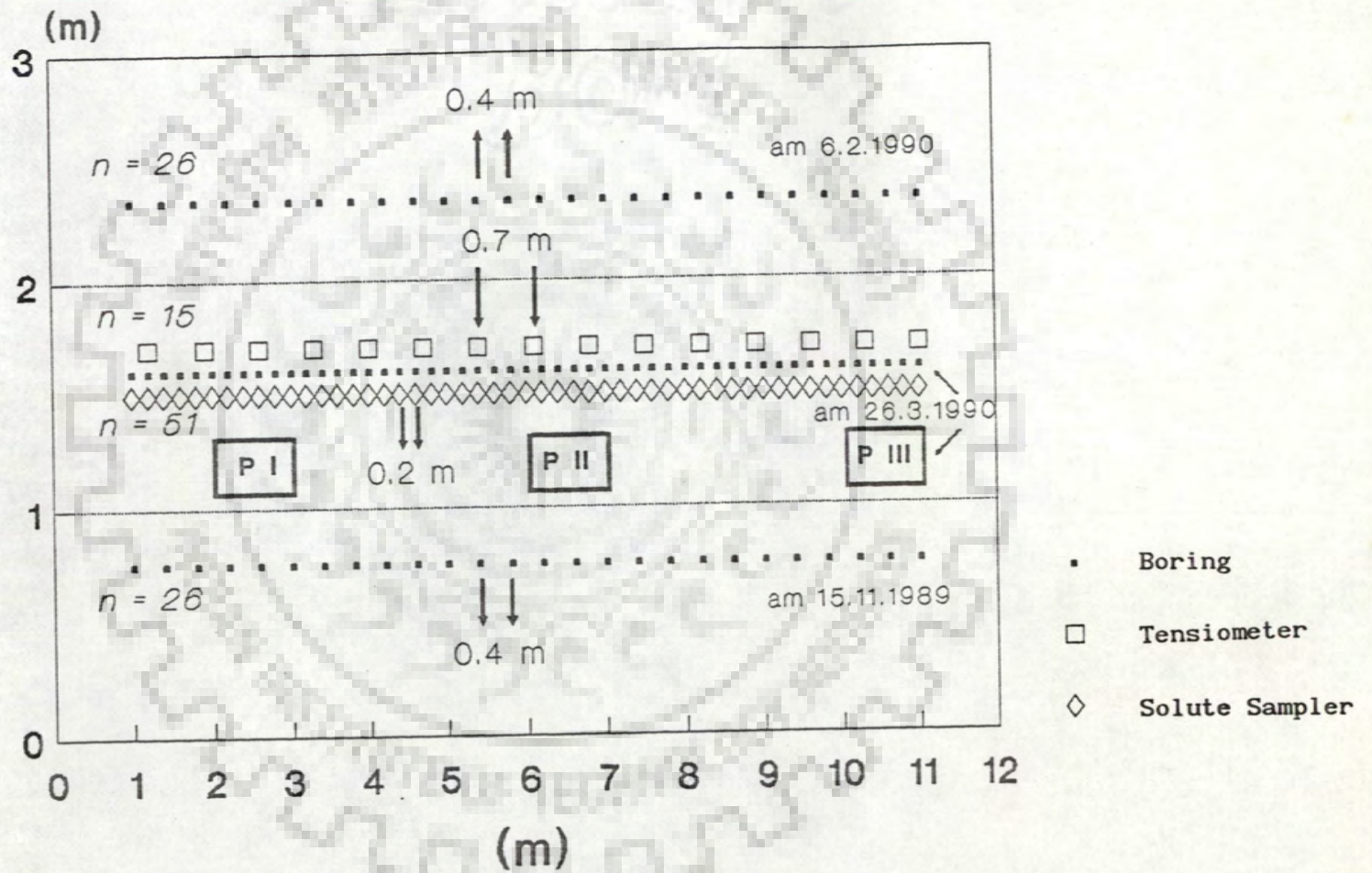
Fig. 4.32. Schematic diagram of field site (Böttcher and Strebel's experiment).

personal communcation).

Numerical simulation of the break through curve and bromide amount in depth, under conditions identical to the field experiment was carried out using the model for single phase non-reactive solute transport.

4.2.3.1 Data

4.2.3.1.1 Soil characteristics

The soil type is gley-podzol in medium fine sand and comprises of two horizons, A (upto 35 cms, rich in organic material) and B (> 35 cms). The reported soil characteristics of the two layers are given in table 4.1. These characteristics are reported to have been determined by laboratory experiments.

4.2.3.1.2 Initial and Boundary Conditions (Soil Moisture)

(i) Initial condition

$$h(z,0) = f(z) \qquad 0 \le z \le Z \qquad (4.42)$$

where, Z is the total depth of the flow domain.

(ii) Upper Boundary Condition

$$q(0,t) = Q(t) \qquad (4.43)$$

where, $Q(t)$ is the net input at the ground comprising of precipitation and evaporation. The actual evaporation values were computed using the unsaturated flow model of Duynisveld and Strebel (1983), with the help of the climatic data recorded during the experimental period. Further, using the recorded precipitation data, the net input at the ground was computed.

(iii) Lower Boundary Condition

The lower boundary condition was taken as the water table, at which the capillary pressure (h) was assigned zero (pressure=atmospheric pressure).

$$h(Z,t) \quad = \quad 0.0 \tag{4.44}$$

The depth to water table [i.e., the lower boundary condition, described by equation (4.44)] was time variant and was monitored throughout the experimental period.

Table 4.1

Soil Characteristics of the two layers.

First layer			Second layer		
θ	h(cm)	K(cm/day)	θ	h(cm)	K(cm/day)
0.05	60000.0	0.1×10^{-6}	0.01	60000.0	0.1×10^{-7}
0.06	15000.0	0.1×10^{-6}	0.02	15000.0	0.1×10^{-7}
0.07	10000.0	0.1×10^{-6}	0.03	10000.0	0.5×10^{7}
0.1	1000.0	0.5×10^{-4}	0.05	1000.0	0.1×10^{-4}
0.14	300	0.4×10^{-3}	0.06	300.0	0.1×10^{-3}
0.17	100.0	0.1×10^{-1}	0.07	100.0	0.5×10^{-2}
0.2	60.0	0.5×10^{-1}	0.09	60.0	0.2×10^{-1}
0.245	40.0	0.68	0.125	40.0	0.3
0.28	30.0	5.0	0.15	30.0	3.0
0.34	20.0	16.0	0.22	20.0	12.0
0.4	10.0	55.0	0.29	10.0	78.0
0.46	0.0	300.0	0.38	0.0	800.0

4.2.3.1.3 Initial and boundary Conditions (Solute Concentration)

(i) Initial condition

$$c(x,0) \quad = \quad 0.0 \qquad 0 \le x \le X \tag{4.45}$$

where X is the total depth of solute domain. The value of X was taken below the greatest depth to water table recorded during the simulation period.

(ii) Upper Boundary Condition

$$c(0,0) \quad = \quad c_o \tag{4.46}$$

where, c_o is the concentration of bromide applied at the ground at the beginning of the experiment. The amount of bromide applied at the ground was taken as 5.61 gBr$^-$/m^2 *.

$$qc(0,t) - \theta D \frac{\partial c(0,t)}{\partial z} = 0 \tag{4.47}$$

(iii) Lower Boundary Condition

$$\frac{\partial c(X,t)}{\partial x} = 0 \tag{4.48}$$

Moisture profiles in depth and time were simulated (Fig. 4.33) (measured experimental data of soil moisture were not available). To simulate spatial and temporal concentration distribution, two different dispersivity values (i.e., $\lambda=1.5$ cm and $\lambda=2.0$ cm) were used.

---

* The amount of bromide appplied on 22.9.89 was 7.5 gBr$^-$/m^2 (=75 kg/ha). On 15.11.89, 26 borings were made to sample the soil down to 120 cms in 10 cm depth increments. The mean recovery of bromide was 5.61 gBr$^-$/m^2 (=56.1 kg/ha). The mean concentration profile in depth also gave the same mean recovery of bromide. Thus, a loss of about 25% Br$^-$ was observed. This loss of Br$^-$ was probably due to wind erosion from the soil surface during the time between Br$^-$ application and the first considerable precipitation in October 89, which leached the Br$^-$ into the soil matrix.
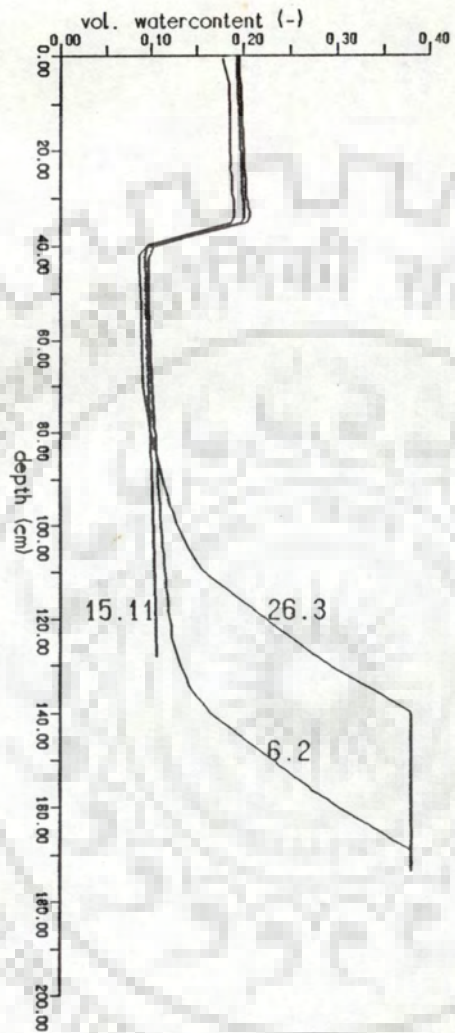
Fig. 4.33. Simulated Moisture Profiles.

4.2.3.2   Experimental Curves

The experimental curves used for comparison comprise of,

(i)   mean bromide breakthrough curve at a depth of 120 cm.

(ii)   mean bromide amount in depth on 15.11.89 and 6.2.90.

The mean breakthrough curve at a depth of 120 cm was based on measurements by suction cups at 51 locations. The soil was more or less homogeneous in nature, but the time of arrival of solute in all the 51 cups was different. This indicates a large horizontal variability in the pore water velocity. This was attributed to differences in the soil moisture contents in a horizontal plane, which were quite prominent in depths > 50 cm (Böttcher, 1991 ; personal communication).

4.2.3.3   Results and Discussion

The variation in solute transport observed at different locations was possibly caused by horizontal transport. The proposed model simulates one dimensional vertical solute transport and does not account for horizontal variability.

The simulated bromide breakthrough curves for the two λ values were superposed on the measured mean breakthrough curve. From Fig. 4.35 and 4.36, it can be seen that the simulated breakthrough curves generally lie between the reported ± 95 confidence interval. However, for $\lambda=2.0$ cm the measured and simulated breakthrough curves were closer.

Profiles of bromide amounts in depth were also simulated using the two dispersivity values. Superposing the mean measured data of
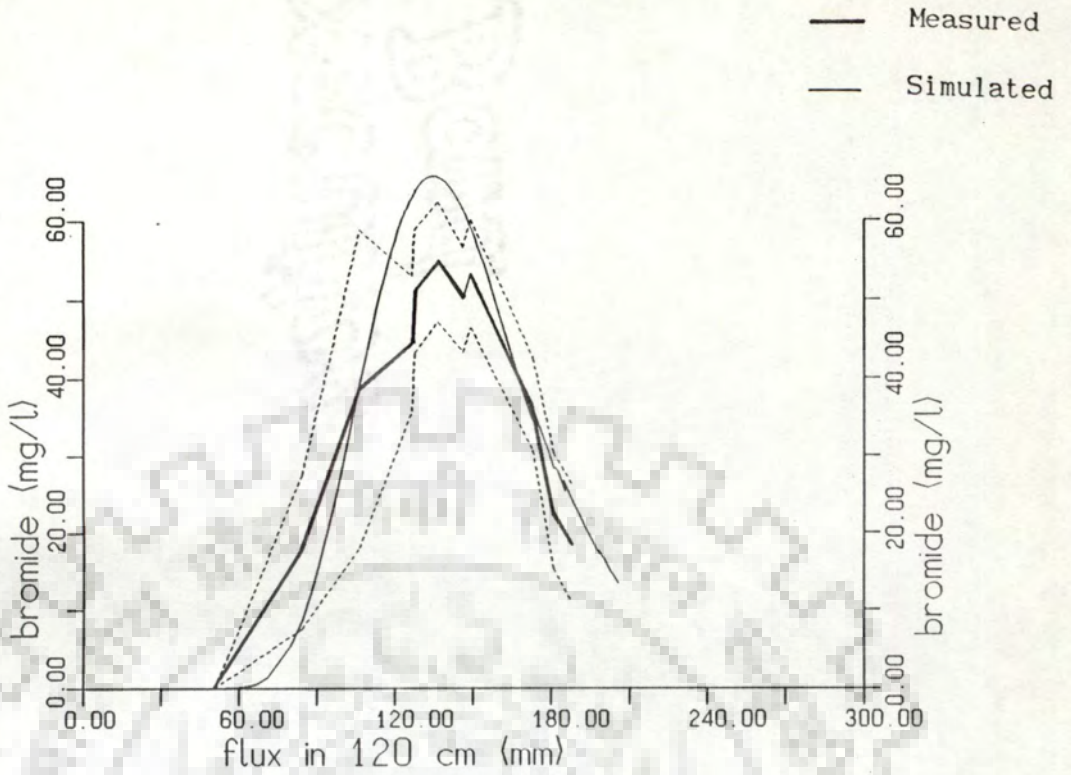
Fig. 4.34. Mesured mean and simulated bromide breakthrough curve (depth=120 cm, λ=1.5 cm).
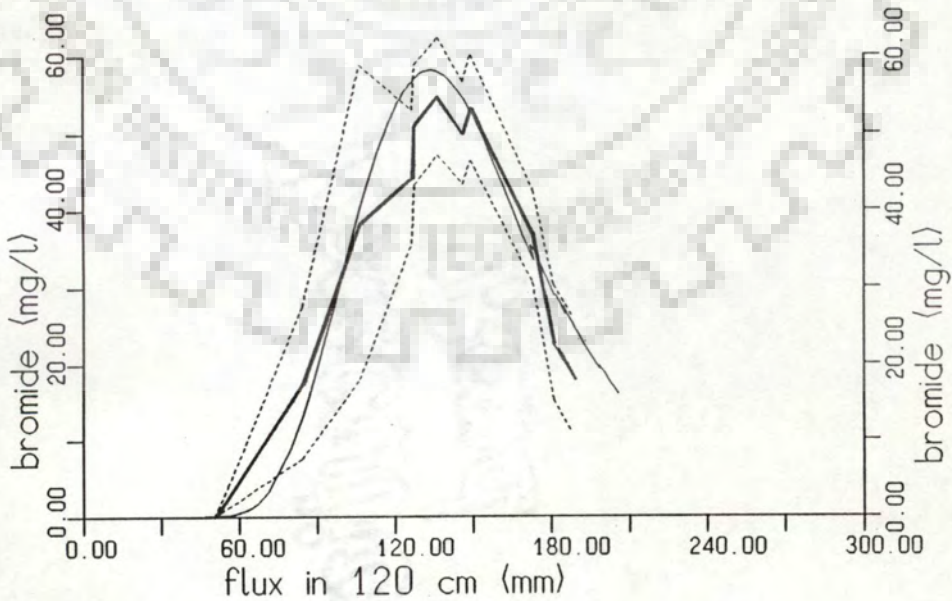
Fig. 4.35. Mesured mean and simulated bromide breakthrough curve (depth=120 cm, λ=2.0 cm).

bromide amount in dpeth on the two dates shows a reasonably good agreement (Figs. 4.37 and 4.38). Again the higher dispersivity value (λ=2.0 cm) gave a closer reproduction.

4.3 MASS BALANCE ERROR

Following the procedure described in section 3.5, relative mass balance errors were computed at all discrete times for each simulation. The errors remained negligible($<$0.1 %) for all the simulations.
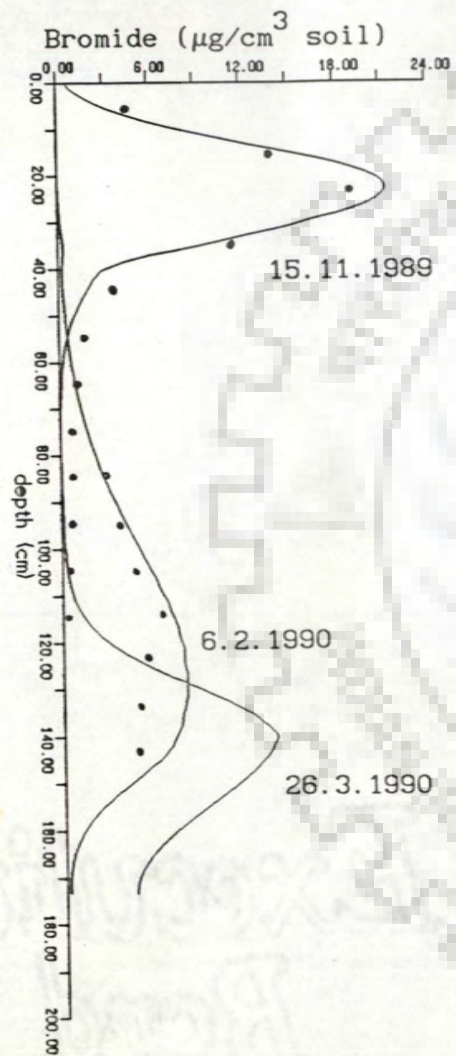
Fig. 4.36. Mesured mean and simulated bromide
amounts in depth (λ=1.5 cm).
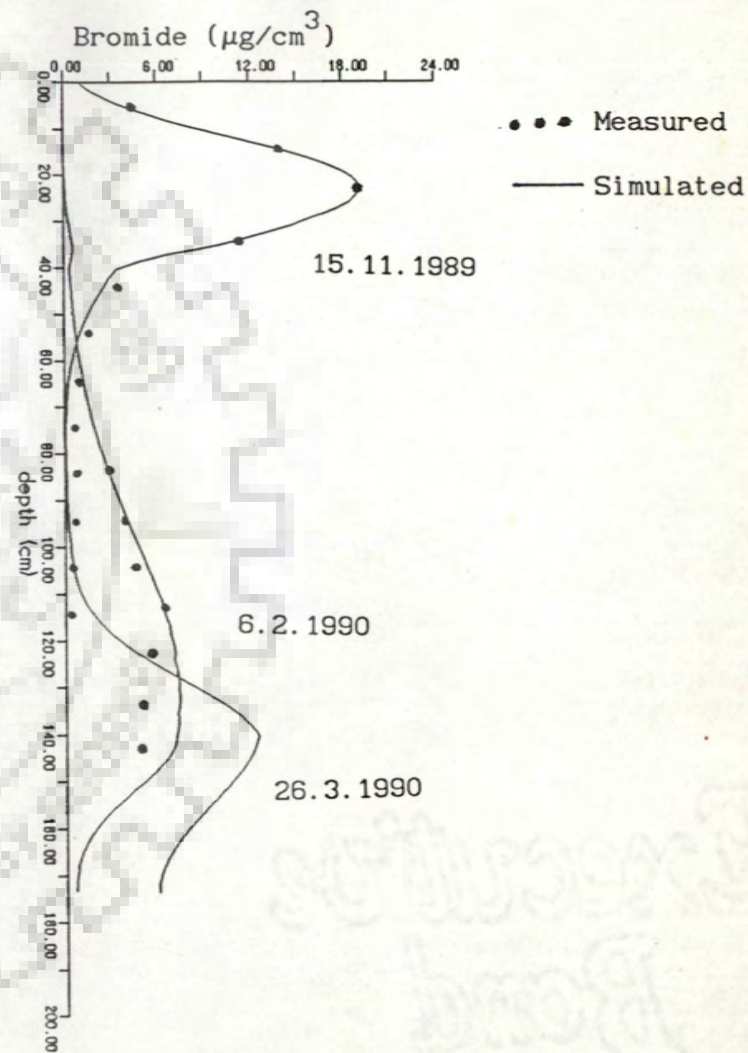
Fig. 4.37. Mesured mean and simulated bromide
amounts in depth (λ=2.0 cm).

CHAPTER 5

MODEL APPLICATION

Applicability of the model to real life problems has been demonstrated by considering the problems of salt accumulation and transport through the unsaturated zone.

5.1 ESTIMATING SALT ACCUMULATION IN THE SOIL PROFILE

Use of saline water subject to evapotranspiration during the summer months and a subsequent poor monsoon over the years, leads to salt build up in the top soil. Salt build up in the root zone is particularly harmful to plantgrowth during its germination stage and to a lesser extent during the later growth stages, depending upon its tolerance to soil salinity. To overcome this problem irrigation in excess of evapotranspiration is applied, and is known as leaching requirement. The current practice is to use the salt storage equation (Van der Molen, 1973) for estimating salt accumulation in the root zone required for designing leaching requirement. A more rational estimation of salt accumulation can be carried out using numerical models (as the one developed in the present study).

The present model (accounting for two phase non-reactive solute transport, refer section 3.4.6) was used to simulate the salt accumulation in a loam soil (a typical agricultural soil in North India), during a normal rainfall year and under irrigation schedules prevalent around Roorkee. The period of simulation commencing from the sowing of wheat crop (15th Nov) covers the harvesting of wheat, sowing

and harvesting of paddy crop and two fallow periods. It terminates on 15th Nov. of the following year (refer table 5.1).

<center>Table 5.1</center>
<center>Cropping schedule</center>

Wheat	15th	Nov.	15th	Mar.
Fallow	16th	Mar.	30th	June
Rice	1st	July	15th	Oct.
Fallow	16th	Oct.	15th	Nov.

In case of wheat and rice pre-sowing operations were neglected. Casual unirrigated crops were asssumed to grow during the two fallow periods. Further these crops were assumed to evapotranspire like the reference crop i.e., actively growing green grass having a root zone depth of 30 cm. The water used for irrigating the two crops (i.e., wheat and rice) was assumed to be considerably saline (1.5 mmho/cm). Salt build up in the root zone was also computed using the salt storage equation (Van der Molen, 1973) and compared with the model simulated values.

5.1.1 Flow Equation

5.1.1.1 Input at the Ground

The assigned net input at the ground, comprising of irrigation and rainfall, are as follows.

5.1.1.1.1 Irrigation

Irrigation scheduling was assigned as per local practice (Tripathi, 1991; personal communication). This allows an application of 7.5 cms of irrigation water at an interval of 20 days for the wheat

crop. For the rice crop, the frequency of water application increases to every 7th day. The application of water is assumed to be carried out uniformly over a period of 6 hrs, from the start of the day. Further, for both the crops irrigation was ceased 15 days before the date of harvest.

5.1.1.1.2 Rainfall

The data of daily rainfall at Roorkee during the year 1981-82 (which was a near normal rainfall year) were used for the study (refer table 5.2). The rainfall was assumed to be uniform throughout the day. Losses due to interception and direct evaporation were ignored.

5.1.1.2 Upper Boundary Condition

The upper boundary condition (i.e., the boundary condition at the ground surface) may vary from Neuman (entire input infilters) to Dirichlet (ponding or just saturation is maintained) and vice-versa, depending on the intensity and duration of the net input at the ground (refer section 3.4.3).

5.1.1.3 Evapotranspiration

Evapotranspiration from the root zone was estimated in accordance with the following equation (Doorenbos et al., 1979).

$$ET/PET = 1 \qquad\qquad \theta \geq \theta_t \qquad\qquad (5.1a)$$

$$ET/PET = 0 \qquad\qquad \theta \leq \theta_{wp} \text{ or } \theta \geq \phi \qquad\qquad (5.1b)$$

$$ET/PET = \frac{\theta - \theta_{wp}}{\theta_t - \theta_{wp}} \qquad\qquad \theta_{wp} < \theta < \theta_t \qquad\qquad (5.1c)$$

where, ET is evapotranspiration, PET is potential evapotranspiration, θ_{wp} is wilting point and θ_t is a threshold moisture content. The equation is shown graphically in Fig. 5.1. The figure reveals that

Table 5.2

Daily Rainfall Values (cm) for the year 1981-82

Date	Nov.	Dec.	Jan.	Feb.	Mar.	Apr.	May.	Jun.	Jul.	Aug.	Sep.	Oct.	Nov.
1							0.76				0.72		
2							1.78						
3							0.82				2.4		
4											0.15		
5										0.35			
6							2.86						
7							0.95	0.3			0.15		
8							0.05						
9						0.58	2.6	8.05		0.24			
10								3.2			0.15		
11								0.28		0.26	1.2		
12											0.1		
13		2.38						0.35		1.44			
14		1.6							0.15	0.08	0.16		
15									0.1				
16				3.45									
17			1.13	0.13						0.22	1.12		
18		0.05	2.13										
19			0.04										
20										4.6			
21													
22								0.3					
23					1.06			0.4		0.1			
24				0.07									
25			1.12	1.0									
26	0.02									0.1			
27									4.3				
28													
29										0.25			
30										7.62			
31										0.23			

Note: Blank entries denote zero values.

Source: Roorkee station, Department of Hydrology, University of   Roorkee, Roorkee (India).
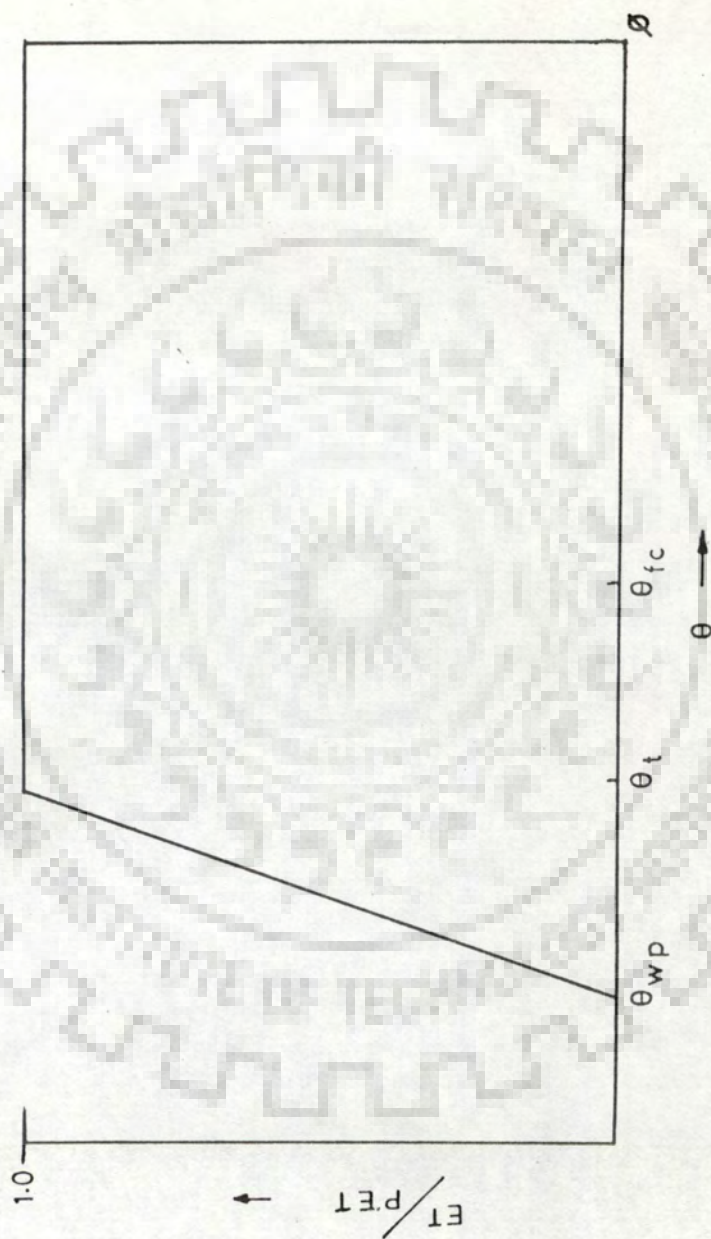
Fig. 5.1. Relation between PET, ET and θ.

evapotranspiration will be zero for moisture contents at or below wilting point and at or above saturation. Further it implies that evapotranspiration will be at the potential rate even if the moisture content falls below that at field capacity (θ_{fc}) by a certain extent. Thus, factor P is defined as (Doorenbos et al., 1979),

$$P = \frac{\theta_{fc} - \theta_t}{\theta_{fc} - \theta_{wp}} \tag{5.2}$$

The various values of PET and P for the two crops and fallow periods are given in table 5.3 (Doorenbos et al., 1979 cited in Mohan Rao, 1986). During the fallow period, factor P remains zero. The values of θ_{fc} and θ_{wp} for loam soil are 0.125 and 0.055 respectively (Rawls et al., 1981 cited in Mohan Rao, 1986).

To account for evapotranspiration during simulation, the sink term in Richards equation [eqn(3.10)] is equated to evapotranspiration. However, in the solute transport equation loss of water due to evapotranspiration is manifested by a loss in the water volumes contained in the moving packets lying in the root zone area (as evapotranspiration takes place only from the root zone). This is done in the following manner.

Referring to section 3.4.3, the volume of water ($ET_{j,k+1/2}$) lost at node j, during the time step Δt_k is,

$$ET_{j,k+1/2} = E_{j,k+1/2} \cdot \Delta t_k \cdot (\Delta z_{j-1} + \Delta z_j)/2 \tag{5.3}$$

Further, $Et_{j,k+1/2}$ is divided among all the moving packets lying wholly or partially within the area of influence of node j. Thus, for p^{th} moving packet, the reduced water volume ($vl_{p,k_{new}}$) is computed as,

Table 5.3
Daily Values of Potential Evapotranspiration and Factor P
Wheat

Stage of growth	Initial	Development	Mid	Late	Harvest
Period	15-30 Nov.	Dec.	Jan.	Feb.	1-15 Mar.
Factor P	0.8	0.8	0.8	0.8	0.8
PET cm.	0.077	0.105	0.193	0.188	0.092

Rice

Stage of growth	Initial	Development	Mid	Late		Harvest
Period	1-20 July	21-31 July	Aug.	1-15 Sep	16-30Sep.	1-15 Oct.
Factor P			doesn't arise			
PET cm	0.591	0.684	0.55	0.569	0.474	0.359

Fallow (reference crop)

Stage of growth	doesn't arise								
Period	Mar.	Apr.	May.	June	Jul.	Aug.	Sep.	Oct.	Nov.
Factor P	0.0	0.0	0.0	0.0	0.0	0.0	0.0	0.0	0.0
PET cm	0.41	0.583	0.716	0.75	0.526	0.458	0.474	0.359	0.22

$$vl_{p,k_{new}} = vl_{p,k_{old}} - \frac{vl_{p,k_{old}}}{nv_{j,k}} ET_{j,k+1/2} \qquad (5.4)$$

$$j=1,2.....n_r$$

where, n_r is the node number at which the root zone ends and $nv_{j,k}$ i

the volume of water (per unit plan area) at node j (refer section 3.4.5

5.1.1.3.1 Root Zone Depth

Evapotranspiration is effective only upto the depth of plan

root present in the soil. The root zone depth increases with time

Fortnightly root zone depths for the wheat and rice crops were availabl

(Mohan Rao, 1986 ; refer table 5.4). The root zone depths were assume

to increase instantaneously at each fortnight. During the fallow perio

a time invariant root zone depth of 30 cms was adopted.

Table 5.4

Depth of Root Zone in (cm) During the various Fortnights

Fortnight	1	2	3	4	5	6	7	
Wheat	32.5	72.5	102.5	132.5	142.5	152.5	162.5	17
Rice	32.5	62.5	62.5	62.5	62.5	62.5	62.5	

5.1.1.4   Lower Boundary Condition

The lower boundary condition was taken as the water table, a

which   the   capillary   pressure   (h)   was   assigned   as   zer

(pressure=atmospheric pressure) . The depth to water table was taken a

400 cm and was assumed to be time invariant.

5.1.1.5   Initial Condition

The   soil   moisture   profile   in   depth   at   the   beginning   o

simulation was taken as the dynamic equilibrium profile reported b

Mohan   Rao   (1986).   [The   dynamic   equilibrium   profile   is   estimate

(commencing from arbitrary initial conditions) by operating the model.

for a number of years for the same yearly data. The operation is continued till the simulated initial conditions, at the beginning of two consecutive years are practically identical]. The adopted soil-moisture profile is given in Fig. 5.2a.

5.1.1.6   Soil Characteristics

Following relations for K vs θ (Brooks and Corey, 1964) and θ vs h (Mohan Rao et al., 1989) were adopted,

$$K = K_s \left[\frac{\theta - \theta_r}{\phi - \theta_r} \right]^4 \qquad\qquad \theta > \theta_r \qquad (5.5a)$$

$$= 0 \qquad\qquad \theta \leq \theta_r \qquad (5.5b)$$

$$\theta = \phi - \frac{\theta_r}{h_b} h \qquad\qquad 0 \leq h \leq h_b \qquad (5.6a)$$

$$= \exp\left[\frac{\ln(\phi - 2\theta_r)}{h_b} h \right] + \theta_r \qquad h > h_b \qquad (5.6b)$$

where, h_b is the bubbling pressure.

Following values of θ_r, ϕ, K_s and h_b reported for loam soil (Rawls et al., 1980 cited in Mohan Rao, 1986) were used.

θ_r = 0.027 K_s = 0.011 cm/min
ϕ = 0.463 h_b = 40.12 cm.

5.1.1.7   Space and Time Discretization

To solve Richards equation, the flow domain was discretized into a finite number of nodes, based on a constant spatial increment (Δz) of 5 cms. For application of irrigation and rainfall intensity equal to or higher than 5 cm/day, a time step (Δt) of 5 mins was used. For lower rainfall intensities a time step (Δt) of 30 mins was used.
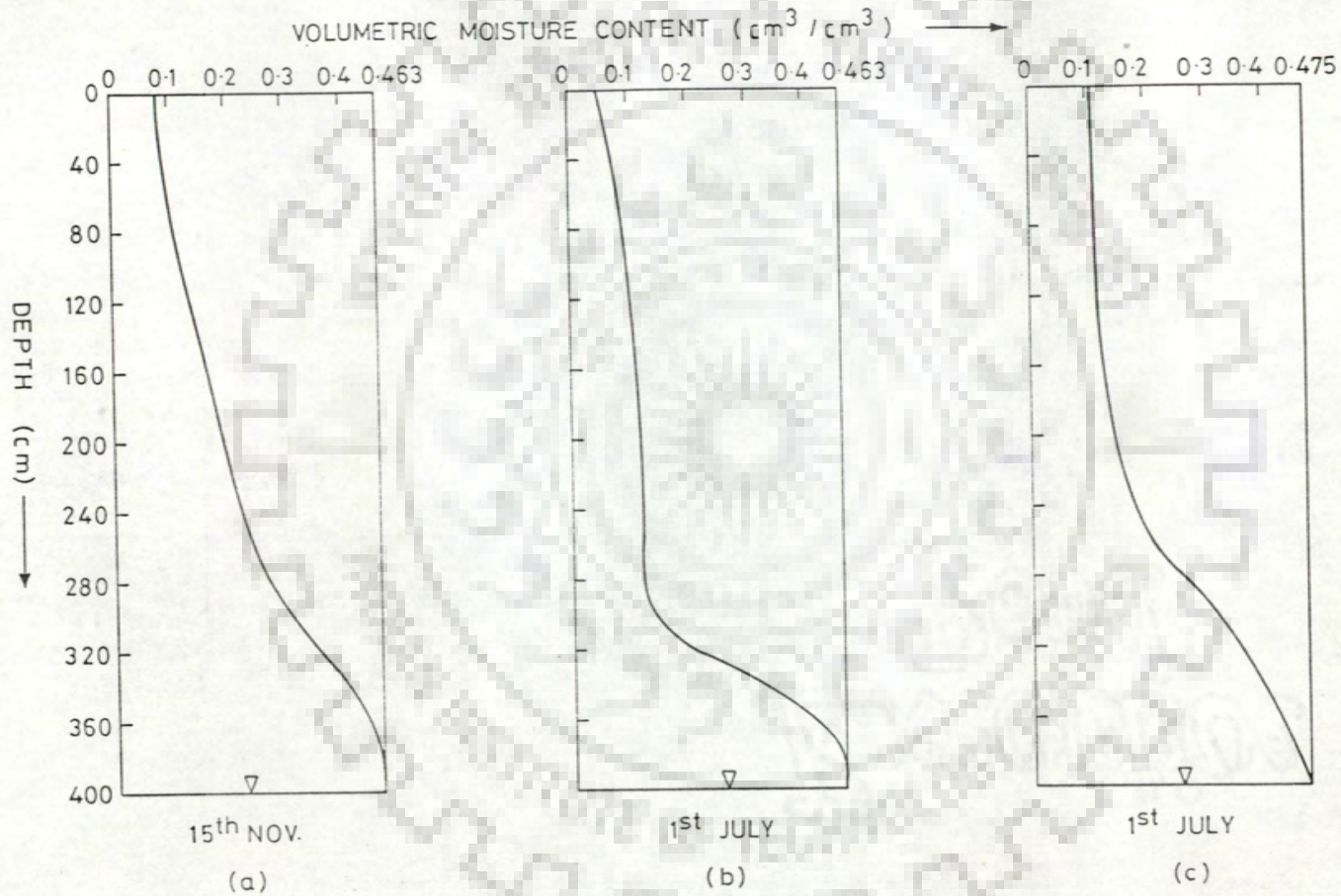
Fig. 5.2. Dynamic equilibrium profiles, (a) loam soil, (b) loam soil, (c) clay soil (Mohan Rao, 1986).

5.1.2 Solute Transport Equation

The initial soil profile was assumed to be salt free. Thus, the initial concentration value throughout the soil profile remains zero. The concentration input at the ground was in the form of a pulse, carried by the irrigation water. The concentration value of the irrigation water was taken as 1.5 mmho/cm (c_o = 960 mg/l). The rainfall was assumed to be salt free.

The immobile water content was assumed to be equal to θ_r (θ_{im} = 0.027). Evapotranspiration was assumed to take place only from the mobile phase. The value of the mass transfer coefficient (α) was taken as 0.00005 min^{-1}.

The following values (Russo, 1988a) were assigned to the parameters of the mobile hydrodynamic dispersion coefficient [refer equation (3.6)].

a = 0.005

b = 10.0

D_o = 0.0007 cm^2/min.

λ = 1.0 cm.

5.1.2.1 Space and Time Discretization

To discretize the solute into moving packets a strip thickness of 2 cms was used. The superposed spatial grid (refer section 3.4.5.1) used for computing change in concentration due to transfer of solute into/out of the immobile phase, coincides with the spatial grid used for solving Richards equation. However, the total depth of it extends 20 cms below the water table (refer section 3.4.4.1.1).

Again, the time steps used for solving the solute transport equation, were the same as those used for solving Richards equation (refer section 5.1.1.7).

5.1.3 Model Output

The output comprises of mobile concentration (c_m) profiles in depth at the end of every 20 days, over the enitre simulation period. They are represented in Figs 5.3-5.9.

5.1.4 Conceptual Model

The prevalent practice for estimating salt build up in the root zone necessary for designing leaching requirement is to use the salt storage equation (Van der Molen, 1973). The conceptual model based on the salt storage equation assumes that the soil in the root zone medium behaves like a reservoir with a bypass. This assumption is based on the observation of incomplete mixing of solute infiltrating into the soil, with the soil solution. Part of the solute may move through large pores and percolate below the root zone without mixing. If c_o is the concentration of the infiltrating solute and c is the conc. of the soil solution, then the solute concentration c_{ef} arriving at the lower boundary of the root zone is expressed as,

$$c_{ef} = f_e c + (1-f_e)c_o \tag{5.7}$$

where, f_e is the fraction of the percolating solute having a concentration of the soil solution and $(1-f_e)$ fraction has the concentration of the infiltrating solute.

5.1.4.1 Salt Storage Equation

Based on the concept described above the change in salt storage in the root zone over a certain period of time is written as (Van der Molen, 1973),
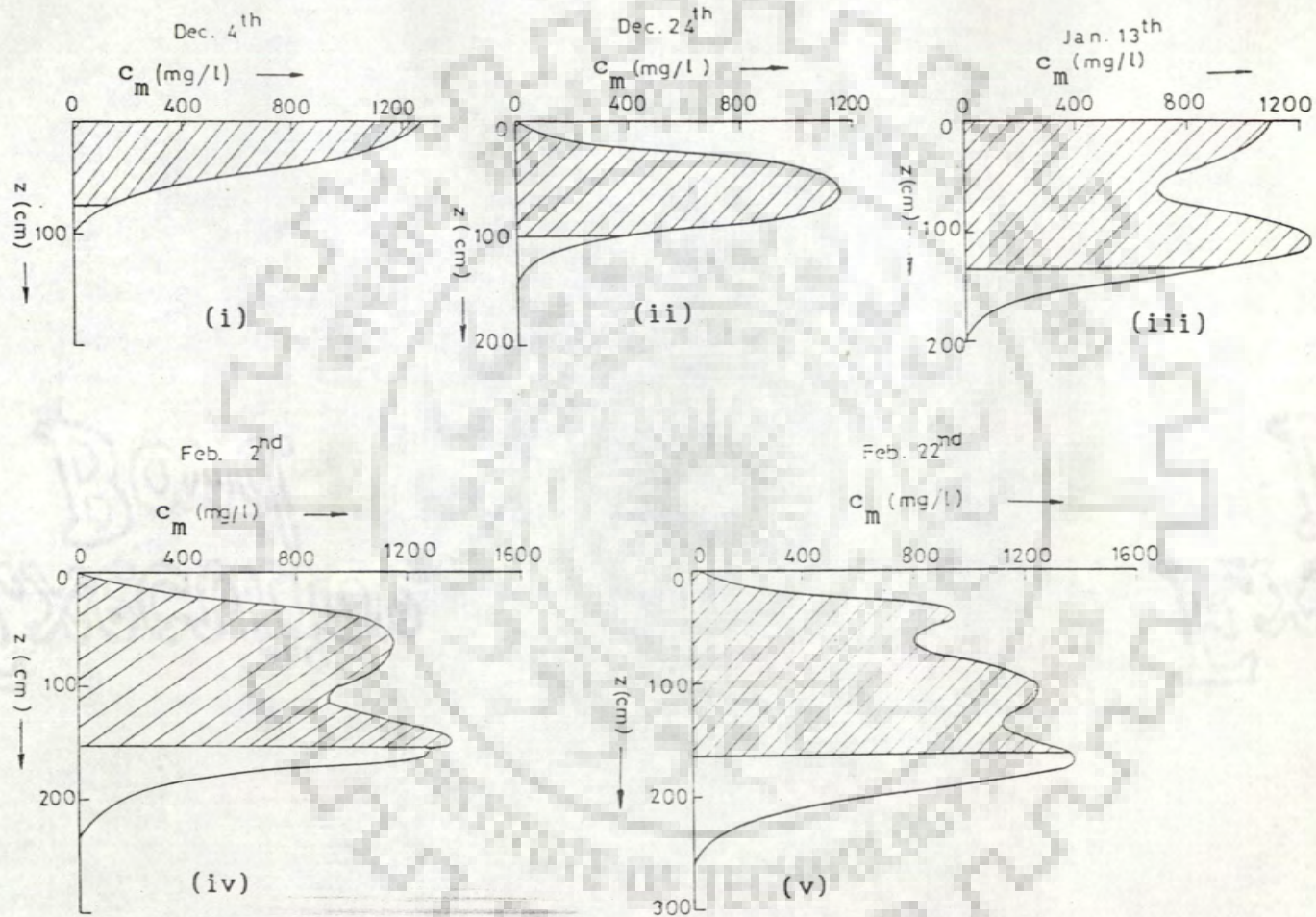
Fig. 5.3. Salt accumulation in the soil profile.
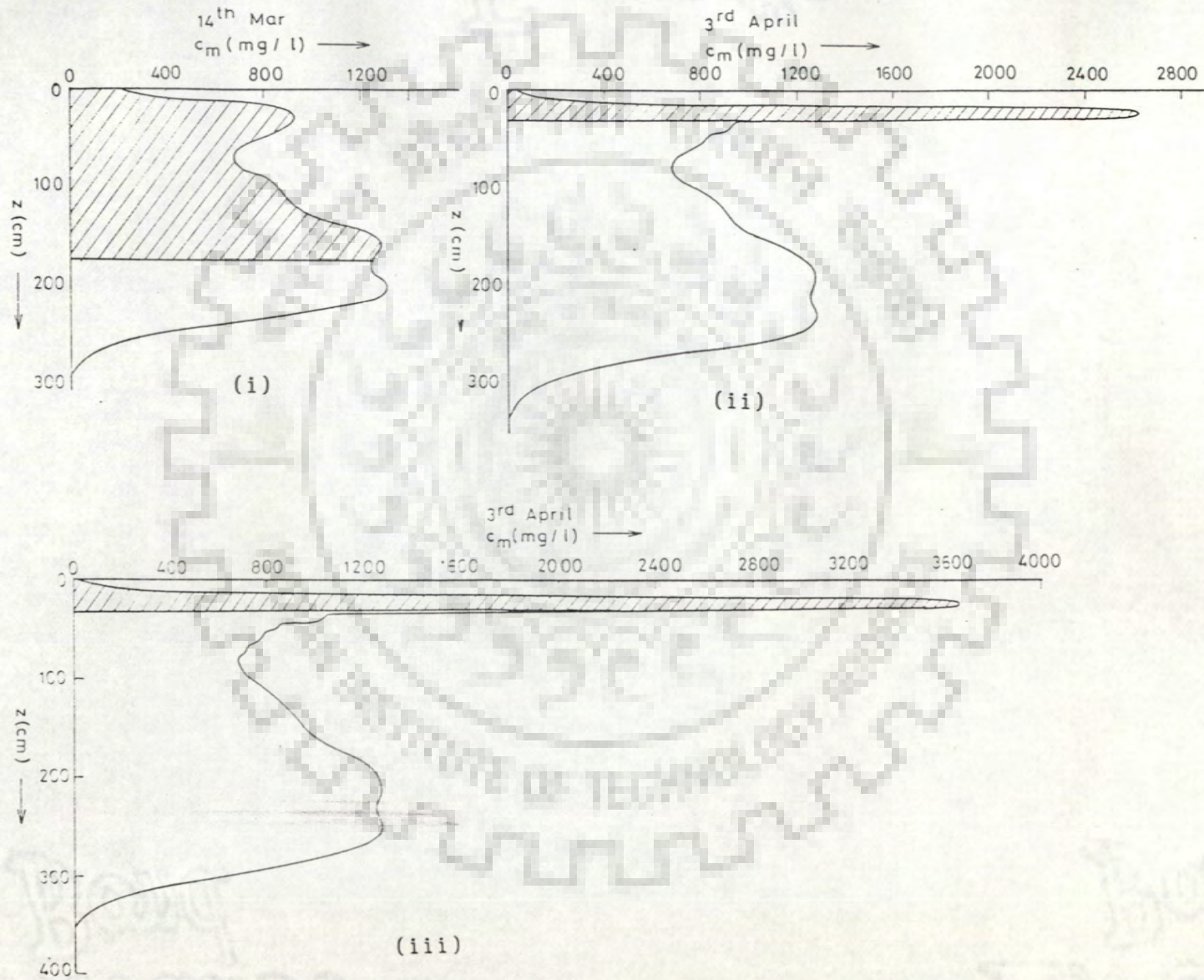
Fig. 5.4. Salt accumulation in the soil profile.
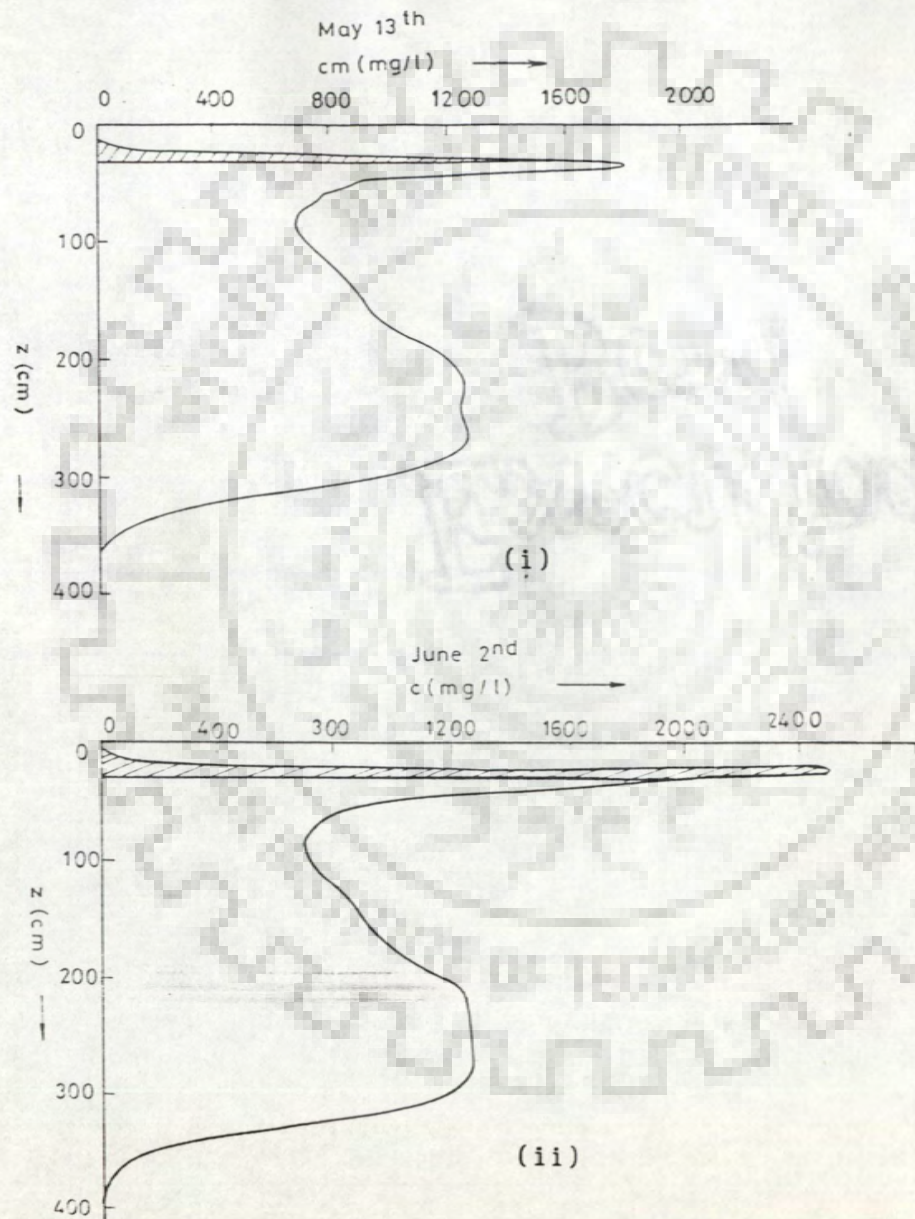
Fig. 5.5. Salt accumulation in the soil profile.
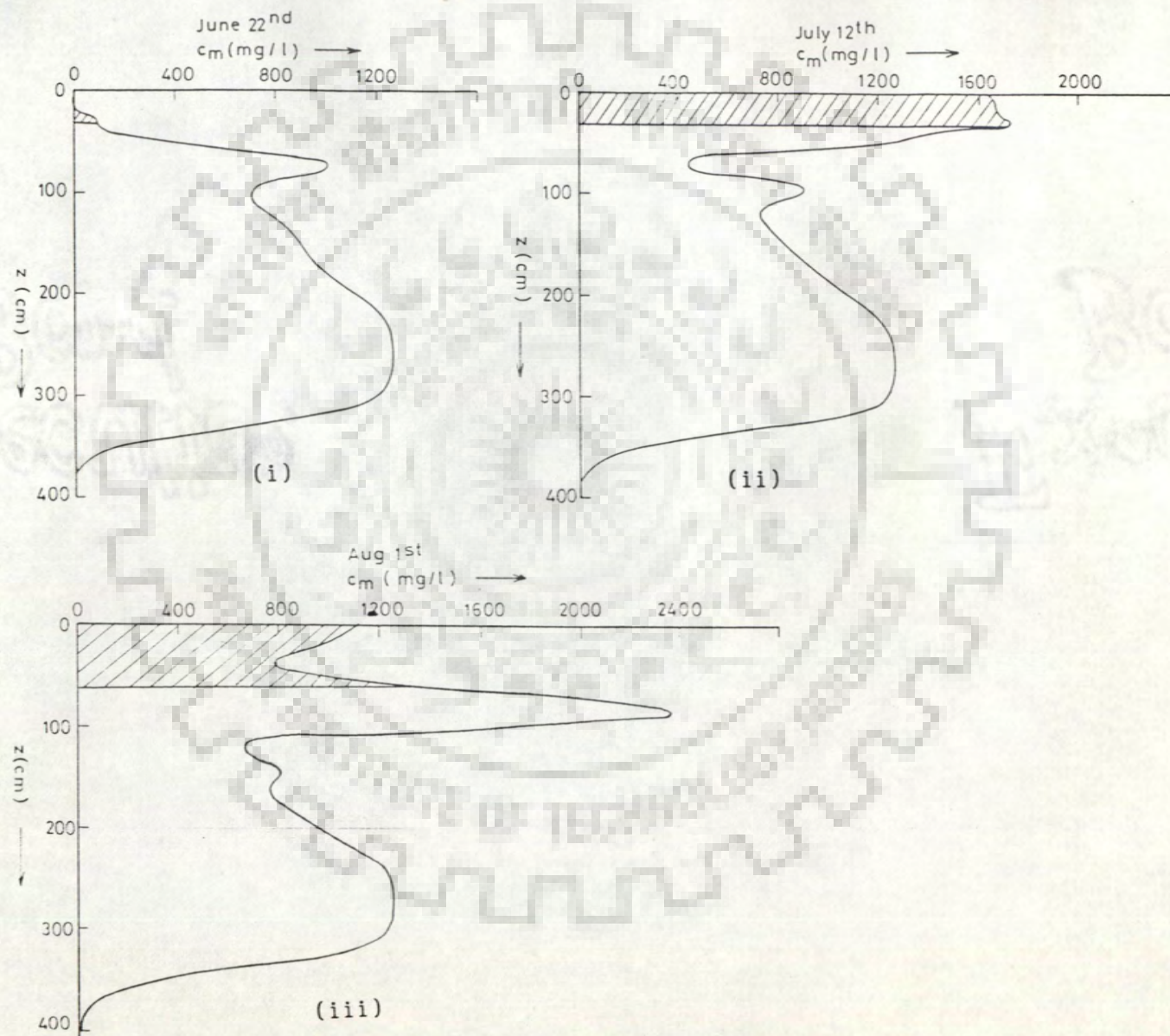
Fig. 5.6. Salt accumulation in the soil profile.
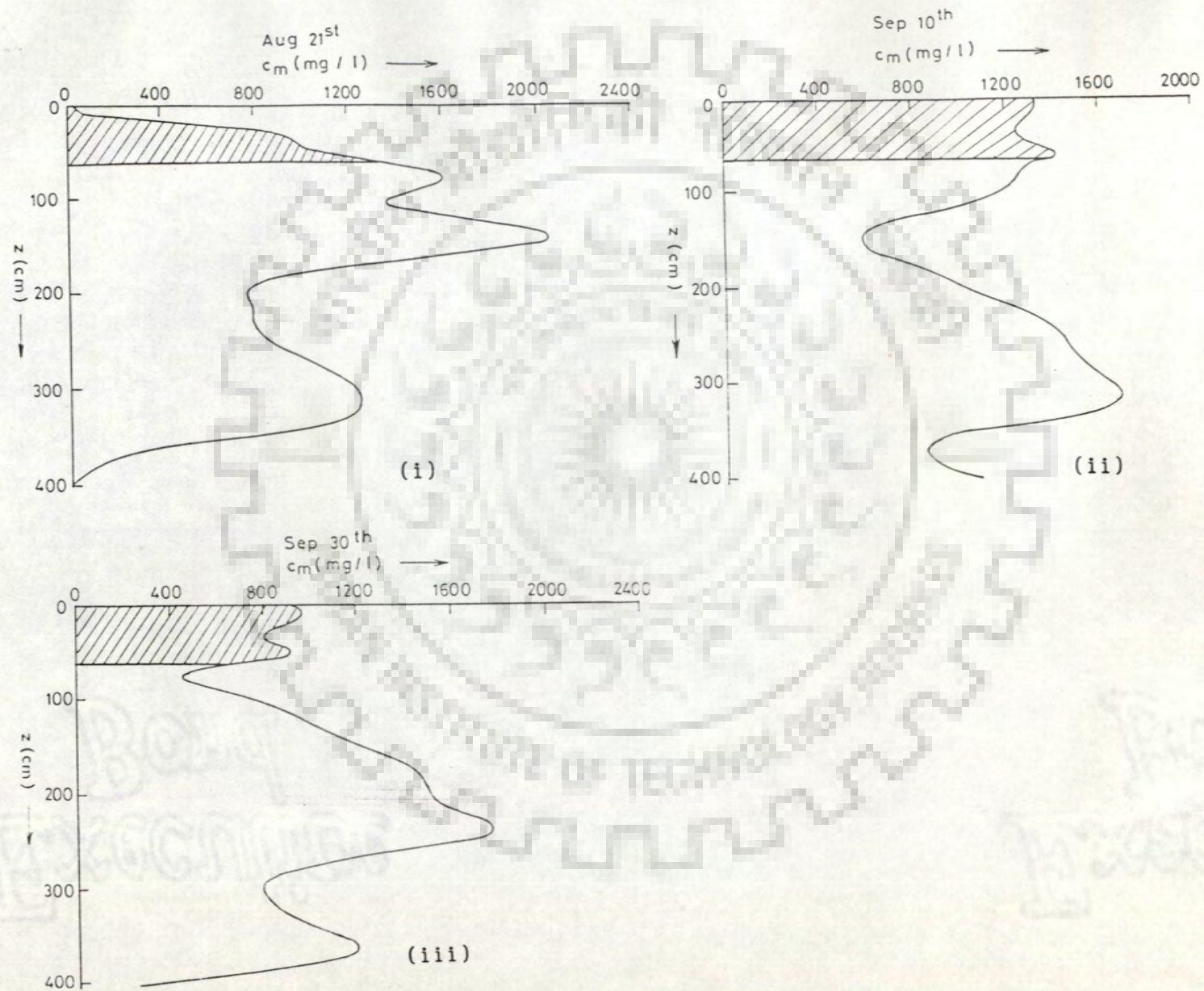
Fig. 5.7. Salt accumulation in the soil profile.
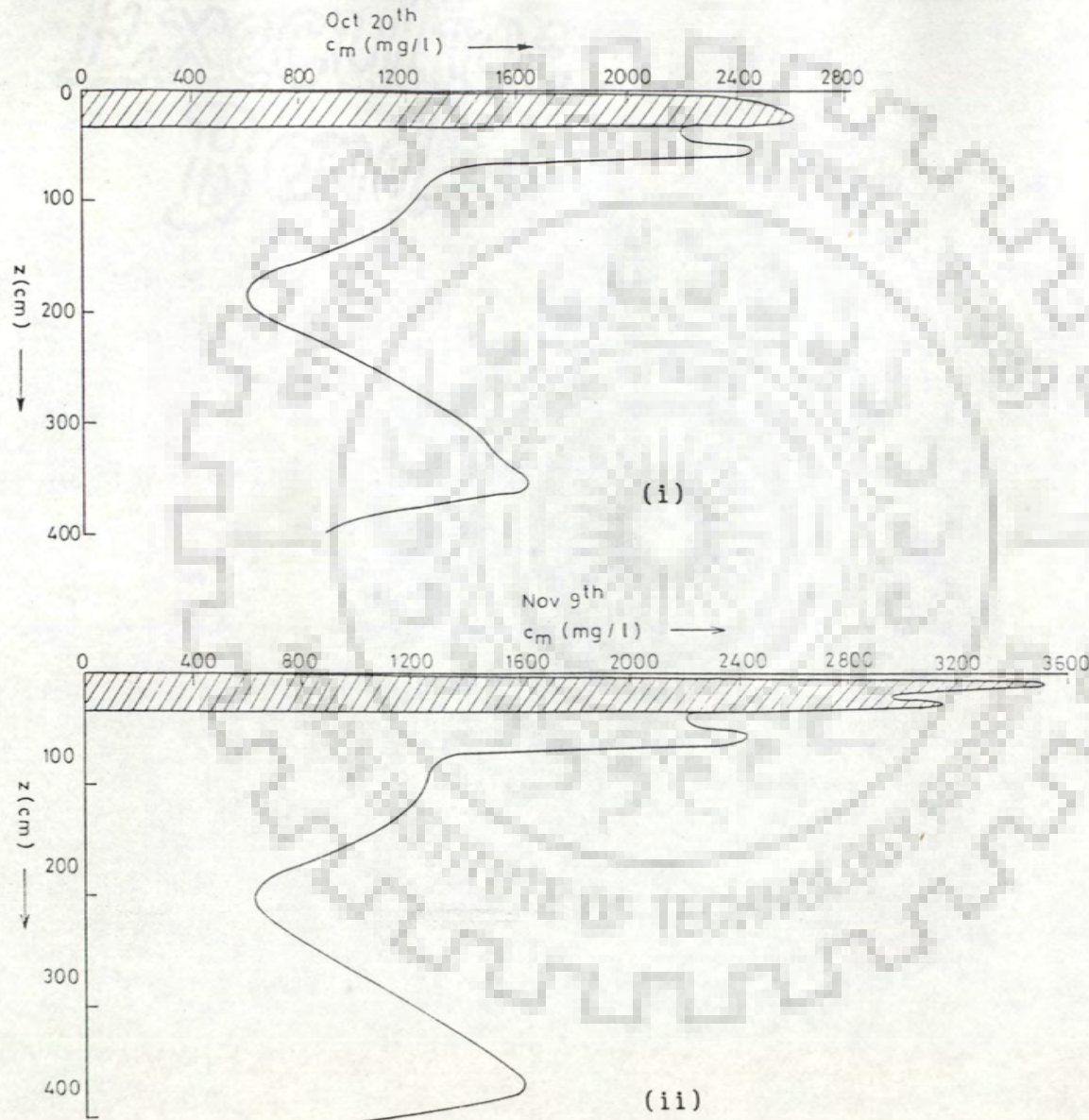
Fig. 5.8. Salt accumulation in the soil profile.
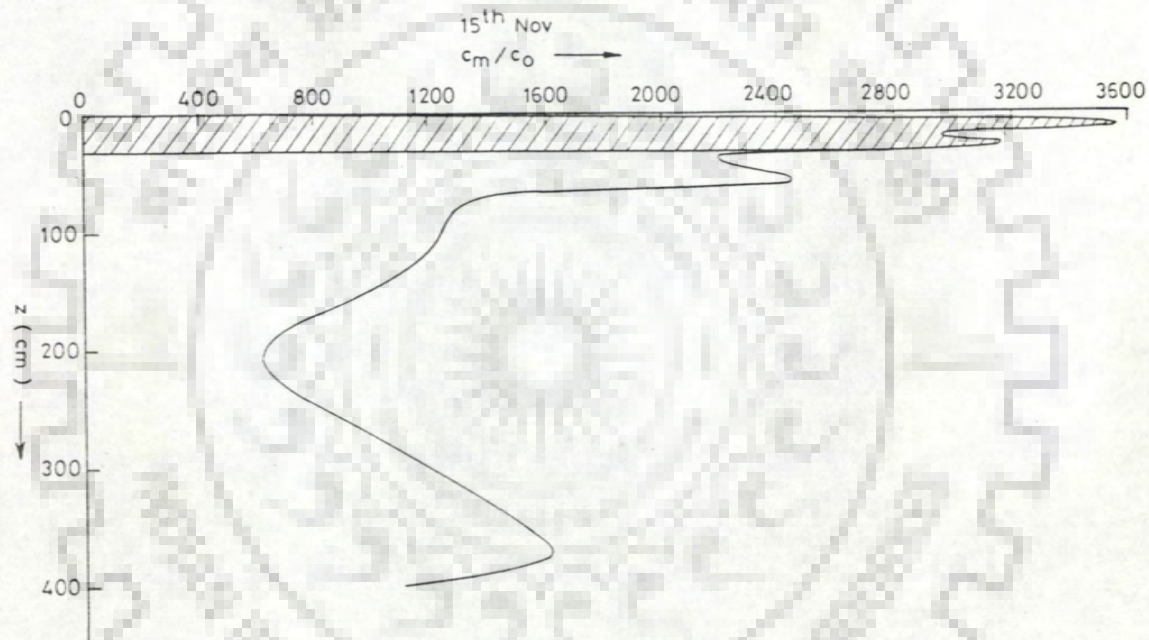
Fig. 5.9. Salt accumulation in the soil profile.

$$\Delta Z' = \frac{Ic_o - (1 - f_e)R^* c_o - \dfrac{f_e R^* Z_1'}{W_{fc}}}{1 + \dfrac{f_e R^*}{2W_{fc}}} \qquad (5.8)$$

where, $\Delta Z'$ is the change in salt content of the root zone, c_o is the concentration of the irrigation water, I is irrigation water applied (or required), f_e is the leaching efficiency, Z_1' is the initial salt content of the root zone, W_{fc} is the amount of moisture in the root zone assuming the moisture content to be at field capacity, R^* is the net downward percolation.

Again,

$$R^* = I - E + P$$

where, E is evapotranspiration and P is precipitation.

$$\Delta Z' = Z_1' - Z_2'$$

where, Z_2' is the salt content in the rootzone at the end of the period.

$$W_{fc} = \theta_{fc} d_t$$

where, d_t is the depth of root zone.

5.1.4.1.1 Underlying Assumptions

(i) All salts are highly soluble and do not precipitate.

(ii) Salts carried by rainfall are negligible.

(iii) Moisture content in the root zone remains at field capacity.

The value of f_e was taken as 0.5 for loam soil. However, when negative percolation ($R^* < 0$) occurs f_e was taken as 1 (complete mixing). Using equation (5.8) and the data set described previously, salt contents in the root zone for wheat and rice were computed at the same time intervals (at every 20th day). The initial salt content in the root zone for the rice crop was taken as per the model output.

5.1.5   Results and Discussions

Model simulated mobile concentration profiles over the entire period of simulation are shown from Fig 5.3 to Fig. 5.9. The concentration profile at the end of the year is shown in Fig.5.9. The average concentration in the root zone is almost three times that of the applied irrigation water and the overall soil-solute concentration profile is considerable as compared to an initially salt free soil profile. Also from Fig. 5.4(ii) and 5.4(iii) it can be seen that during the month of April (fallow period), when rainfall is negligible (refer table 5.2), there is a sudden increase in the concentration in the root zone, due to evapotranspiration through the reference crop.

5.1.5.1   Salt Balance

The amount of salt retained by the soil profile and the amount of salt leached to the water table were cmputed as follows.

(i) Total salt amount infiltrated into the soil profile during the period of simulation (15th Nov. – 15th Nov.) : Salt amount infiltrated into the soil profile during a single irrigation application was calculated , by integrating the product of infiltration rate (q) and the concentration of the irrigation water (c_o) over the time of a single application [$\int_0^{t_o} qc_o dt, t_o =6hrs$]. Thus, the total salt amount infiltrated into the soil profile was computed by summing the salt amountsinfiltrated during each irrigation application. And is,

$$= 136.8 \text{ mg/cm}^2$$

(ii) Total salt amount retained in the soil profile : This was calculated by integrating the product of the concentartion and the soil moisture over the depth of the soil profile ($\int_0^Z c\theta \, dz$). And is,

$$= 92.2 \text{ mg/cm}^2$$

(iii)   Thus, the salt amount leached to the water table,

	Total salt amount		Total salt amount
=	infiltrated into the	−	retained in the soil
	soil profile		profile

= 44.6 mg/cm^2

Thus, for the assigned irrigation schedule, at the end of the simulation period 67 % of the total infiltrated salt amount was retained in the soil profile.

5.1.5.2   Comparison with the salt storage equation

The average salt concentration and salt content in the root zone (as computed by the model and by the salt storage equation) for the wheat and rice crops are given in table 5.5a and 5.5b respectively. It can be seen that the salt storage equation has under-estimated the salt concentration as well as salt contents for the wheat crop. However, for the rice crop, the salt storage equation has generally overestimated the salt concentration and salt contents in the root zone.

The deviations in the results obtained by the two approaches is mainly caused by the assumptions underlying the salt storage equation. Thus, the use of the salt storage equation for estimating salt accumulation in the root zone in order to compute leaching requirement may not always be reliable.

5.2   POLLUTANTS JOINING THE WATER TABLE DURING A HEAVY MONSOON

Water percolating through waste material at the ground diss-olves the pollutants in it and subsequently carries them through the unsaturated soil profile. Depending upon the type of soil and the amount of water percolating through it, non-conservative pollutants may in time join the water table and adversely effect the water quality. Or

Table 5.5a

Average salt concentration and salt content in the root zone
of wheat crop

Date	Model Computed		Computed with the help of the salt storage equation	
	Salt conc. mg/l	Salt Content mg/cm^2	Salt conc. mg/l	Salt content mg/cm^2
4th Dec.	763.34	6.90	383.44	3.47
24th Dec.	791.96	13.36	258.91	3.32
13th Jan.	985.09	18.63	417.62	6.92
2nd Feb.	980.01	23.69	432.76	8.25
22nd Feb.	931.82	26.02	468.59	9.52
14th Mar.	910.00	25.62	543.79	11.72

Table 5.5b

Average salt concentration and salt content in the root zone
of rice crop

Date	Model computed		Computed with the help of the salt storage equation	
	Salt conc. mg/l	Salt Content mg/cm^2	Salt conc. mg/l	Salt content mg/cm^2
12th July	1660.68	7.22	2293.08	9.31
1st Aug.	996.21	12.03	1749.02	13.66
21st Aug.	783.88	12.90	1403.17	10.96
10th Sep.	873.28	13.13	1107.71	8.63
30th Sep.	1295.17	11.70	2121.12	16.57

depending on the time of travel, they may be degraded to harmless levels
or get adsorbed by the soil. However, conservative pollutants will
sooner or later join the water table. Heavy rainfall is particularly

helpful in accelerating the transport. The travel time of conservative pollutants to join the water table is smaller compared to the travel time of non-conservative pollutants (which react with the soil matrix and in the process get retarded). Thus, if the time of degeneration of a non-conservative pollutant is less than the travel time of a conservative pollutant under identical conditions, the disposal of the non-conservative pollutant on the ground could be assumed to be safe.

The model developed in the present work (two phase non-reactive solute transport) was used to study the transport of a pollutant (assumed to be abundantly available at the ground) through two soil profiles (comprising of loam and clay soils respectively) during a monsoon season [1st July to 17th Nov. (140 days)]. Each of the soil profile was assumed to be 400 cms thick, extending from ground surface to water table. Daily rainfall data of an above normal rainfall year were taken. As has already been stated, heavy rainfall is helpful in accelarating the transport. Thus, a safer limit is arrived at. Conditions of operation were identical for both soil types.

5.2.1   Flow Equation

5.2.1.1   Net Input at the Ground

The assigned net input at the ground comprising of rainfall is as follows.

5.2.1.1.1 Rainfall

The data of daily rainfall at Roorkee during the year 1988 (which was an above normal rainfall year) were used for the study (refer table 5.5). Rainfall was assumed to be uniform throughout the day.

Losses due to interception and direct evaporation were not considered.

5.2.1.2   Upper Boundary Condition

The upper boundary condition (i.e., the boundary condition at the ground surface) varied from Neuman (entire input infilters) to Dirichlet (ponding or just saturation is mantained) and vice-versa, depending on the intensity and duration of the net input at the ground refer section 3.4.3).

5.2.1.3   Evapotranspiration

The area was assumed to be covered with grasses (reference crop). Evapotranspiration was estimated as described previously (refer section 5.1.1.3). Daily values of PET and P for the reference crop during the period of simulation are given in table 5.3. (Doorenbos et al., 1979 cited in Mohan Rao, 1986). The values of θ_{fc} and $\theta_{\omega p}$ for loam soil are 0.125 and 0.055 (refer section 5.1.1.3). The values for clay are 0.225 and 0.15 respectively (Rawls et al., 1980 cited in Mohan Rao, 1986).

5.2.1.3.1 Root Zone Depth

The reference crop was assumed to have a time invariant root zone depth of 30 cm.

5.2.1.4   Lower Boundary Condition

The lower boundary condition was taken as the water table at which the capillary pressure head (h) was assigned as zero (pressure = atmospheric pressure). The depth to water table was taken as 400 cms and it is assumed to be time invariant.

Table 5.6

Daily Rainfall Values (cm) for the year 1988

Date	July	Aug.	Sep.	Oct.	Nov.
1		7.43			
2		0.3			
3	4.2	2.36			
4	4.22	0.02			
5	15.5	1.56			
6	4.1				
7	3.1				
8	0.1	3.88	1.26		
9		2.54	1.6		
10		3.76			
11					
12	0.18	0.18			
13	0.62	1.18			
14	0.86	1.44			
15	0.18	4.02			
16	0.16				
17	0.08				
18		4.98			
19	0.2	0.76			
20	1.6	0.46			
21	0.13		0.03		
22	1.15	0.05	0.4		
23		1.4	3.29		
24	5.4	6.4	3.78		
25	0.2	6.38	13.9		
26					
27	2.14		3.7		
28	0.03				
29					
30	0.1				
31	4.46				

Note: Blank entries denote zero values
Source: Roorkee station, Department of Hydrology, University of Roorkee
         Roorkee.

5.2.1.5   Initial Condition

For both soil profiles the initial moisture profile in depth were taken as the dynamic equilibrium profiles (refer section 5.1.1.5) reported by Mohan Rao (1986). The adopted moisture profiles are given in Figs. 5.2b and 5.2c.

5.2.1.6   Soil Characteristics

The K vs θ and θ vs h relations were taken the same as described previously (refer section 5.1.1.6). Following values of θ_r, $\emptyset$, K_s and h_b reported for clay soil (Rawls et al., 1980 cited in Rao, 1986) were used.

$$\theta_r = 0.09 \qquad K_s = 0.001 \text{ cm/min}$$

$$\emptyset = 0.475 \qquad h_b = 85.0 \text{ cm}$$

For the values of θ_r, $\emptyset$, K_s and h_b for loam soil refer to section 5.1.1.6.

5.2.1.7   Space and Time Discretization

To solve Richards equation the flow domain was discretized into a finite number of nodes, based on a constant spatial increment (Δz) of 5 cms.

For rainfall intensities equal to or higher than 5 cm/day a time step (Δt) of 5 mins was used. For lower rainfall intensities a time step (Δt) of 30 mins was used.

5.2.2   Solute Transport Equation

The initial soil profiles were assumed to be salt free. Thus, the initial values of c_i were taken as zero for the entire depth under consideration.

The pollutant was assumed to be completely soluble in the rainfall. As the supply of pollutant was assumed to be abundant at the ground, the pollutant concentration in the infiltrating water was assigned a relative concentration value of 1 unit and the relative concentration distribution in the soil water at different discrete space and time points were estimated. The concentration input at the ground was again in the form of a pulse input carried by the rainfall. This was valid for both soil profiles.

The immobile water content was taken equal to θ_r. Thus, for loam soil $\theta_{im} = 0.027$ and for clay soil $\theta_{im} = 0.09$. The mobile water content was variable, depending upon the total moisture content ($\theta_m = \theta - \theta_{im}$). Evapotranspiration was assumed to take place only from the mobile solute phase. Rest of the parameters required for solving the solute transport equation were taken to be the same as described previously (refer section 5.1.2) except the value of a, which changes for clay soil and was taken as 0.002 (Russo, 1988a).

4.2.2.1 Space and Time Discretization

To discretize the solute into moving packets a strip thickness of 2 cms was used. The superposed spatial grid (refer section 3.4.5.1) used for computing change in concentration due to transfer of solute into/out of the immobile phase, coincides with the spatial grid used for solving Richards equation. However, the total depth of it extends 50 cms below the water table (refer section 3.4.4.1.1).

Again, the time steps used for solving the solute transport equation were the same as those used for solving Richards equation (refer section 5.2.1.7).

5.2.3　Model output

Cumulative solute depth/c_o joining the water table vs time for loam soil is represented in Fig. 5.10. (c_m/c_o) profiles in depth at the end of every 20 days, over the entire simulation period, for the two soils are represented in Figs. 5.11 and 5.12 for loam soil and Figs. 5.13 and 5.14 for clay soil.

5.2.4　Results and Discussion

For clay soil the cumulative depth of solute/c_o joining the water table even towards the end of the simulation period is negligible-caused only by dispersion. However, for loam soil (Fig. 5.10) the convective front reaches the water table in about 80 days time. Thus, beyond 80 days the cumulative depth of solute/c_o joining the water table is appreciable for loam soil. Comparing the two sets (Figs. 5.11-5.12 and Figs. 5.13-5.14) of concentration proifles it can be seen that the pollutant travels at a much faster rate in loam soil as compared to the clay soil.
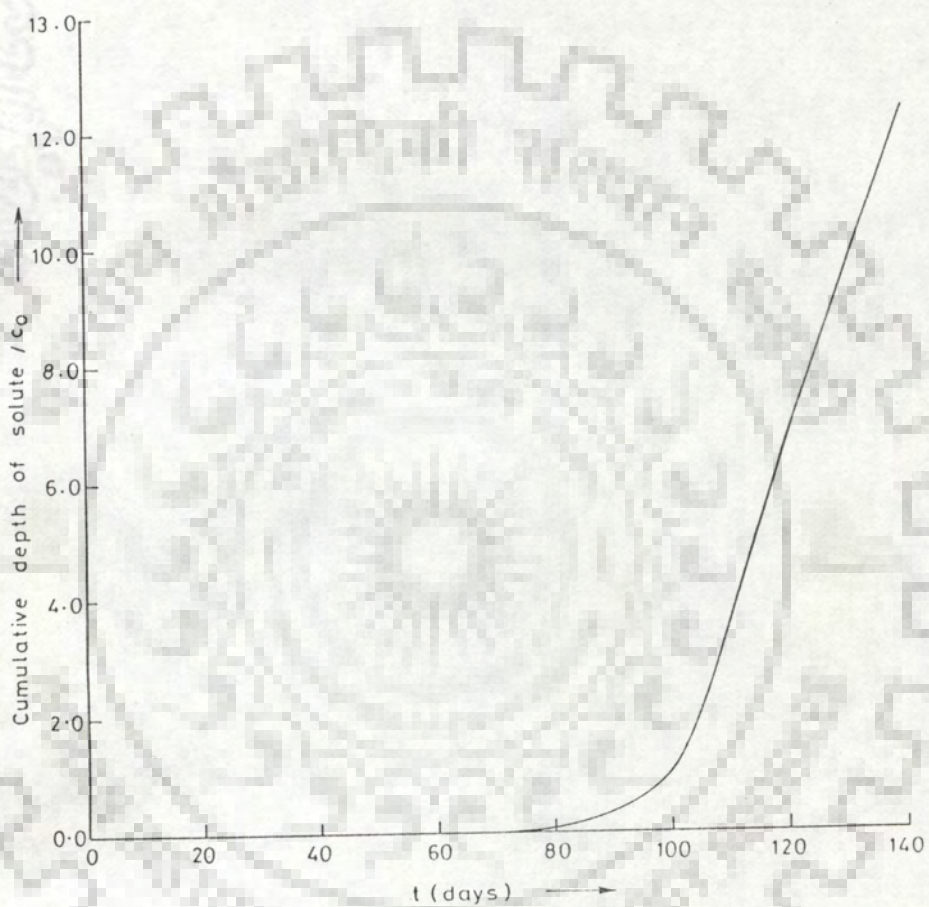
Fig. 5.10. Pollutant joining the water table (loam soil).
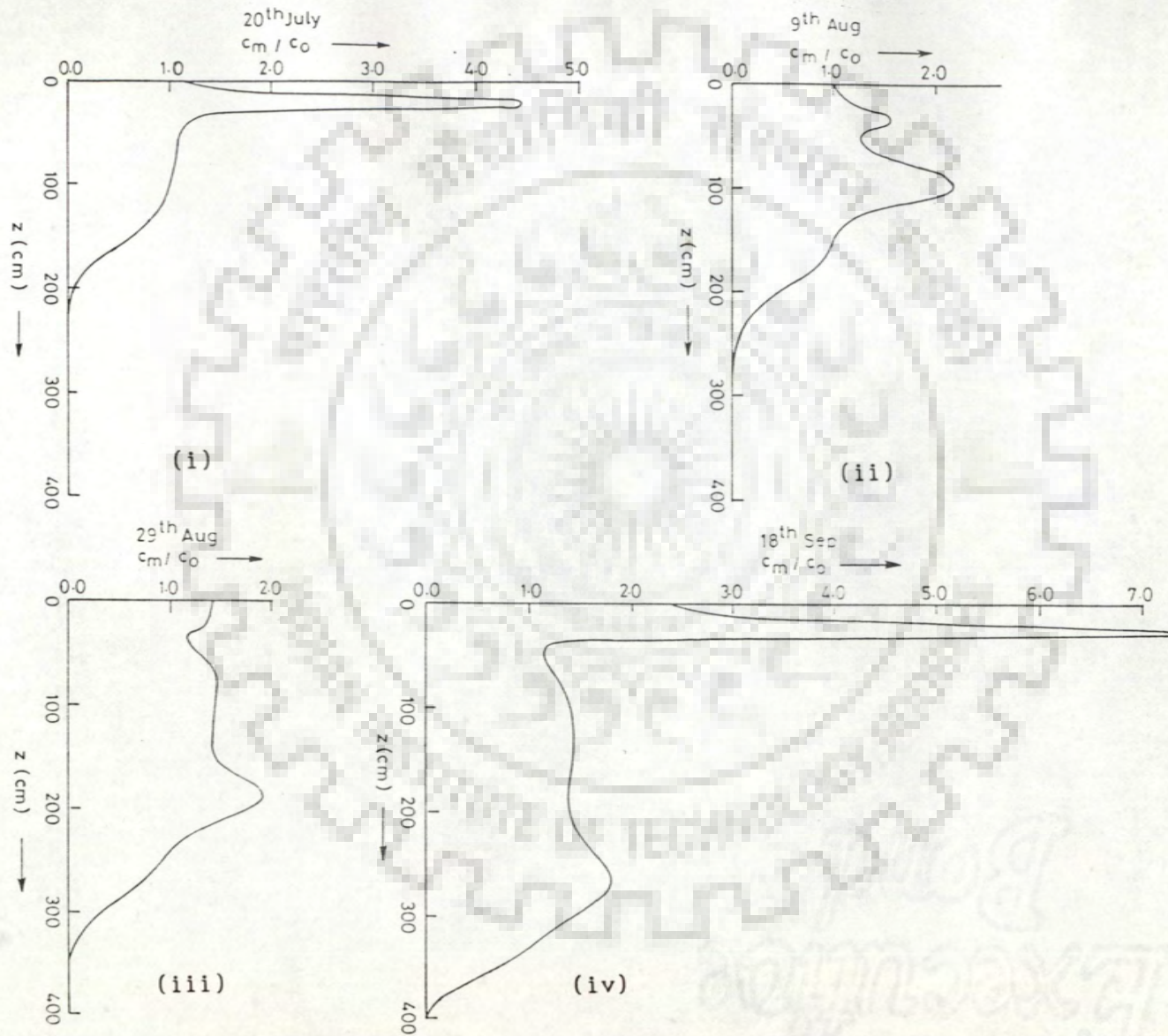
Fig. 5 11. c_m/c_o vs. depth profiles (loam soil).
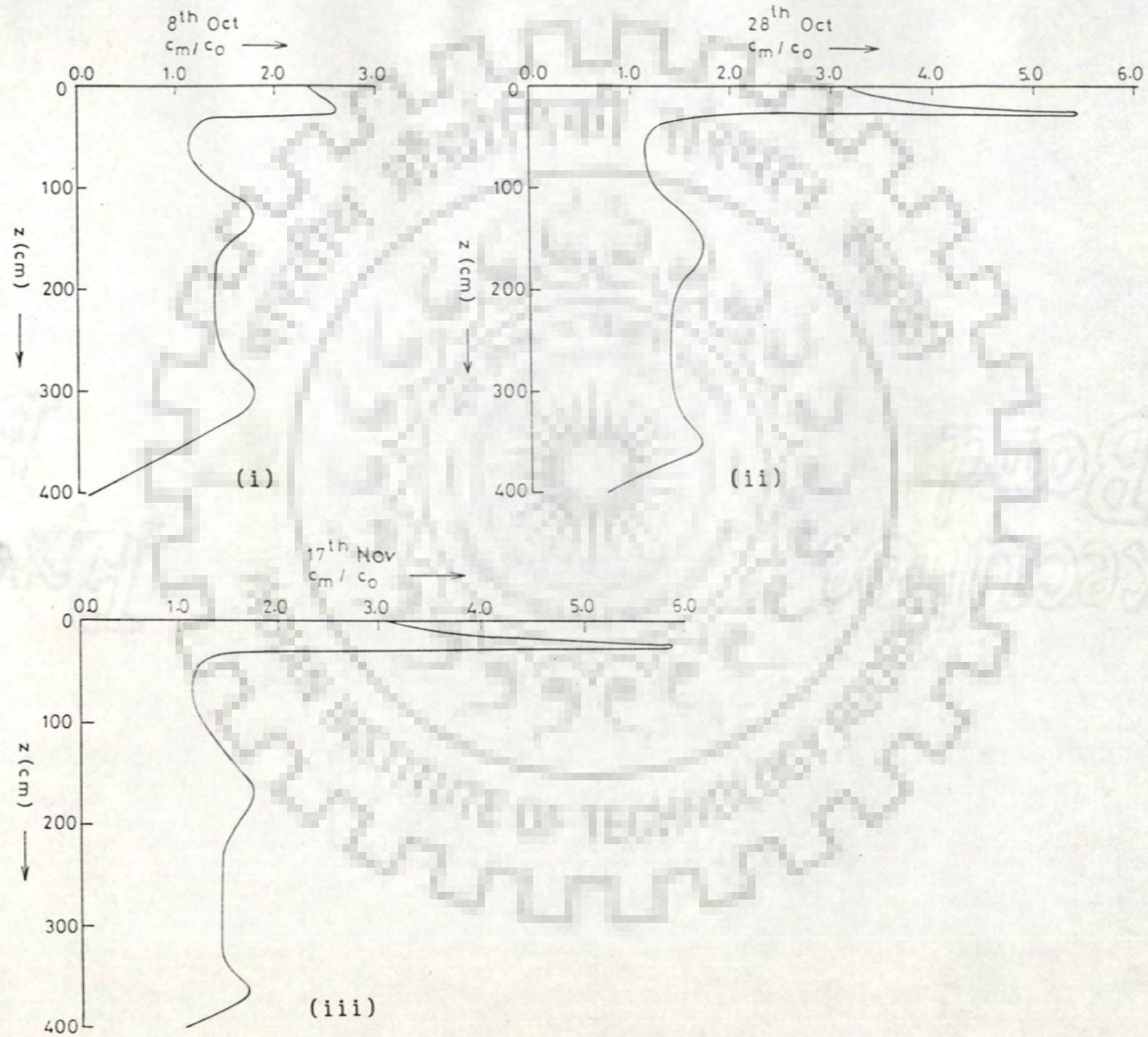
Fig. 5 12. c_m/c_o vs. depth profiles (loam soil).
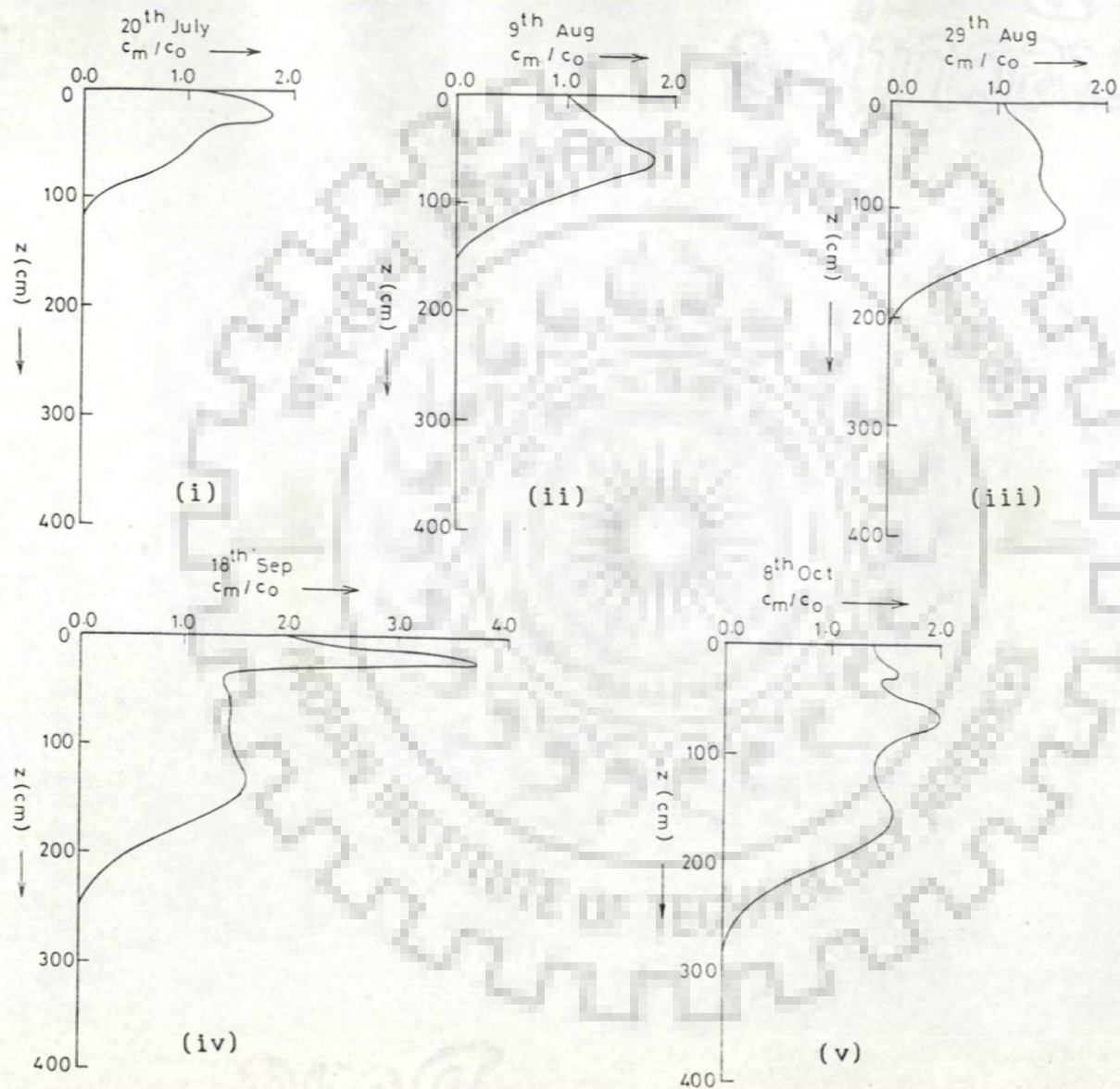
Fig. 5 13. c_m/c_o vs. depth profiles (clay soil).
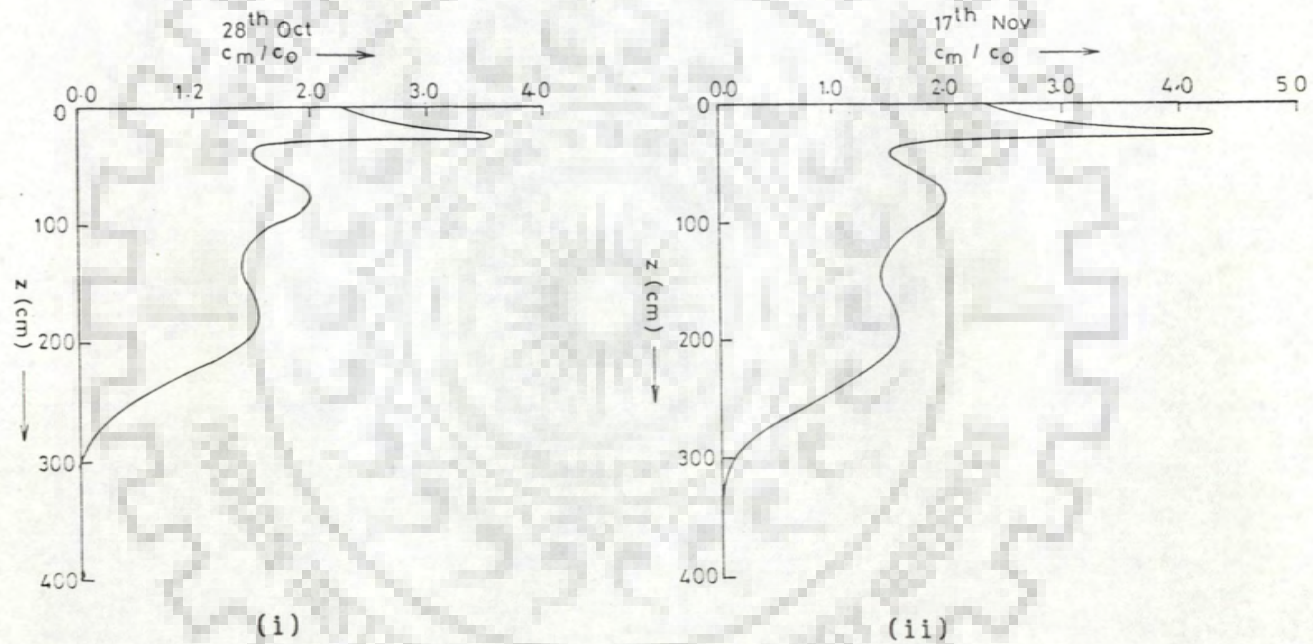
Fig. 5 14. c_m/c_o vs. depth profiles (clay soil).

CHAPTER 6

CONCLUSION

A numerical model has been developed for simulation of vertical unsteady state two phase reactive solute transport in an unsatuarated porous medium extending from the ground surface to the water table. The model provides, among others, solute concentrations at pre-stipulated discrete depth time points. The solute matrix interac-tion is described by first order linear *kinetic* adsorption-desorption (single phase) and linear equilibrium adsorption-desorption (two phase) isotherms. Convective transport is computed by the method of characteristics, while diffusive-dispersive transports and adsorption-desorption by the soil matrix are computed subsequently by implicit finite difference. The solutions of the transport equations require spatial and temporal distributions of moisture and flux. These distributions are obtained by solving the head form of Richards equations, which governs one dimensional unsteady state flow in an unsaturated porous medium. The solution of Richards equation is accomplished by the Crank-Nicolson finite difference scheme. The non-linearity is taken care of by Picard's iteration method. The prominent conclusions of the study are as follows,

1.   The model is capable of reproducing available analytical solutions.

(i)   The model computed concentration profiles and breakthrough curves obtained with a time step of 1 min and strip thickness of 1 cm,

matched well with the corresponding analytical solutions. Increasing the time step to 15 mins, caused no change in the solution for single phase non-reactive solute transport. However, for two phase non-reactive solute transport, increasing the time step to 15 mins caused some deviation between the model simulated breakthrough curve and the corresponding analytical solution.

(ii) The model reproduced the analytical solution even at very low dispersivities ($\lambda=0.1$ cm). This suggests that the proposed procedure of breaking up the total transport among convective and dispersive components and computing the former by method of characteristics eliminates the problem of numerical dispersion and oscillations.

2. Reproduction of two field experimental results by the model has been reasonably good. Prominent details are as follows,

(i) Warrick's experiment (Warrick et al.,1971)

(a) Considering the solute transport to be single phase non-reactive, a lag between the time to peak concentration was observed between the simulated and measured concentration profiles. This lag could be minimized by considering the presence of an immobile phase. A reasonable agreement was obtained for θ_{im} = 0.06 and λ = 1.5 cm.

(b) Time (depth) variability of λ was observed. To match the peak concentration values, increasing values of λ had to be used (λ = 0.7 cm at 9 hrs, λ = 0.9 cm at 11 hrs, λ = 1.0 cm at 17 hrs).

(ii) Böttcher and Strebel's experiment (Böttcher and Strebel, 1989; unpublished data)

The reported breakthrough curves measured at 51 locations show a considerable variation. This was possibly caused by a horizontal

transport, due to lateral variations of soil moisture. Although the proposed model does not account for horizontal transport, the simulated concentration distribution in space and time compared reasonably well with the measured mean distribution of concentration.

3.   Relative mass balance error remained negligible (<0.1%) at all the discrete times for each simulation.

4.   The model is capable of estimating salt accumulation in the root zone due to application of saline irrigation water. Apart from the salt accumulation in the root zone, the model can also provide estimates of the salts leached down to the water table.
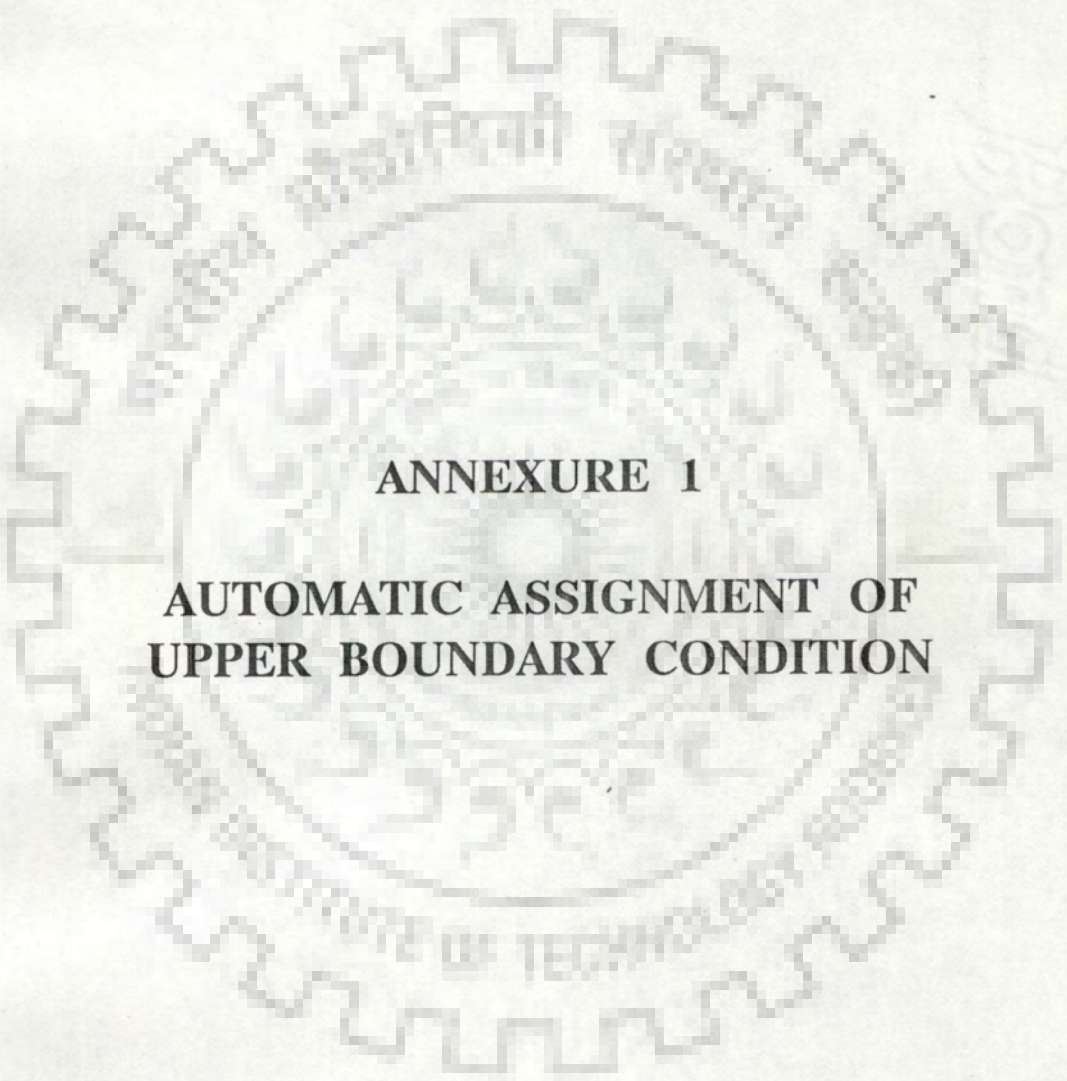
Salt accumulation in the root zone for a yearly cropping schedule irrigated by considerably saline irrigation water (1.5 mmho/cm) has been estimated using the proposed model. Results were compared with those obtained by the salt storage equation, which assumes the soil medium in the root zone to be a reservoir with a bypass (Van der Molen, 1973). A considerable deviation between the two results was observed, which may have been caused by the assumption on which the salt storage equation is based. Thus, the proposed model can be employed to arrive at more rational estimates of the leaching requirement.

5.   The model is capable of estimating volume of pollutant transferred to the water table.

The model was employed to estimate the volume of pollutant (abundantly available at the ground) transferred from ground surface to the water table, during an above normal monsoon season at Roorkee, extending from 1st July to 17th Nov. (140 days). The water table was

assumed to occur at a depth of 400 cms (below the ground), which is a typical depth to water table around Roorkee. Model simulated results indicated that for a clayey unsaturated medium, the pollutant joining the water table, right till the end of the simulation period (140 days) remained negligible (caused only by diffusive-dispersive transport). However, for a loamy unsaturated medium the convective front reached the water table in about 80 days time.
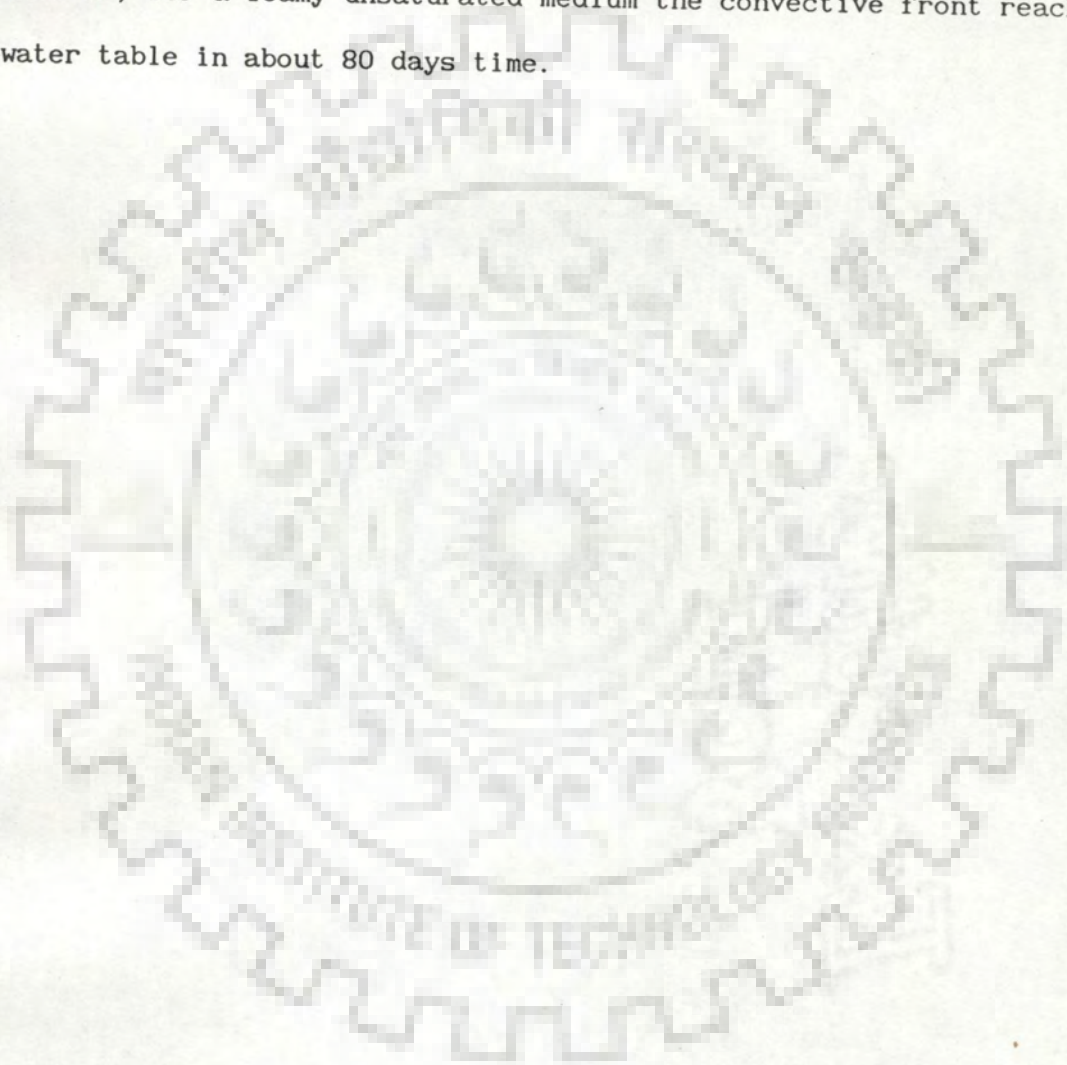
ANNEXURE 1

AUTOMATIC ASSIGNMENT OF UPPER BOUNDARY CONDITION

Automatic Assignment of Upper Boundary Condition

The type of boundary condition at the ground during the simulation period may alternate between Neuman and Dirichlet types, depending upon the intensity and duration of the net input at the ground (refer section 3.4.3). The following algorithm was adopted to implement such alternating boundary conditions.

At the beginning of a time step Δt_k i.e., k^{th} discrete time, the following possibilities are encountered.

1. $h_{1,k}$ is positive (i.e., the top soil remains unsaturated), implying that the boundary condition is of Neuman type.

2. $h_{1,k}$ is zero (i.e., just saturation is maintained) or negative (i.e., ponding has occurred), implying that the boundary condition is of Dirichlet type.

Beginning from either of the two conditions stated above, at the end of the time step Δt_k i.e., $(k+1)^{th}$ discrete time and m^{th} iterations for each condition the following situations may arise.

Condition 1.

(i) $h_{1,k+1}^{(m)}$ remains positive (i.e., the boundary condition remains of Neuman type). Simulation in the subsequent time step is carried out in the same manner as the current one.

(ii) $h_{1,k+1}^{(m)}$ is zero or negative (i.e., saturation or ponding has occurred). If $h_{1,k+1}^{(m)}$ is negative Δt_k is reduced successively, till $h_{1,k+1}^{(m)}$ becomes zero or very small, in which case a zero value is assigned. For simulation during the subsequent time step a Dirichlet boundary condition is assigned.

Condition 2.

At the end of the time step $h_{1,k+1}^{(m)}$ is computed using the mass balance of ponded water at node 1, as follows,

$$h_{1,k+1}^{(m)} = h_{1,k} + (K_{1+1/2,k} \frac{h_{2,k} - h_{1,k} + \Delta z_1}{\Delta z_1} + K_{1+1/2,k+1}^{(m)} \frac{h_{2,k+1}^{(m)} - h_{1,k+1}^{(m)} + \Delta z_1}{\Delta z_1})$$

$$\frac{\Delta t}{2} + (\theta_{1,k+1}^{(m)} - \theta_{1,k}) \Delta z_1/2 - I.\Delta t + E_{1,k+1/2}^{(m)}.\Delta t.\Delta z_1/2$$

where, I is the total input (rainfall + irrigation) and E is evapotranspiration. Again, the following two situations may arise,

(i) $h_{1,k+1}^{(m)}$ remains zero or negative (i.e., the boundary condition remains of Dirichlet type). Simulation during the subsequent time step is carried out in the same manner as the current one.

(ii) $h_{1,k+1}^{(m)}$ is positive or zero (i.e., the boundary condition has changed from Dirichlet to Neuman type). If $h_{1,k+1}^{(m)}$ is positive Δt_k is reduced till $h_{1,k+1}^{(m)}$ attains a small positive value. For simulation in the subsequent time step a Neuman boundary condition is assigned.

ANNEXURE 2

COMPUTER CODE

FLOW CHART OF THE MAIN PROGRAM

FLOW CHART A (SUBROUTINE SOLVE)

ITERATION = 0.0

ADVANCE ITERATION — (C)

IS NETS EQUAL 1

NO → CALL SINK TO COMPUTE EVAPOTRA-NSPIRATION IN THE ROOT ZONE AREA (REFER SECTION 5.1.1.3)

YES

SETTING UP OF TRIDIAGONAL COEFFICIENT MATRIX FOR THE FINITE DIFFERENCE APPROXIMATION OF RICHARDS EQUANTION (REFER EQN. 3.11)

CALL BST TO SOLVE THE MATRIX

CHECK FOR CHANGOVER IN BOUNDARY CONDITION AND CHANGE IF REQUIRED (REFER SECTION 3.4.3)

CHECK FOR CONVERGENCE

IS CONVERGENCE ACHIEVED

NO → IS ITERATION NUMBER LESS THAN ITR — YES → (C)

YES

NO → REDUCE TIME STEP

CALL THETA TO COMPUTE MOISTURE DISTRIBUTION

RETURN

FLOW CHART B (SUBROUTINE TRANS)

CALL MODCOR TO INCREMENT THE CUMULATIVE WATER VOLUMES (PER UNIT PLAN AREA) OF CO-ORDINATES AND ESTIMATE THE CONVECTIVE TRANSPORT BY COMPUTING NEW POSITIONS OF THE MOVING PACKETS (REFER SECTION 3.4.4.1.1)

GENERATE NEW MOVING PACKETS IF REQUIRED (REFER SECTION 3.4.4.1.2)

CALL EXCMOV TO COMPUTE SOLUTE VOLUME (PER UNIT PLAN AREA) LEAVING THE DOMAIN AT THE LOWER BOUNDARY (REFER SECTION 3.4.4.1.3)

COMPUTE CHANGE IN CONCENTRATION OF MOVING PACKETS DUE TO HYDRODYNAMIC DISPERSION. RECOMPUTE SOLUTE VOLUMES (PER UNIT PLAN AREA) CONTAINED IN MOVING PACKETS (REFER SECTION 3.4.4.2 AND 3.4.4.2.1)

CALL VOLSOL TO COMPUTE NODAL CONCENTRATION, SOLUTE AND WATER VOLUMES (PER UNIT PLAN AREA) BY LOCATING THE MOVING PACKETS IN EACH NODAL AREA OD INFLUENCE (REFER SECTION 3.4.5.1)

IS NMKT EQUAL 1

YES

NO

COMPUTE ADSORBED CONCENTRATION OF SOIL MATRIX ACCOUNTING FOR FIRST ORDER LINEAR KINETIC ADSORPTION-DESORPTION. RECOMPUTE NODAL SOLUTE CONCENTRATION AND CHANGE IN NODAL SOLUTE VOLUME (PER UNIT PLAN AREA) (REFER SECTION 3.4.5.2)

d

ll

(II)

IS
THC EQUAL 0.0
OR
ALPHA EQUAL 0.0

NO

YES

COMPUTE IMMOBILE CONCENTRATION
BY ACCOUNTING FOR TRANSFER OF
SOLUTE INTO/OUT OF THE IMMOBILE
PHASE RECOMPUTE NODAL MOBILE
CONCENTRATION AND CHANGE IN
NODAL SOLUTE VOLUMES (PER
UNIT PLAN AREA)
(REFER SECTION 3.4.6.4)

(d)

CALL MODSOL TO MODIFY SOLUTE
VOLUMES (PER UNIT PLAN AREA)
CAUSED BY CHANGE IN NODAL
SOLUTE VOLUME (PER UNIT PLAN
AREA)
(REFER SECTION 3.4.5.3)

RETURN

```
* SOLUTE TRANSPORT IN AN UNSATURATED POROUS MEDIUM EXTENDING FROM GROUND
* TO WATER TABLE ---- PROGRAMMED BY SULEKHA GUPTA
*------------------------------------------------------------------------
* DEFINATION OF VARIABLES
*------------------------------------------------------------------------
*         NDP : NUMBER OF NODES IN THE FLOW DOMAIN
*         NMAX : NUMBER OF NODES IN THE SOLUTE DOMAIN
*         NT : NUMBER OF TIME STEPS
*         NOB : NUMBER OF DAILY OBSRERVATIONS
*         ITR : MAXIMUM NUMBER OF ITERATIONS USED IN PICARD'S ITERATION
*               METHOD
* CONDITIONAL SWITCHES
*         IOPT = 0 : NEUMAN BOUNDARY CONDITION
*         IOPT = 2 : DIRICHLET BOUNDARY CONDITION
*         NWTV = 1 : TIME VARIANT WATER TABLE (DEFAULT TIME INVARIANT
*                    WATER TABLE
*         NETS = 1 : EVATRANSPIRATION NOT ACCOUNTED FOR (DEFAULT
*                    EVAPOTRANSPIRATION ACCOUNTED FOR
*         NMKT = 1 : LINEAR KINETIC ADSORPTION-DESORPTION ACCOUNTED FOR
*                    (DEFAULT LINEAR KINETIC ADSORPTION-DESORPTION NOT
*                    ACCOUNTED FOR)
*------------------------------------------------------------------------
*         DTM : TIME STEP
*         TOTIRR : TIME DURATION OF A SINGLE IRRIGATION APPLICATION
*         EPS : SMALL POSITIVE VALUE FOR DEFINING THE PERMISSIBLE ERROR
*               IN PICARD'S ITERATION METHOD
*------------------------------------------------------------------------
*         POR : POROSITY ; SAT : SATURATED CAPILLARY CONDUCTIVITY ; SSM :
*         BUBBLING PRESSURE ; FFC : FIELD CAPACITY ; WP : WILTING POINT ;
*         THR : RESIDUAL MOISTURE CONTENT
*------------------------------------------------------------------------
*         PAT : MINUTES IN A DAY
*         C0 : INPUT SOLUTE CONCENTRATION ; TSTR : STRIP THICKNESS
* PARAMETERS
*         THC : IMMOBILE MOISTURE CONTENT ; D0 : MOLECULAR DIFFUSION
*         COEFFICIENT IN A FREE WATER SYSTEM ; A0,A10 : EMPIRICAL CONSTA-
*         NTS CHARACTERIZING THE SOIL ; AML : DISPERSIVITY ; P : FRACTION
*         OF ADSORPTION SITES LOCATED IN THE MOBILE SOIL MATRIX ; RO :
*         BULK DENSITY OF SOIL ; CONS : EMPIRICAL DISTRIBUTION COEFFICIENT
*         ALPHA : FIRST ORDER RATE COEFFICIENT GOVERNING TRANSFER OF
*         SOLUTE INTO/OUT OF THE IMMOBILE PHASE ; BETA : FIRST ORDER RATE
*         COEFFICIENT GOVERNING EXCHANGE BETWEEN SOLUTE AND SOIL MATRIX
*------------------------------------------------------------------------
*         DELZ : SPATIAL INCREMENT IN THE FINITE DIFFERENCE GRID
*         HPRI : INITIAL CAPILLARY HEAD DISTRIBUTION
*         CI : INITIAL CONCENTRATION DISTRIBUTION
*------------------------------------------------------------------------
*         NYR : YEAR OF SIMULATION ; NMNTH : MONTH OF SIMULATION ; NDT :
*         DATE OF SIMULATION ; RAIN : RAINFALL INTENSITY (DAILY) ; PET :
*         POTENTIAL EVAPOTRANSPIRATION (DAILY) ; PF : P FACTOR ; API :
*         DEPTH OF APPLIED IRRIGATION ; RZD : DEPTH OF ROOT ZONE ; NOROOT
*         : NODE NUMBER AT WHICH ROOT ZONE ENDS
*------------------------------------------------------------------------
```

```
*          ERR : RELATIVE MASS BALANCE ERROR
*          THE : MOISTURE CONTENT
*          ECE : CONCENTRATION OF SATURATION EXTRACT
*          CCM : MOBILE CONCENTRATION
*          CIM : IMMOBILE CONCENTRATION
*          CC1 : AVERAGE CONCENTRATION IN THE ROOT ZONE
*          ADN1 : AVERAGE SOLUTE VOLUME (PER UNIT PLAN AREA) IN THE ROOT
*                 ZONE
*          WTSOL : VOLUME OF SOLUTE (PER UNIT PLAN AREA) JOINING THE WATER
*                  TABLE
*------------------------------------------------------------------------
           DIMENSION WADPT(800),CMD(800),SMY(800),VLT(800),CUMET(800)
           DIMENSION DZS(120),ECE(120),COT(120),S(120)
           DIMENSION NNA(120),INA(120,100),DV(120),DV1(120)
           COMMON/DAT/DELZ(120),HAD(120),B1(120),THE(120),HPR1(120),AP(120)
           COMMON/CONN/CCM(120),VLA(120),VLX(120),CIM(120)
           1,XV(120),XU(120),XF(120)
           COMMON /CONC/VLL(800),X(800),Y(800),SOL(800),XWAT(800),
           1YWAT(800)
           COMMON/CONST/POR,SAT,PAT,SSM,FFC,WP,POW,THR,RZD,PF,PET,THC
           COMMON/INDEX/TSTR,C0,A0,A10,AML,D0,CFS,SUMVL,EFL,ALPHA,BETA
           1P,RO,CONS
           OPEN(UNIT=1,DEVICE='DSK',FILE='LR2.DAT')
           OPEN(UNIT=2,DEVICE='DSK',FILE='LR1.DAT')
           OPEN(UNIT=3,DEVICE='DSK',FILE='WHTSAL.OUT')
           OPEN(UNIT=4,DEVICE='DSK',FILE='FLUX.OUT')
           READ(1,*)NDP,NMAX,NT,NOB,ITR,IOPT,NWTV,NETS,NMKT
           READ(1,*)DTM,TOTIRR,EPS
           READ(1,*)POR,SAT,PAT,SSM,FFC,WP,POW,THR
           READ(1,*)C0,CI,TSTR,D0,A0,A10,AML,ALPHA,THC,P,RO,CONS,RX,KS
           READ(1,*)(DELZ(I),I=1,NMAX-1)
           READ(1,*)(HPR1(I),I=1,NDP)
           READ(1,*)(CI(I),I=1,NDP)
           IF (NMKT.EQ.1) GO TO 5
           RX=RO
           KS=CONS
           RO=0.0
           CONS=0.0
5          CONTINUE
           SUM1=0.0
           DO 101 I=1,NMAX
           IF (I.GT.NDP) GO TO 102
           JTL=I
           B1(I)=THETA(HPR1(I),JTL)
           GO TO 101
102        B1(I)=POR
101        CONTINUE
           SOLIV=0.0
           DO 10 J=1,NMAX
           IF (J.GT.NDP) CI(J)=0.0
           SOLIV=SOLIV+CI(J)*B1(J)
10         CONTINUE
           AP(1)=(COND(B1(1),1)+COND(B1(2),2))/2.0
```

```
        DFR=(HPR1(1)+DELZ(1)-HPR1(1))
        DV(1)=DFR*AP(1)/(DELZ(1))
        CALL DPEC(NMAX,DZS,XF,XV,XU)
        CALL INICON(NMAX,XF,TSTR,B1,THC,CI,P,RO,CONS,NTP)
        NTT=NTP
        CALL VOLSOL(NMAX,XV,XU,NTT,X,Y,SOL,VLL,VLA,VLX,COT,CCM,
        1NNA,INA)
        CTM=0.0
        IX=0
        IRR=0
65      CMDTM=0.0
        IRR1=0
        API=0.0
        WTOD=WTNW
655     IX=IX+1
        READ(2,*)NYR,NMNTH,NDT,RAIN,PET,PF,API
        TYPE *,NYR,NMNTH,NDT,RAIN,PET,PF,API
        IF (IX.EQ.1)  GO TO 205
        IF (NDT.EQ.1.OR.NDT.EQ.16) GO TO 205
        GO TO 210
205     IF (IX.EQ.2.AND.NDT.EQ.16) GO TO 210
        READ(2,*)RZD,NOROOT
210     CONTINUE
        CMRAIN=RAIN
        RAIN=RAIN/PAT
        IF (NWTV.EQ.1) GO TO 889
        IF (IX.GT.1) CALL WATBLE(WTOD,WTNW,NDP)
889     LMN=0
        IF (API.EQ.0.0) GO TO 225
        IRR=1
        IRR1=1
        APIRI=API/TOTIRR
        TYPE *,APIRI
        DPTAPI=0.0
225     FLUX1=RAIN+APIRI
        IOPT=0
        IF (HPR1(1).LE.0.0) IOPT=2
        INX=INX+1
        DO 166 IT=1,NT
        DV1(1)=DV(1)
        IF (IT.EQ.1) GO TO 62
        IF (DELTAT.EQ.TSP) GO TO 62
        IF (AD.EQ.HAX) GO TO 62
        DELTAT=DT
        NP=1
        GO TO 60
62      DELTAT=DTM
        TSP=DELTAT
        AD=0.0
        DT=0.0
        NP=0
60      CALL SOLVE(NDP,IOPT,ITR,NETS,NOROOT,EPS,DELTAT,FLUX1,XU,XV
        1,BAL,STOR,S,DT)
```

```
        AD=AD+DT
        IF (IND.EQ.0.OR.NP.NE.0) GO TO 69
        HAX=DT*(2**IND)
        IND=0
69      CTM=CTM+DELTAT
        CMDTM=CMDTM+DELTAT
        CFL=CFL+BAL
        CMS=CMS+STOR
        FLUX=FLUX1
        TYPE *,CTM,FLUX
        IF (IOPT.EQ.0) GO TO 80
        DFR=(HPR1(2)+DELZ(1)-HPR1(1))
        DV(1)=DFR*AP(1)/(DELZ(1))
        FLUX=(DV1(1)+DV(1))/2.0
        TYPE *,IOPT,FLUX
80      SUMIFS=SUMIFS+FLUX*DELTAT*C0
        CALL MCURVE(NDP,B1,DELZ,THC,P,RO,CONS,NMD,WADPT,CMD)
        IF (NETS.EQ.1) GO TO 79
        CALL SOLET(NOROOT,NNA,INA,NTT,NTP,VLX,XV,XU,S,X,Y,VLL,
       1RZD,DELTAT,CUMET)
79      CONTINUE
        CALL MODCOR(NTP,NMD,FLUX,CUMET,SUMVL,CFS,WADPT,CMD,DELTAT,SMY)
        CALL TRANS(NMAX,NTT,NTP,FLUX,DELTAT,THC,SMY,NNA,INA,NMKT)
        IF (IRR.EQ.0) GO TO 288
        DPTAPI=DPTAPI+APIRI*DELTAT
        TYPE *,DPTAPI,API
        IF (DPTAPI.LT.API) GO TO 288
        APIRI=0.0
        IRR=0
        FLUX1=RAIN
288     SUMV=0.0
        DO 901 K=1,NTT
        SUMV=SUMV+SOL(K)
901     CONTINUE
        SUMV=SUMV+EFL
        SUMC=0.0
        DO 902 J=1,NMAX
        SUMC=SUMC+CCM(J)*VLX(J)+CIM(J)*(XU(J)-XV(J))*THC
        SUMV=SUMV+CIM(J)*(XU(J)-XV(J))*THC
902     CONTINUE
        SUMC=SUMC+EFL
        TYPE *,IT,CMDTM,SUMIFS,SUMV
        IF (CMDTM.EQ.PAT) GO TO 67
166     CONTINUE
67      IF (INX/20*20.EQ.INX) GO TO 784
        IF (IX.EQ.1) GO TO 784
        GO TO 780
784     WTSOL=0.0
        DEPTH=XF(NDP)
        IF (NWTV.NE.1) DEPTH=WTNW
        DO 787 K=1,NTP
        IF (X(K).LE.DEPTH) GO TO 787
        IF (Y(K).LT.DEPTH) GO TO 789
```

```
            WTSOL=WTSOL+SOL(K)
            GO TO 787
789         WTSOL=WTSOL+SOL(K)*(X(K)-DEPTH)/(X(K)-Y(K))
787         CONTINUE
            ERR=(SUMIFS-SUMC-SOLIV)/SUMIFS
            WTSOL=WTSOL+EFL
            WRITE(4,*)NYR,NMNTH,NDT
            WRITE(4,*)(THE(I),I=1,NDP)
            DO 782 J=1,NDP
            ECE(J)=(CCM(J)*(THE(J)-THC)+CIM(J)*THC)/POR
782         CONTINUE
            WRITE(3,*)NYR,NMNTH,NDT
            WRITE(3,*)ERR
            WRITE(3,*)NDP,NMAX
            WRITE(3,*)(ECE(J),J=1,NDP)
            WRITE(3,*)(CCM(J),J=1,NMAX)
            WRITE(3,*)(CIM(J),J=1,NMAX)
            ADN1=0.0;ADN2=0.0;ADN3=0.0
            ADN4=0.0;ADN5=0.0;ADN6=0.0
            DO 883 J=1,NOROOT
            ADN1=ADN1+(CCM(J)*(THE(J)-THC)+CIM(J)*THC)*(XU(J)-XV(J))
            ADN2=ADN2+THE(J)*(XU(J)-XV(J))
883         CONTINUE
            CC1=ADN1/ADN2
            WRITE(3,*)CC1,ADN1
780         IF (IX.LT.NOB) GO TO 65
            STOP
            END
            FUNCTION THETA(TUF,JTL)
C THIS FUNCTION COMPUTES MOISTURE CONTENT VALUES
            COMMON/CONST/POR,SAT,PAT,SSM,FFC,WP,POW,THR,RZD,PF,PET,THC
            IF(TUF.GT.SSM)GO TO 100
            THETA=POR-THR*TUF/SSM
            GO TO 101
100         THETA=EXP(ALOG(POR-2.0*THR)*TUF/SSM)+THR
101         IF(THETA.GT.POR)THETA=POR
            RETURN
            END
            FUNCTION COND(TUF,JTL)
C THIS FUNCTION COMPUTES CAPILLARY CONDUCTIVITY VALUES
            COMMON/CONST/POR,SAT,PAT,SSM,FFC,WP,POW,THR,RZD,PF,PET,THC
            COND=SAT*((TUF-THR)/(POR-THR))**POW
            IF (TUF.EQ.POR) COND=SAT
            IF (TUF.LE.THC) COND=0.0
            RETURN
            END
            SUBROUTINE DPEC(NMAX,DZS,XF,XV,XU)
C THIS SUBROUTINE COMPUTES CUMULATIVE NODAL DEPTHS AND NODAL AREA
C OF INFLUENCE
            DIMENSION DZS120),XF(120),XV(120),XU(120)
            SUM1=0.0
            DO 3 J=2,NMAX
            SUM1=SUM1+DZS(J-1)
```

```
             XF(J)=SUM1
3            CONTINUE
             XF(1)=0.0
             DO 155 J=1,NMAX
             IF (J.EQ.1) GO TO 1100
             XV(J)=XF(J-1)+0.5*(XF(J)-XF(J-1))
             GO TO 1122
1100         XV(J)=XF(J)
1122         CONTINUE
             IF (J.EQ.NMAX) GO TO 1155
             XU(J)=XF(J+1)-0.5*(XF(J+1)-XF(J))
             GO TO 1177
1155         XU(J)=XF(J)
1177         CONTINUE
155          CONTINUE
             RETURN
             END
             SUBROUTINE INICON(NMAX,XF,TSTR,B1,THC,CI,P,RO,CONS,NTP)
C THIS SUBROUTINES COMPUTES THE TOTAL NUMBER OF MOVING PACKETS, THEIR
C COORDINATE POSITIONS, WATER AND SOLUTE VOLUMES (PER UNIT PLAN AREA)
C CONTAINED IN THEM AND CUMULATIVE WATER VOLUMES (PER UNIT PLAN AREA)
C CORRESPONDING TO THE CO-ORDINATES AT THE BEGINNING OF SIMULATION
             DIMENSION XF(120),B1(120),CI(120)
             DIMENSION XTH(800),YTH(800),WCON(800),CPX(800),CPY(800),
             CPI(800)
             COMMON /CONC/VLL(800),X(800),Y(800),SOL(800),XWAT(800),
             1YWAT(800)
             NTP=0
             CTM=0.0
             TTE=PAT
             RNM=XF(NMAX)/TSTR
             NNM=IFIX(RNM)
             DO 35 K=NTP+1,NTP+NNM
             Y(K)=(FLOAT(NTP+NNM)-FLOAT(K))*TSTR
             X(K)=Y(K)+TSTR
35           CONTINUE
             NTP=NTP+NNM
             NTT=NTP
             MP2=NTP+1
             DO 31 K=1,NTP
             DO 30 J=1,NMAX-1
             IF (X(K).LT.XF(J).OR.X(K).GT.XF(J+1)) GO TO 30
             XTH(K)=B1(J)+(B1(J+1)-B1(J))*(X(K)-XF(J))/(XF(J+1)-XF(J))
             CPX(K)=CI(J)+(CI(J+1)-CI(J))*(X(K)-XF(J))/(XF(J+1)-XF(J))
             GO TO 29
30           CONTINUE
29           DO 28 J=1,NMAX-1
             IF (Y(K).LT.XF(J).OR.Y(K).GT.XF(J+1)) GO TO 28
             YTH(K)=B1(J)+(B1(J+1)-B1(J))*(Y(K)-XF(J))/(XF(J+1)-XF(J))
             CPY(K)=CI(J)+(CI(J+1)-CI(J))*(Y(K)-XF(J))/(XF(J+1)-XF(J))
             GO TO 31
28           CONTINUE
31           CONTINUE
```

```
         DO 33 K=1,NTP
         WCON(K)=(XTH(K)+YTH(K)-2.0*(THC+P*RO*CONS))/2.0
         VLL(K)=(X(K)-Y(K))*(XTH(K)+YTH(K)-2.0*(THC+P*RO*CONS))/2.0
         CPI(K)=(CPX(K)+CPY(K))/2.0
         SOL(K)=VLL(K)*CPI(K)
33       CONTINUE
         DO 39 L=1,NTP
         K=NTP-L+1
         SUMXW=SUMXW+(X(K)-Y(K))*WCON(K)
         XWAT(K)=SUMXW
         IF (K.EQ.NTP) GO TO 39
         SUMYW=SUMYW+(X(K+1)-Y(K+1))*WCON(K+1)
         YWAT(K)=SUMYW
39       CONTINUE
         YWAT(NTP)=0.0
         RETURN
         END
         SUBROUTINE VOLSOL(NMAX,XV,XU,NTT,X,Y,SOL,VLL,VLA,VLX,COT
        1,CCM,NNA,INA)
C THIS SUBROUTINE COMPUTES NODAL WATER AND SOLUTE VOLUMES (PER UNIT
C PLAN AREA)
         DIMENSION XV(120),XU(120),VLX(120),COT(120),CCM(120),NNA
        1(120),INA(120,100),VLA(120)
         DIMENSION X(800),Y(800),SOL(800),VLL(800)
         DO 55 J=1,NMAX
         VLA(J)=0.0
         VLX(J)=0.0
         NNA(J)=0.0
55       CONTINUE
         SUMSOL=0.0
         DO 50 J=1,NMAX
         DO 60 K=1,NTT
         IF (X(K).LE.XV(J).OR.Y(K).GE.XU(J)) GO TO 60
         IF (Y(K).LE.XV(J).AND.X(K).GE.XU(J)) GO TO 53
         IF (Y(K).LT.XV(J).AND.X(K).GT.XV(J)) GO TO 66
         IF (Y(K).LT.XU(J).AND.X(K).GT.XU(J)) GO TO 71
         VLA(J)=VLA(J)+SOL(K)
         VLX(J)=VLX(J)+VLL(K)
         GO TO 75
66       VLA(J)=VLA(J)+SOL(K)*(X(K)-XV(J))/(X(K)-Y(K))
         VLX(J)=VLX(J)+VLL(K)*(X(K)-XV(J))/(X(K)-Y(K))
         GO TO 75
71       VLA(J)=VLA(J)+SOL(K)*(XU(J)-Y(K))/(X(K)-Y(K))
         VLX(J)=VLX(J)+VLL(K)*(XU(J)-Y(K))/(X(K)-Y(K))
         GO TO 75
53       VLA(J)=VLA(J)+SOL(K)*(XU(J)-XV(J))/(X(K)-Y(K))
         VLX(J)=VLX(J)+VLL(K)*(XU(J)-XV(J))/(X(K)-Y(K))
75       NNA(J)=NNA(J)+1
         KN=NNA(J)
         INA(J,KN)=K
60       CONTINUE
         IF (VLX(J).EQ.0.0) GO TO 50
         COT(J)=VLX(J)/(XU(J)-XV(J))
```

```
           CCM(J)=VLA(J)/VLX(J)
50         CONTINUE
           RETURN
           END
           SUBROUTINE WATBLE(WTOD,WTNW,NDP)
C THIS SUBROUTINE MODIFIES THE NUMBER OF NODES, THEIR POSITIONS
C AND CAPILLARY HEAD VALUES IN CASE OF A VARIABLE WATER TABLE
           COMMON/DAT/DELZ(120),HAD(120),B1(120),THE(120),HPR1(120),AP(12(
           NDOLD=NDP
           DTW=WTOD-DELZ(NDP-1)
           PRH=HPR1(NDP-1)
           HNS=0.5*DELZ(NDP-2)
           ZZ=DELZ(NDP-2)
           DFWT=WTNW-WTOD
           IF (DFWT)5,10,15
15         DFWT=DFWT+DELZ(NDP-1)
           NDP=NDP-1
50         DFWT=DFWT-ZZ
           IF (DFWT.LT.0.0) GO TO 60
           DELZ(NDP)=ZZ
           NDP=NDP+1
           GO TO 50
60         DFWT=DFWT+ZZ
           IF (DFWT.EQ.0.0) GO TO 70
           IF (DFWT.LT.HNS) GO TO 80
           NDP=NDP+1
           DELZ(NDP-1)=DFWT
           GO TO 70
80         DELZ(NDP-1)=DELZ(NDP-1)+DFWT
70         HPR1(NDP)=0.0
           GO TO 10
5          DFWT=DFWT+DELZ(NDP-1)
           NDP=NDP-1
           IF(DFWT.LT.0.0) GO TO 5
           IF (DFWT.EQ.0.0) GO TO 55
           IF (DFWT.LT.HNS) GO TO 40
           NDP=NDP+1
           DELZ(NDP-1)=DFWT
           GO TO 55
40         DELZ(NDP-1)=DELZ(NDP-1)+DFWT
55         HPR1(NDP)=0.0
10         CONTINUE
           IF (NDP.LE.NDOLD) GO TO 678
           DXDN=0.0
           DO 673 J=NDOLD,NDP
           DXDN=DXDN+DELZ(J-1)
           HPR1(J)=PRH*(WTNW-(DTW+DXDN))/(WTNW-DTW)
673        CONTINUE
           DO 678 J=NDOLD,NDP
           JTL=J
           B1(J)=THETA(HPR1(J),JTL)
678        CONTINUE
           RETURN
```

```
        END
        SUBROUTINE SOLVE(NDP,IOPT,ITR,NETSNNOROOT,EPS,DELTAT,RAIN
       1,XU,XV,BAL,STOR,S,DT)
C THIS SUBROUTINE SOLVES RICHARDS EQUATION AND PROVIDES THE LATEST
C VALUES OF CAPILLARY HEADS AND MOISTURE CONTENTS
        DIMENSION SA(120),STO1(120),FTHE(120),AP1(120),STO(120)
       1,XU(120),XV(120)
        DIMENSION B(120),A(120),C(120),D(120),H(120),F(120),S(120)
        COMMON/DAT/DELZ(120),HAD(120),B1(120),THE(120),HPR1(120),AP(120
        LMN=LMN+1
        KIN=1
        IF (LMN.NE.1) GO TO 3801
        DO 5 I=1,NDP-1
        JTL=I
        AP(I)=(COND(B1(I),JTL)+COND(B1(I+1),(JTL+1)))/2.0
5       CONTINUE
        STO(1)=(-HPR1(1)+HPR1(2)+DELZ(1))/DELZ(1)*AP(1)
        C1=STO(1)
        G1=(-HPR1(NDP-1)+HPR1(NDP)+DELZ(NDP-1))/DELZ(NDP-1)*AP(NDP-1)
        STO(NDP-1)=G1-(-HPR1(NDP-2)+HPR1(NDP-1)+DELZ(NDP-2))/DELZ(NDP-2
       1*AP(NDP-2)
        STO(NDP)=G1
        DO 1000 I=2,NDP-2
        STO(I)=(-HPR1(I)+HPR1(I+1)+DELZ(I))/DELZ(I)*AP(I)
       1-(-HPR1(I-1)+HPR1(I)+DELZ(I-1))/DELZ(I-1)*AP(I-1)
1000    CONTINUE
        DO 3800 I=1,NDP
        STO1(I)=STO(I)
3800    CONTINUE
3801    CONTINUE
        NPT=IOPT
        DO 1266 I=1,NDP
        SA(I)=STO(I)
1266    CONTINUE
900     CONTINUE
        IOPT=NPT
        DO 1 I=1,NDP
        THE(I)=B1(I)
        AP1(I)=AP(I)
        STO(I)=SA(I)
        HAD(I)=HPR1(I)
1       CONTINUE
        DO 110 M=1,ITR
        IF (NETS.EQ.1) GO TO 111
        CALL SINK(NDP,NOROOT,B1,THE,XU,XV,S,DELTAT)
111     CONTINUE
        DO 10 I=1,NDP-1
        JTL=I
        AP(I)=(COND(THE(I),JTL)+COND(THE(I+1),(JTL+1)))/2.0
10      CONTINUE
        DO 68 I=1,NDP
        JTL=I
        IF (I.GT.1.AND.I.LT.NDP) GO TO 69
```

```
       IF (I.EQ.1) GO TO 70
       GO TO 75
70     IF (IOPT.GT.0) GO TO 71
       A(I)=0.0
       B(I)=AP(I)/DELZ(I)-DELZ(I)/DELTAT*DIFU(JTL)
       C(I)=-AP(I)/DELZ(I)
       D(I)=-HPR1(I)*DELZ(I)/DELTAT*DIFU(JTL)-2.0*RAIN+STO(I)+AP(I)
      1+2.0*S(I)
       GO TO 68
75     A(I)=0.0
       B(I)=1.0
       C(I)=0.0
       D(I)=0.0
       GO TO 68
71     A(I)=0.0
       B(I)=1.0
       C(I)=0.0
       D(I)=HAD(I)
       GO TO 68
69     CONTINUE
       JTL=I
       A(I)=-AP(I-1)/DELZ(I-1)
       B(I)=AP(I-1)/DELZ(I-1)+AP(I)/DELZ(I)-DIFU(JTL)*(DE
      1LZ(I-1)+DELZ(I))/DELTAT
       C(I)=-AP(I)/DELZ(I)
       D(I)=-DIFU(JTL)*(DELZ(I-1)+DELZ(I))*HPR1(I)/DELTAT+
      1STO(I)+AP(I)-AP(I-1)+2.0*S(I)
68     CONTINUE
       CALL BST(NDP,A,B,C,D,H)
       DO 73 I=1,NDP
       F(I)=H(I)
73     CONTINUE
       IF (IOPT.GT.0) GO TO 502
       IF (HPR1(1).GT.0.0.AND.F(1).GT.0.0) GO TO 504
       IF (F(1).GT.-0.01.AND.HPR1(1).LT.0.01) F(1)=0.0
       IF (F(1).NE.0.0) GO TO 1100
       IOPT=2
       GO TO 1110
502    F(1)=HPR1(1)+(STO(1)+AP(1)*(HAD(2)-HAD(1)+DELZ(1))/DELZ(1))
      1*DELTAT/2.0+(THE(1)-B1(1))*DELZ(1)/2.0-RAIN*DELTAT+S(1)*DELTAT
       IF (HPR1(1).LE.0.0.AND.F(1).LE.0.0) GO TO 504
       IF (HPR1(1).GT.-0.01.AND.F(1).LT.0.01) F(1)=0.001
       IF (F(1).NE.0.001) GO TO 1100
       IOPT=0
       GO TO 1110
504    DO 505 K=1,NDP
       PERR=F(K)*EPS
       IF (PERR.EQ.0.0) GO TO 507
      IF(ABS(HAD(K)-F(K)).LE.ABS(PERR)) GO TO 507
       GO TO 605
507    JTL=K
       FTHE(K)=THETA(F(K),JTL)
       ERD=FTHE(K)*EPS
```

```
        IF (ABS(THE(K)-FTHE(K)).LE.ABS(ERD)) GO TO 505
        GO TO 605
505     CONTINUE
        GO TO 1110
605     DO 600 I=1,NDP
        JTL=I
        HAD(I)=F(I)
        THE(I)=THETA(HAD(I),JTL)
600     CONTINUE
110     CONTINUE
1100    DELTAT=DELTAT/2.0
        IND=IND+1
        DT=DELTAT
        GO TO 900
1110    CONTINUE
        DO 700 I=1,NDP
        JTL=I
        HAD(I)=F(I)
        THE(I)=THETA(HAD(I),JTL)
700     CONTINUE
        DO 800 I=1,NDP-1
        JTL=I
        AP(I)=(COND(THE(I),JTL)+COND(THE(I+1),(JTL+1)))/2.0
800     CONTINUE
        STO(1)=(-HAD(1)+HAD(2)+DELZ(1))/DELZ(1)*AP(1)
        C2=STO(1)
        G2=(-HAD(NDP-1)+HAD(NDP)+DELZ(NDP-1))/DELZ(NDP-1)
        1*AP(NDP-1)
        STO(NDP)=G2
        STO(NDP-1)=G2-(-HAD(NDP-2)+HAD(NDP-1)+DELZ(NDP-2))/DELZ
        1(NDP-2)*AP(NDP-2)
        DO 1050 I=2,NDP-2
        STO(I)=(-HAD(I)+HAD(I+1)+DELZ(I))/DELZ(I)*AP(I)
        1-(-HAD(I-1)+HAD(I)+DELZ(I-1))/DELZ(I-1)*AP(I-1)
1050    CONTINUE
        STO(NDP)=G2
        COM=RAIN*DELTAT
        IF (IOPT.GT.0) COM=(C1+C2)*DELTAT/2.0
        OUT=(G1+G2)*DELTAT/2.
        EVTP=0.0
        DO 1070 J=1,NOROOT
        EVTP=EVTP+S(J)*DELTAT
1070    CONTINUE
        BAL=COM-(OUT+EVTP)
        STOR=TRP(NDP)
        DO 3700 I=1,NDP
        B1(I)=THE(I)
        HPR1(I)=HAD(I)
3700    CONTINUE
        C1=C2
        G1=G2
        RETURN
        END
```

```
          SUBROUTINE SINK(NDP,NOROOT,B1,THE,XU,XV,S,DELTAT)
C THIS SUBROUTINE COMPUTES NODAL EVAPOTRANSPIRATION VALUES
          DIMENSION B(120),B1(120),THE(120),XU(120),XV(120),S(120)
          COMMON/CONST/POR,SAT,PAT,SSM,FFC,WP,POW,THR,RZD,PF,PET,THC
          THMC=FFC-(FFC-WP)*PF
          SSS=PET/(PAT*RZD)
          DO 10 J=1,NDP
          B(J)=(B1(J)+THE(J))/2.0
          S(J)=0.0
10        CONTINUE
          DO 50 J=1,NOROOT
          IF (B(J).GE.THMC) GO TO 30
          IF (B(J).LE.WP.OR.B(J).GE.POR) GO TO 40
          S(J)=SSS*(B(J)-WP)/(THMC-WP)*(XU(J)-XV(J))
          IF (J.EQ.NOROOT) S(J)=S(J)*(RZD-XV(J))/(XU(J)-XV(J))
          GO TO 20
30        S(J)=SSS*(XU(J)-XV(J))
          IF (J.EQ.NOROOT) S(J)=SSS*(RZD-XV(J))
          GO TO 20
40        S(J)=0.0
20        SVR=S(J)*DELTAT
          AVSM=(B(J)-THR)*(XU(J)-XV(J))
          IF (J.EQ.NOROOT) AVSM=(B(J)-THR)*(RZD-XV(J))
          IF (AVSM.LT.0.0) AVSM=0.0
          IF (SVR.GT.AVSM) SVR=AVSM
          S(J)=SVR/DELTAT
50        CONTINUE
          RETURN
          END

          FUNCTION DIFU(JTL)
C THIS FUNCTION COMPUTES SPECIFIC MOISTURE CAPACITY
          COMMON/DAT/DELZ(120),HAD(120),B1(120),THE(120),HPR1(120),AP(120
          COMMON/CONST/POR,SAT,PAT,SSM,FFC,WP,POW,THR,RZD,PF,PET,THC
          TUF1=(HPR1(JTL)+HAD(JTL))/2.0
          AC=ALOG(POR-2.0*THR)/SSM
          IF(TUF1.GT.SSM)GO TO 1000
          IF (TUF1.EQ.SSM) GO TO 887
          DIFU=-THR/SSM
          RETURN
1000      DIFU=EXP(AC*TUF1)*(AC)
          IF(DIFU.GE.0.0)STOP'ERROR-SPEC'
          RETURN
887       CONTINUE
          A1=THETA(TUF1+0.001,JTL)/0.002
          A2=THETA(TUF1-0.001,JTL)/0.002
          DIFU=A1-A2
          IF(DIFU.GE.0.0)STOP'ERROR-SPEC'
          RETURN
          END
          FUNCTION TREP(NDP)
C THIS FUNCTION COMPUTES THE CHANGE IN MOISTURE STORAGE
          COMMON/DAT/DELZ(120),HAD(120),B1(120),THE(120),HP1(120),AP(120)
```

```
          AREA=0.0
          DO 100 KM=2,NDP-1
          AREA=AREA+(THE(KM)-B1(KM))*(DELZ(KM-1)+DELZ(KM))/2.
  100     CONTINUE
          TREP=AREA+(THE(1)-B1(1))*(DELZ(1))/2.+(THE(NDP)-B1(NDP))
         1*DELZ(NDP-1)/2.
          RETURN
          END
          SUBROUTINE BST (N,A,B,C,D,H)
C THIS SUBROUTINE SOLVES THE TRI-DIAGONAL COEFFICIENT MATRIX
C USING THOMAS ALGORITHM
          DIMENSION A(800),B(800),C(800),D(800)
          DIMENSION AL(800),BT(800),Y(800),H(800)
          AL(1)=B(1)
          BT(1)=C(1)/B(1)
          DO 100 I=2,N
          AL(I)=B(I)-A(I)*BT(I-1)
          BT(I)=C(I)/AL(I)
  100     CONTINUE
          Y(1)=D(1)/AL(1)
          DO 200 I=2,N
          Y(I)=(D(I)-A(I)*Y(I-1))/AL(I)
  200     CONTINUE
          H(N)=Y(N)
          DO 300 I=2,N
          II=N-I+1
          H(II)=Y(II)-BT(II)*H(II+1)
  300     CONTINUE
          RETURN
          END
          SUBROUTINE TRANS(NMAX,NTT,NTP,FLUX,DELTAT,THC,SMY,NNA,INA,NMKT)
C THIS SUBROUTINE SOLVES THE SOLUTE TRANSPORT EQUATIONS
          DIMENSION COT(120),CCD(120),CIMP(120),NNA(120),INA(120,100)
          DIMENSION DIS(800),HRC(800),VLT(800),DFC(800),CSO(800),
         1WCON(800),SMY(800)
          DIMENSION A(800),B(800),C(800),D(800),H(800)
          COMMON/DAT/DELZ(120),HAD(120),B1(120),THE(120),HPR1(120),AP(120)
          COMMON/CONN/CCM(120),VLA(120),VLX(120),CIM(120)
         1,XV(120),XU(120),XF(120)
          COMMON /CONC/VLL(800),X(800),Y(800),SOL(800),XWAT(800),
         1YWAT(800)
          COMMON/INDEX/TSTR,C0,A0,A10,AML,D0,CFS,SUMVL,EFL,ALPHA,
         1P,RO,CONS,RX,KS
          XL=Y(NTP)
          IF (SUMVL.GE.0.0) GO TO 99
          GO TO 101
   99     CFS=CFS+FLUX*DELTAT*C0
          IF (XL.LT.TSTR) GO TO 101
          ETP=XL/TSTR
          NMP=IFIX(ETP)
          DSL=(ETP-NMP)*TSTR
          SLSUM=0.0
          DO 107 K=NTP+1,NTP+NMP
```

```
        VLL(K)=TSTR*SUMVL/XL
        SOL(K)=TSTR*CFS/XL
        Y(K)=DSL+(FLOAT(NTP+NMP)-FLOAT(K))*TSTR
        X(K)=Y(K)+TSTR
        XWAT(K)=X(K)*SUMVL/XL
        YWAT(K)=Y(K)*SUMVL/XL
        SLSUM=SLSUM+SOL(K)
107     CONTINUE
        NTP=NTP+NMP
        XL=DSL
        SUMVL=YWAT(NTP)
        CFS=CFS-SLSUM
101     CONTINUE
        EXDP=XF(NMAX)
        CALL EXCMOV(NTP,EXDP,EFL)
        IF (XL.EQ.0.0) GO TO 115
        NTT=NTP+1
        VLL(NTT)=SUMVL
        SOL(NTT)=CFS
        X(NTT)=XL
        Y(NTT)=0.0
        XWAT(NTT)=SUMVL
        YWAT(NTT)=0.0
        GO TO 114
115     NTT=NTP
114     DO 105 K=1,NTT
        DIS(K)=X(K)-Y(K)
        HRC(K)=SOL(K)/VLL(K)
        WCON(K)=VLL(K)/(X(K)-Y(K))-P*RO*CONS
105     CONTINUE
        DO 110 K=1,NTT-1
        AVW=(WCON(K)+WCON(K+1))/2.0
        WIP=A10*AVW
        DFC(K)=D0*A0*EXP(WIP)+AML*ABS(SMY(K))
110     CONTINUE
        DO 69 K=1,NTT
        IF (K.GT.1.AND.K.LT.NTT) GO TO 73
        IF (K.EQ.NTT) GO TO 72
        GO TO 74
72      AX=2.0*((WCON(K-1)+WCON(K)))*(DFC(K-1))/
        1(DIS(K)*(DIS(K)+DIS(K-1)))
        A(K)=-AX
        B(K)=(WCON(K)+P*RO*CONS)/(DELTAT)+AX
        C(K)=0.0
        D(K)=HRC(K)*(WCON(K)+P*RO*CONS)/DELTAT
        GO TO 69
74      AX=2.0*((WCON(K+1)+WCON(K)))*(DFC(K))/
        1(DIS(K)*(DIS(K)+DIS(K+1)))
        A(K)=0.0
        B(K)=(WCON(K)+P*RO*CONS)/(DELTAT)+AX
        C(K)=-AX
        D(K)=HRC(K)*(WCON(K)+P*RO*CONS)/(DELTAT)
        GO TO 69
```

```
73        CONTINUE
          ATH=(WCON(K)+WCON(K+1))/2.0
          BTH=(WCON(K-1)+WCON(K))/2.0
          A(K)=-(2.0*DFC(K-1))*(BTH)/(DIS(K)*(
          1DIS(K)+DIS(K-1)))
          B(K)=(WCON(K)+P*RO*CONS)/DELTAT+(2.0*DFC(K))*
          1(ATH)/(DIS(K)*(DIS(K)+DIS(K+1)))+(2.0*DFC(K-1))*(BTH
          2)/(DIS(K)*(DIS(K)+DIS(K-1)))
          C(K)=-(2.0*DFC(K))*(ATH)/(DIS(K)*(DIS(K)+DIS(K+1)))
          D(K)=HRC(K)*(WCON(K)+P*RO*CONS)/DELTAT
69        CONTINUE
          CALL BST(NTT,A,B,C,D,H)
          DO 88 K=1,NTT
          CSO(K)=H(K)
88        CONTINUE
          DO 106 K=1,NTT
          SOL(K)=CSO(K)*VLL(K)
106       CONTINUE
          CALL VOLSOL(NMAX,XV,XU,NTT,X,Y,SOL,VLL,VLA,VLX,COT,CCM,
          1NNA,INA)
          IF (THC.EQ.0.0.OR.ALPHA.EQ.0.0) GO TO 78
          DO 121 J=1,NMAX
          IF (NMKT.NE.1) GO TO 122
          CIM(J)=(ALPHA*DELTAT*CCM(J)+CIMP(J)*(THC+(1-P)*RO*CONS))
          1/((THC+(1-P)*RO*CONS)+ALPHA*DELTAT)
          CCM(J)=CCM(J)-(CIM(J)-CIMP(J))*(THC+(1-P)*RO*CONS)/COT(J)
          GO TO 121
122       CIM(J)=(ALPHA*DELTAT*KS*CCM(J)+CIMP(J))/(1.0+ALPHA*DELTAT)
          CCM(J)=CCM(J)-RX*(CIM(J)-CIMP(J))/COT(J)
121       CONTINUE
          DO 123 J=1,NMAX
          CCD(J)=(CIMP(J)-CIM(J))*(THC+(1-P)*RO*CONS)/COT(J)
          IF (NMKT.EQ.1) GO TO 124
          CCD(J)=(CIMP(J)-CIM(J))*RX/COT(J)
124       CIMP(J==CIM(J)
123       CONTINUE
          CALL MODSOL(NTT,NMAX,NNA,INA,VLA,VLX,CCD,XU,XV,X,Y,SOL)
78        IF (NTT.EQ.NTP) GO TO 79
          CFS=SOL(NTT)
79        CONTINUE
          RETURN
          END
          SUBROUTINE MCURVE(NDP,B1,DELZ,THC,P,RO,CONS,NMD,WADPT,CMD)
C THIS SUBROUTINE COMPUTES THE CUMULATIVE WATER VS DEPTH PROFILE
          DIMENSIONB1(120),DELZ(120),WADPT(120),CMD(120)
          SUM2=0.0
          SUM3=0.0
          LNDP=1
          DO 73 J=2,NDP
          SUMDP=0.0
          PSTP=ABS(B1(J)-B1(J-1))
          NDIV=IFIX(PSTP/0.002)
          IF (PSTP.LT.0.002) NDIV=1
```

```
          DDZ=DELZ(J-1)/FLOAT(NDIV)
733       LNDP=LNDP+1
          SUMDP=SUMDP+DDZ
          SUM3=SUM3+DDZ
          CMD(LNDP)=SUM3
          STAG=(B1(J-1)-(THC+P*RO*CONS))
          IF (STAG.LT.0.0) STAG=0.0
          SUM2=SUM2+(2.0*STAG+(B1(J)-B1(J-1))*
         1(SUMDP+SUMDP-DDZ)/DELZ(J-1))*DDZ*0.5
          WADPT(LNDP)=SUM2
          IF (SUMDP.LT.DELZ(J-1)) GO TO 733
73        CONTINUE
          WADPT(1)=0.0
          NMD=LNDP+1
          CMD(NMD)=CMD(LNDP)+15.0*DELZ(NDP-2)
          WADPT(NMD)=WADPT(LNDP)+(B1(NDP)-THC+P*RO*CONS)*15.0*DELZ(NDP-2)
          RETURN
          END
          SUBROUTINE DONNA(X,ARG,VAL,Y,NDIM,IER)
C THIS SUBROUTINE PROVIDES LINEAR INTERPOLATION
          DIMENSION ARG(800),VAL(800)
          IER=0
          KDIM=NDIM-1
          IF (ARG(1).GT.ARG(2)) GO TO 1
          IF (X.LT.ARG(1).OR.X.GT.ARG(NDIM)) GO TO 100
          DO 2 I=1,KDIM
          IF (X.GE.ARG(I).AND.X.LE.ARG(I+1)) GO TO 3
2         CONTINUE
3         Y=VAL(I)+(X-ARG(I))*(VAL(I+1)-VAL(I))/(ARG(I+1)-ARG(I))
          RETURN
1         IF (X.GT.ARG(1).OR.X.LT.ARG(NDIM)) GO TO 100
          DO 4 I=1,KDIM
          IF (X.LE.ARG(I).AND.X.GE.ARG(I+1)) GO TO 5
4         CONTINUE
5         Y=VAL(I)+(X-ARG(I))*(VAL(I+1)-VAL(I))/(ARG(I+1)-ARG(I))
          RETURN
100       IER=1
          RETURN
          END
          SUBROUTINE SOLET(NOROOT,NNA,INA,NTT,NTP,VLX,XV,XU,S,X,Y,
         1VLL,RZD,DELTAT,CUMET)
C THIS SBBROUTINE MODIFIES THE WATER VOLUMES (PER UNIT PLAN AREA) OF
C MOVING PACKETS DUE TO LOSS OF WATER BY EVAPOTRANSPIRATION
          DIMENSION NNA(120),INA(120,100),VLX(120),XV(120),XU(120)
         1,S(120)
          DIMENSION X(800),Y(800),VLL(800),CUMET(800),ETS(800),VLT
         1(800)
          DO 399 K=1,NTT
          VLT(K)=VLL(K)
399       CONTINUE
          I=NOROOT
          IF (RZD.EQ.XU(I)) GO TO 411
          VLX(I)=0.0
```

```
                DO 411 KK=1,NNA(I)
                K=INA(I,KK)
                IF (Y(K).GE.RZD) GO TO 411
                IF (Y(K).LT.XV(I).AND.X(K).GT.RZD) GO TO 413
                IF (Y(K).LT.XV(I).AND.X(K).GT.XV(I)) GO TO 414
                IF (Y(K).LT.RZD.AND.X(K).GT.RZD) GO TO 415
                VLX(I)=VLX(I)+VLL(K)
                GO TO 411
413             VLX(I)=VLX(I)+(RZD-XV(I))/(X(K)-Y(K))*VLL(K)
                GO TO 411
414             VLX(I)=VLX(I)+(X(K)-XV(I))/(X(K)-Y(K))*VLL(K)
                GO TO 411
415             VLX(I)=VLX(I)+(RZD-Y(K))/(X(K)-Y(K))*VLL(K)
411             CONTINUE
                XYZ=XU(I)
                XU(I)=RZD
                ADD=0.0
                DO 300 L=1,NTT
                K=NTT-L+1
                ETS(K)=0.0
                CUMET(K)=0.0
                SUME=0.0
                DO 310 J=1,NOROOT
                IF (X(K).LE.XV(J).OR.Y(K).GE.XU(J)) GO TO 310
                IF (Y(K).LT.XV(J).AND.X(K).GT.XU(J)) GO TO 320
                IF (Y(K).LT.XV(J).AND.X(K).GT.XV(J)) GO TO 330
                IF (Y(K).LT.XU(J).AND.X(K).GT.XU(J)) GO TO 340
                ETS(K)=VLT(K)/VLX(J)*S(J)*DELTAT
                GO TO 350
330             ETS(K)=VLT(K)*(X(K)-XV(J))/((X(K)-Y(K))*VLX(J))*S(J)*DELTAT
                GO TO 350
340             ETS(K)=VLT(K)*(XU(J)-Y(K))/((X(K)-Y(K))*VLX(J))*S(J)*DELTAT
                GO TO 350
320             ETS(K)=S(J)*DELTAT
350             VLL(K)=VLL(K)-ETS(K)
                SUME=SUME+ETS(K)
310             CONTINUE
                ADD=ADD+SUME
                CUMET(K)=ADD
300             CONTINUE
                XU(NOROOT)=XYZ
                IF (NTT.EQ.NTP) CUMET(NTP+1)=0.0
                RETURN
                END
                SUBROUTINE MODCOR(NTP,NMD,FLUX,CUMET,SUMVL,CFS,WADPT,CMD
                1,DELTAT,SMY)
C THIS SUBROUINE MODIFIES THE CUMULATIVE VOLUMES (PER UNIT PLAN AREA) O
C WATER CORRESPONDING TO THE MOVING COORDINATES AND COMPUTES THEIR NEW
C POSITIONS
                DIMENSION CUMET(800),SMY(800),SM(800),XOLD(800),YOLD(800)
                DIMENSION WADPT(120),CMD(120)
                COMMON /CONC/VLL(800),X(800),Y(800),SOL(800),XWAT(800),
                1YWAT(800)
```

```
          DO 34 K=1,NTP
          XOLD(K)=X(K)
          YOLD(K)=Y(K)
34        CONTINUE
          MPR=0
          DO 36 K=1,NTP
          XWAT(K)=XWAT(K)+FLUX*DELTAT-CUMET(K)
          YWAT(K)=YWAT(K)+FLUX*DELTAT-CUMET(K+1)
          IF (YWAT(K).GT.0.0) GO TO 36
          SUMVL=XWAT(K)
          CFS=CFS+SOL(K)
          MPR=MPR+1
36        CONTINUE
          NTP=NTP-MPR
          IF (MPR.EQ.0) SUMVL=YWAT(NTP)
          DO 26 K=1,NTP
          CALL DONNA(XWAT(K),WADPT,CMD,X(K),NMD,IER)
          IF(IER.NE.0)STOP'ERROR IN INT1'
          SM(K)=(X(K)-XOLD(K))/DELTAT
          CALL DONNA(YWAT(K),WADPT,CMD,Y(K),NMD,IER)
          IF (IER.NE.0) TYPE *,K,Y(K)
          IF(IER.NE.0)STOP'ERROR IN INT2'
          SMY(K)=(Y(K)-YOLD(K))/DELTAT
26        CONTINUE
          RETURN
          END
          SUBROUTINE EXCMOV(NTP,EXDP,EFL)
C THIS SUBROUTINE EXCLUDES MOVING PACKETS LEAVING THE DOMAIN
          COMMON /CONC/VLL(800),X(800),Y(800),SOL(800),XWAT(800),
         1YWAT(800)
43        CONTINUE
          DO 40 IK=1,NTP
          IF (X(IK).LE.EXDP) GO TO 40
          IF (Y(IK).LT.EXDP) GO TO 441
          EFL=EFL+SOL(IK)
          DO 442 L=IK,NTP-1
          X(L)=X(L+1)
          Y(L)=Y(L+1)
          VLL(L)=VLL(L+1)
          SOL(L)=SOL(L+1)
          XWAT(L)=XWAT(L+1)
          YWAT(L)=YWAT(L+1)
442       CONTINUE
          NTP=NTP-1
          GO TO 43
441       EFL=EFL+SOL(IK)*(X(IK)-EXDP)/(X(IK)-Y(IK))
          SOL(IK)=SOL(IK)-SOL(IK)*(X(IK)-EXDP)/(X(IK)-Y(IK))
          XWAT(IK)=XWAT(IK)-(X(IK)-EXDP)*VLL(IK)/(X(IK)-Y(IK))
          VLL(IK)=VLL(IK)-VLL(IK)*(X(IK)-EXDP)/(X(IK)-Y(IK))
          X(IK)=EXDP
40        CONTINUE
          RETURN
          END
```

```
      SUBROUTINE MODSOL(NTT,NMAX,NNA,INA,VLA,VLX,CCD,XU,XV,X,Y,SOL)
C THIS SUBROUTINE MODIFIES SOLUTE VOLUMES (PER UNIT PLAN AREA) CONTAINED
C IN THE MOVING PACKETS
      DIMENSION NNA(120),INA(120,100),VLA(120),CCD(120),XU(120)
     1,XV(120),VLX(120)
      DIMENSION X(800),Y(800),SOL(800),VLT(800)
      DO 669 K=1,NTT
      VLT(K)=SOL(K)
669   CONTINUE
      DO 78 J=1,NMAX
      IF (CCD(J).EQ.0.0) GO TO 78
      DO 70 KK=1,NNA(J)
      K=INA(J,KK)
      IF (CCD(J).LT.0.0.AND.VLA(J).LT.1.0E-35) GO TO 78
      IF (CCD(J).GT.0.0) GO TO 57
      RT=VLT(K)/VLA(J)
      IF (Y(K).LT.XV(J).AND.X(K).GT.XV(J)) RT=VLT(K)*(X(K)-XV(J))/
     1((X(K)-Y(K))*VLA(J))
      IF (Y(K).LT.XU(J).AND.X(K).GT.XU(J)) RT=VLT(K)*(XU(J)-Y(K))/
     1((X(K)-Y(K))*VLA(J))
      IF (Y(K).LE.XV(J).AND.X(K).GE.XU(J)) RT=1.0
      GO TO 59
57    RT=(X(K)-Y(K))/(XU(J)-XV(J))
      IF (Y(K).LT.XV(J).AND.X(K).GT.XV(J)) RT=(X(K)-XV(J))/
     1(XU(J)-XV(J))
      IF (Y(K).LT.XU(J).AND.X(K).GT.XU(J)) RT=(XU(J)-Y(K))/
     1(XU(J)-XV(J))
      IF (Y(K).LE.XV(J).AND.X(K).GE.XU(J)) RT=1.0
59    CSV=RT*CCD(J)*VLX(J)
      SOL(K)=SOL(K)+CSV
      IF (SOL(K).GE.0.0) GO TO 70
      TYPE 56
56    FORMAT(5X,'CONTENT OF A MOVING POINT GETTING NEGATIVE')
      STOP
70    CONTINUE
78    CONTINUE
      RETURN
      END
```

REFERENCES

Aris, R., (1956), ' On the dispersion of a solute in a fluid flowing through a tube', Proc. Roy Soc. Ser. A, Vol. 225, 473-477.

Bachmat, Y., (1969), 'Hydrodynamic dispersion in a saturated homogeneous porous medium at low Peclet numbers and nonhomogeneous solution', Water Resour. Res.,Vol.5, No.1, pp. 139-143.

Bear,J., (1972), 'Dynamics of fluids in porous media', American Elsvier, New York, 764 pp.

Bear, J., (1979), 'Hydraulics of groundwater', McGraw-Hill, Israel, 567 pp.

Bear, J. and Bachmat, Y., (1967),'A generalized theory on hydrodynamic dispersion in porous media', Proc. Int. Ass. Sci. Hydrol. Symp. Haifa, Publ. No.72.

Bear, J. and Todd, D.K., (1960), 'The transition zone between fresh and salt waters in coastal aquifers', University of California', Water Resources Centre Contrib., No.29.

Bear, J., Zaslavsky, D. and Irmay, S., (1968), ' Physical principles of water percolation and seepage ', Unesco, Paris.

Biggar, J.W. and Nielsen, D.R., (1963),' Miscible displacement: IV. Mixing in glass beads ', Soil Sci. Soc. Am. Proc., Vol.27, pp. 11-13.

Biggar, J.W. and Nielsen, (1976), 'Spatial variability of the leaching characteristics of a field soil', Water Resour. Res., Vol.12, No.1, pp. 78-84.

Bolt, G.H. (ed.), (1982), ' Soil chemistry B. Physco Chemical Models', Elsvier, Amsterdam, 527 pp.

Böttcher, J. and Strebel, O.,(1989), (Scientists, B.G.R, Hannover, Germany), Personal Discussion.

Böttcher, J.,(1990),(Scientist, B.G.R, Hannover, Germany), Personal Communication.

Brenner, H., (1962), ' The diffusion model of longitudinal mixing in beds of finite length. Numerical values ', Chem. Eng. Sci., Vol.17, pp. 229-243.

Bresler, E., (1973a), ' Simultaneous transport of solute and water under transient unsaturated flow conditions', Water Resour. Res., Vol.9, No.4, pp. 975-986.

Bresler, E., (1973b), ' Anion exclusion and coupling effects in non-steady transport through unsaturated soils: I. Theory', Soil Sci. Soc. Am. Proc. , Vol.39, pp. 604-613.

Bresler, E. and Hanks, R.J. (1969), ' Numerical method for estimating simultaneous flow of water and salt in unsaturated soils' Soil Sci. Soc. Am. Proc., Vol.33, pp. 827-832.

Bresler, E., Kemper, W.D. and Hanks, R.J., (1969), ' Infiltration, redistribution and subsequent evaporation of water from soil as affected by wetting rate and hysteresis', Soil Sci. Soc. Am. Proc., Vol.33, pp. 832-840.

Brooks, R.H. and Corey, A. T., (1964), ' Hydraulic properties of porous media ', Hydrology Paper no.3, Colorado State University, Ft. Collins.

Bruch, J.C. and Zyvoloski, G., (1974), 'Solution of equation for vertical unsaturated flow of soil water ', Soil Science,

Vol.116, pp. 417-422.

Butters, G.L., Jury, W.A. and Ernst, F.F., (1989), ' Field scale transport of bromide in an unsaturated soil : 1. Experimental methodology and results', Water Resour. Res. , Vol.25, No.7, pp. 1575-1582.

Burdine, N.T., (1953), 'Relative permeability calculations from pore size distribution data', Trans. A.M.I.E., Vol. 198, pp. 71-77.

Campbell, G.S., (1974), ' A simple method for determining unsaturated conductivity from moisture retention data', Soil Science, Vol.117, No.6, pp. 311-314.

Cameron, D.A. and Klute, A., (1977), 'Convective -dispersive solute transport with a combined equilibrium and kinetic adsorption model', Water Resour. Res. , Vol.13, No.1, pp. 183-188.

Cavalieri, F. and Russo Spena, A.,(1984),'Wastewater utilization in the problem of water resources management', Finite Elements in Water Resources, (J.P. Laible et al., eds.), pp. 339-351.

Charbeneau, R.J., (1981), 'Groundwater contaminant transport with adsorption and ion exchange chemistry: Method of characteristics for the case without dispersion', Water Resour. Res., Vol.17., No.3, pp. 705-713.

Chaudhari, N.M., (1971), 'An improved numerical technique for solving multidimensional miscible displacement equations', Soc. Petrol. Eng. J., Vol.11, pp. 277-284.

Childs, E.C., (1967), 'Soil moisture theory', Advan. Hydrosci. (Ven T. Chow, ed.), Vol.4, pp. 73-117.

Childs, E.C. and Collis-George, N., (1950), 'The permeability of porous materials', Proc. Roy. Soc. (London) A, Vol.201, pp. 392-405.

Cleary, R.W. and Adrian, D.D., (1973), 'Analytical solution of the convective-dispersive equation for cation adsorption in soils', Soil Sci. Soc. Am. Proc. ,Vol.37, pp. 197-199.

Coats, K.H., and Smith, B.D., (1964), 'Dead end pore volume and dispersion in porous media', Soc. Pet. Eng. J., Vol.4, pp. 73-84.

Corey,A.T., (1957), 'Measurement of water and air permeability in unsaturated soils', Soil Sci. Soc. Am. Proc., Vol.21, pp.7-10.

Corey, J.C., Hawkins, R.H. and Overman, R.F., (1970), 'Miscible displacement measurements within laboratory columns using the gamma photoneutron method', Soil Sci. Soc. Am. Proc., Vol.34, pp. 854-858.

Dane, J.H. and Mathis, F.H., (1981), 'An adaptive finite difference scheme for the one dimensional water flow equation', Soil Sci. Soc. Am. J., Vol.45, No.6, pp. 1048-1054.

Deans, H.H., (1963),'A mathematical model for dispersion in the direction of flow in porous media', Soc. Pet. Eng. J., Vol.3, pp. 49-52.

De Josselin De Jong, G., (1958), Longitudinal and transverse diffusion in granular deposits', Trans. Amer. Geophys. Un., Vol.39, No.1, pp. 67-74.

De Smedt, F. and Wierenga, P.J., (1978a), 'Solute transport through soil with non-uniform water content', Soil Sci. Soc. Am. J., Vol.42, No.1, pp. 7-10.

De Smedt, F. and Wierenga, P.J., (1978b), 'Approximate analytical solution for solute flow during infiltration and redistribution', Soil Sci. Soc. Am. J., Vol.42, No.3, pp. 407-412.

De Smedt, F. and Wierenga, P.J., (1979a), 'Mass transfer in porous media with immobile water' J. Hydrol., Vol.41, pp. 59-67.

De Smedt, F. and Wierenga, P.J., (1979b), 'A generalized solution for solute flow in soils with mobile and immobile water', Water Resour. Res., Vol.15, No.5, pp. 1137-1141.

De Smedt, F and Wierenga, P.J., (1984), 'Solute transfer through columns of glass beads', Water Resour. Res., Vol. 20, No.2, pp. 225-232.

Doorenbos, J. and Kasam, A.H., (1979), 'Crop yield response for water', Irrigation and drainage division, FAO-ROME, paper No.33.

Duynisveld, W.H.M. and Strebel, O., (1983), 'Entwicklung von simulationsmodellen fur den transport von gelosten stoffen in wasserungesattigten boden und locker-sedimenten', Texte 17/83, unweltbundesamt Berlin: 197 S.

Fried, J.J., (1968), 'Changement dechelle dans un milieu poreux applieque a le tude de la dispersion dun traceur dans un fluide', Ann. Ponts Chaussees (V), pp. 285-295.

Fried, J.J. and Combarnous, M.A., (1971), 'Dispersion in porous media', Advan. Hydrosci., (Ven T. Chow, ed.), Vol.7, pp. 169-282.

Gaudet, J.P., Jegat, H., Vachaud, G. and Wierenga, P.J., (1977), 'Solute transfer, with exchange between mobile and stagnant

water, through unsaturated sand', Soil Sci. Soc. Am. J., Vol.41, No.4, pp. 665-671.

Garder, A.O., Jr., Peaceman, D.W. and Pozzi, A.L., Jr., (1964), 'Numerical calculations of multidimensional miscible displacement by the method of characteristics', Soc. Pet. Eng. J., Vol.4, No.1, pp. 26-36.

Gehrson, N.D. and Nir, A., (1969), 'Effects of boundary conditions of models on tracer distribution in flow through porous mediums', Water Resour. Res., Vol.5, pp. 830-839.

Giesel, W., Renger, M. and Strebel, O., (1973), 'Numerical treatment of the unsaturated flow equation - comparison of experimental and computed results', Water Resour. Res., Vol.9, No.1, pp. 174-177.

Gottschlich, C.F., (1963), 'Axial disperison in a packed bed', A.I.Ch.E.J., Vol.9, pp. 88-92.

Gray, W.G. and Pinder, F., (1976), 'An analysis of the numerical solution of the transport equation', Water Resour. Res., Vol.12, No.3, pp. 547-555.

Green, W.H. and Ampt, G.A., (1911), 'Studies on soil physics: I flow of air and water through soils', J. Agr. Sci., Vol.4, pp. 1-24.

Gupta, R.K., Millington, R.J. and Klute, A., (1973), 'Hydrodynamic dispersion in unsaturated porous media: I. Concentration distribution during dispersion', J. Indian Soc. Soil Sci., Vol.21, No.1, pp. 1-7.

Gupta, S.K. and Singh, S.R., (1980), 'Analytical solutions for predicting solute movements and their interpretation in

reclamation', J. Hydrol., Vol.45, pp. 133-148.

Gureghian, A.B., Ward, D.S. and Cleary, R.W., (1979), 'Simultaneous transport of water and reacting solute through multilayered soils under transient unsaturated flow conditions', J. Hydrol., Vol. 41, pp. 253-278.

Hanks, R.J. and Bowers, S.A., (1962), 'Numerical solution of the moisture flow equation for infiltration into layered soils', Soil Sci. Soc. Am. Proc., Vol.26, pp. 530-534.

Hanks, R.J., Klute, A. and Bresler, E., (1969), 'A numerical method for estimating infiltration, redistribution, drainage and evaporation of water from soil', Water Resour. Res., Vol.5, pp. 1064-1069.

IBM, (1967), 'System 360. Continuous system modelling program (360A-CX-16X)', User's Manual Data Processing Division, 122 East Post Road, White Plains, New York, N.Y.

IBM, (1972), 'System/360. Continuous system modelling program (360-CX-16X), User's Manual, IBM Publ. no.GH 20-636704, IBM Corporation, White Plains, New York, N.Y.

Irmay, S., (1954), 'On the hydraulic conductivity of unsaturated soils', Trans. Am. Geophys. Un., Vol.35, pp. 463-468.

Kemper, W.D. and Van Schaik, J.C., (1966), 'Diffusion of salts in clay water systems', Soil Sci. Soc. Amer. Proc., Vol.30., pp. 534-540.

Klute, A., (1952), 'A numerical method for solving the flow equation for water in unsaturated materials', Soil Sci. , Vol. 73, No.2, pp. 105-116.

Khaleel, R. and Redell, D.L., (1985), 'Miscible displacement in

porous media: MOC solution', J. Irrg. Drain. Eng., Vol.III, No.1, pp. 45-64.

Khaleel, R. and Redell, D.L., (1986), 'Computer notes - MOC solution of convective - dispersion problem', Groundwater, Vol.24, No.6, pp. 798-807.

Kirda, C., Nielsen, D.R., and Biggar, J.W., (1973), 'Simultaneous transport of chloride and water during infiltration', Soil Sci. Soc. Am. Proc., Vol.37, No.3, pp. 339-345.

Klinkenberg, L.J., (1957), 'Pore size distribution of porous media and displacement experiments with miscible liquids', J. Petrol. Technol, Vol.210, pp. 366-369.

Krupp, H.K. and Elrick, D.E., (1968), 'Miscible displacement in an unsaturated glass bead medium', Water Resour. Res., Vol.4, No.4, pp. 809-815.

Lai, S.H. and Jurinak, J.J., (1971)'Numerical approximation of cation exchange in miscible displacement through soil columns', Soil Sci. Soc. Am. Proc., Vol.35,.

Lai, S.H. and Jurinak, J.J., (1972), 'Cation adsorption in one dimensional flow through soils: Numerical solution', Water Resour. Res., Vol.8, No.1, pp. 99-107.

Lapidus, L. and Amundson, N.R., (1952), 'Mathematics of adsorption in beds', J. Phys. Chem., Vol.56, pp. 984-988.

Lindstorm, F.T., Haque, R., Freed, V.H. and Boersma, L, (1967), 'Theory on the movement of some herbicides in soils', Environ. Sci. Technol., Vol.1, pp. 561-565.

Marino, M.A., (1974), 'Distribution of contaminants in porous media flow', Water Resour. Res., Vol.19, No.2, pp. 1013-1018.

Marle C., and Defrenne, P., (1960), 'La description mathematique du deplacement de fluides miscibles dans un milieu poreux', Rapp. Inst. Fr. Fetrole No.5433.

Miller, R., Biggar, J.W. and Nielsen, D.R., (1965), 'Chloride displacement in Panoche clay loam in relation to water movement and distribution', Water Resour. Res., Vol.1, pp. 63-75.

Misra, C. and Mahapatra, S.N., (1989), 'Prediction of salt transport during leaching of saline soils for reclamation', J. Hydrol., Vol.106, pp. 185-189.

Mohan Rao, K.M., (1986), 'Hydrological response of unsaturated zone upto water table', Ph.D. Thesis, University of Roorkee, Roorkee (India), 266 pp.

Mohan Rao, K.M., Kashyap, D. and Chandra, S., (1989), 'A functional relation for capillary suction vs moisture content', Proceedings of the International workshop on Appropriate Methodologies for Development and Management of Groundwater Resources in Developing Countries, NGRI, Hyderabad, India, Vol.I, pp. 405-409.

Mualem, Y., (1976) 'A new model for predicting the hydraulic conductivity of unsaturated porous media', Water Resour. Res., Vol.12, No.3, pp. 513-522.

Neuman, S.P., (1981), 'An eularian lagrangian numerical scheme for the dispersion - convection equation using conjugate space-time grids', J. Comp. Phys. Vol.41, No.2, pp. 270-294.

Neuman, S.P. and Sorek, S., (1982), 'Eularian - lagrangian methods for advection - dispersion', Finite Elements in Water

Resources, (K.P. Holz et al, eds.), Springer - verlag Berlin Heidelberg New York, pp. 14-41.

Nielsen, D.R., and Biggar, J.W., (1961), 'Miscible displacement in soils: I. Experimental information', Soil Sci. Soc. Am. Proc., Vol.25, pp. 1-5.

Nielsen, D.R., and Biggar, J.W. (1962), 'Miscible displacement in soils: II Theoretical considerations', Soil Sci. Soc. Am. Proc., Vol.26, pp. 216-221.

Nielsen, D.R., Kirkham, D. and van Wijk, W.R.,(1961), 'Diffusion equation calculations of field soil water infiltration profiles', Soil Sci. Soc. Am. Proc., Vol. 25, pp. 165-168.

Ogata, A., (1970), 'Theory of dispersion in a granular medium', U.S. Geol., Surv. Prof. Pap., 411-I.

Olsen, S.R. and Kemper, W.D., (1968),'Movement of nutrients to plant roots', Adv. Agron., Vol.30, pp. 91-151.

Parkar, J.C. and van Genuchten, M. Th., (1984), 'Determining transport parameters from laboratory and field experiments', Virginia Agric. Exp. Stn. Bull. 84-3, 96 pp.

Parlange, J.Y., and Starr, J.L., (1978), 'Dispersion in soil columns: effects of boundary conditions and irreversible reactions', Soil Sci. Soc. Am. J., Vol.42, No.1, pp. 15-18.

Parlange, J.Y., Lisle, I. and Broaddock, R.D., (1982), 'The three parameter infiltration equation', Soil Sci., Vol.133, No.6, pp. 337-341.

Philip, J.R., (1955),'Numerical solution of equations of the diffusion type with diffusivity concentration dependent', Trans Faraday Soc., Vol.51, pp. 885-892.

Philip, J.R., (1957a), 'The theory of infiltration :1.', Soil, Sci., Vol.83, pp. 345-357.

Philip, J.R., (1957b), 'The theory of infiltration :2. The profile at infinity', Soil Sci., Vol.83, pp. 435-448.

Philip, J.R., (1958), 'The theory of infiltration :6. Effect of water depth over soil', Soil Sci., Vol.85, pp. 278-286.

Philip, J.R., (1969), 'Theory of infiltration ', Advan. Hydrosci Vol.5, pp. 215-296.

Porter, L.K., Kemper, W.D., Jackson,R.D. and Stewart, B.A., (1960), 'Chloride diffusion in soils as influenced by moisture content', Soil Sci. Soc. Am. Proc., Vol.24, pp. 460-463.

Rawls, W.J.,Brakensiek, D.L. and Saxton, K.E.,(1981), 'Soil water characteristics', Paper No. 81-2510 for presentation at the 1981 winter meeting of ASAE.

Remson, I., Drake, R.L. and Mc Neary, S.S.,(1965), 'Vertical drainage of an unsaturated soil',J. Hydraulic Div., ASCE, Vol. 91, pp. 55-74.

Remson, I., Hornberger, G.M. and Molz, F.J., (1971), 'Numerical methods in subsurface hydrology', Wiley Interscience, 389 pp.

Richards, L.A., (1931), 'Capillary conduction of liquids in porous mediums', Physics 1, pp. 318-333.

Rubin, J. (1967), 'Numerical methods for analyzing hysteresis affected, post - infiltration redistribution of soil moisture', Soil Sci. Soc. Am. Proc. Vol.31, pp. 13-20.

Rubin, J., and Steinhardt, R., (1963), 'Soil water relations during rain infiltration: I. Theory', Soil Sci. Soc. Am. Proc., Vol.27, pp. 246-251.

Rubin, J., Steinhardt, R. and Reiniger, P., (1964), 'Soil water relations during rain infiltration: II. Moisture content profiles during rains of low intensities', Soil Sci. Soc. Am. Proc., Vol.28, pp. 1-5.

Russo, D., (1988a), 'Numerical analysis of the nonsteady transport of interacting solutes through unsaturated soil : 1.Homogenous systems', Vol.24, No.2, pp. 271-284.

Russo, D., (1988b), 'Numerical analysis of the nonsteady transport of interacting solutes through unsaturated soil: 2. Layered systems', Vol.24, No.2, pp. 285-290.

Russo, D., Jury, W.A. and Butters, G.L., (1989a), 'Numerical analysis of solute transport during transient irrigation: 1. The effect of hysteresis and profile heterogeneity', Water Resour. Res., Vol.25, No.10, pp. 2109-2118.

Russo, D., Jury, W.A. and Butters, G.L., (1989b), 'Numerical analysis of solute transport during transient irrigation: 2. The effect of immobile water', Water Resour. Res., Vol.25, No.10, pp. 2119-2127.

Saffman, P.G., (1959), 'A theory of dispersion in a porous medium', J. Fluid Mech., Vol.6, Part 3, pp. 321-349.

Saffman, P.G., (1960), 'Dispersion due to molecular diffusion and macroscopic mixing in flow through a network of capillaries', J. Fluid Mech., Vol.7, Part 2, pp. 194-208.

Scheideggar, A.E., (1954), ' Statistical hydrodynamics in porous media ', J. Appl. Phys., No. 25, pp. 994-1001.

Scheideggar, A.E., (1961), 'General theory of dispersion in porous media', J. Geophys. Res., Vol.66, pp. 3273-3278.

Scheideggar, A.E., (1963), 'The physics of flow through porous media', University of Toronto Press., 313 pp.

Scott, E.J., Hanks, R.J., Peters, D.B. and Klute, A., (1962), 'Power series solution of the one-dimensional diffusion equation for exponential and linear diffusivity function', USDA. ARS 41-64, Sept.

Selim. H.M. and Mansell, R.S., 1976, 'Analytical solution of the equation for transport of reactive solutes through soils', Water Resour. Res., Vol.12, No.3, pp. 528-532.

Skopp, J. and Warrick, A.W., (1974), 'A two phase model for the miscible displacement of reactive solutes in soil', Soil Sci. Soc. Am. J., Vol.38, No.4, pp. 545-550.

Slichter, C.S., field measurement of the rate of movement of underground waters', U.S. Geol. Survey, Water Supply Paper, No. 140.

Smajstrla, A.G., Redell, D.L.and Hiller, E.A., (1975), 'Simulation of miscible displacement in soils using the method of characteristics', Transactions of ASAE, Vol. 18, No.3, pp. 281-287.

Staple, W.J., (1966),'Infiltration and redistribution of water in vertical columns of loam soil', Soil Sci. Soc. Am. Proc., Vol.30, pp. 553-558.

Stone, H.L. and Brian, P.L.T.,(1963),'Numerical solution of convective transport problems', A.I.Ch.E.J., Vol.9, NO.5, pp. 681-688.

Swartzendruber, D.,. (1969), 'The flow of water in unsaturated soils', In: Flow through porous media, R.J.M., De Wiest (ed.),

Academic press, pp. 229-237.

Taylor, G.I., (1953), 'Dispersion of soluble matter in solvent flowing slowly through a tube', Proc. Roy. Soc. Ser. A, Vol. 212, pp. 186-203.

Tripathi, S.K., (1991), (Reader in Agronomy, U.O.R., Roorkee, India), Personal Discussion.

Vachaud, G. and Thony, J.L., (1971), 'Hystersis during infiltration and redistribution in a soil column at different initial water contents', Water Resour. Res., Vol.7, No.1, pp. 111-127.

Van de Pol, R.M., Wierenga, P.J. and Nielsen, D.R., (1977), 'Solute movement in a field soil', Soil Sci. Soc. Am. J., Vol.141, No.1, pp. 10-13.

Van der Molen, W.H., (1973), 'Salt balance and leaching requirement', Drainage pricniples and Applications, (J. Kesser et al, eds.), International Institute for Land Reclamation and Improvement, Wageningen, Netherlands, Pub. No.16, Vol.II, pp. 59-100.

van Genuchten, M.Th.,(1976), 'On the accuracy and efficiency of several numerical schemes for solving the convective-dispersive equation', Finite Elements in Water Resources, (W.G.Gray, G.F. Pinder and C.A. Brebbia, eds.) Pentech Press London, pp. 1.71-1.90.

van Genuchten, M.Th., (1980), 'A closed form equation for predicting the hydraulic conductivity of unsaturated soils', Soil Sci. Soc. Am. J., Vol. 44, No.5, pp. 892-898.

van Genuchten, M.Th., (1981), 'Analytical solutions for chemical transport with simultaneous adsorption, zero order production

and first order decay', J. Hydrol., Vol.49, pp. 213-233.

van Genuchten, M.Th., (1982), 'A comparison of numerical solutions of the one-dimensional unsaturated saturated flow and mass transport equations', Adv. Water Resour., Vol.5, pp. 47-55.

van Genuchten, M.Th. and Gray, W.G., (1978), 'Analysis of some dispersion corrected numerical schemes for solution of the transport equation', Int. J. Num. Meth. Eng., Vol.12, pp. 387-404.

van Genuchten, M.Th and Wierenga, P.J., (1974), 'Simulation of one-dimensional solute transport in porous media', New Mexico State Univ., Agric. Exp. Stn. Bull. 628, 40 pp.

van Genuchten, M.Th. and Wierenga, P.J., (1976), 'Mass transfer studies in sorbing porous media: I. Analytical solutions', Soil Sci. Soc., Am. J., Vol.40, No.4, pp. 473-480.

van Genuchten, M.Th. and Wierenga, P.J., (1977), 'Mass transfer studies in sorbing porous media II. Experimental evaluation with tritium ($3H_2O$)', Soil Sci. Soc. Am. J., Vol.41, No.2, pp. 278-285.

van Genuchten, M.Th., Wierenga, P.J. and O' Connor, G.A., (1977), 'Mass transfer studies in sorbing porous media: III. Experimental evaluation with 2,4,5-T', Soil Sci., Soc. Am. J., Vol.41, No.2, pp. 278-285.

Van Ommen, H.C., Van Genuchten, M.Th., Van der Molen, W.H. Dijksma, R. and Hulshof,J., (1989a), 'Experimental and theoretial analysis of solute transport from a diffuse source of pollution', J. Hydrol., Vol. 105, pp. 225-251.

Van Ommen, H.C., Dijksma, R., Hendrickx, J.M.H., Dekker, L.W.,

Hulshof., J. and Van der Heuvel, M., (1989b),'Experimental assesment of preferential flow paths in a field soil', J. Hydrol., Vol.105, pp. 253-262.

Von Neuman, J. and Richtermyer, R.D., 1950, J. App. Phys., Vol.21, pp. 232-237.

Varoglu, E. and Finn, W.D.L, (1978), 'A finite element method for the diffusion-convection equation', Finite Elements in Water Resources, (C.A. Brebbia, W.G. Gray and G.F. Pinder, eds.), Pentech Press, London, pp. 4.3-4.20.

Warrick, A.W., Biggar, J.W.and Nielsen, D.R., (1971), 'Simultaneous solute and water transfer for an unsaturated soil', Water Resour. Res., Vol.7, No.5, pp. 1216-1225.

Whitaker, S., (1967), 'Diffusion and dispersion in porous media', A.I.Ch.E.J., Vol. 13, No.3, pp. 420-427.

Wood, A.L. and Davidson J.M., (1975), 'Fluometuron and water content distributions during infiltration: Measured and calculated', Soil Sci. Soc. Am. Proc., , Vol.39, pp. 820-825.

Youngs, E.G., (1957), 'Moisutre profiles during vertical infiltration' Soil Science, Vol. 84, pp. 283-290.